Speleothem Growth Rate and Palaeoclimate

Andy Baker

Department of Geography

A thesis submitted to the University of Bristol in accordance with the requirements of the degree of Ph.D. in the Faculty of Science.

October 1993

ABSTRACT

An initial study of the palaeoclimate signal contained within speleothem growth was undertaken by investigating regional variations in speleothem growth frequency. It was demonstrated that about 500 analyses in such a regional compilation were necessary to generate a statistically significant curve which did not suffer from sample bias. However, few such regions are likely to have such a large data set. That from north west Europe did provide a useful palaeoclimate record, giving evidence of multiple interstadial events within isotope stage 3, and a significantly low level of growth within stage 5a.

An investigation was undertaken into the palaeoclimate signal contained in variations of speleothem growth rate, based on the theory derived by Dreybrodt (1981) and Buhmann and Dreybrodt (1985) from calcite precipitation kinetics. It was demonstrated that growth rate increases with increasing calcium ion concentration, temperature and water flux (drip rate for stalagmites, water film thickness for flowstones and seasonal variations in water availability for both speleothems); turbulent flow conditions and cave air pCO_2, which theoretically affect growth rate, were demonstrated to be insignificant. If water flux, calcium concentration and temperature all increase with improving climate, growth rate increases may reflect climatic improvement. In particular, it was demonstrated that stalagmites should be most sensitive to changes in calcium concentrations, temperature, and seasonal shut-off of the water feed, whilst flowstones would also be sensitive to changes in water film thickness.

Theoretical growth rates were tested for recently forming speleothems in excavated caves and mines. For these, minimum growth rates were determined by knowing the date of excavation of the cave or mine, and the growth rate determining variables were measured over the course of a year. It was demonstrated that the theory accurately predicted growth rates for both stalagmites and flowstones within the 2σ errors based on variations in calcium ion concentration and water film thickness. However, flowstones generally grew slower than that predicted by the theory, due to the seasonal shut-off of the water supply feeding these samples. For flowstones at Kent's Cavern, growth rate was observed to increase with increasing water availability, for stalagmites at Lower Cave, growth rate was shown to increase with increasing drip rate.

Assuming a good prediction of growth rate by the theory, applications to Quaternary speleothems were undertaken to determine past calcium ion concentration, temperature and water flux. Growth rates were determined by thermal ionisation mass spectrometric uranium-series dating. The growth rate of one Holocene sample from Sutherland demonstrated that variations in growth rate over the last 7 ka did not depend on temperature variations, but either to changes in calcium concentrations due to vegetation change or a non-linear response to changes in water flow. Growth rates were also determined for two flowstones from Yorkshire which had grown over the last 200 ka. However, the very fast growth rates in these samples prevented a precise record from being obtained.

Mass spectrometric dating also provided a record of the timing of growth commencement and cessation. This was shown to be more complex than previously considered; in particular the Holocene growth of the Sutherland stalagmite commenced 5 ka after glacier retreat in the region, the Yorkshire flowstone from Lancaster Hole had seven growth phases, each for only 1-3 ka, five of which correlated with solar insolation maxima. In contrast, another flowstone from Stump Cross in Yorkshire was shown to grow in both interglacial, interstadial and glacial periods of the last 200 ka.

An investigation was made into the use of $^{13}C/^{12}C$ ratios to determine the type of plant community at the time of speleothem formation, and whether a non-biogenic source of CO_2 was present. ^{13}C analyses of the Stump Cross flowstone gave elevated ^{13}C not explicable by the plant communities present, nor were high enough to have a non-biogenic source. Further investigations are needed, but this evidence suggests caution in interpreting ^{13}C records for flowstones.

An annual signal of growth rate and growth rate variability was obtained from ultra-violet microscopic analysis of luminescent banding within speleothems. Banding was demonstrated to be annual by mass spectrometric uranium-series dating, but was only preserved in 10% of all samples. Variability of growth rate for the Holocene Sutherland stalagmite was compared to the theoretical annual variability of growth rate derived from annual variations in the growth rate determining variables observed today, and a good agreement was observed. Furthermore, for one period of growth, a 4-5 year period of rapid growth rate was demonstrated to correlate with the Hekla 3 volcanic eruption in Iceland.

ACKNOWLEDGEMENTS

Work presented in chapter two was improved by critical discussions with David Richards, Chris Proctor and Dave Gordon. Collaboration with Derek Ford and Henry Schwarcz at McMaster University, who provided unpublished data for the regional compilations, greatly improved the cumulative frequency curves.

Correspondence with Wolfgang Dreybrodt at Bremen University helped improve the content of chapter three. Jane Brandt is thanked for providing information on splash effects.

Many fieldwork volunteers made the work in chapter four possible. These include Angus Tillotson, Sam Stratham, Andy Farrant, Dawn Lawrence, Tim Davie, Mark Mulligan, Simon Cannell, Stella Matthews, James Bracey, Ro Charlton and Chris Proctor. In particular, Angus Tillotson provided initial information on the mine sites, and Andy Farrant introduced me to the world of caving. Fieldwork in Kent's Cavern was made possible with the permission of Kent's Cavern Showcaves.

The work in chapter five would not have been possible without the facilities provided by Larry Edwards at the University of Minnesota. Thanks to David Richards, Warren Beck, John Hoff and Sarah Gray for help in my mass spectrometry training; also Christina Gallup, Yemane Asmerom, Greg Gratton and Peter Jansson for accommodation. Emi Ito provided facilities for the carbon isotope analyses and had an excellent taste in tea. Thanks also to Reed McEwan for explaining how to use a carbon line and for running samples. The flowstone sample from Stumps Cross Caverns was collected with the permission of Gordon Hanley at the showcave.

Derek Ford and Yavor Shopov at McMaster University provided initial encouragement in the field of luminescence banding. The work presented here would not have been possible without the help of Tony Philpott for his photographic expertise, Mark Cheshire at the University Safety Office for providing the ultra-violet microscope facilities, and Chris Kidd for help with digitising. Chris Proctor and Sian Davies helped in the fruitless fieldwork search for recent banded speleothems.

This project was funded by a NERC studentship to Pete Smart. In particular, their continued support of travel to both the U.S.A. and Canada is gratefully acknowledged. Thanks also to Larry Edwards, who funded one trip to the U.S.A.

Special thanks to all those who helped me through the three years. In particular, Mike, Jane, Dawn, Rupert, Sian and the Indian Food Centre for some happy times in Horfield; and my parents, who helped me through a difficult period. This thesis has been completed despite being present in Brownes Folly Mine as there was a roof fall (thanks to Tim Davie for sticking it out), getting injured on a solo fieldwork trip (thanks to the farmer at Manor Farm, Charterhouse for getting me to hospital), and seeing an engine blow-up over Iceland while flying to Minnesota.

Pete Smart provided guidance, encouragement and generous quantities of beers throughout the three years.

This thesis is dedicated to my grandfather, Alfred Baker.

This thesis is the original work of the candidate except where acknowledgement is given and has not been submitted for a higher degree in this or any other University.

Andy Baker

October 1993

SUMMARY OF CONTENTS

DETAILED CONTENTS

LIST OF TABLES

LIST OF FIGURES

LIST OF PLATES

CHAPTER ONE

INTRODUCTION

1.1 Palaeoclimate Studies

"Geologic data provide a surprisingly rich set of results that enable us to peer into the future with some level of insight concerning the consequences of a greenhouse warming. ... The magnitude and rate of warming could be comparable to or exceed any that has occurred in earth history." conclusion of Crowley and North (1991), p261.

Palaeoclimate change can provide us with important insights into the mechanisms behind potential future climatic fluctuations. In particular, global climate models (GCMs), which aim to predict future climate change, are extrapolating into a future for which parallel conditions may not exist today. Modelling the climate change over the last glacial-interglacial cycle, for which severe changes in temperature and precipitation have occurred, allow scientists to obtain a measure of the accuracy of the GCM climate change predictions. Two major collaborative palaeoclimate GCM projects have been run for the last 20 ka (CLIMAP, 1976; 1981; 1984; and COHMAP, 1988), with varying degrees of success. Table 1.1 shows the areas of best agreement between these models and the empirical palaeoclimate evidence, and shows that for many regions and times, the models do not perform well. This may be due to deficiencies in our ability to model physical processes, but better records of palaeoclimate change would also lead to better GCM performance and prediction.

"Palaeo-Modelling Scorecard"

Region and Time		*Model-Data Agreement*
N. High-Latitude	(18 ka)	Very Good
Low-Latitude	(18 ka)	Poor
Low-Latitude	(9 ka)	Very Good
S. High-Latitude	(18 ka)	Fair
Ocean Circulation	(18 ka)	Insufficient Work

Table 1.1. Status of model-data agreements for various time and space slices over the last 20,000 years. (From Crowley and North (1991); after Crowley (1989)).

Theoretical models of the changes in palaeoclimate have also been developed, and also depend on empirical records of palaeoclimate change. These theoretical approaches have been constantly revised as improved palaeoclimate records have become available. Original models were based on changes in solar insolation reaching the earth due to orbital forcing, which was proposed to predict the timing of the Quaternary glaciations (figure 1.1) (Milankovitch, 1941). The effect of this forcing mechanism has been preserved in the ocean sediment foraminifera ^{18}O isotope record, which has in turn been demonstrated to give a record of changes in global ice volume (Shackleton, 1977; Shackleton and Opdyke, 1973; Martinson et al, 1987; figure 1.1). More recently, more detailed palaeoclimate records have shown that the relationship between solar insolation, ice volume and palaeoclimate change is not simple, containing feedback mechanisms which could potentially cause catastrophic changes in climate. In particular, glacial meltwater flows have been proposed to cut off Atlantic deep water circulation (Broecker et al, 1988), causing rapid cooling of the globe during the Younger Dryas (≈ 10 ka) and perhaps at 6 other times during the last 700 ka (Sarnthein and Tiedeman, 1990). However, subsequent coral reef evidence suggested that meltwater input actually decreased during the Younger Dryas period of cooling (Fairbanks, 1989), and thus glacial meltwater could not cause the cooling. A new theory based upon a salt oscillator was proposed as a suitable mechanism causing deep water shut-off (Broecker, 1990). However, at the present time, the actual affect of glacial melting on deep water circulation is unclear, with various records from the North Atlantic giving conflicting evidence as to whether deep water flows actually ceased in the Younger Dryas (Lehman and Keigwin, 1992; Veum et al, 1992). Further palaeoclimate evidence will help an improved palaeoclimate theory to be developed, linking changes in ocean and atmospheric circulation, ice volume and insolation.

Many sources of empirical evidence for palaeoclimate change have been used both as a basis for the CLIMAP and COHMAP studies and in other studies but these often have considerable shortcomings. Improvements in GCM performance and the development of theoretical models will only come from the investigation of other palaeoclimate records. In particular, these should contain information which is:

a) Precisely dated. In particular, absolute dating techniques (^{14}C, uranium-series) are preferable to incremental techniques (ice-layers, tree-rings) which are preferable to age equivalence techniques (palaeomagnetism, pollen zones).

b) They should contain absolute rather than relative information on palaeoclimate change. For example, absolute measures of climate change from isotopic data (temperature derived from ^{18}O isotopes in the ice cores) are better than those

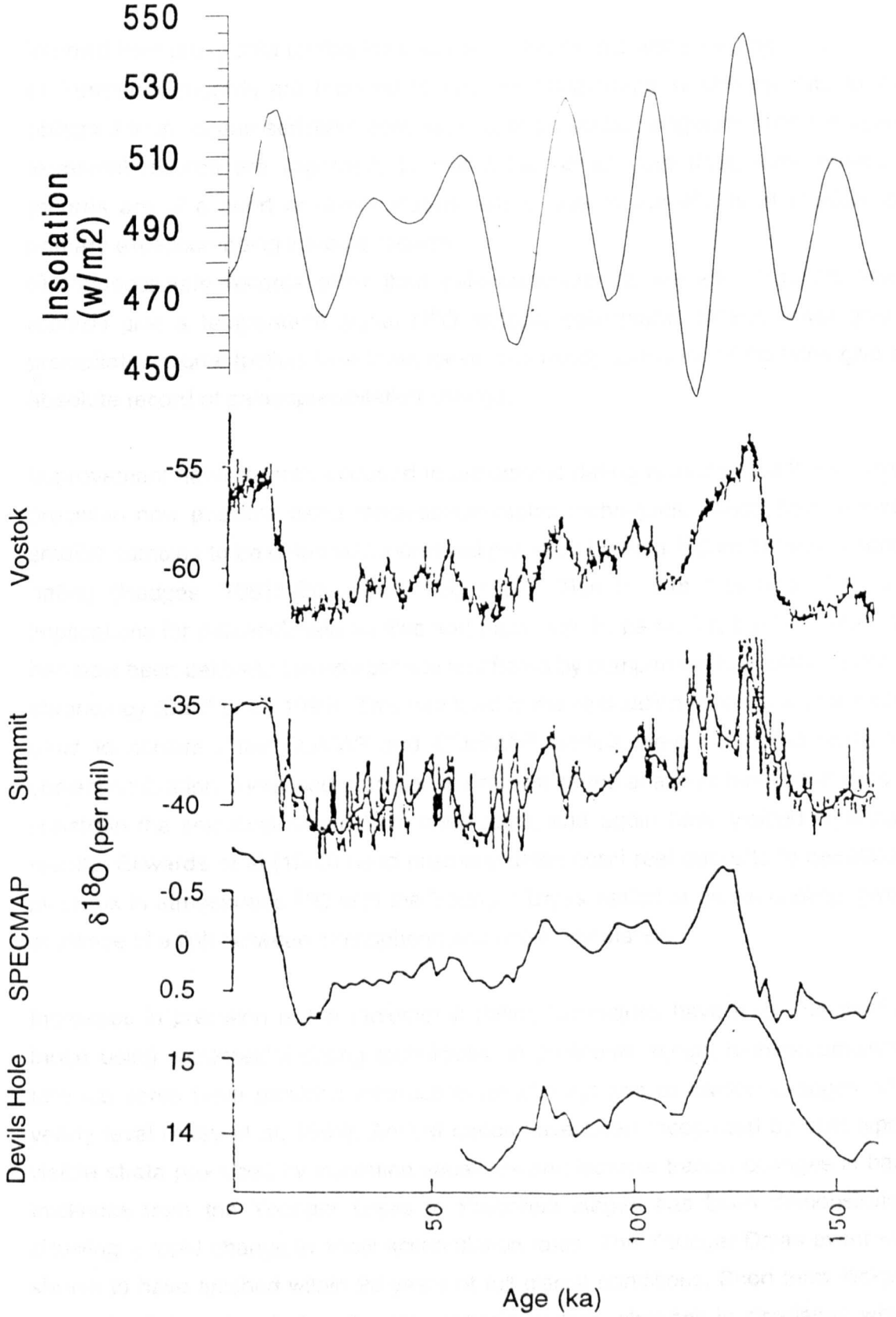

Figure 1.1. Comparison of solar insolation for July, 60 °N, and oxygen isotope records. The insolation record is from Berger and Loutre (1991); the other records are from the Vostok and Summit ice cores (Lorius et al, 1987; Dansgaard et al, 1993); the marine oxygen isotope record (Martinson et al, 1987) and the Devils Hole vein calcite (Winograd et al, 1992).

inferred from proxy data (global ice volume) or relative records (tree-ring width).
c) Terrestrial records are required to provide complementary climate data to that obtained from ocean sediment core studies. In particular, long-term (10^5-10^6 years) terrestrial records are important, to match the ocean core data. Most terrestrial records are of a short or discontinuous nature, due to the effects of erosion, the primary exception being ice-core records.
d) Palaeoclimate records other than palaeotemperature are also required. Many records give a temperature signal (^{18}O isotope, coleoptera, pollen), fewer give a precipitation signal (pollen, lake level, loess, tree rings), and none of the latter give an absolute record of palaeoprecipitation change.

Improvement have recently occurred in radiometric dating techniques with increased precision now possible using mass-spectrometric techniques. These have allowed smaller samples to be dated with increased precision by both ^{14}C and uranium series dating (Hedges, 1981; Edwards et al, 1987). This in turn has had significant implications for palaeoclimate studies and modelling. In particular, the ^{14}C timescale has now been calibrated to an absolute timeframe by comparison to a uranium-series chronology (Bard et al, 1990). This had lead to the realisation that many of the sites used to constrain the CLIMAP and COHMAP models were not dated using the correct calibration. Increased precision in uranium series analyses have been used to constrain the sea-level record from coral reefs, and again have yielded significant results. Edwards et al (1993) used precisely dated coral reef deposits to correlate a plateaux in atmospheric ^{14}C with the Younger Dryas period of global cooling, giving evidence of a link between atmospheric and ocean circulation.

Increases in precision of the radiometric dating techniques have been matched by those using incremental dating techniques. In particular, recent high accumulation rate ice cores have provided information on atmospheric circulation changes on a yearly level (Alley et al, 1993). Annual bands have been recognised by dust types, visible strata produced by insolation variations and isotopic traces; changes in band thickness from the Younger Dryas to Preboreal stages has been demonstrated, showing a rapid change in snow accumulation rates. The Younger Dryas event was shown to have finished within 20 years of full glacial conditions. Short term 'flickers' have also been identified in the atmospheric system; changes in circulation which occurred on a 5-20 year interval for at least the last 50 ka (Taylor et al, 1993). Recognised by variations in the dust content in an ice core, these also suggest rapid reorganisations of atmospheric circulation. Continuing research into these events will provide further understanding into climate change phenomenon.

The availability of new terrestrial palaeoclimate records in recent years has provided a base for the challenging of some of the conventional theories of climate change. Long ice core records have been obtained from Antarctica and Greenland (Dansgaard et al, 1982; Lorius et al, 1985; Dansgaard et al, 1993; figure 1.1). These have provided a wider range of terrestrial palaeoclimate signals, including temperature from ^{18}O isotopes (Jouzel et al, 1987) and CO_2 variations (Barnola et al, 1987). These have highlighted the differences between terrestrial and marine records; for example, the ^{18}O isotope record shows two bistable modes of atmospheric circulation, either glacial or interglacial, throughout the last 250 ka. More recently, another terrestrial ^{18}O isotope record from a vein calcite has been demonstrated to reflect the record obtained from the ocean cores, but with mass spectrometric uranium series ages showing an offset of 6 ka (Winograd et al, 1992; Ludwig et al, 1992). This has lead to doubts over both the timing of the marine ^{18}O isotope record, the global synchroneity of terrestrial and marine records, the importance of solar forcing and the applicability of uranium series dating to subaqueous vein calcite (Winograd et al, 1992; Edwards and Gallup, 1993; Shackleton, 1993).

This study aims to investigate the potential of a palaeoclimate signal derived from the speleothem record. This is undertaken with respect to the factors presented earlier, namely, that it is a precisely dated terrestrial record which may provide a high resolution palaeoclimate record, including one of precipitation.

1.2 Speleothem Studies

Speleothems have a recognised potential as a source of palaeoclimate information. They are very well preserved in the fossil record, as their location in subaerial caves gives them comparatively more protection than surface deposits from erosion events. Furthermore, they commonly form a geochemically 'closed system', that is, their geochemical constituents are not changed from the day of their formation. Thus if these properties contain any palaeoclimate information, they will be preserved and measurable today. Finally, speleothems can be reliably dated by radiometric dating techniques, the most important of which is uranium-series dating. This allows age determinations to be made for the last 350 ka (using alpha-spectrometry) or 500 ka (using mass spectrometry).

Speleothems were first dated by the uranium-series technique by Rosholt and Antal

(1962), later work was undertaken by Cherdyntsev (1971). Routine implementation of the technique was first performed at McMaster University, Canada, from the mid-1970's (Thompson, 1973; Harmon, 1975; and many others). Alpha-counting of the radioactive decay of ^{238}U to ^{234}U to ^{230}Th allowed ages to be determined with a precision of 5-10% from samples of 20-100 g size. Most recently, mass spectrometric techniques have been developed, which allow the determination of uranium-series ages to a much higher precision (≈ 1%) from samples of under 1 g weight (Edwards et al, 1987). First applied to coral samples, applications to speleothems have just commenced (Li et al, 1989; Dorale et al, 1992; Richards et al, in prep).

Speleothems have long been recognised as valuable sources of palaeoclimate information. Original work undertaken by Hendy (Hendy and Wilson, 1968; Hendy, 1971) demonstrated that an ^{18}O isotope signal may be preserved in the samples when they have been deposited in isotopic equilibrium. This has been investigated in more recent studies (Thompson et al, 1976; Gascoyne et al, 1978), together with the record of the isotopic composition of fluid inclusions within the speleothems, preserved through D/H ratios (Schwarcz et al, 1976; Schwarcz and Younge, 1983). For some samples it has been demonstrated that a palaeotemperature signal may be obtained. Early work also concentrated on the signal contained within the timing of speleothem growth. For samples from regions subjected to sea-level rise, growth hiatuses could be used to define the timing of these events (for example, Bermuda, Harmon et al, 1978; the Bahamas, Gascoyne et al, 1979). Terrestrial samples were also found to grow during periods of climatic improvement (Gascoyne et al, 1983; Hennig et al, 1983; Gordon et al, 1989), suggesting that growth was dependant on climatic conditions. More recent work has investigated the potential palaeoclimate record from trace elements (Gascoyne, 1983), and pollen contained within speleothems (Bastin, 1979; Bastin et al, 1988).

Analysis of speleothems has undergone similar trends in recent years to match those taking place in other fields of palaeoclimate studies. In particular, there is a move towards higher resolution records. Mass spectrometric uranium-series analyses can provide ages of a precision of under 1% from 1 g samples. This has allowed the better constraint of the timing of growth hiatuses (Li et al, 1989). High precision dating can now be used to constrain the equally high resolution ^{18}O isotope, fluid inclusion and trace element records. The former has already been undertaken by Dorale et al (1992), fluid inclusion and trace element work is currently being developed by other workers. Additionally, the recent work on banding within speleothems, which has been proposed to be annual in nature (Shopov et al, 1989),

may raise the precision to an equivalent to that of ice-core records. Future developments in ion-probe techniques may allow the measurement of both trace element and isotope variations on a sub-annual level.

This thesis forms an integral part of the trend towards developing higher precision palaeoclimatic signals from speleothems. In particular, it aims to investigate the potential signal contained within speleothem growth rates. Growth rate information can be obtained routinely from mass spectrometric dates obtained upon the sample; these can also be used to constrain stable isotopic and trace element records. It would be hoped that the future will see such combined studies on individual speleothem providing a comprehensive suite of palaeoclimate information.

1.3 Thesis Aims

This thesis has the simple aim of investigating the palaeoclimate record contained within speleothem growth rate variations. Initial work investigates our understanding of the mechanisms of speleothem growth. This is used as a base to aid interpretation of the palaeoclimate record preserved in the speleothem growth frequency record from different regions of the world (chapter two; part of this chapter has been published elsewhere (Baker et al (1993a)). The sensitivity of speleothem growth to palaeoclimate and other factors is then evaluated using the kinetic growth rate theory of Buhmann and Dreybrodt (1985a) (chapter three). This is undertaken by testing growth rates predicted from theory against actual rates from speleothems growing today (chapter four). Finally, the significance of growth rate variations for speleothems growing over the last glacial-interglacial cycle are assessed using high precision dating techniques, both mass-spectrometric uranium series dating (chapter five) and annual luminescence banding (chapter six; part of which has been published in Baker et al (1993b)). Chapter seven summarises the palaeoclimate signal contained in speleothem growth rate, and points to future applications and research areas.

CHAPTER TWO

SPELEOTHEM GROWTH FREQUENCY AND PALAEOCLIMATE

2.1 Introduction

As introduced in the previous chapter, speleothems provide a wide range of potential palaeoclimatic signals. The most basic of these is that provided solely by the timing of periods of speleothem growth. This record can be used to gain a greater understanding of the mechanisms of speleothem growth, and their relationship to climate change, and is investigated here for several regions of the world which have different climate regimes today. The record of speleothem growth is then used as a basis for more detailed investigations into the relationship between palaeoclimate, speleothem growth phases and speleothem growth rate, developed in chapters 3 to 6.

2.2 Speleothem Growth Mechanisms and Palaeoclimate

The degassing of groundwaters which contain elevated carbon dioxide concentrations is thought to be the most important mechanism for speleothem (and non-hydrothermal spring deposited travertine) deposition, a mechanism which has been well documented elsewhere (Holland et al, 1964; White, 1976; Gordon et al, 1989). The elevated carbon dioxide ion concentration is derived from the high partial pressures of CO_2 in the soil atmosphere, generated by microbial processes and root respiration (Dorr & Munnich, 1986). Other growth mechanisms are possible, for example, due to common-ion effects (Atkinson, 1983), evaporation processes (Harmon et al, 1983), elevated sub-glacial pCO_2 levels (C. Smart, unpublished data) and temperature gradient effects (Dreybrodt, 1981). These mechanisms are considered uncommon, and can potentially be identified by the analysis of the ^{13}C isotopic composition, as explained later.

Many factors effect soil CO_2 concentrations, including soil type, texture and horizon, depth, drainage and exposure, vegetation type, soil flora and fauna (Ford and Williams, 1989, p64). However, the dependence of biotic activity on climate has been suggested as producing a climate related signal in speleothem growth. Temperature and precipitation have been shown to affect plant productivity, and hence soil CO_2. Solar insolation also influences temperature and precipitation through orbital forcing variations, as well as having a direct effect on plant respiration.

These factors are detailed below. If a potential palaeoclimate signal is indicated by speleothem growth, then it will be a complex one, with the relative importance of water supply, temperature, and insolation levels unknown.

a) Temperature. Soil CO_2 production is strongly dependent on soil temperature (Dorr & Munnich, 1989), and elevated soil CO_2 concentrations have been measured for many regions today (Miotke, 1974; Smith and Atkinson, 1976; Woo and March, 1977). In regions of cold climate, with lower CO_2 production levels (Poole and Miller, 1982) and potentially lower soil CO_2 concentrations and a shorter growing season, speleothem growth may be expected to occur for only a small part of the year, or may even become completely inhibited. This sparse speleothem growth is observed in arctic or high alpine regions today.

Although a strong soil CO_2 production rate - temperature relationship is observed, this is not reflected in a soil CO_2 concentration - temperature relationship. Particular stress has been placed on the latter; models were developed to obtain a global empirical equation linking soil pCO_2 and temperature (Drake and Wigley, 1975; Drake, 1980), measured by back-calculating from empirical spring and well water pCO_2 data (Harmon et al, 1975; Trainer and Heath, 1976; Smith and Atkinson, 1976). The final form of the models (Drake, 1980; Drake, 1983) accounted for the reduction in bacterial productivity in the soil due to the death of aerobic bacteria as soil pCO_2 increases:

$$pCO_2 = \{ (0.21-pCO_2) / 0.21 \} pCO_2^* \qquad (2\text{-}1)$$

where $\log pCO_2^* = -1.97 + 0.04T$

and T is the mean annual temperature.

The model predicts increasing pCO_2 with temperature, and is shown in figure 2.1. Data which did not fit this empirically based equation at low temperatures was explained to be due to recurrent glaciations replenishing soil zone carbonate in these regions. Fish (1978) and Miller (1982) have criticised the data upon which this empirical relationship is based, arguing that it is unrealistic as it includes only diffuse flow springs; in reality fast flow routes for which equilibrium calcium concentrations may not be reached would obscure the pCO_2 - temperature relationship. Miller (1982) also criticised the open system / glacial till replenishment explanation of divergent data as this could not explain the over prediction of initial soil pCO_2 levels from a few sites in high temperature areas. Finally, the model makes the assumption that spring and well waters can be used as a measure of soil $pC0_2$, when a range of evolution pathways between 'open' or 'closed' systems are possible between the soil atmosphere and the spring sources.

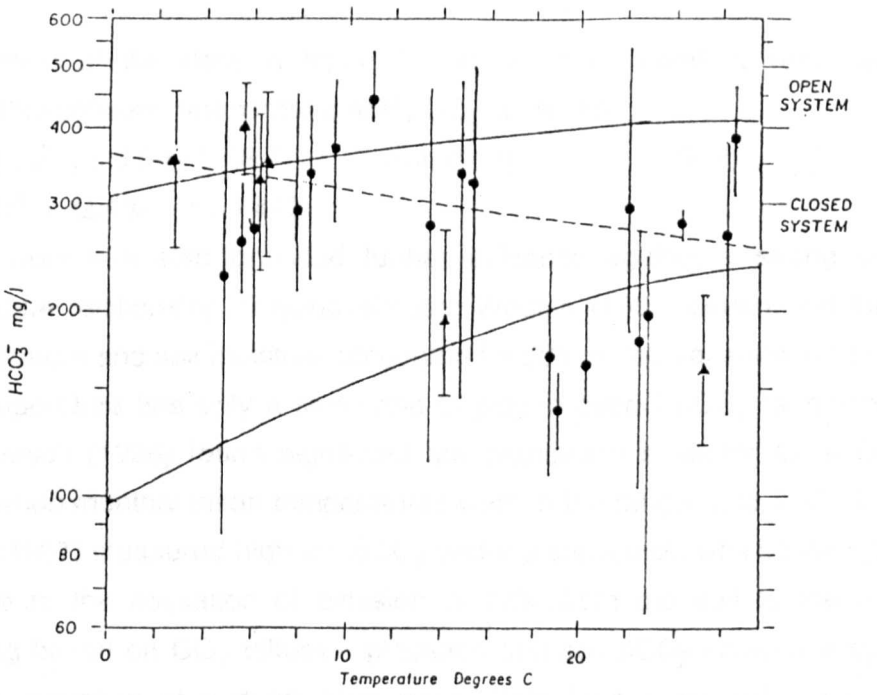

Figure 2.1. Equilibrium HCO_3^- concentrations derived from pCO_2 values at various temperatures from the model of Drake (1980) for both open and closed system evolution (solid lines). Data points represented by dots are from Trainer and Heath (1976), triangles are from other sources quoted in Drake (1980). Open error bars indicate the range, closed bars indicate the standard deviation. The dashed line indicates the regression line for the empirical data.

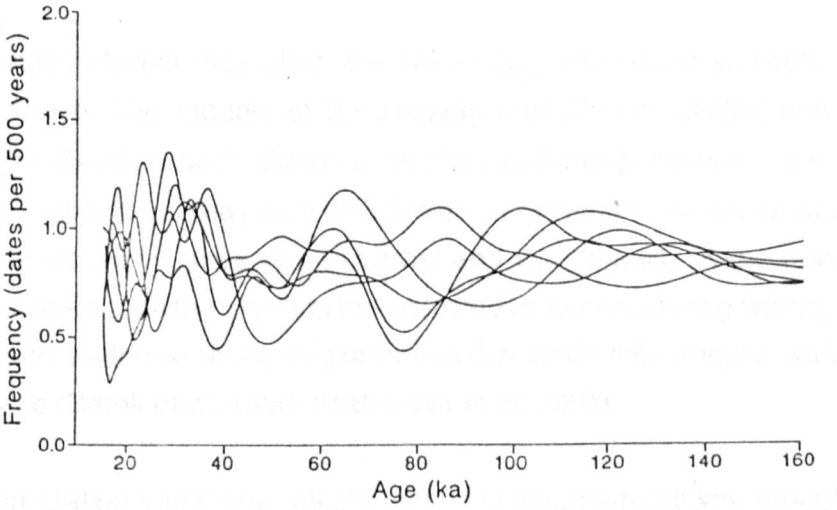

Figure 2.2. Cumulative frequency distribution of 520 randomly generated uranium series ages, using a standard deviation of 0.075 of the age.

Examination of the data in figure 2.1 shows that overall a very weak inverse relationship between temperature and pCO_2 is present:

$$[Ca^{2+}] = 3.59 - 5.38\,T \qquad (mmol\ l^{-1}) \qquad (2\text{-}2)$$

$R^2 = 22.4\%$ $r = -.473$

Recent work has also provided further evidence against a strong soil pCO_2 - temperature relationship. Buyanovsky and Wagner (1983) determined that changes in temperature and soil moisture accounted for 50% of the variation in soil pCO_2, and thus temperature has only a small role to play in overall pCO_2 determination. Dorr and Munnich (1986) found significant soil respiration in winter for a German soil profile, when monthly mean temperatures were in the range -2 to 3 °C. Solomon and Cerling (1987) measured high soil pCO_2 under a snowpack, which they hypothesized was due to the cessation of diffusion of CO_2 from the soil to the atmosphere. Modelling based on CO_2 diffusion predicted that soil pCO_2 could rise by up to x15 with the formation of a deep snow pack. Data from a tropical region (Malaysia) demonstrated soil pCO_2 and dissolved calcium concentrations at the same level to that from temperate regions (Crowther, 1984). Finally, recent finite difference and finite element modelling of soil CO_2 transport and production (Suarez and Simsnek, 1993; Simsnek and Suarez, 1993) has also demonstrated the complexity of factors affecting soil CO_2 production and transport. They showed that temperature, water movement, O_2 concentration and depth below surface all influenced soil pCO_2; and they successfully tested their model results against the data of Buyanovsky and Wagner (1983).

b) Precipitation levels may affect the soil pCO_2, and hence speleothem growth, as detailed above. The models of Buyanovsky and Wagner (1983) and Simsnek and Suarez (1993) have both shown a strong relationship between soil CO_2 and soil moisture. Precipitation may also directly limit speleothem growth, as recharge may be reduced or cease in times of permafrost and ice advance (Kane and Stein, 1984), and speleothem growth may thus be restricted or halted. During warm periods growth may also be limited at times of extreme aridity when little surplus water is available for recharge (Brook et al, 1990; Kashiwaya et al, 1991).

c) Solar insolation variations will also affect speleothem growth through its effect on soil CO_2 concentrations, as increased plant productivity and respiration would be expected with increasing insolation. Whole plant respiration has been shown to be strongly positively correlated with insolation (see review in Amthor, 1989); root respiration has been observed to correlate with photosynthesis (and hence

insolation) for rye-grass, wheat, peas and maize (Hansen and Jensen, 1977; Mahon, 1977; Massimino et al, 1981; Gerbaud et al, 1988), although further experiments are necessary, especially on plants which use the C3 photosynthetic pathway. Insolation variations would also influence temperature and precipitation. King (1973) demonstrated a 25 day shorter frost free season at Eskdalemuir, Scotland, between sunspot maxima and minima, which would lower plant productivity, yet change in surface insolation due to sunspot cyclicity is estimated at only 0.2 W m^{-2} (Kyle et al, 1985), much less than occurs during astronomically forced Milankovitch cycles (40 W m^{-2}). This further complicates any soil pCO_2 - temperature relationship when extrapolated over the Quaternary timescale, as it is not known the extent to which vegetation systems are affected by changes in insolation. Even if a significant soil pCO_2 - temperature relationship did exist today, as suggested by Drake (1980, 1983), it would not be applicable to previous inter-glacials and interstadials, during which insolation maxima were different.

Non-biotic growth mechanisms may also obscure any climate related signal. Several mechanisms have been proposed, but most are distinguishable from biotic sources. Atkinson (1983) proposed that the presence of sulphur in groundwaters, derived from pyrite, may give rise to a common-ion effect which may permit growth when climatic conditions were not suitable, as for instance in the growth of sub-glacial speleothems within Castleguard Cave. However, other mechanisms have also been proposed to explain growth at this site (increased pCO_2 in basal glacial meltwaters; C.Smart, unpublished data). Furthermore, Buhmann and Dreybrodt (1987) found that foreign ions had no significant effect on altering growth rates. Few examples of foreign ion effects have been found elsewhere, probably due to few significant sources of sulphate (gypsum, anhydrate, pyrite), and dolomite. Speleothems formed by evaporative processes may also occur (Harmon et al, 1983), as may those which form solely due to an decrease in temperature between the water source and cave atmosphere, increasing calcite dissolution, and causing speleothem deposition within the cave (the temperature effect; Dreybrodt, 1982). Both of these processes, plus growth due to elevated pCO_2 basal meltwaters and common ion effects, are thought to be distinguishable from conditions when biotic pCO_2 was present by elevated ^{13}C values contained within the calcite (Dreybrodt, 1982; Geyh et al, unpublished data).

Atmospheric CO_2 has a ^{13}C isotopic composition of -6 per mil, whereas soil CO_2 derived from plant respiration has ^{13}C values in the range -26 to -20 per mil for plants using the C3 photosynthetic pathway, and from -16 to -10 per mil for those using the C4 pathway (Cerling, 1984). After fractionation processes, It has been suggested that

these three ^{13}C ranges even after fractionation remain distinguishable in speleothem calcite (Dreybrodt, 1982; Brook et al, 1990). CO_2 derived from a biotic C3 pathway (typical of temperate and arctic plants) would give ^{13}C values in the range -14 to -8 per mil; that from a biotic C4 pathway (typical of plants adapted to severe aridity) in the range -8 to +2 per mil. Speleothems which grew without the presence of a biotic CO_2 source would have a ^{13}C concentration in the range +4 to +10 per mil. However, such elevated ^{13}C levels have only been found in one study of Alpine speleothems (Geyh et al, unpublished data), although subglacial calcite precipitates have also been found to have elevated ^{13}C (Sharp et al, 1990).

The use of $^{13}C/^{12}C$ ratios to determine the source of pCO_2 causing speleothem deposition is developed in chapter 5. It is considered here that non-biotic growth mechanisms are probably uncommon as they have rarely been demonstrated to occur today. If a biotic mechanism dominates, then speleothem growth periods may potentially be used to obtain a palaeoclimate signal, increased levels of growth occurring in periods of increasing warmth and/or precipitation and/or insolation. This signal is now investigated further, by examining the cumulative growth frequency of speleothem deposition for regions of differing climate regimes.

2.3 The Development of the Growth Frequency Technique

The first investigations of the growth frequency of speleothems were made by Gascoyne et al (1983) and Hennig et al (1983). These used a histogram technique to investigate the temporal variability of alpha-spectrometric age determinations from samples from both Yorkshire and on a global basis respectively. However, the techniques used suffered from many drawbacks, as demonstrated by Gordon and Smart (1984) and Gordon (1987). They introduced a cumulative growth frequency method, which summed the distributed error probabilities for all individual age analyses using a 500 year time interval. Similar techniques have also been applied by Geyh (1971) to ^{14}C chronologies; an improved speleothem compilation was presented by Gordon et al (1989) for the United Kingdom, and the technique was later applied to coral reef growth frequencies by Smart and Richards (1992).

Several improvements have been made to the technique in this study, in order to obtain a more accurate record from which a better understanding of the mechanisms of speleothem growth can be obtained. In previous work, screening of the data was undertaken by removing any analyses which showed evidence of contamination (activity ratio of $Th^{230}/Th^{232} < 20$) or of analytical problems (thorium or uranium yield

of less than 10%). Analyses yielding infinite ages were also omitted. However, these compilations failed to correct for systematic variations in calculated ages between different laboratories, due to use of different values for the half life of ^{230}Th. In this study, the dates were recalculated from the isotopic analytical ratios using a single ^{230}Th decay constant of 9.195×10^{-6} a^{-1} (Meadows et al, 1980). The influence this had on the calculated ages varied both between laboratories and within individual laboratories over time. For example, early analyses from McMaster University (Thompson et al, 1976) showed variations of ± 12 ka from the published ages. More recent results were more accurate. A more surprising finding was that for one laboratory (Institute of Geology, Beijing; Shusen et al, 1988), errors were underestimated by up to 50%.

A second problem in previous studies using the cumulative growth frequency approach was the lack of statistical testing undertaken. Rigourous testing of the significance of individual peak and troughs in growth frequency is necessary if there is to be confidence when interpreting the cumulative frequency growth curve in terms of enhanced or restricted speleothem abundance. This can be undertaken by generating random data sets having the same age range and analytical uncertainty as the actual data set; such an approach was previously used in the evaluation of ^{14}C dated sea-level data (Geyh, 1980; Shennan, 1979). Data sets of random ages were generated with standard deviations equal to 0.075 of the age (the average value of the one standard deviation uncertainty of the real alpha-spectrometric dates). Results of 6 such runs for a sample size of 520 analyses is shown in Figure 2.2.

Sets of 40 runs was used to determine the 95% ($\approx 2\sigma$) probability bounds for individual peaks and troughs being generated solely by chance for different size samples. Figure 2.3 compares the 95% confidence levels generated for sample sizes of 40, 80, and 340 dates. It can be seen that as sample size increases, the mean cumulative frequency also increases (as would be expected). The 95% confidence interval for young ages is always the widest, due to the high precision of these analyses which leads to higher variability in the cumulative growth frequency. More importantly it can be seen that for small samples no interpretations can be made for low levels of cumulative growth frequency in the period 0-40 ka. For example, a minimum sample size of 100 analyses is necessary before recognition of low levels of growth associated with isotope stage 2 is possible.

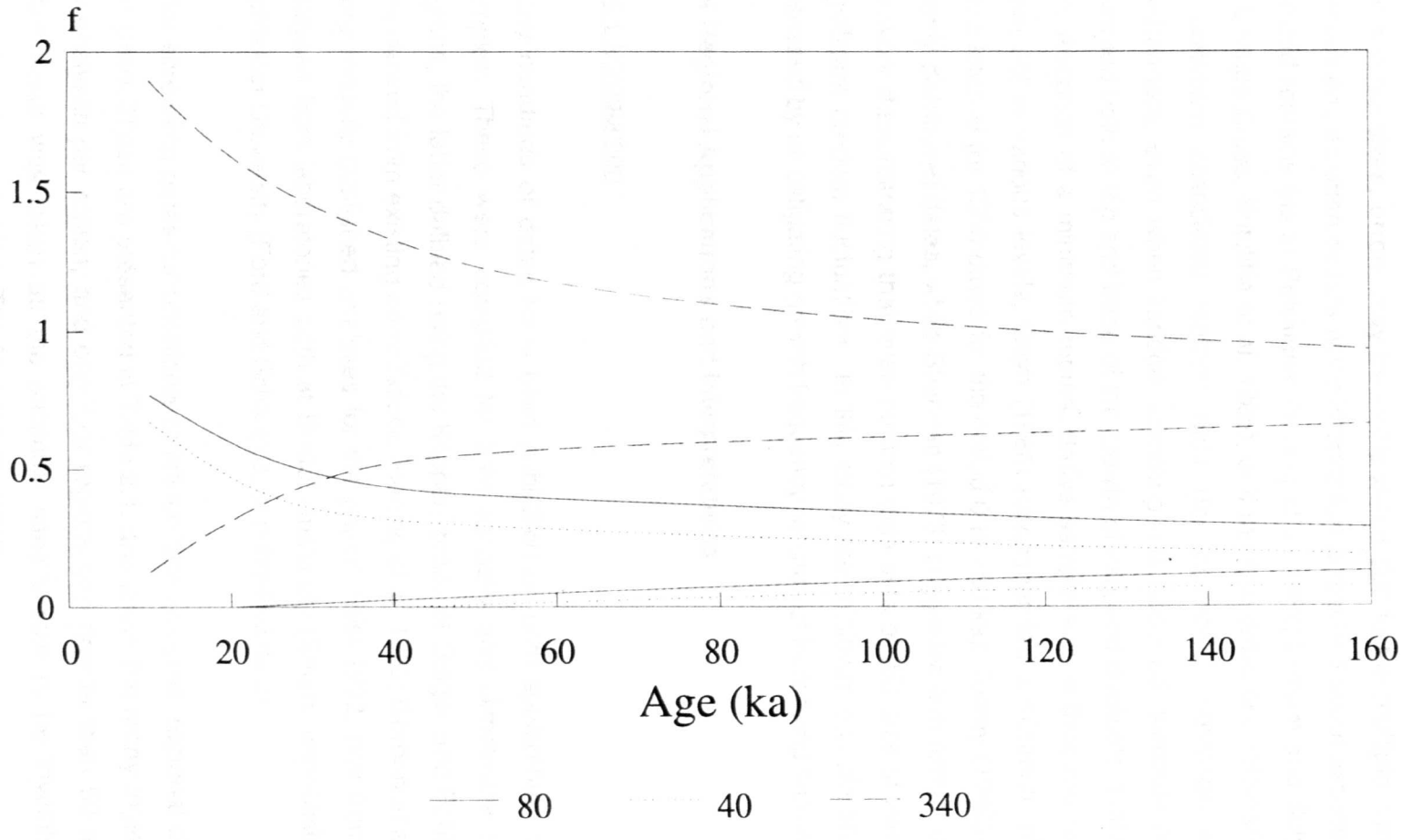

Figure 2.3 Comparison of 95% confidence intervals for random run simulations of 40, 80 and 340 analysis samples

Although the generation of random runs provides us with confidence levels, care must also be taken not to overlook the problem of sampling error. In particular, for low sample sizes, errors may be incorporated due to the multiple sampling of one speleothem, as often occurs when information is required about associated faunal or hominid remains (as at Petralona, Hennig et al, 1982; Latham and Schwarcz, 1992, or Stumps Cross, Sutcliffe et al, 1985), or if multiple dates are obtained on a sample to constrain associated isotopic data (for example; Thompson et al, 1976). Furthermore, even when random sampling has occurred, samples are commonly analysed both at top and base of the growth phase, and duplicate analyses are often run. Adoption of a minimum representative sample size is thus desirable. This has been set at various levels; Geyh (1980) recommended a minimum of 4 dates per class interval (or 1300 dates for the period 0 to 160 ka); Tooley (1982) a total of 400 evenly distributed dates, while Shennan (1979) suggested a minimum of 1000 dates, his work demonstrating that even random data sets of this size showed statistically significant random fluctuations. In this study the minimum sample size required is assessed by investigating growth frequency records of increasing sample size.

2.4 Regional Applications and Interpretations

2.4.1 Introduction

Many hundreds of dates have been published on both speleothem and travertine samples. These were compiled for both spatially and climatically homogeneous regions, the latter defined using the Köppen zones of Geiger and Pohl (1953). Data was derived from existing compilations (Hennig et al, 1983; Gordon et al, 1989), from more recently published analyses for the period 1984-1992, and from unpublished analyses from laboratories both at Bristol University (Smart, unpublished data) and McMaster University (Ford and Schwarcz, unpublished data).

After screening dates for unreliable or infinite age analyses, regional data sets were compiled. These are presented in Table 2.1, and show that many regions had under 40 analyses per region, and only four regions had greater than 60 analyses. This latter value was taken as the minimum sample size to be investigated for the presence of sample bias. The four regions were:

a) Pyrenees (65 analyses). Speleothems came from two sites, Caune de l'Arago and the Grotte Pierre St. Martin, under 100 km apart but at 2000 m altitude difference. The former had 35 dates from only 12 stalagmites associated with bone layers in an

Europe		
U.K.	388	⎫
Belgium	52	⎬ North-West Europe 520
Germany	80	⎭
Pyrennes, France	65	
Picos Mountains, Spain,	37	
Dordogne, France	31	
Baltic states	28	
Greece	22	
Italy	8	
Norway	7	
Alps, France	6	
North America		
Viginia / W. Virginia	68	
Arid USA (Köppen B only)	48	
Minnesota/Iowa	41	
Vancouver / B. Columbia	40	
Mexico (Köppen A only)	13	
Ontario / Quebec	7	
New York State	3	
Missouri	3	
Asia		
China	75	
Israel	20	
Tibet	4	
Russia	2	
India	2	
Others		
Tasmania	43	
South Australia	35	
Mulu	7	
Somalia	8	
New Guinea	6	
Eygpt	3	
Belize	1	

Table 2.1. Size of the regional speleothem data sets, derived from the published literature and unpublished analyses from McMaster University and Bristol University. Only finite, uncontaminated analyses are included, which come from sites not affected by sea-level rise.

archaeological deposit; the latter had no obvious bias in the distribution of speleothems (30 analyses).

b) Atlantic Mid - U.S.A. (68 analyses), all speleothems from Kentucky, Virginia and West Virginia states.

c) China (75 analyses), all speleothem analyses from Guizhou Province and Eastern China.

d) North West Europe (520 analyses), compiled from speleothem and travertine dates from the British Isles, Belgium and Germany.

The Pyrenees region was not analysed because of the probable sampling bias from Caune de l'Arago and the altitudinal differences between the two sites, both probably causing sampling and climatic biases. Compilations from the latter three regions are presented below.

2.4.2 The East Coast U.S.A.

A compilation of 68 speleothem dates was made from the states of Virginia, West Virginia and Kentucky. This region is characterised by a warm, temperate climate (Köppen type Cfa; Köppen and Geiger, 1954); mean annual temperatures are 11-14 °C, with an annual precipitation of 900 mm exceeding evaporation. The region lies outside the glacial maxima limits of the North American ice sheet (Denton and Hughes, 1981). The sources of the analyses used in this compilation are shown in table 2.2.

Source	Number of Analyses
Thompson et al (1976)	28
Harmon (1975)	11
Thompson (1973)	16
D.C. Ford (unpublished)	13
	TOTAL = 68

Table 2.2. Sources of data compiled for the central west coast U.S.A. cumulative frequency curve.

The results of the cumulative frequency curve for a sample size of 70 analyses are shown in figure 2.4a. From the figure it can be seen that the only significant period of speleothem growth occurred between 60 and 80 ka, a surprising result, as this would

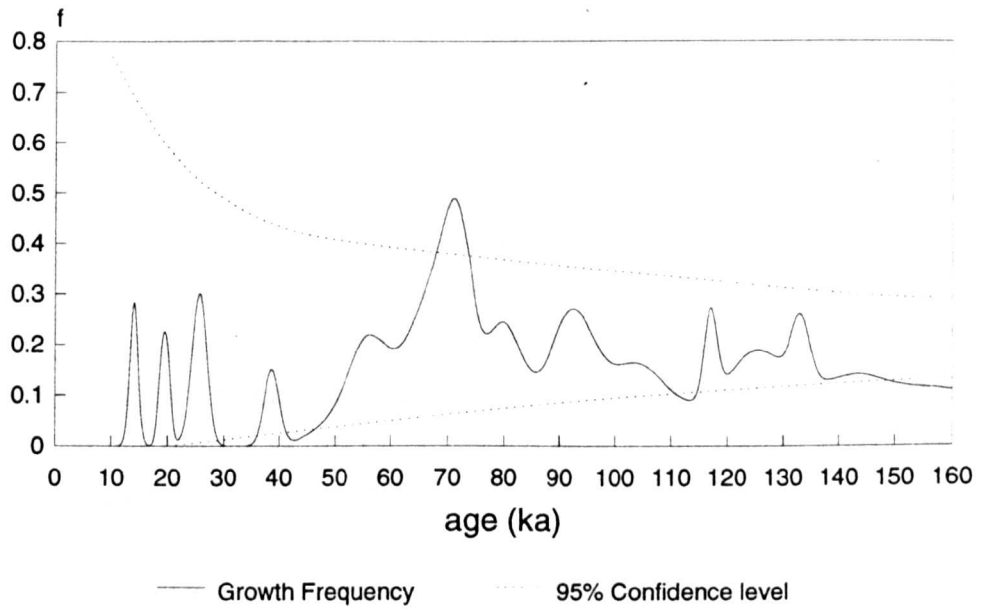

Figure 2.4a. Cumulative growth frequency for 68 analyses.

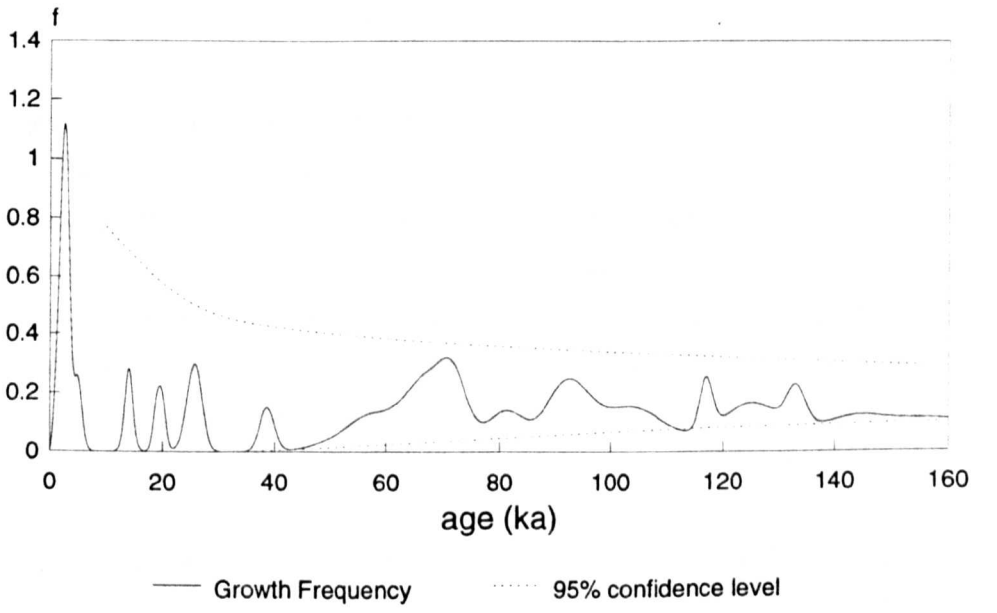

Figure 2.4b. Cumulative frequency after removal of duplicate analyses.

correlate with an isotope stage 4 cool period. Closer analysis of the data set, however, revealed significant sampling error even in a sample of this size. In particular, 26 analyses were obtained from just three samples (NB1, NB5, and GV2 in Thompson, 1976), and 13 of these analyses were in the range 60-80 ka. If duplicate analyses were removed from the data set, 57 dates would remain, with no statistically significant growth periods (figure 2.4b).

This second result has two explanations. One is that the small sample size makes it very possible that sample bias still occurs. The second is that there is a genuine palaeoclimate component to the record. Glacial periods are not reflected in the record, with growth occurring within isotope stages 2, 4 and 6, although all at a statistically insignificant level. This may suggest that both temperatures were above freezing, and that there was a groundwater supply available at these times. The latter requires significant precipitation, which may be confirmed by the record of aeolian deposits in the last glacial maximum, which shows a prevailing wind direction from the north west (Wells, 1983). This would be consistent with the continuing action of the jet stream, 'anchored' by the ice sheet, with low pressure systems intensifying in the region of strong temperature gradient (Crowley and North, 1991, p73). GCM output for the region shows a predicted increase in precipitation minus evaporation of up to 4 mm/day at 18 ka because of this effect (Rind and Peeteet, 1985). Furthermore, glacial maximum temperatures from regions at this latitude show a decline of only 5-10 °C in mean annual temperature. (with a greater decline in winter temperatures) (Crowley and North, 1991, p52-53). This drop in temperature would not be enough to limit speleothem growth.

If a genuine palaeoclimate signal is contained within this cumulative frequency record, then it demonstrates the problem of statistically testing a growth record for a region where no significant changes in growth frequency are expected to occur (also likely for equatorial regions with high levels of insolation, precipitation and temperature). If the growth frequency peaks and troughs all fall within the confidence levels of the technique, then no interpretation of the record can be made, and other techniques are necessary to provide palaeoclimate information (potentially including growth rates; chapter 3).

The significant sampling bias found in this compilation suggests that a sample size of only 60 analyses is too small to provide a reliable growth frequency record. Thus regions of smaller numbers of analyses are not analysed here. The compilation from China, with 75 analyses, is now investigated.

2.4.3 China

2.4.3.1 Introduction

The region considered in this compilation is shown in figure 2.5. It consists of a wide geographical area, but one dominated by the warm temperate climate of eastern China (Köppen classifications Cfa and Cwa; Köppen and Geiger, 1954). Mean annual temperatures vary from 11 °C in the north and east (Shanzi), to 19 °C in the south and west (Guangxi). The whole area is characterised by a strong seasonal variation in temperatures (20-30 °C difference between January and July mean annual temperatures), and also a strong seasonality of precipitation. Between 600 mm and 1100 mm of precipitation falls each year, with most of this concentrated in the monsoon season (June - September). Significant soil moisture deficits occur in winter, with low temperatures and precipitation, whilst flooding is common during the monsoon season.

Uranium series analyses from China were compiled from the work of Shusen et al (1988), and total 75 dates in all. The calculated cumulative frequency curve is shown in figure 2.6, together with the 95% confidence intervals.

2.4.3.2 Interpretation

Correlations with the statistically significant peaks and troughs of the growth frequency record are made with both the orbitally tuned oxygen isotope record (Martinson et al, 1987), and the loess record from China (Liu et al, 1985; Lu et al, 1987; Kukla et al, 1988). The results are shown in table 2.3. and figure 2.7.

No interpretation of the signal is possible in the period 0-25 ka, due to the low number of dates in the compilation. Before this date, several speleothem growth peaks occur within isotope stage 3, only one of which (peak B) is statistically significant. There are no statistically low levels of growth frequency in this isotope stage. Correlations between these growth peaks (A - C) and isotope events are shown in table 2.3. Three further periods of significantly high growth levels occur at 72.5 - 81 ka, 85 - 91 ka and 101 - 102 ka (peaks E to G). These correlate with oxygen isotope events within substages 5a and 5c.

No significantly high or low growth levels can be observed to correlate with oxygen isotope substage 5e, a point which is discussed further below. Significantly low levels of growth occur at 56 - 67 ka (trough D), and correlates with oxygen isotope stage 4.

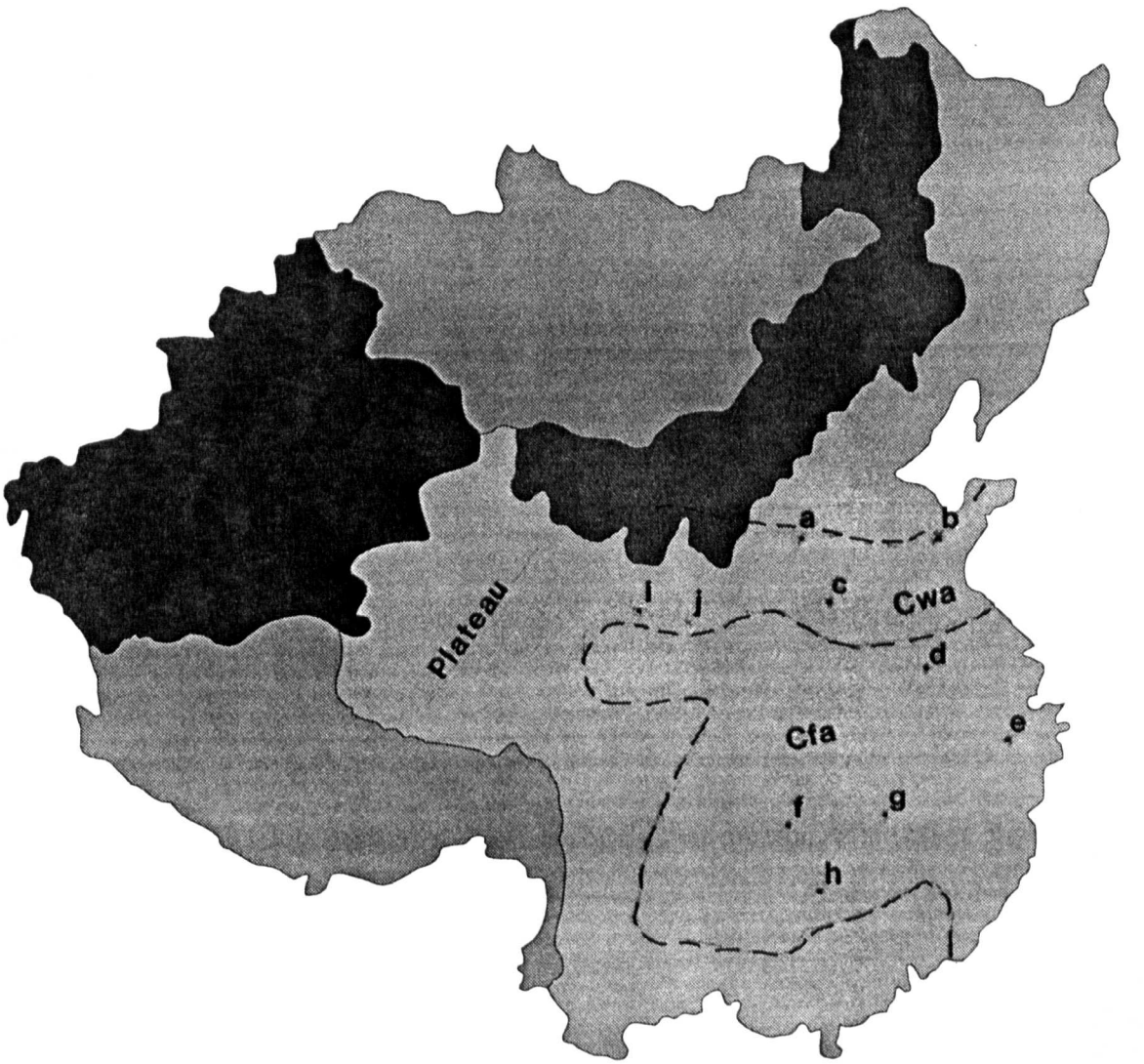

Figure 2.5. China, showing speleothem sampling regions, location of loess profiles mentioned in text and Koppen climatic zones. Speleothems were compiled from: (a) Shanzi, (b) Shandong, (c) Henan, (d) Anhui, (e) Zhejiang, (f) Guizhou, (g) Hunan, (h) Guangxi provinces. Loess magnetic susceptibility records were from profiles at: (i) Lanzhou, (j) Xifeng. The Quinghan-Xizang Plateau is shown in west China; Köppen climate zones by dashed lines.

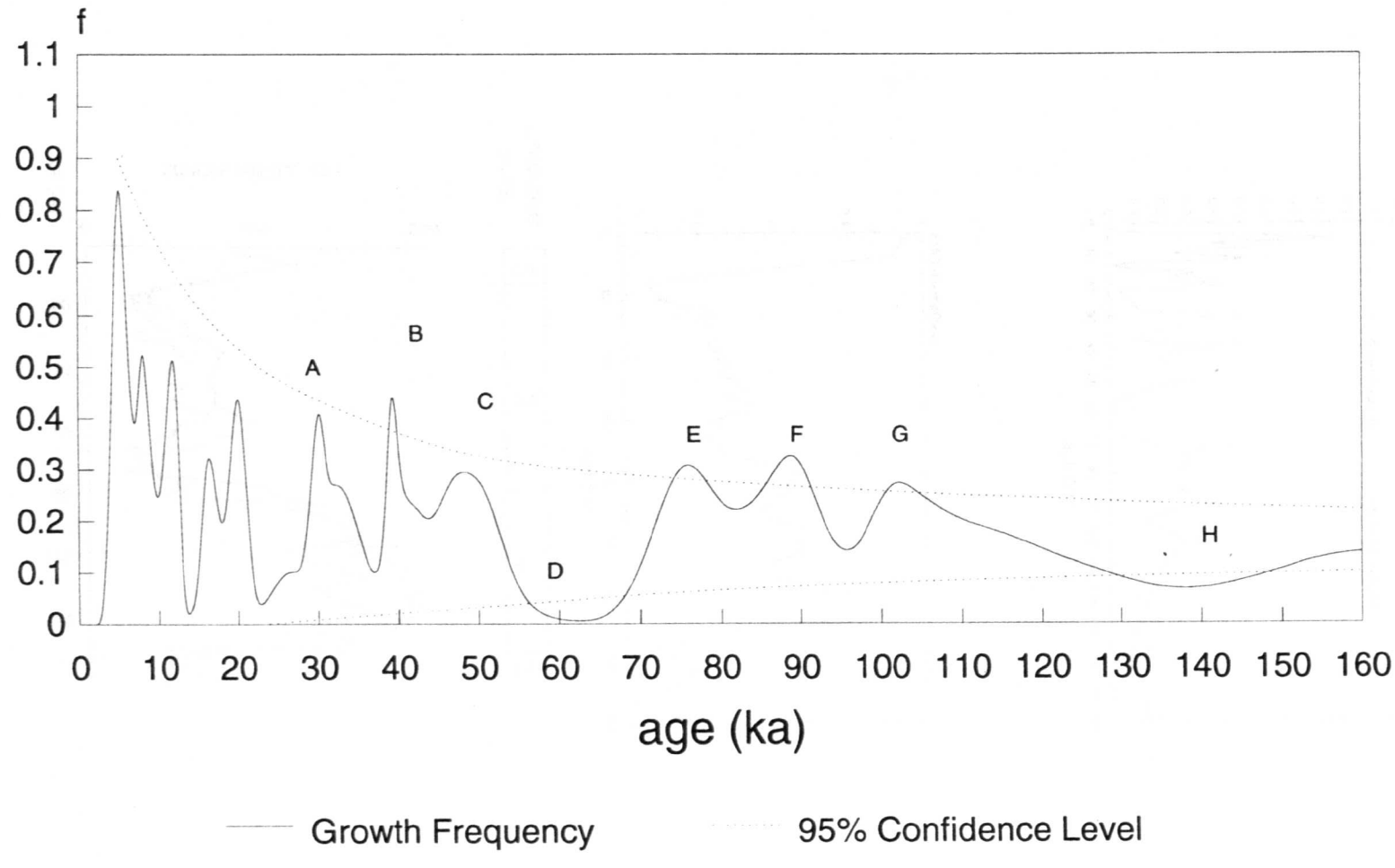

Figure 2.6. Cumulative growth frequency for the China compilation.

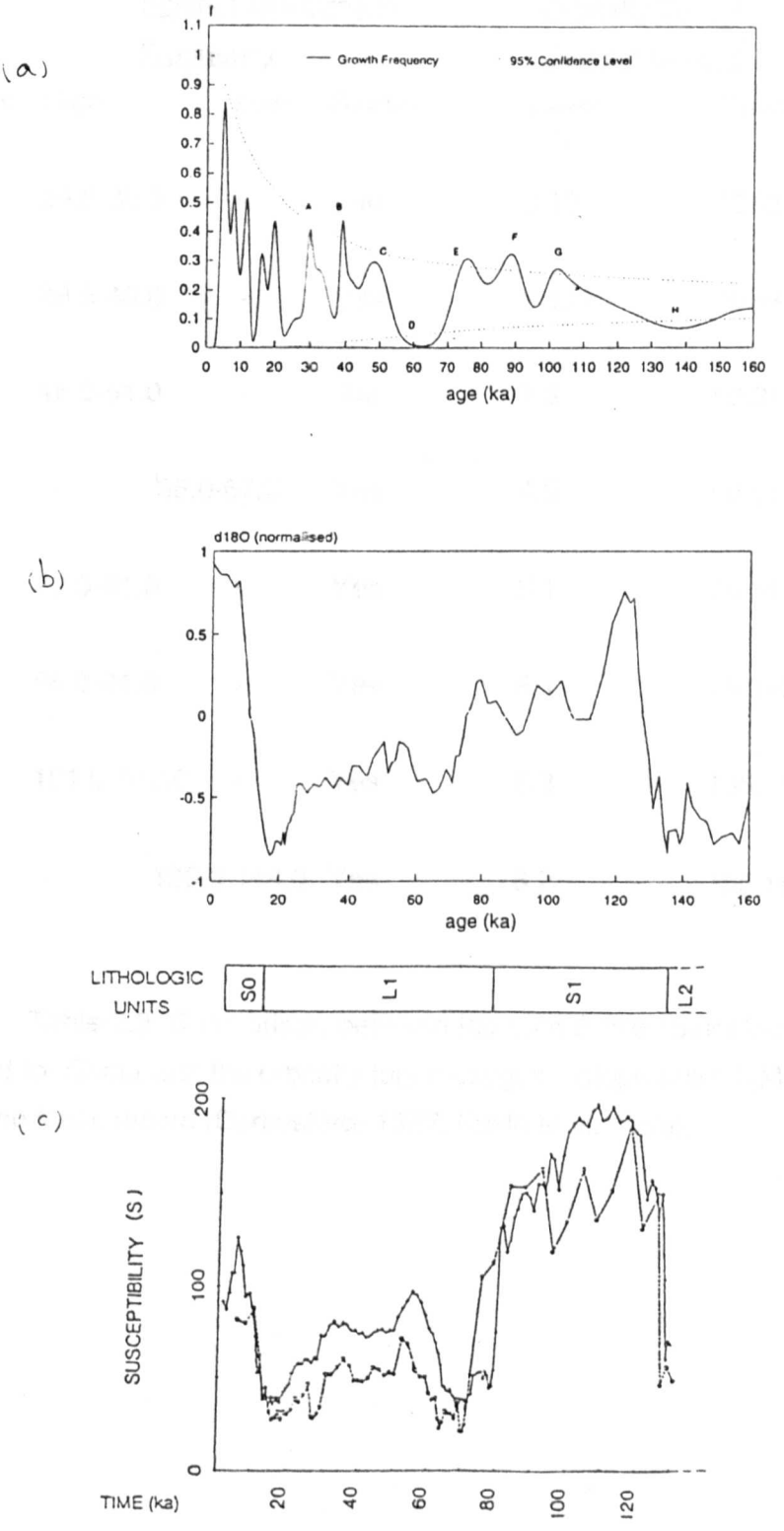

Figure 2.7. Palaeoclimate evidence relevent to the China speleothem record. a. The speleothem growth frequency record. b. The normalised oxygen isotope record from Martinson et al (1987). c. The magnetic susceptibility records from Xifeng (dotted line) and Luochuan (solid line) (Lu et al, 1987).

	Speleothem Growth Frequency			Orbitally Tuned Oxygen Isotope		Loess record
Peak	*High*	*Low*	*Signif?*	*Event*	*Timing*	
A	29.5-30.5	-	No	3.1?	33.0±2.5	L_{1-s}?
B	38.5-40.0	-	Yes	3.13?	40.5±6.5	L_{1-s}?
C	48.0-51.0	-	No	3.3	50.2±3.9	L_{1-s}?
D	-	56.0-67.0	Yes	4.0	60.0±5.6	?
E	72.5-81.0	-	Yes	5.1	79.3±3.6	S1?
F	85.0-91.0	-	Yes	5.1	79.3±3.6	S1
G	101.0-102.0	-	Yes	5.3	105.1±4.2	S1
H	-	129.0-148.0	Yes	6.2	135.1±4.24	L2

Table 2.3. Comparison between the cumulative speleothem growth frequency record for China with the orbitally tuned oxygen isotope record (Martinson et al, 1987) and the loess record (Derbyshire, 1987; Kukla et al, 1988).

Preceding this, the only other significantly low level of growth, at 130 - 148 ka (trough G), correlates with oxygen isotope stage 6; detail within this period is not discernible due to the low precision of analyses at this age.

The speleothem growth signal can be used to further interpret the loess / palaeosol record. Only three periods of palaeosol formation are recognised over the period 0 - 160 ka (Derbyshire, 1987; Kukla, 1987; Kukla et al, 1988). Two, consistent over the whole of the Chinese record, are correlated with isotope stages 1 and 5 (palaeosols S0 and S1). The other, which is only occasionally observed, is assumed to correlate with an improvement in climate within stage 3 (Malan Loess $L_{1\text{-}S}$; Kukla, 1987). The speleothem record, on the other hand, shows many more periods of significant growth, and is precisely dated.

Liu et al (1985) examine the conditions necessary for palaeosol formation. For the Luochuan sequence (for location see figure 2.5), a palaeotemperature and precipitation record was developed from $CaCO_3$ and iron oxide variations. This suggested a mean annual temperature of 12 °C for S1 (stage 5), and between 0 and 3 °C for loess L1. Annual precipitation also declined from 600-700 mm in palaeosol S1 to 200-300 mm within loess L1. The loess data suggests that during speleothem peaks A-C, climate was close to the threshold which would prevent speleothem growth from occurring (sub-zero temperatures and very low precipitation). If the strong seasonality and monsoon nature of the climate persisted within the interstadial periods but outside the insolation maxima, then this would explain the significant growth phases, as precipitation would occur in summer months when temperatures would be above freezing and a high soil pCO_2 likely, allowing speleothem growth to occur. However, little is known about the variation of monsoonal behaviour over time. Prell and Kutzbach (1987) suggest a strong correlation between monsoon intensity and solar insolation maxima. However, the latter are estimated to have occurred within isotope stage 3 at 58 and 32 ka (Berger and Loutre, 1991), which do not coincide with the speleothem peaks A to C. Hence some other explanation must sought for the speleothem record, possible if it provides a more sensitive record of short term changes in climate.

Two periods of statistically significant low growth levels correlate with isotope stage 4, and isotope stage 6 and loess L2. The glacial record is poorly interpreted in China (Derbyshire, 1987). Four major glaciations are recognised at present, although these may actually represent multiple events in reality. It is certain that no one major ice sheet covered the Qinghan-Xizang plateau (figure 2.5), or approached the region

considered here. Of the four glaciations recorded, it would be expected that one of these would be that within isotope stage 6, due to the global severity of this event; if so a consequent decrease in temperature and precipitation in south and east China would explain the low speleothem growth frequency record. The isotope stage 2 glaciation is not visible in this record due to the inability to resolve events before 25 ka in this compilation. However, significantly low levels of growth are observed within stage 4, a similar signal to that obtained in North West Europe (see following section), and possibly reflects an ice advance associated with this isotope stage, or may be a function of sample bias in such a small data set.

A surprising result is the lack of significantly high levels of growth in isotope substage 5e, although speleothem growth does occur at a non-significant level. This could be due to more arid conditions occurring than in substages 5c and 5a, limiting speleothem growth. Kashiyawa et al (1991) suggest that decreased growth levels could occur when temperatures are high due to high soil moisture deficits developing in summer months. However, GCM output for the region for 126 ka predicts both increased temperatures and precipitation (Prell and Kutzbach, 1987), with increased monsoonal activity strongly correlated to increased solar insolation at ≈ 126 ka. Furthermore, palaeosol S1 is correlated with the whole of isotope stage 5; Kukla et al (1988) calculate that palaeosol formation occurred over at least a period of 40 ka, which would cover isotope stages 5e through 5a (assuming a constant rate of soil formation). TL dates upon the palaeosol give ages of 84±10 ka and 110 ka (no error bars quoted) (Nishimura et al, 1984), which do not constrain the palaeosol formation period any further. A sequence at Xifeng (Lu et al, 1987) has been argued to contain a tripartite magnetic susceptibility record within soil S1 (figure 2.7). This would correspond to the three substages, making it very likely to have formed throughout isotope stage 5. However this record is based on very few data points, and is also poorly temporally constrained, and therefore may not necessarily represent all of stage 5. Pollen evidence from the palaeosol does not clarify the situation; pollen within the soil is of a woodland steppe variety, with no climatically demanding species, but mixing effects make it uncertain as to whether this record applies to the whole of stage 5.

These results provide no rationale for the low growth frequency observed in stage 5e from the speleothem record, and the reasons for this therefore remain unknown. Samples which do grow in substage 5e show a wide spatial spread over the whole region considered in the compilation, thus regional variations are unlikely. Dividing the data set into smaller regions is not possible due to the small number of dates

within the compilation. Forming definite conclusions from a growth frequency peak which is statistically insignificant is difficult. An explanation may come from the presence of sampling bias within such a small data set of under 100 dates, with more analyses, growth frequency within sub-stage 5e may increase to significant levels. Also possible is a systematic error in the age determinations from the laboratory; if the cumulative frequency curve of figure 2.6 is lagged by ≈ 20 ka, then it would fit the expected peak pattern of maxima in substages 5a, 5c and 5e. Such an error in age determinations could be caused by incorrect spike calibration; it has already been noted that the errors associated with the age determinations were underestimated by 50%. More precise conclusions can be reached with the analysis of further Chinese speleothem samples.

2.4.3.3 Conclusions

Correlations between the speleothem growth frequency and the loess / palaeosol record are possible, and show differences in the palaeoclimate signal contained within them. Uncertainties contained within the palaeoclimatic interpretation of both sets of data and the low number of analyses in the speleothem growth frequency record mean that precise determination of the causes of this variation are difficult. As a result, further insight into the mechanisms of speleothem growth are limited, with growth generally correlating with warm and / or wet climate phases. The possibility of lower growth in stage 5e due to increased aridity is discussed, but no conclusion can be reached.

2.4.4. The Growth Record for North West Europe

2.4.4.1 Introduction

The geographical area considered in this compilation is shown in Figure 2.8 and is characterised by having been ice-covered or marginal to ice sheets during glacial stages. The present day climate is temperate with rain at all seasons and cool short summers (Köppen climate type Cfb; Köppen and Geiger, 1953). Any spatial variations in temperature that exist within the region today are small compared to the magnitude of climatic variations in the Quaternary. Mean annual temperatures have been estimated to have varied by approximately 15 °C between glacial and interglacial stages (Atkinson et al, 1987).

Data for this compilation (Table 2.4) have been derived from published and unpublished sources, 520 dates in total were compiled using the cumulative growth frequency technique. The resulting curve and statistical testing is shown in figure 2.9.

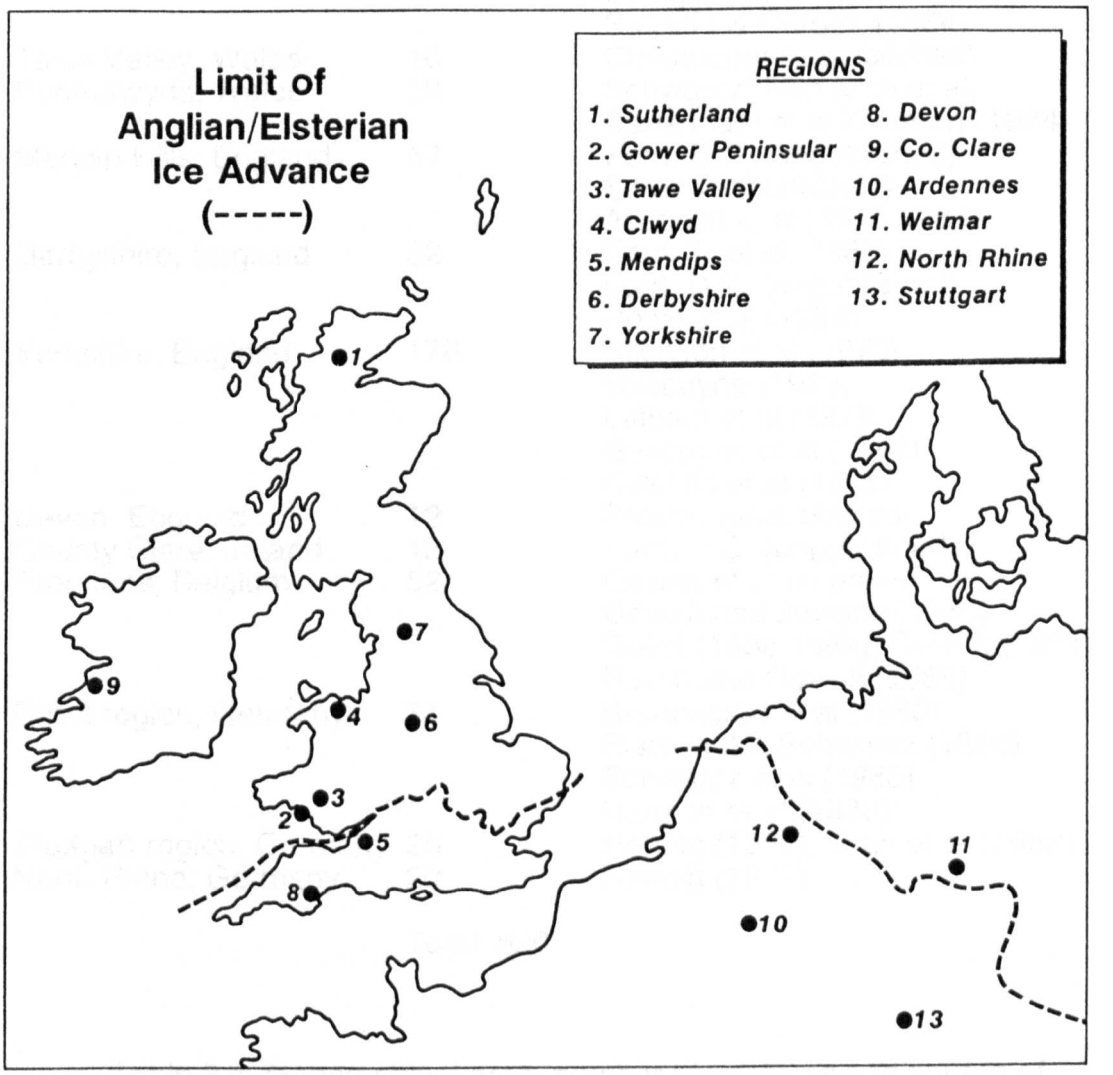

Figure 2.8. Location of karst regions from which samples in the North West Europe compilation were derived.

Location	*Number*	*Source*
Sutherland, Scotland	15	Ford, D.C. (unpublished) Atkinson et al (1986)
Gower, Wales	9	Ford, D.C. (unpublished) Stringer et al (1986) Sutcliffe & Currant (1984)
Tawe Valley, Wales	16	Christopher (unpublished)
Pontnewydd, Wales	39	Schwarcz, Ivanovich et al, Debenham et al in Green (1984)
Mendip Hills, England	57	Ford, D.C. (unpublished) Smart (unpublished) Atkinson et al (1978,1984)
Derbyshire, England	52	Ford, T. et al (1983) Ford, D.C. (unpublished) Rowe et al (1989)
Yorkshire, England	176	Atkinson et al (1978) Gascoyne (1979) Latham et al (1979) Gascoyne et al (1983) Sutcliffe et al (1985)
Devon, England	12	Proctor (unpublished)
County Clare, Ireland	12	Ford, D.C. (unpublished)
Ardennes, Belgium	52	Gewelt et al (in press) Gewelt and Juvigne (1986) Quinif (1986,1989), Gewelt (1985) Bastin and Gewelt (1986)
Erfurt region, Germany	34	Brunnacker et al (1983) Blackwell & Schwarcz (1986) Schwarcz et al (1988) Harmon et al (1980)
Stuttgart region, Germany	26	Hennig (1979), Grun et al (1982)
North Rhine, Germany	20	Hennig (1979)
	Total: 520	

Table 2.4. Geographical area, number of analyses and source of uranium series ages on secondary carbonate deposits included in the compilation for North-West Europe.

Many periods of significant growth frequency levels are visible. These are interpreted on both a chronological and palaeoclimatic basis.

2.4.4.2 Chronological Interpretation

The cumulative growth frequency record is compared with the orbitally tuned oxygen-isotope chronology of Martinson et al (1987) (figure 2.9, table 2.5) to see if growth phases can be used to define the timing of warm (enhanced growth) and cold (limited growth) periods by taking the timing of the peaks and troughs as a simple binary signal. For isotope stage 5, comparisons with the oxygen-isotope record use the generally used sub-stages as defined by Shackleton (1969) are employed, while in stages 2 to 4 the comparisons are made with isotope events as defined by Pisias et al (1984).

Initial very high levels of growth frequency (A on Figure 2.9) correlate with the Holocene interglacial, the large number of dates under this peak create a tail, adversely affecting the timing of the isotope stage 2 minima (event 2.2; trough B). Peak C, although not statistically significant, provides evidence of an improvement in climate and probably correlates with event 3.1. Peaks D, F1 and F2 give a good correlation with events 3.13, 3.3 and 3.31. The double peak structure of peak F is significant; the runs of random dates generated double peaks in fewer than 10% of all cases. The presence of these in the cumulative frequency curve is therefore unlikely to be due to random fluctuations, and the F1/F2 doublet is probably real. The significantly low level of growth at trough E does not correlate with any recognisable event in the orbitally tuned oxygen isotope chronology, but does correlate with a cool and arid period in the Grande Pile pollen record (Figure 2.9), a point discussed later. In stage 5, peak H and trough I could correlate with the isotope sub-stages 5a and 5b, or alternatively be fluctuations within stage 4. The multiple peaks J1-3 thus could either contain the whole of stage 5, or alternatively just substages 5c to 5e, a debate developed in the next section. Peaks J1 - J3 can not be adequately differentiated; this may be due to favourable palaeoclimatic conditions throughout this period; more probably it is due to the large counting errors associated with analyses of this age (typically 5-10% at 110 ka), which obscures any possible reductions in growth frequency.

The growth frequency record has a reliable and internally consistent radiometric time-base, and thus provides a useful alternative to the orbitally tuned oxygen isotope record which is widely used as a general Quaternary timescale. The record appears to give a good correlation with the oxygen isotope record, suggesting that it contains

Isotope		Orbital Tuned $\delta^{18}O$ Isotope	Coral Reef	Secondary Carbonate Growth Periods		
Stage	*Event*			*Peak*	*Timing*	*95% significant?*
2	2.2	17.9±1.4	-	B	22-27	Yes (-)
	3.1	25.4±5.9	33.0±2.5	C	28-31	Yes (-)
	3.13	43.9±4.7	40.5±6.5	D	35-42	No
3	-	-	-	E	44-46	Yes (-)
	3.3	50.2±3.9	50.0±2.0	F1	49-56	Yes (+)
	3.31	55.5±5.0	62.5±6.0	F2	56-62	Yes (+)
4	4.22	65.2±6.1	- ⎫			
	4.23	68.8±4.2	- ⎬	G	63-71	Yes (-)
	4.24	70.8±4.0	- ⎭			
			⎧	H	72-78	No
	5.1	79.3±3.6	81.5±5.5 ⎨	I	79-81	Yes (-)
			⎩	J1	87-98	Yes (+)
5	5.33	103.3±3.4	102.5±2.5	J2	98-115	Yes (+)
	5.5	123.8±2.6	122±15.0	J3	115-133	Yes (+)

Table 2.5. Timing of isotope stages from different chronological records. Oxygen isotope dates from Martinson et al (1987), coral reef uranium series ages from Smart and Richards (1992). Statistical significance of growth record shown, + and - indicating significantly low and high levels respectively. For reasoning behind correlations see text.

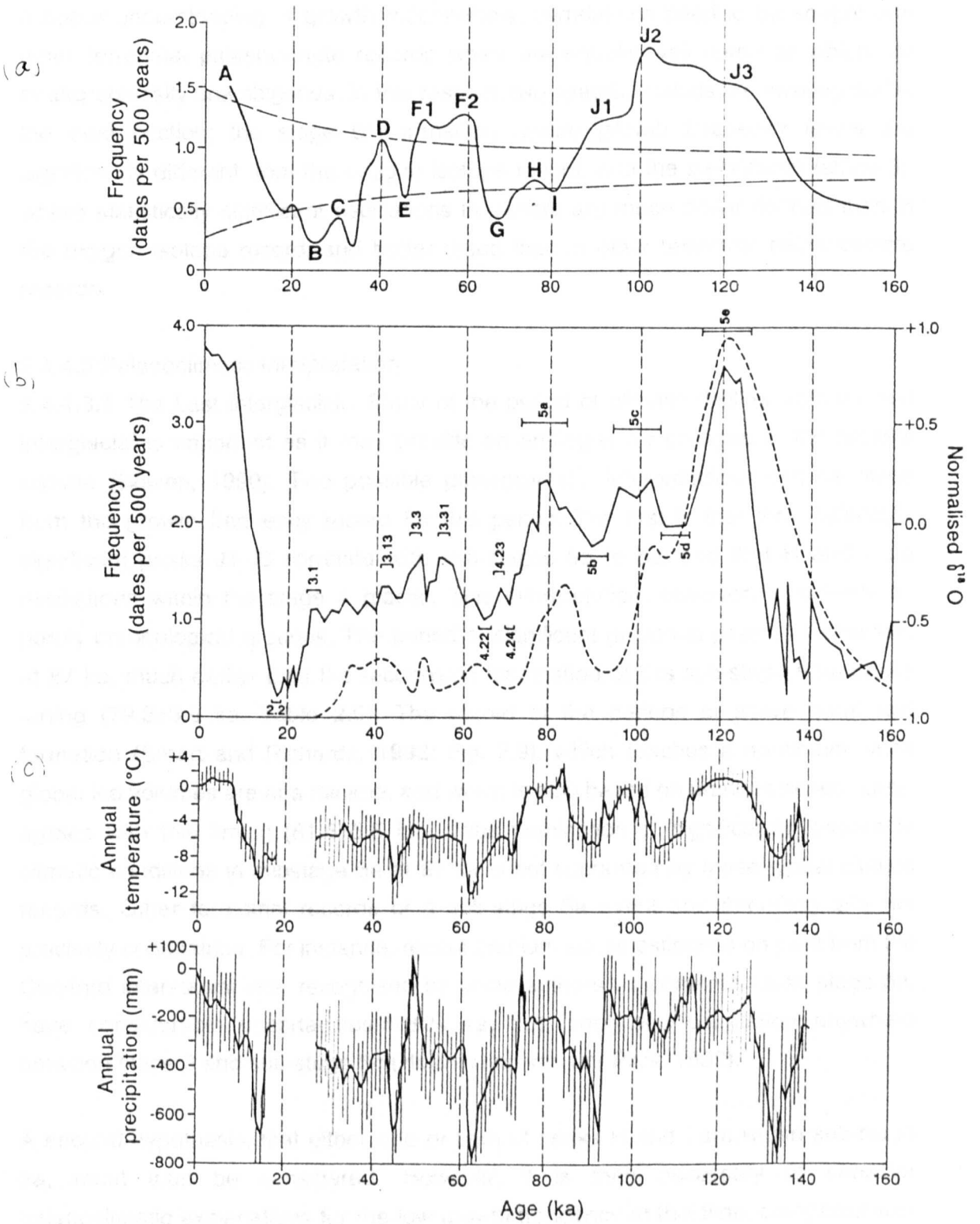

Figure 2.9. Comparison of palaeoclimatic records for the period 0-160 ka. a. The secondary carbonate growth record. b. Oxygen isotope record (Martinson et al, 1987; events from Pisias et al, 1984) and coral growth frequency (Smart and Richards, 1992). c. Grande Pile pollen record of temperature and precipitation deviations from present (Guiot et al, 1989)

a palaeoclimate signal. However, precise interpretation of this signal is difficult due to the dependence of growth on both warm and / or wet conditions for growth. To obtain a better understanding of growth mechanisms, correlations need to be sought with other terrestrial palaeoclimate records which are equally well dated or which are stratigraphically unambiguous. In this respect, two specific periods are investigated in the next section; the stage 5/4 transition, where growth frequency levels are significantly different from the oxygen isotope record, and the pleniglacial (stage 3), where statistically significant oscillations in climate are much better defined than in the oxygen isotope record, and better dated than in other terrestrial palaeoclimate records.

2.4.4.3 Palaeoclimatic Interpretation

2.4.4.3.1 The Last Interglacial. Study of the period of climatic decline from the last interglacial is important as it may provide an analogue for changes in the present climate (Bowen, 1990). Two possible palaeoclimatic interpretations can be made from the growth frequency record for this period. The first is that the statistically significant peaks J1-J3 correlate with sub-stages 5a to 5e, and that H and I are oscillations within the stage 4 glacial. This interpretation, however, is unlikely on purely chronological grounds. The period of significant growth at peak J1 terminates at 87 ka, much earlier than the recognised termination of this sub-stage from orbital tuning (79.3±3.6 ka; Table 2.5). The record of the periods of active coral reef formation (Smart and Richards, 1992; Fig. 2.9), which reaches a maximum when global ice volumes are at a minima, and which is also based on uranium series dates, agrees with this timing (81.5±5.5 ka). Thus termination of significantly favourable climatic conditions in substage 5a at 87 ka is not supported by these global climate records. Other terrestrial records of a sub-stage 5a event are chronologically not precisely constrained. For instance, recent uranium series estimates on peat from the Chelford interstadial site, recognised by some authors as correlated with stage 5a, have considerable uncertainties(86±24 ka; 1σ), permitting correlation anywhere between stage 3 and sub-stage 5c (Heijinis and van der Plick, 1992).

A second hypothesis, that either one or both of peaks H and I are within sub-stage 5a, must thus be considered. However, it is then necessary to consider palaeoclimatic explanations for the low growth frequency at this time, compared with earlier stage 5 warm periods (Figure 2.9). Such an explanation could either be related to a decrease in temperature or an increase in aridity. The palaeotemperature record from pollen in North West Europe suggests that isotope stage 5 had three periods of interglacial or interstadial character; the British Ipswichian and European

Eemian (sub-stage 5e), followed by the European Brorup (sub-stage 5c) and Odderade (sub-stage 5a). The Brorup is actually bipartite, being divided into the Dutch Brorup and Amersfoort interstadials, separated by a cooler period (Zagwijn, 1990). The record at Grande Pile (Guiot et al, 1989; Figure 2.9) does not show the Eemian to be significantly warmer than the subsequent interstadials. Conversely, Zagwijn (1990) observes a more northerly limit of *Abies* in the Eemian in north west Europe than in the Brorup or Odderade, and the evidence from British pollen records supports this suggestion with the presence of *Acer monsperssulanum* at several Ipswichian sites including Stone and Trafalgar Square (Godwin, 1975, p171). Cooling of the sub-stage 5a palaeoclimate compared to that in 5c is not evident either in the German pollen record (Gr ger, 1990; Behre, 1989), where a mean July temperature of perhaps 13-15 °C for sub-stages 5a and 5c is postulated, or in the record from Grande Pile (Guiot et al, 1989).

The oxygen isotope record, figure 2.9 from Martinson et al (1987), suggests from ice volume evidence that the Eemian was warmer than the other two sub-stages. This is also supported by the presence of a distinctive warm "hippopotamus fauna" in Victoria Cave, Yorkshire, associated speleothem dates range from 135 ± 8.5 to 114 ± 5 ka (Gascoyne et al, 1981; 1983). Some evidence of a deterioration of climate in England at the end of stage 5 is available however, with the presence of a cold fauna including wolverine *(Gulo gulo)* at Stump Cross Caverns, Yorkshire, overlain by speleothem dated to 83 ± 6 ka by alpha-spectrometry (Sutcliffe et al, 1985), and 80 ± 1 ka by mass spectrometry (chapter 5).

Thus the pollen record provides no evidence of a significant difference in temperature between sub-stages 5a and 5c. The faunal record at Stump Cross may signify a cooling of the climate at the end of stage 5a (an earlier timing would be in contradiction with the pollen records presented above), but its age constraint is insufficient to be certain as to its relevance here. Thus we must consider if the decrease in growth frequency during stage 5a could be due to a decrease in precipitation. Unfortunately palaeoprecipitation indicators are not well developed for the fossil record. Kashiwaya et al (1991), in a spectral analysis of speleothem abundance in Britain, suggested that in the period 70-100 ka variation in water abundance was as important for speleothem development as that of temperature. Wind blown sands are evident in many cave sites on the south coast of Britain and could possibly provide an indication of increased aridity although they may simply be a function of sediment availability due to lowering sea-levels. At present they can only be constrained to a post-Ipswichian age at Bacon Hole (Stringer et al, 1986) and

between 110 and 55 ka at Minchin Hole (Proctor, unpublished data). Loess deposits are widespread through the region considered in this compilation, although the ages of many have been determined using thermoluminescence dating, there is still considerable uncertainty as to their accuracy when applied to sediments over 50 ka (Wintle, 1990). A palynological palaeoprecipitation record has been developed by Guiot et al (1989) at Grande Pile. The average annual precipitation estimated for stage 5e is similar to that for stage 5c (≈ 200 mm below present levels), with a relatively minor decrease associated with the intervening cooler stage (figure 2.9). Stage 5a is on average slightly drier (≈ 300 mm below present levels) and is preceded and followed by very arid intervals (although there is less certainty about the 5b aridity, Seret, pers. commun., 1992). This evidence thus supports a suggestion that decreased speleothem and travertine growth in stage 5a is caused by a reduction in effective precipitation.

The increase in aridity in substage 5a could be associated with the preliminary stages of the glacial advance which culminated in stage 4. If the Fennoscandian ice advance commenced during stage 5, this could lead to the development of a semi-permanent high pressure systems over the continent (Spaulding, 1991), which would result in a drier, more continental climate. The very low level of secondary carbonate growth evident in isotope stage 4 (trough G) is certainly an important indication of the subsequent severity of climate. There is also more direct terrestrial evidence for the timing and extent of this glacial advance. Recent thermoluminescence dates on glacial deposits from Denmark and Poland signify ice advances around 60-70 ka (no error bars quoted) (Kronberg, (1988), quoted in Olsen, (1990)); and the most recent TL dates from Danish meltwater deposits have yielded ages in the range 73-75 ± 7 ka (Kronberg and Mejdahl, 1990), confirming an early glaciation. There is also renewed debate over an Early Devensian (stage 4) glaciation in Scotland and North England (Bowen, 1990); although at this time Worsley (1991) contends that the evidence for such an advance is inconclusive.

Therefore, evidence from other palaeoclimate indicators suggests that the decline cumulative growth frequency in sub-stage 5a was due to an increase in aridity, probably due to the initial stages of growth of the Fennoscandian ice sheet which caused development of a more continental climate over much of North West Europe. The decrease in speleothem growth frequency due to this factor shows the importance of water supply in controlling speleothem growth. More detailed work investigating variations in growth rate over this period would be useful in providing

further understanding of growth mechanisms and provide further palaeoclimatic evidence for this time (chapters 3 and 5).

2.4.4.3.2. The Isotope Stage 3 (Pleniglacial) Record. The speleothem and travertine growth frequency record provides a detailed record of climate change in isotope stage 3; other deposits from this period often provide good palaeoclimatic records but have poor chronological control (for example, the coleoptera record of the 'Upton Warren' interstadial gives an excellent temperature record but is constrained only by a minimum radiocarbon ages of ≈ 42 ka (Coope, 1975)). The growth frequency record shows periods of significant climate change which are precisely dated, and can thus be used as a temporal framework into which these other records may be fitted. The record shows two distinct periods of enhanced deposition in the pleniglacial period, from approximately 35 to 42 ka (peak D; event 3.13), and from 49 to 62 ka (peaks F1 and F2; events 3.3 and 3.31), with an intervening period of below average growth (trough E; an undefined event in Pisias et al (1984) and Martinson et al (1987)). This is in agreement with the division of isotope stage 3 into three substages suggested by Pujol and Turon (1986). Statistically, this record indicates significantly warm (wet) 3.3 and 3.31 events, followed by the significantly cool (dry) and short duration undefined event at trough E. This trough corresponds with a cold, dry period in the Grande Pile record, although the very wet period immediately preceding this and corresponding with peak F1 has similar growth frequency to peak F2 which correlates with a drier interval. Further, chronologically less well constrained, evidence of a stage 3 cool and dry period has been found by Ran et al (1990) in the Netherlands, where ice-wedge casts were dated to a minimum age of 36.6 ka, and overly sediments contained pollen of a chionophilous dwarf shrub tundra. If this correlation with the speleothem trough is correct it indicates a mean annual temperature of -2.4 to -6 °C, discontinuous permafrost and relatively dry conditions. Van Vliet-Lanoe (1990) also suggests discontinuous permafrost in North West Europe during this time, although exact timing is unknown. This cool period can not however be found in two more southerly climate records; the pollen record at Les Echets (Guiot et al, 1989) and the mollusc record in loesses at Alsace (Rousseau and Puisségur, 1990). This may indicate a strong north-south climatic gradient, as suggested Pons et al (1990) from the French pollen record, or perhaps a limited duration further south.

The most northern European stage 3 interstadial site with a good temporal constraint is probably the 'Oerel' peat deposit in Germany (Behre, 1989), which directly overlays 3 peat beds correlated with isotope stage 5. This probably correlates with the

significant F1/F2 peaks (events 3.3 / 3.31), its pollen of *Betula nana*, *Salix*, *Juniperus*, *Calluna* and *Empetrum* indicating a treeless shrub tundra with moist conditions. Placing other interstadial sites is more problematic; Behre (1989) notes that the Dutch sites of Moershoofd, Hengelo and Denekamp may not even be inter-stadial in character since the presence of peat bogs in itself is not a climatic indicator because they can form solely due to geomorphic factors. Their chronological positioning based on radiocarbon dates is also not justified as the technique is at the limit of its dating range and the published dates from the three sites form a continuous scatter rather than individual peaks (see graph in Zagwijn, 1983). The Upton Warren interstadial possibly correlates with the period 49-59 ka (peaks F1/F2), but again a better time constraint of this site is necessary. The growth frequency record also shows a very limited growth period at about 29 ka (peak C), possibly correlating with a stage 3.1 event. This is also recorded terrestrially by a weak arctic brownearth soil in Germany dated to approximately 28-30 ka by TL analysis of overlying loess and by ^{14}C dating (Zöller *et al*, 1988; Zöller and Wagner, 1989).

In conclusion, over this time period the climate of North West Europe was cool, with frequent periods of climatic oscillation. Three phases of improved (warm and/or wet) conditions, events 3.31, 3.3 and 3.13 are here dated at 59-62, 49-56 and 35-42 ka (with perhaps also a very slight climatic improvement occurring in event 3.1 (28-31 ka)) are evident; the many European 'interstadial' sites probably fall within these events but detailed correlations are not presently possible. A significant cool and / or arid phase (trough E) occurs at 45 ka, but is not represented in the oceanic record, possibly due to it's brief duration and the smoothing of the ocean core record by bioturbation.

2.4.4.4 Conclusions

It is argued here that speleothem growth phases are precisely dated but provide a complex palaeoclimatic indicator which appear sensitive to both temperature and aridity. Independent changes in either one or both of these can determine periods of enhanced or reduced growth. Mechanisms of speleothem growth can be interpreted in combination with evidence from other deposits giving less ambiguous palaeoclimatic information; however, the latter are often poorly dated. The correlations presented here show good agreement with the oxygen isotope record, showing the predominance of a palaeoclimate signal. Variations from the oxygen-isotope record are explained as being palaeoclimatically significant. During substage 5a, significantly low levels of secondary carbonate growth are shown to be associated with a deterioration in climate preceding the stage 4 glacial maxima,

whilst in stage 3 the growth frequency record provides a good framework into which 'interstadial' sites can be fitted. Studies from other climatically distinct regions may help give further insight into the palaeoclimatic influences on growth frequency.

2.5. Conclusions

The growth frequency records presented here, although developed from a comparatively crude technique, have provided improved insight into the timing and causes of speleothem growth phases. In particular, correlations were observed between periods of growth and non-growth and the oxygen isotope, loess and pollen records for the regions considered here, although they often suffered from limitations in dating of the comparative records. Comparisons with regions of desert, semi-arid and tropical climate regimes was not possible, due to the very low number of analyses available for these regions.

A palaeoclimate signal was observed within the growth frequency record from North West Europe. Less clear signals were contained in the records from China and the U.S.A., probably due to sampling bias occurring due to the low number of analyses contained within each compilation. The use of this technique in regional compilations provides us with information which may not have been obtainable from individual samples. However, the relative importance of the factors affecting speleothem growth are still unknown from this approach. The strong correlation with other palaeotemperature records suggests the influence of temperature, however no simple relationship exists between soil pCO_2 and temperature. Also of importance may be the influence of Milankovitch insolation maxima; increased solar insolation may lead to increased soil pCO_2 through increased plant productivity. A strong relationship between Milankovitch cyclicity and speleothem growth frequency was demonstrated by Kashiwaya et al (1991). Alternatively, low levels of growth may be due to limited water supply, as demonstrated for north west Europe in sub-stage 5a. This is particularly important, as palaeoprecipitation records are not preserved in most palaeoclimate indicators, and demonstrates a complex relationship between terrestrial climate change and solar forcing.

The potential for preserving a palaeoprecipitation signal can be investigated further through better understanding of speleothem growth mechanisms, described theoretically in recent work by Dreybrodt (Dreybrodt, 1980, 1981, 1988; Buhmann and Dreybrodt, 1985a). In developing a model of speleothem deposition based on chemical kinetics, growth rate determining variables have been determined.

Understanding growth rate variability will also provide insight into the precise causes of speleothem growth cessation and thus the timing of growth phases. This work is developed in chapter 3, with the aim of evaluating any possible palaeoclimate, and especially palaeoprecipitation, signal contained within the growth rate record.

CHAPTER THREE

SPELEOTHEM GROWTH RATE AND PALAEOCLIMATE

3.1 Introduction

Chapter Two demonstrated that the temporal distribution of speleothem age analyses contained a palaeoclimate component. This signal was complex, being dependant on several variables which affect speleothem growth. A theoretical understanding of how these variables control speleothem growth would potentially allow an improved palaeoclimatic interpretation of the speleothem growth record. Recent work by Dreybrodt has developed such a theory, based on the kinetics of the calcite precipitation process, details of which are presented in Dreybrodt (1980, 1981, 1988) and Buhmann and Dreybrodt (1985a, 1987). An overview of the theory is presented here, followed by a critical assessment of its potential to provide an improved understanding of the palaeoclimate signal; both in terms of a better understanding of the conditions necessary to cause speleothem growth cessation, and also from variations in growth rate.

3.2 Development of Growth Rate Theory

The first attempt to develop a kinetic model of speleothem growth was made by Dreybrodt (1980). The model considers stalagmite formation from a constant supply of water dripping onto a plane stalagmite surface, precipitation occurring from a stagnant thin film of water remaining on the stalagmite cap. The water drops are saturated with respect to calcite, and slowly degass until the CO_2 concentration of the solution equals that of the cave air (figure 3.1a). With degassing, calcite precipitation may occur by the reaction:

$$Ca^{2+} + 2HCO_3^- \rightarrow CaCO_3 + CO_2 + H_2O \qquad (3\text{-}1)$$

the steps of which are shown in figure 3.1b. The rate determining steps for the reaction were considered, and four processes were shown to potentially limit precipitation rates. These were:

a) the diffusion of CO_2 molecules within the solution.

b) the diffusion of Ca^{2+} and CO_3^{2-} within the solution.

c) deposition of $CaCO_3$ at the surface.

d) production of CO_2 at the surface.

Dreybrodt (1980) considered the kinetics of each reaction using the calcite dissolution experiments of Reddy and Nancollas (1970, 1971). They reported that

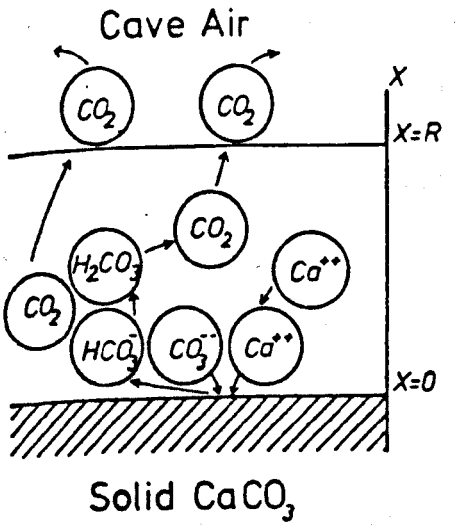

Figure 3.1a. Model of the stagnant fluid film on a stalagmite cap (from Dreybrodt, 1980).

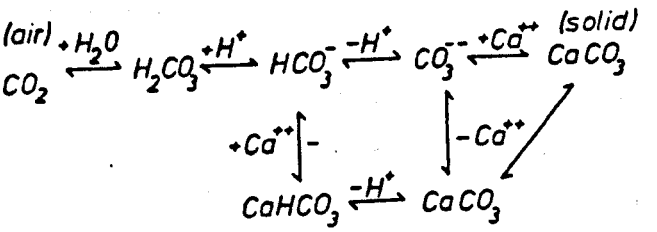

Figure 3.1b. Reactions in the $CaCO_3$ - CO_2 - H_2O - air system (from Dreybrodt, 1980).

from the four potentially limiting reactions, the production of CO_2 at the solid surface was shown to be rate determining. This in turn depended on the calcium concentration of the water, water film thickness and temperature.

Dreybrodt (1981) developed the kinetic theory further by using the empirical data from the more recent dissolution experiments performed by Plummer et al (1978, 1979). These yielded different results from the earlier work of Reddy and Nancollas, although the reasoning for this remains unclear. Calcite deposition is described by the rate equations:

$$dCa^{2+} / dt = \kappa_1(H^+) + \kappa_2(H_2CO_3^+) + \kappa_3 - \kappa_4(Ca^{2+})(HCO_3^-) \qquad (3\text{-}2)$$

where $\kappa_{1\text{-}4}$ are temperature dependent rate constants (Plummer et al (1978, 1979)). Dreybrodt (1981) reported an approximate doubling in the predicted growth rates compared to those using the Reddy and Nancollas equation.

Later work by Buhmann and Dreybrodt (1985a) incorporated an additional rate determining step and tested the equation experimentally. In this more complex formulation, diffusion limited reactions ((a) and (b) earlier), rate determining reactions at the surface ((c) and (d) earlier), and CO_2 - $H_2CO_3^0$ conversion (a previously omitted rate determining reaction), were all considered simultaneously using an iterative procedure. Results showed that both precipitation and dissolution rates could be approximated by the equation:

$$\text{growth rate} = \alpha\,([Ca^{2+}]_{eq} - [Ca^{2+}]) \quad (\text{mmol cm}^{-2}\,\text{s}^{-1}) \qquad (3\text{-}3)$$

$$\text{when } [Ca^{2+}] > 0.2\,[Ca^{2+}]_{eq}$$

where α = f(film thickness, cave air pCO_2, temperature, flow regime)

Temperature was shown to affect growth rate, because the CO_2 - $H_2CO_3^0$ reaction (previously omitted) is strongly temperature dependent. Film thickness variations were also important; under conditions of thin film thickness, CO_2 conversion is rate determining; under high film thicknesses diffusion limited reactions become important (only thin films had been considered by Dreybrodt (1980, 1981)). Cave pCO_2 levels are also an important factor as they control the diffusion gradient across the water film. Finally, dynamic flow conditions were also incorporated into the model for the first time; under a turbulent flow regime the diffusion coefficient is $x10^4$ higher than for molecular diffusion which occurs under laminar flow.

Final developments of the model were made by Dreybrodt and Franke (1987) and Dreybrodt (1988). Based on the earlier work on minimum diameter stalagmites (Curl, 1973), growth rates were calculated for stalagmite formation under slow drip rates, during which growth rate is limited due to the supersaturated water film on the

stalagmite cap reaching equilibrium before a new supersaturated water drip falls. Assuming complete mixing of drops, Dreybrodt and Franke (1987) showed that growth rate is determined by:

$$d[Ca^{2+}]/dt = (R ([Ca^{2+}]_{eq} - [Ca^{2+}]) (1 - e^{(-t\alpha/R)})) \quad (3\text{-}4)$$

where R is film thickness, α is as defined in equation (3-3), and t is the time between drips. Under high drip rates, they showed that the equation simplifies to equation (3-3). Finally by multiplying equation (3-4) throughout by the surface area of the stalagmite, and then solving for the stalagmite diameter, it was shown that:

$$d = (4 V / \pi \alpha t)^{0.5} \quad (3\text{-}5)$$

where V is the drip volume, and d is the stalagmite diameter, and that drip rate information may therefore be determinable from stalagmite diameters.

The growth rate theory has been tested experimentally by Buhmann and Dreybrodt (1985a). The experiments were performed for both dissolution and precipitation; full experimental details are given in Buhmann and Dreybrodt p204-9. For dissolution experiments, the empirical results gave a time constant (τ) for the dissolution reaction which was too high, giving dissolution rates slower than predicted by the theory. The theoretical time constants had to be 'fitted' by a correction factor, which varied between x1.5 and x2.5 of the growth rate. However, the experiments did show the dependence of growth rate on temperature, pCO_2 and film thickness. Similarly, growth rate was shown to increase with turbulent flow conditions, although again a similar correction factor had to be fitted.

Precipitation experiments were performed by dripping water drops onto a calcite slab of known weight embedded into a stalagmite cap, which was later removed and reweighed. The experimental results are shown in figure 3.2. Buhmann and Dreybrodt (1985a) claim that agreement between experiment and theory is good, and that no fitting factor is necessary. However, closer inspection shows that growth rate is systematically higher than that predicted from theory, with a correction factor of x1.5 necessary for experiments at 10 °C (although only two data points are present), and of x1.25 at 20 °C.

It is not known why there is this difference between experimental and theoretical results. Reddy et al (1981) show that a variation of up to x2 is present in the Plummer et al (1978, 1979) dissolution experiments upon which the growth rate theory is based, especially at high pCO_2 levels ($\approx$ 0.3 atm) and low supersaturations. Several reasons for this were proposed, including the omission of an additional reaction step in the rate equations, or crystallographic reasons, either a reduction in growth site

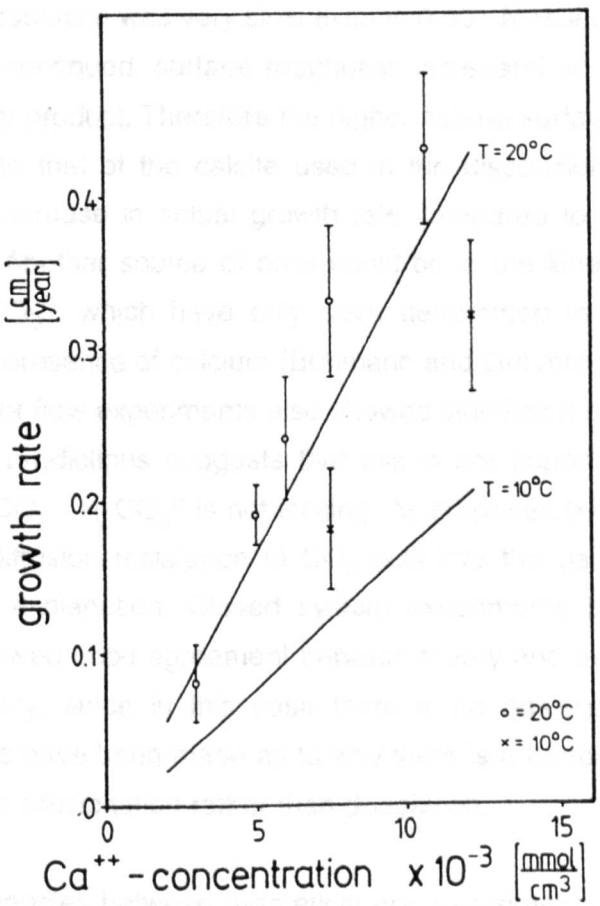

Figure 3.2. Experimental growth rates of $CaCO_3$ at temperatures of 10 °C and 20 °C for varying calcium ion concentrations. pCO_2 is $3x10^{-4}$ atm. Theoretical results are shown by the solid line, and assume a film thickness of 0.1 mm (from Buhmann and Dreybrodt, 1985).

density or a crystallisation mechanism change as reactions approach equilibrium. Compton and Daly (1984) noted a significant increase in the value of the solubility product κ_2 derived from their dissolution experiments using a rotating disc, and those of Plummer et al (1979) which used calcite powders. They later showed that surface roughness was important in controlling dissolution rate. Using freshly cleaved crystals, dissolution was very slow even in 0.001 N HCl (Compton et al, 1986), but as dissolution continued, surface roughness increased and thus changed the value of the solubility product. Therefore the higher natural surface roughness of speleothems compared to that of the calcite used in the dissolution experiments may cause a significant increase in actual growth rate compared to the theory (Dreybrodt, pers. commun.). Another source of error could be in the kinetic constants of the reaction CO_2 - $H_2CO_3^0$, which have only been determined in pure H_2O - CO_2 solutions, without the presence of calcium (Buhmann and Dreybrodt, 1985a). However, the fact that turbulent flow experiments also showed significant disagreement between actual and model predictions suggests that this is not important, as under turbulent flow conditions CO_2 - $H_2CO_3^0$ is not limiting. As proposed by Stumm and Morgan (1981), additional diffusion resistance to CO_2 built into the gas-liquid boundary could also provide an explanation. Closed system experiments by Buhmann and Dreybrodt (1985b) showed good agreement between theory and experiment and would confirm this possibility, since in this case there is no gas-liquid boundary. However, no explanations have been made as to why there is a better fit between experiment and theory under precipitation rather than dissolution.

The discrepancies between theoretical and experimental growth rates suggests that direct application to palaeoclimate studies must be treated with caution. There is the possibility that the as yet unknown cause of this error is not constant for all values of temperature, precipitation or calcium concentrations. Until this has been determined, growth rate theory can not be used to give absolute measures of temperature, calcium or water flux variations. However, relative changes in growth rate from multiple samples formed under given temperature, precipitation and calcium concentration levels may prove the constancy of this error, and give a valid record of palaeoclimate change. Furthermore, the x2 error in growth rate may be insignificant compared to changes in growth rate which may have occurred over the Quaternary period.

3.3 Critical Analysis of Growth Rate Theory

3.3.1 Sensitivity of Growth Rate to Determining Variables

As discussed in section 3.2, several variables influence growth rate; calcium concentration, temperature, cave air pCO_2, and hydrological conditions (water film thickness, turbulent or laminar flow conditions, and drip rate). Two different deposition environments can be considered; flowstone deposition, with theoretically continuous water supply, and stalagmite deposition, where slow drip rates may limit growth rate. Growth rates for both stalagmites and flowstones were calculated from the growth rate equations (3-3 and 3-4)* using Fortran 77 programs, and the relative importance of each of the variables affecting growth rate was investigated over the range of conditions expected in the cave environment. Each variable is considered in detail below.

3.3.1.1 Calcium

The sensitivity of growth rate to calcium ion concentration variations is shown in figure 3.3 for both flowstones and stalagmites. When holding temperature and film thickness constant, calcium concentrations in dripwaters have a significant influence on growth rate. Increasing calcium ion concentration increases growth rate linearly, the rate of which is shown in figure 3.3. For stalagmites, the rate of increase is less for fast drip rates than for slow. Unfortunately because of the absence of any well defined calcium - temperature relationship (section 2.2), temperature may not be substituted for calcium ion concentration, and thus the elimination of calcium from consideration in the growth rate equations is not possible.

3.3.1.2 Temperature

The influence of temperature on growth rate is shown in figure 3.4 for both flowstone and stalagmite deposition. Holding calcium ion concentration and film thickness constant, an increase in temperature is shown to give an exponential increase in growth rate. The effect of temperature is greater at high rather than low temperatures. Drip rate variations are also shown to significantly affect the temperature - growth rate relationship for stalagmite samples, with a lower rate of increase of growth rate with temperature than that for flowstones.

3.3.1.3 Cave Air pCO_2

Few studies of cave air pCO_2 levels have been undertaken, due to measurement difficulties. Ek and Gewelt (1984) compiled data from caves world-wide, and found a

* And the tabulated values for α for varying T & pCO_2 from Dreybrodt (1988)

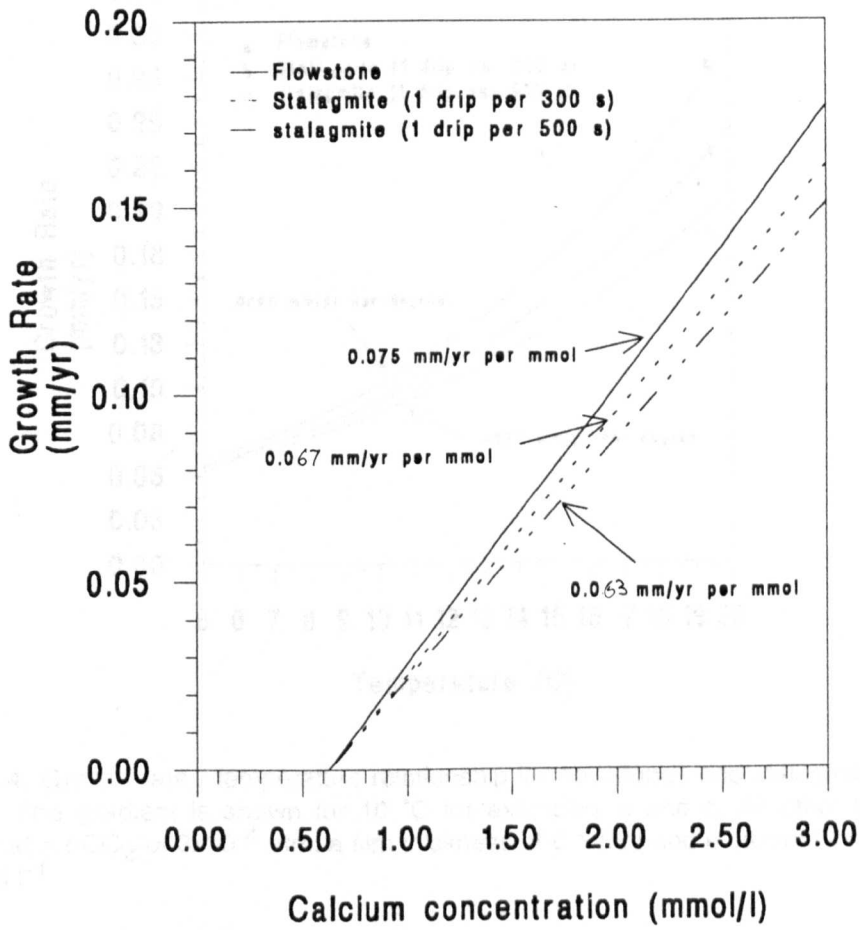

Figure 3.3. Growth rate / calcium relationship for flowstones and stalagmites. All other variables are held constant at a temperature of 10 °C, a pCO_2 of $3x10^{-4}$ atm and a film thickness of 0.1 mm.

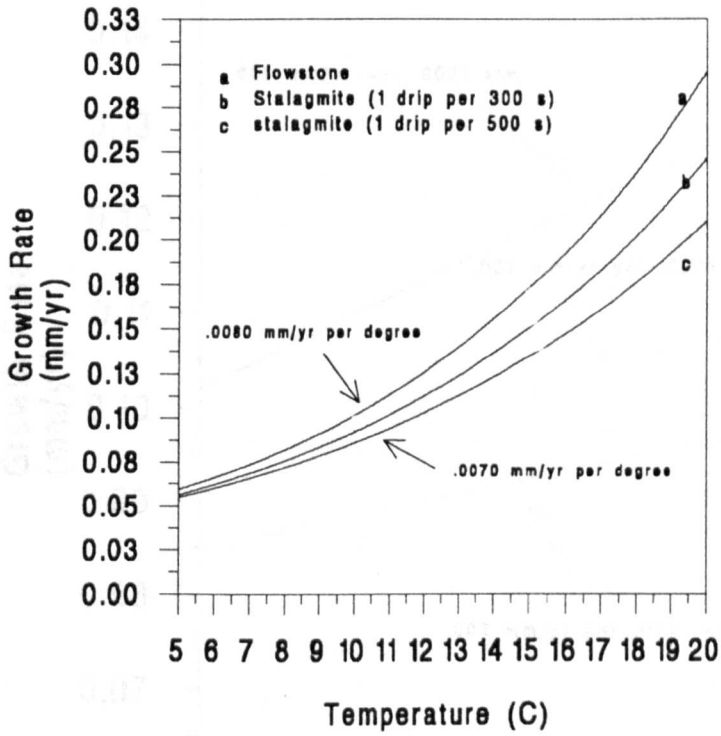

Figure 3.4. Growth rate / temperature relationship for flowstones and stalagmites over the range 5-20 °C. The gradient is shown for 10 °C for examples a and c. All other variables are held constant at a pCO_2 of $3x10^{-4}$ atm, a film thickness of 0.1 mm and a calcium ion concentrations of 2.0 mmol l^{-1}.

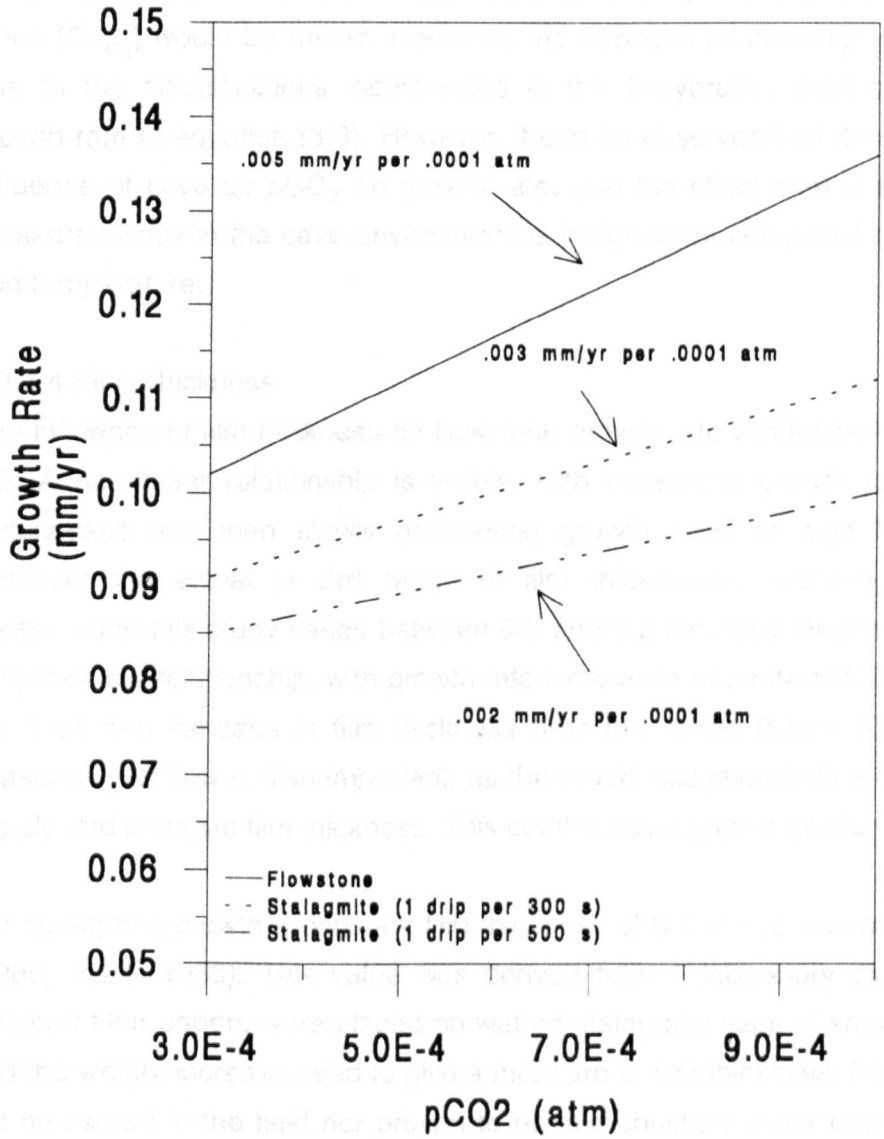

Figure 3.5. Growth rate / pCO_2 relationship for both stalagmites and flowstones. All other variables are held constant at a temperature of 10 °C, a calcium concentration of 2.0 mmol l^{-1}, and a water film thickness of 0.1 mm.

range of pCO_2 levels from $3x10^{-4}$ atm (atmospheric concentration) to $5x10^{-3}$ atm, although they state that the higher values must be treated with caution due to probable CO_2 contamination during measurement from human respiration. The influence of pCO_2 levels on growth rate are shown in figure 3.5; the expected relationship would be of an increasing pCO_2 leading to a decrease in growth rate, since $[Ca_{eq}]$ would be raised. However, the opposite relationship is observed here, due to the simplifications incorporated in the Dreybrodt model by approximating growth rate to equation (3-3). However, it can be observed that there is only a small influence of cave air pCO_2 on growth rate, and the effect over the range of partial pressures likely in the cave environment is insignificant compared to that of calcium and temperature.

3.3.1.4 Film Thickness

The influence of film thickness on flowstone growth rate variations is shown in figure 3.6. A non-linear relationship is visible, with increasing growth rates for low film thicknesses and then slowly decreasing growth rates at high film thicknesses. However the actual ($\pm$ 2σ) range of film thicknesses occurring on flowstones measured in this study varies between 0.0 and 0.2 mm (see chapter 4). This greatly simplifies the relationship, with growth rate increasing at a rate of 0.05 - 0.01 mm yr^{-1} per 0.01 mm increase in film thickness over this range (figure 3.6). However the seasonality of flow is also important, as the model assumes both a continuous water supply and constant film thickness. This point is developed in section 3.3.3.

For stalagmite growth a constant film thickness of 0.1 mm is assumed by Dreybrodt (1980, 1981, 1988). This value was derived from a laboratory experiment, where weighed filter papers were placed on wetted stalagmite caps of known surface area, and the weight increase used to give a measure of film thickness. Film thickness was not measured in the field nor proven to remain constant under changing flow rates. This has been investigated in this study (see chapter 4), where no relationship between drip rates and film thickness was observed. Hence for stalagmites, growth rate is more sensitive to drip rate variability than changes in water film thickness.

Film thickness also has an influence on the flow regime. Figure 3.7 shows the influence on growth rate of flow regime, which may become turbulent when the film thickness exceeds 1 mm. An order of magnitude increase in growth rate can be seen under turbulent flow conditions, growth rate being far more sensitive to this variable than the others affecting growth rate. However, it is not known whether film thicknesses are sufficient for turbulent flow to actually occur on speleothem

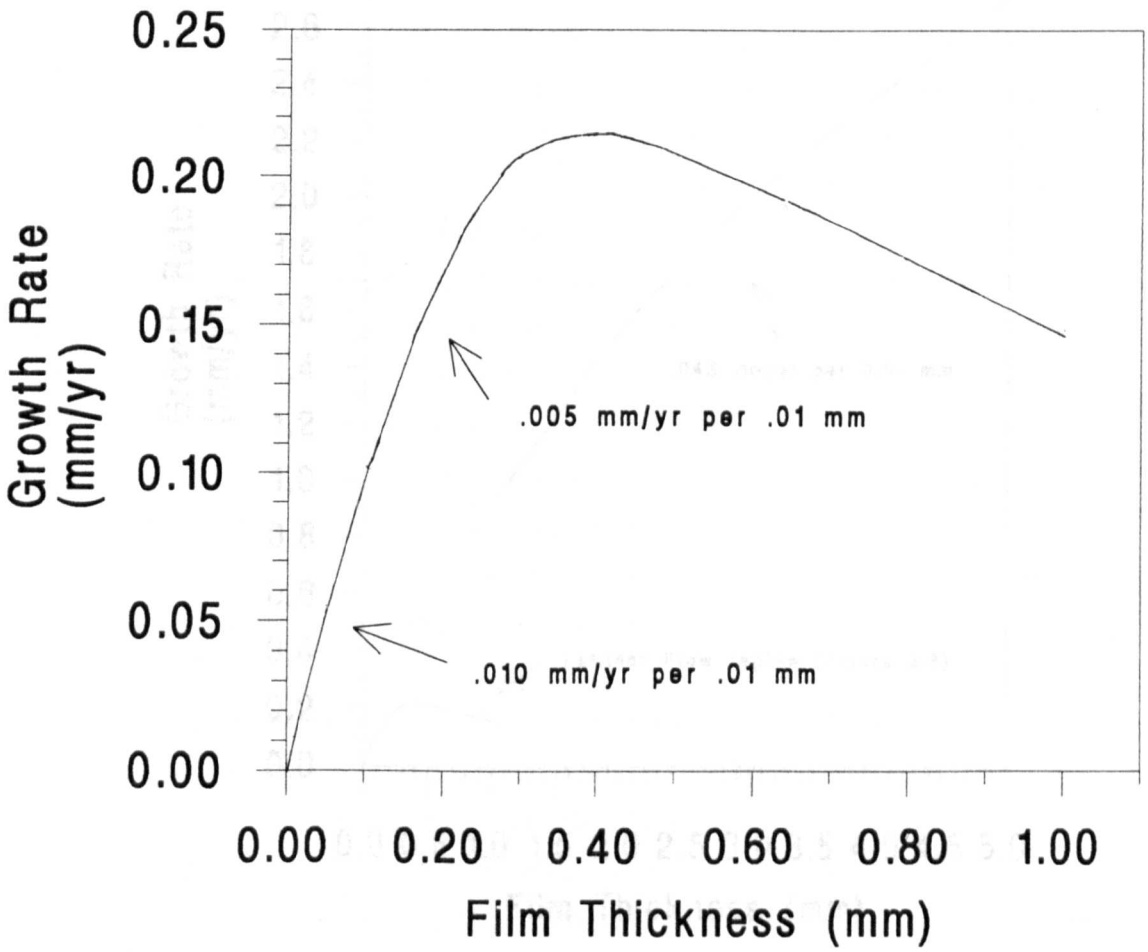

Figure 3.6. Growth rate / film thickness relationship under laminar flow conditions. All variables are held constant at a temperature of 10 °C, a pCO_2 of $3x10^{-4}$ atm and a calcium concentration of 2.0 mmol l^{-1}.

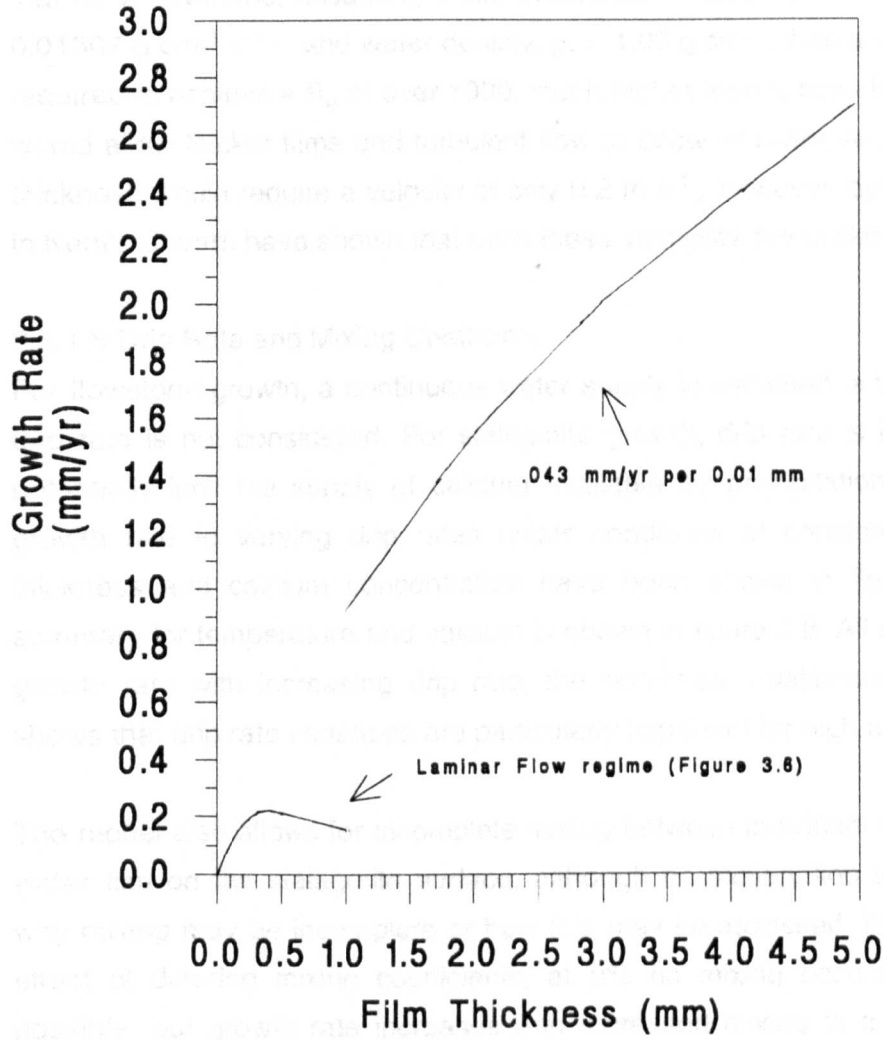

Figure 3.7. The effect of turbulent flow on growth rate for varying film thicknesses. All other variables are held constant at a temperature of 10 °C, calcium ion concentration of 2.0 mmol l^{-1}, and a pCO_2 of $3x10^{-4}$ atm.

formation. Dreybrodt (1988) suggests that turbulent flow is not possible during stalagmite formation, since to obtain a Reynolds Number (R_e) greater than 1000 on a stalagmite of 10 cm diameter (the maximum measured in this study), 100 $cm^3\ s^{-1}$ of water would be needed (approximately 1000 drips per second). Calculations show that for a flowstone, assuming a film thickness, R, less than 0.2 mm; viscosity, η, = 0.01307 g $cm^{-1}\ s^{-1}$; and water density, ρ, = 1.03 g cm^{-3}, then a velocity of 6 m s^{-1} is required to achieve a R_e of over 1000, much higher than is actually possible. Ponding would allow thicker films and turbulent flow to occur at lower velocities. A 6 mm film thickness would require a velocity of only 0.2 m s^{-1}, however, dye trace experiments in Kent's Cavern have shown that even these velocities are unlikely (see chapter 4).

3.3.1.5 Drip Rate and Mixing Coefficient

For flowstone growth, a continuous water supply is assumed, and therefore variable drip rate is not considered. For stalagmite growth, drip rate is important as it may potentially limit the supply of calcium available for precipitation. The sensitivity of growth rate to varying drip rates under conditions of constant temperature, film thickness and calcium concentration have been shown in figures 3.3 to 3.5. A summary for temperature and calcium is shown in figure 3.8. All show an increase in growth rate with increasing drip rate, the non-linear relationship with temperature shows that drip rate variations are particularly important for high temperatures.

The model also allows for incomplete mixing between individual water drops and the water film on the stalagmite surface, although no explanation was proposed as to why mixing may be incomplete or how this may be assessed. Figure 3.9 shows the effect of differing mixing coefficients; at 0% no mixing occurs and no growth is possible, but growth rate increases with increased mixing to a maximum at 100% mixing between drips and the water film. For all practical purposes, mixing coefficient is arbitarily assumed to be 90%, since the energy of a falling drop would be expected to give good mixing, with some loss due to splash effects. No field testing of this value was found to be feasible.

3.3.1.6 Summary

The sensitivity of growth rate to the variables detailed above is shown quantitatively in table 3.1, where the effects on growth rate of a 50% change in each of the variables from an assumed mean value are shown. It can be seen that for all variables which have a significant effect on growth rate, the effect on growth rate is positive. In particular, it shows that the effect of calcium ion concentration on growth rate is more significant than that of temperature or film thickness. Both pCO_2 and drip rate

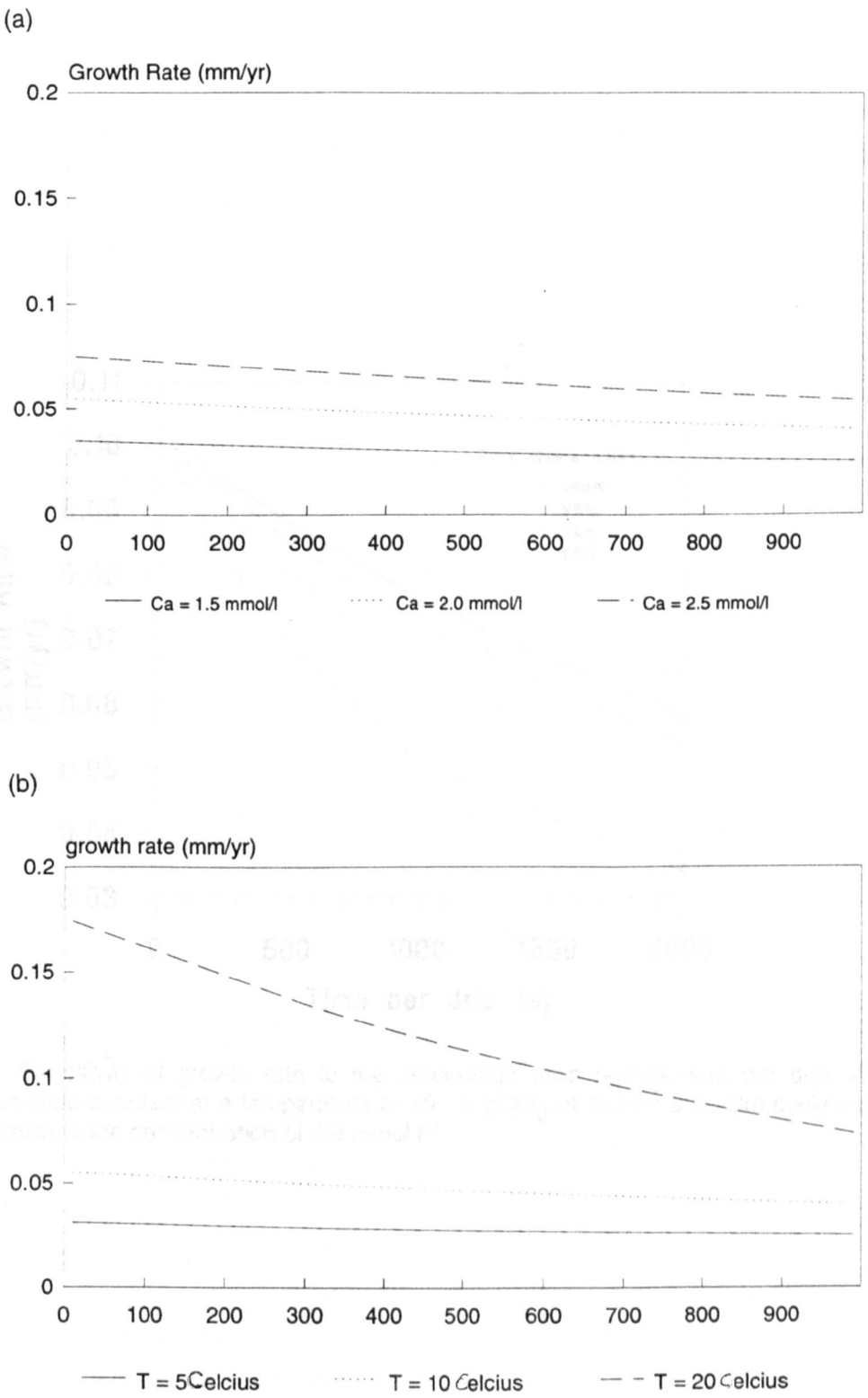

Figure 3.8. (a) Growth rate / drip rate relationship under varying calcium ion concentrations. All other variables held constant at a pCO_2 of $3x10^{-4}$ atm, temperature of 10 °C and a film thickness of 0.05 mm. (b) Growth rate / drip rate relationship under varying temperatures. All other variables held constant at a calcium ion concentration of 2.0 mmol l^{-1}, a film thickness of 0.05 mm, and a pCO_2 of $3x10^{-4}$ atm.

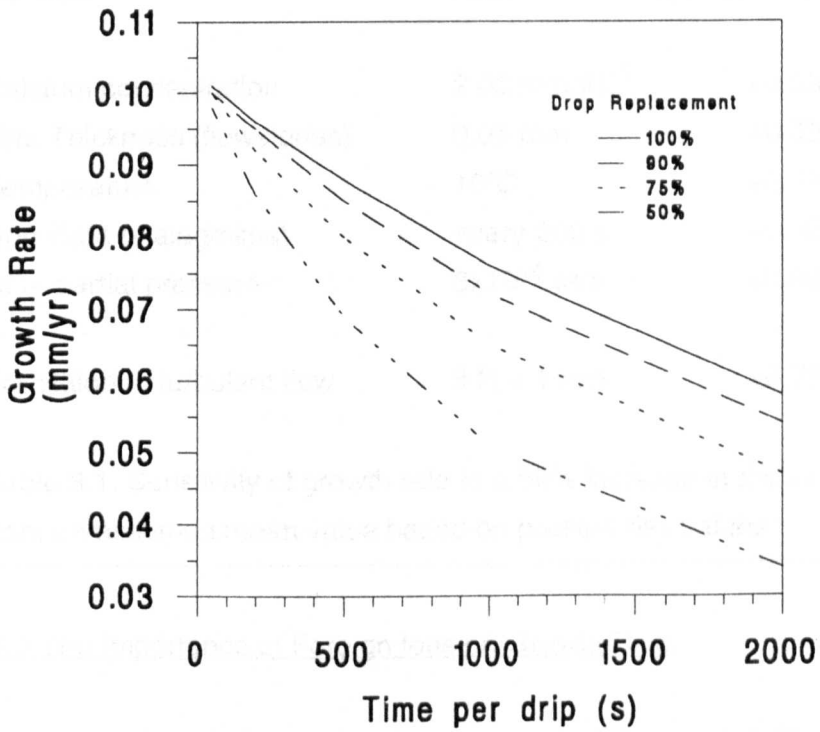

Figure 3.9. Sensitivity of growth rate to the percentage drop replacement per drip. All other variables are held constant at a temperature of 10 °C, pCO_2 of $3x10^{-4}$ atm, film thickness of 0.1 mm and a calcium ion concentration of 2.0 mmol l^{-1}.

are relatively insignificant. The complexity of the effect of changes in water supply are also highlighted as film thickness, drip rate, dynamic flow conditions and seasonality (see section 3.3.3) all effect growth rate. What is now needed is an investigation of how the variables act in combination with one another, especially with respect to potential changes in climatic conditions. This is undertaken in section 3.4. Before the possible effects of climate change on the controlling variables is considered, several other variables of potential significance in controlling growth rate must also be reviewed.

Variable	*Mean*	*Growth Rate Change (mm yr^{-1})*
Calcium concentration	2.00 mmol l^{-1}	+0.037
Film Thickness (flowstones)	0.05 mm	+0.025
Temperature	10°C	+0.018
Drip Rate (stalagmites)	every 200 s	+0.005 - 0.010
CO_2 partial pressure	$3x10^{-4}$ atm	+0.007
- - -	-	-
Transition to turbulent flow	if R = 1 mm	+0.769

Table 3.1. Sensitivity of growth rate to a 50% increase in the value of the variables from an assumed mean value based on present day values

3.3.2 The Importance of Foreign Ions on Growth Rate

The kinetic theory of growth rate assumes calcite precipitation in a pure chemical system. The problem of the influence of foreign ions was addressed by Buhmann and Dreybrodt (1987), when they considered the effect of Mg^{2+}, Na^{+}, SO_4^{2-} and Cl^{-} ions in solution. Four processes were investigated; the ionic strength effect (the effect of adding uncharged substances which change the ionic strength of the water), common-ion effects (the addition of charged substances which change the saturation state of the water), acid - base effects (altering the pH of the solution) and ion - pair effects (the formation of ion pairs such as $CaSO_4^0$ which remove Ca^{2+} from the solution, decreasing the saturation state). Of these, the last was found to be the most important, but overall, growth rates were not significantly affected by the concentrations of foreign ions expected in the cave environment. The effects of $NaSO_4$ and $MgCO_3$ as ion-pairs and common-ions respectively are shown in figure 3.10.

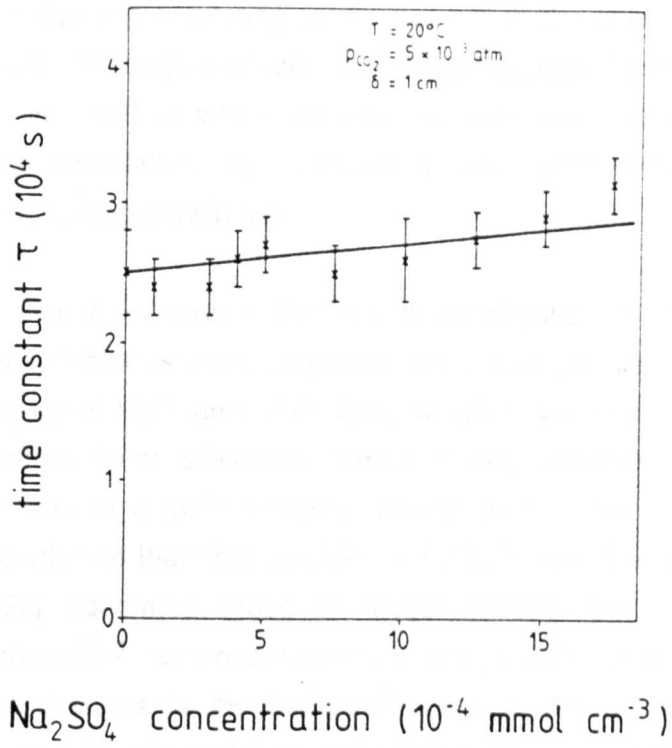

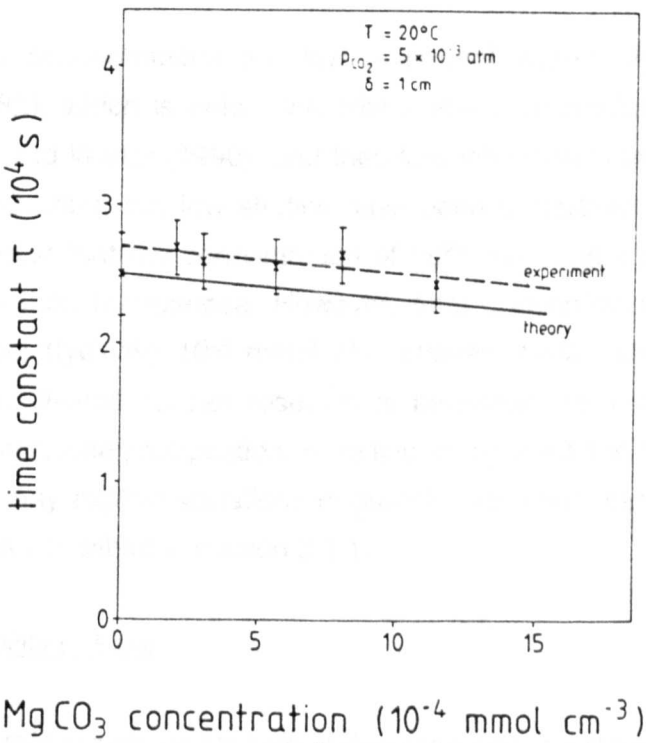

Figure 3.10. Measured time constants of calcite dissolution upon addition of Na_2SO_4 and $MgCO_3$. Solid lines are the theoretically calculated variation of the time constants (from Buhmann and Dreybrodt, 1987).

Buhmann and Dreybrodt (1987) studied the effect of foreign ions on the saturation state of the solution precipitating calcite, but not on the rate equations of Plummer et al (1978, 1979). Although the latter may also be expected to be affected by common-ions, when predicted growth rates were tested experimentally in the presence of common-ions under laboratory conditions, a good agreement was found between the theory and measured growth rate.

A more significant omission is the lack of investigation of other foreign ions which may potentially inhibit or increase growth rates. Of particular importance is the study of the influence of Fe^{2+} and Mn^{2+} ions, which have been demonstrated to inhibit growth in some karst situations. Meyer (1984) observed a x5-10 decrease in precipitation rate at a Mn^{2+} concentration of 0.01 mmol l^{-1}, a significantly higher effect on growth rate than that of Mg^{2+} and SO_4^{2-} ions. The results of Dromgoole & Walter (1990) confirmed those of Meyer (1984), but showed that a higher concentration of Mn^{2+} was necessary to inhibit growth rate (0.1 mmol l^{-1}). They also showed that changes in the Mn^{2+}/Ca^{2+} ratio in the solution were important in determining growth rate variation, rather than changes in Mn^{2+} ion concentration alone.

Manganese concentrations are low in natural waters (typically 10^{-4} mmol l^{-1}; Drever, 1982), which is below the critical levels determined by Meyer (1984) and Dromgoole and Walter (1990), and therefore inhibition is unlikely to occur. Iron may be more important, but few studies have been undertaken. Dromgoole and Walter (1990) suggest that the concentration of Fe^{2+} ions has a much lower influence on growth rate than manganese. However, total concentrations of iron are higher in groundwaters (typically 10^{-3} mmol l^{-1}; Drever, 1982), and thus may be of more significance. Overall, further research is necessary to investigate the influence of other ions on calcite precipitation. Here it is recognised that they may be an important factor, and may explain variations in growth rate which cannot be accounted for by the variables described in section 3.3.1.

3.3.3 Variability of Flow

The growth rate equations for both stalagmites and flowstones assume constant flow. For stalagmites, flow variations control the drip rate variable, but no account has been taken of the frequency of different drip rates over time. For flowstones, water flux is incorporated in the film thickness term, but again temporal variations have not been considered.

Previous workers have suggested that variability of discharge from karst springs and seeps varies with the flow route taken and the amount of storage within the bedrock; in general small discharges are associated with decreasing variability of flow (Smart and Friedrich, 1987). However, measurements of the very low discharges found upon flowstones and especially stalagmites have rarely been obtained, due to the relative difficulty in recording such low flow rates. To obtain an improved understanding of the variability of flow with decreasing discharge, data was compiled in this study for low discharge drip and seep sources. These were associated with both stalagmite and flowstone deposition, and non-calcite depositing drips and seeps. This data was drawn from both published work (Pitty (1966, 1974), Stenner (1973), Friedrich (1981), Villar et al (1985)), and also data collected in this study over the period 1990-1992, from G.B. Cave, Mendips; Kents Cavern, Devon; and Lower Cave, Bristol. In the case of the data compiled from the literature, measurements were made both in terms of drip rate and discharge (l s^{-1}). For the former, a drip volume of 0.15 cm^3 was assumed, to convert values into discharge (actual drip volumes were measured in the field (the average of 20 - 100 drips collected in a measuring cylinder), and averaged 0.17 ± .05 cm^3 (n=11, 1σ error)). The coefficient of variation of discharge was then plotted against the mean discharge for all the data; the results are shown in figure 3.11.

Flow sources can be observed to have a high discharge (> 10^{-5} l s^{-1}) and a wide range of coefficients of variation (2-200%), though most samples fall in the range 20-125%. This reflects the possible range of flow routings onto such samples. Subcutaneous, shaft or vadose flow feeds have relatively fast response times to precipitation events and relatively low storage (Smart and Friedrich, 1987), which would be reflected by highly variable discharge and a high coefficient of variation. This has been observed in this study, where several flowstones only received a water supply in winter, when rainfall is greatest (7 out of 13 samples, chapter 4). Such a limited water availability will effect growth rate. Figure 3.12 shows the effect of having less than 12 months of available water supply for different film thicknesses, and demonstrates that changes in the number of months of water availability are potentially more significant than changes in film thickness.

Drip sources have coefficients of variation in the range 5-200%, though most samples fall within the range 5-75%, a lower range than that observed for flow sources. This probably reflects different flow routing, with low discharge drips being fed by high storage, low variability (seepage) flows (Smart and Friedrich, 1987).

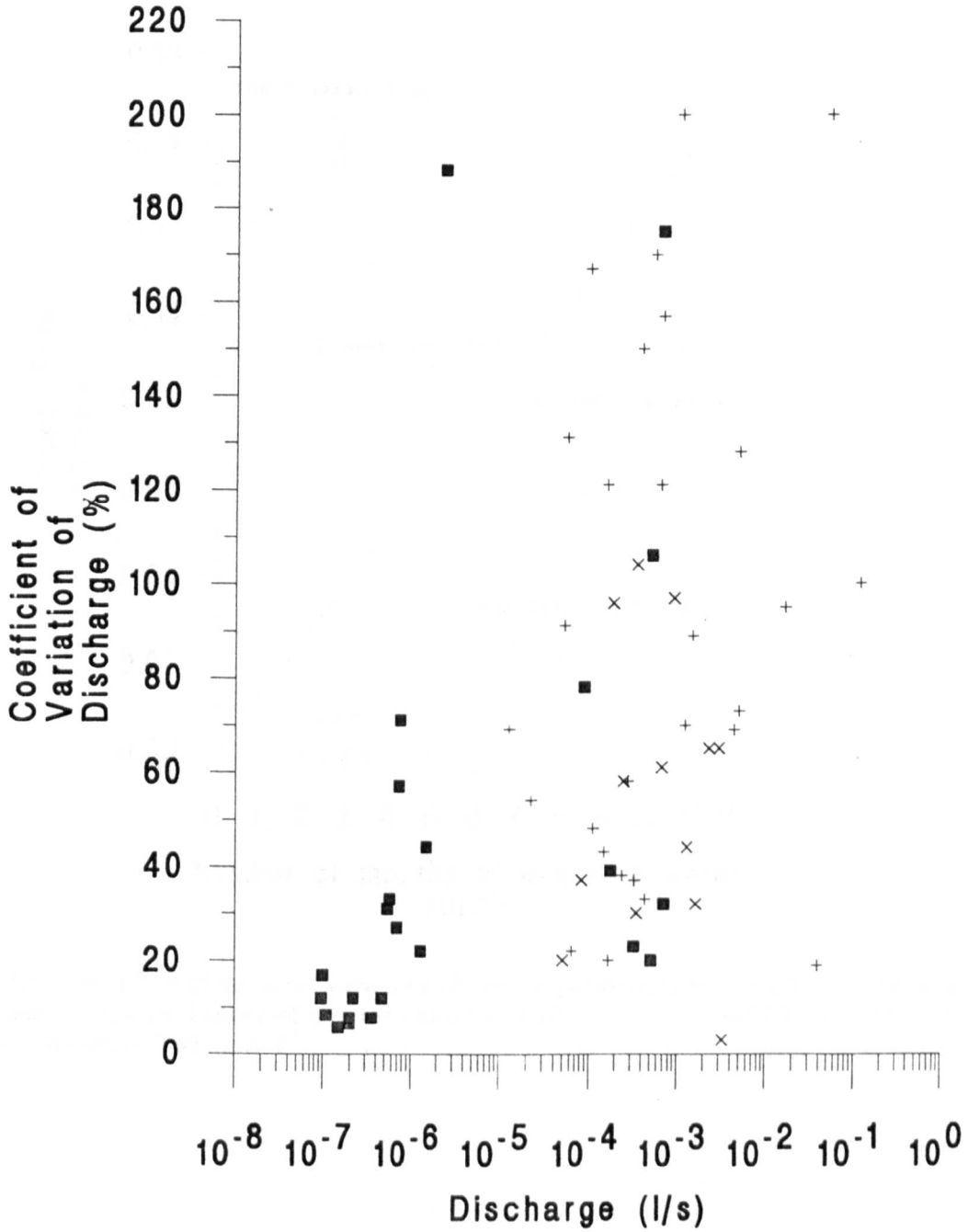

Figure 3.11. Relationship between discharge and discharge variability for cave drips (squares), flows (pluses) and undetermined sources (crosses). The coefficient of variation is related to discharge by the relationship: CV = 62 - 6734 Q with correlation coefficient of 0.03.

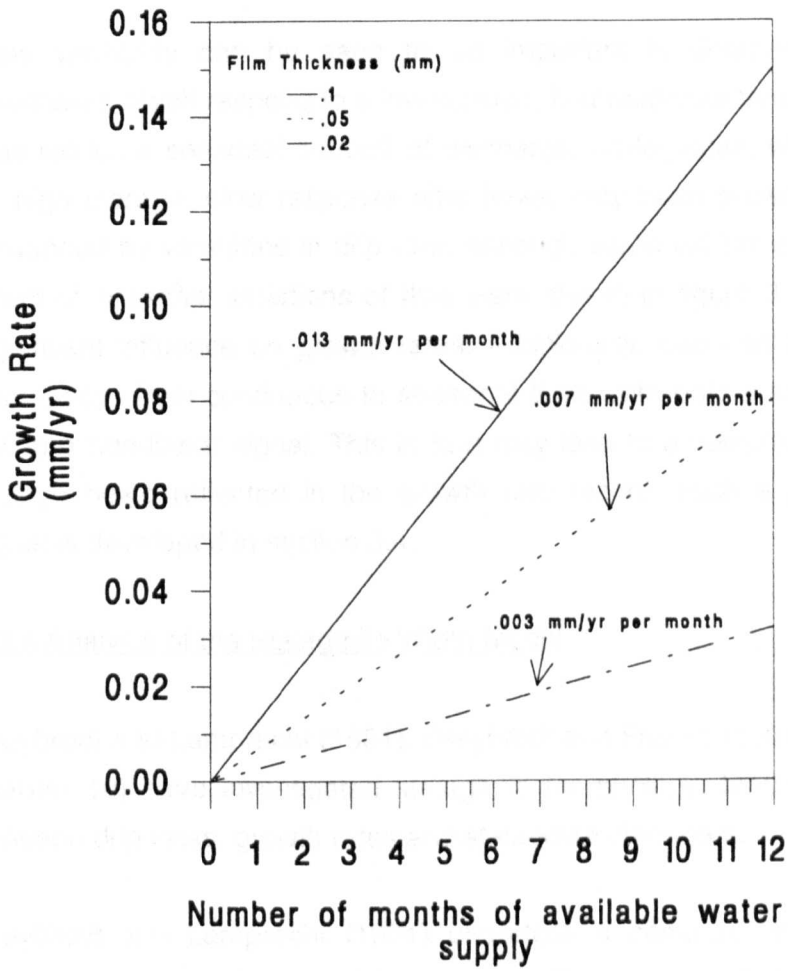

Figure 3.12. The effect of seasonal variations of flow on growth rate for three film thicknesses. All other variables are held constant at a temperature of 10 °C, pCO_2 of $3x10^{-4}$ atm and a calcium ion concentration of 2.63 mmol l^{-1}.

Stalagmites fed by low coefficient of variation feeds may be expected to have a continuous drip supply all year. Variations in drip rate over time may cause changes in growth rate as shown in figure 3.8, rather than seasonal shut-off of water supply. However, some samples exhibit a seasonal shut-off of flow (2 out of 13 samples in this study, chapter 4), with a high coefficient of variation of discharge and water supply only in winter. These samples would be effected as in figure 3.12.

Flow variability can be seen to be important in determining growth rates for flowstones which respond to a low storage, fast response time groundwater flow, and thus exhibit a seasonal shut-off of discharge. Stalagmites, which are commonly fed by high storage, slow response time flows, may have growth rates which are only influenced by variations in drip rate, although some exhibit a seasonal shut-off. The effect of seasonal variations of flow were shown in figure 3.12, and demonstrate a significant influence on growth rates. Additionally, one can speculate that samples may switch from continuous to seasonal flows with only a small change in climate, giving a non-linear signal. This in turn may lead to a complex signal of precipitation change being reflected in the growth rate record; such a potential palaeoclimate signal is developed in section 3.4.

3.3.4 Analysis of the Stalagmite Width Model

Dreybrodt and Lamprecht (1981), Dreybrodt and Franke (1987) and Dreybrodt (1988, chapter 10) have investigated stalagmite morphology, leading to a suggested link between drip rates, growth rates and stalagmite diameters.

Dreybrodt and Lamprecht (1981) undertook a computer simulation of stalagmite growth using a purely geometric approach. They showed that an equilibrium shape is established when a height of x2 the diameter had been reached, and that this equilibrium form does not depend on the angle of the initial growth surface or surface roughness.

A link between equilibrium stalagmite diameter and drip rate was developed by Dreybrodt and Franke (1987). Equation (3-4) was rewritten such that:

$$d[Ca^{2+}]/dt = R\,\varphi\,([Ca^{2+}]_{eqm}-[Ca^{2+}])\,\{1-e^{(-t/T_d)}\}\,x1.174x10^{7} \quad (mm\ yr^{-1})$$

$$t\,\{1-(1-\varphi)\,e^{(-t/T_d)}\} \qquad (3\text{-}6)$$

where T_d is the saturation decay time for each drip, and φ is the amount of water film replacement per drip (assumed 90% - section 3.3.1.5). For equilibrium growth, the solution flowing across the stalagmite has lost supersaturation completely, and

calcite is deposited only over the plane surface area of the stalagmite top, A. Therefore, combining (3-5) and (3-6):

$$d[Ca^{2+}]/dt\ A = D[Ca^{2+}]/dt\ \pi\ d^2 / 4 \qquad (3\text{-}7)$$

where D is the stalagmite diameter. Therefore:

$$D^2 = V\ \{1-(1-\varphi)\ e^{(1-t/T_d)}\}\ 4 / R\ \varphi\ \{1-e^{(-t/T_d)}]\ \pi \qquad (3\text{-}8)$$

Under low flow conditions, the time between drips (t) is much smaller than the saturation decay time (Td), and also assuming φ = 100%, the equation simplifies to:

$$D_{min} = (\ 4\ V / \pi\ R\ \varphi\ )^{0.5} \qquad (3\text{-}9)$$

And under high flow ($T_d >> t$):

$$D = (\ 4\ V / \pi\ \alpha\ t\ )^{0.5} \qquad (3\text{-}10)$$

Under low flow, assuming a constant drip replacement (φ=100%), the minimum diameter is limited only by film thickness (R) and the drip volume (V) (equation 3-9). Both of these measures have been made in this study. R gave values of 0.052 ± 0.031 mm (1σ; n=78; see section 4.3.1.3), and V was found to be 0.17 ± 0.05 cm^3 (1σ; n=11; see section 3.3.3). This gives a range of potential minimum diameter stalagmites of 4.3 to 11.6 cm (1σ range; mean = 6.5 cm). This is in good agreement with that suggested by Dreybrodt (1988) and those observed in caves today.

Under high flow conditions, stalagmite diameter depends on the complex function α and drip rate, t, (equation 3-10), and Dreybrodt (1988) suggested that a relationship between diameter and drip rate may be found in nature. This would allow stalagmite diameter to be used as a proxy measure of drip rate, and allow the elimination of this variable in the determination of growth rate. However, such a simple relationship is unlikely, as there would be expected to be an important relation between stalagmite diameter and drip height, since the latter influences the velocity of a falling drop and thus the amount of splash (Gams, 1981). This relationship can be developed from the literature on soil erosion (Brandt, 1990; Stuttard, 1990) and splash physics (Harlow and Shannan, 1967; Mutchler and Larson, 1971; Cheng, 1977). The Fortran 77 program 'DROP' of Stuttard (1990) has been used here to estimate fall velocities of water drops falling from different heights, which can then be input into the splash equations of Mutchler and Larson (1971) and Cheng (1977). Figure 3.13a shows the theoretical influence of fall height on the drop velocity, and shows a variation of x9 in velocity over the range of heights possible in the cave environment. The amount of splash generated from a falling water drop will be greater as velocity increases. Literature searches could not reveal if theoretical studies had been undertaken of how the amount of splash varies with increasing velocity; however Mutchler and Larson (1971) show that 20% of the drop will be splashed at terminal velocity (9.15 m s^{-1} for a drop of .15 cm^3 volume). Figure 3.13b shows the effect of fall velocity on the

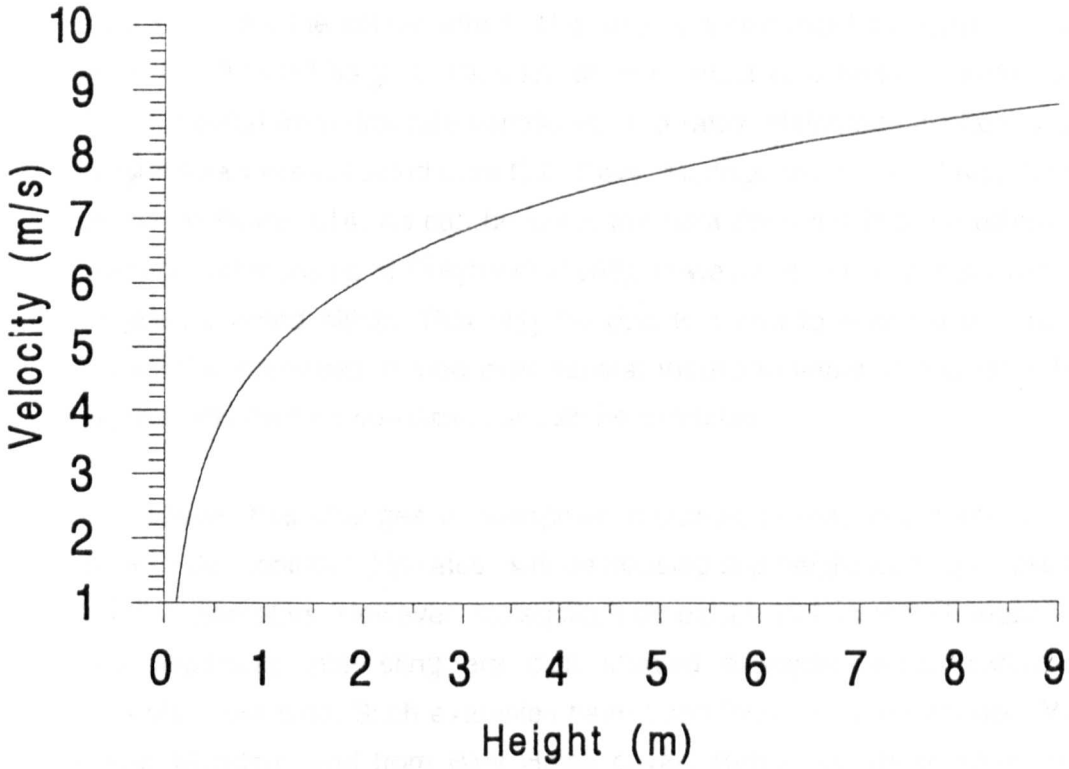

Figure 3.13a. Impact velocity of a falling drip from different fall heights.

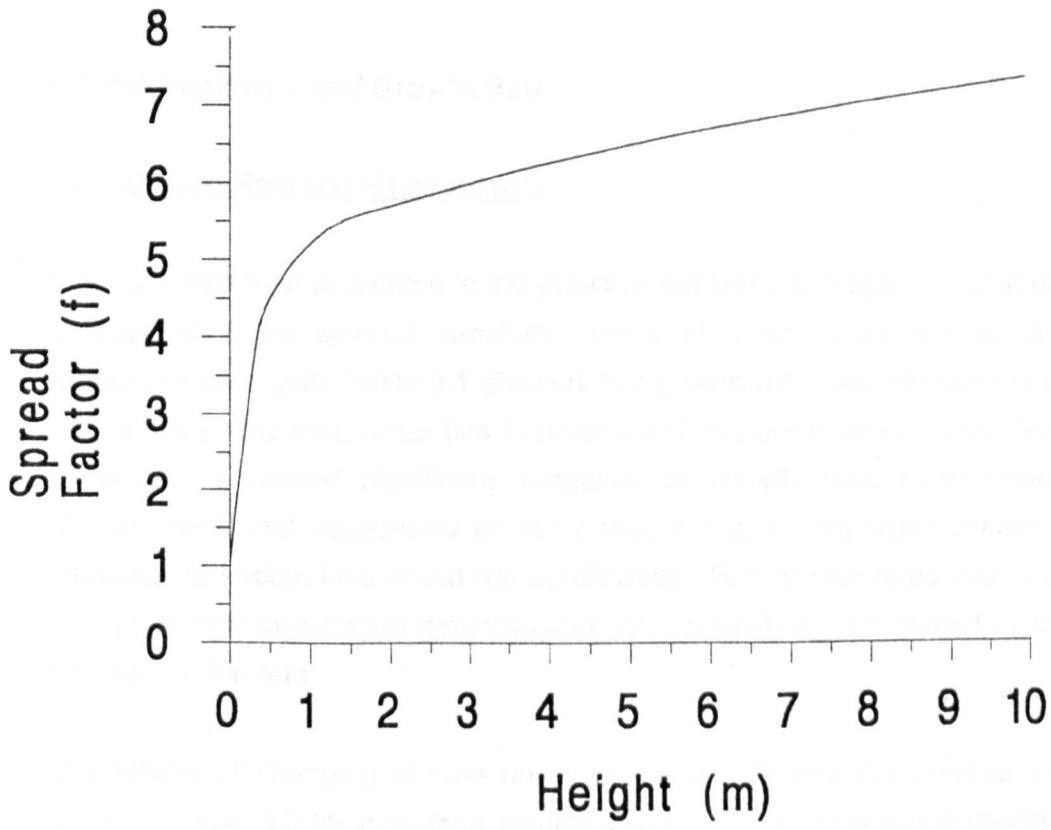

Figure 3.13b. Relationship between the amount of spread of a falling drip upon impact with the stalagmite cap and the drip fall height.

diameter of the drop upon impact, as theorised by Cheng (1977), and which is used as a proxy for the splash effect. This shows a sevenfold increase in drop diameter over 1 to 9 m fall heights. Thus splash may affect stalagmite diameters as much as that expected from drip rate variations. Drip rates, stalagmite diameters and drip fall height data were collected from G.B. Cave, Mendip, and Lower Cave, Bristol, and are shown in figure 3.14. As can be seen, the data does not fit the predicted drip rate / diameter relationship of Dreybrodt (1988); however, no clear pattern with varying fall heights is noted either. This may be due to trying to relate drip rates today and stalagmite diameters formed over several thousand years; if drip rates have varied significantly then no correlation should be expected.

It is shown that changes in stalagmite morphology may occur whilst the samples grow under constant drip rates, with decreasing drip height leading to less splash and smaller diameters. However, stalagmites do exist with frequent changes in diameter, and especially interesting are club shaped examples which exhibit increasing diameter over time. Such examples have been found in Charterhouse Warren Farm Cave, Mendips, and from Blue Holes caves, Bahamas. These samples would be particularly interesting samples to analyse in future studies. For the moment, it is recognised that the no clear relationship would be expected between drip rate and diameter.

3.4 Palaeoclimate and Growth Rate

3.4.1 Growth Rate and Palaeoclimate

From the evidence presented in the previous sections, it is apparent that growth rate is dependent on several variables, some of which may provide a potential palaeoclimate signal. Table 3.1 showed that growth rate was sensitive to increasing temperature, drip rate, water film thickness and calcium concentrations, increases in all of which caused significant increases in growth rate. Furthermore, it was demonstrated that seasonality of water supply was an important variable, that the presence of foreign ions would not significantly effect growth rates over the range of concentrations expected in groundwaters, nor could stalagmite diameters be used as a proxy for drip rate.

The effects of changing climate on all of the growth rate determining variables is shown in table 3.2 for flowstone samples and a variety of possible combinations of changes in calcium concentration, temperature and water flux. Growth rates are

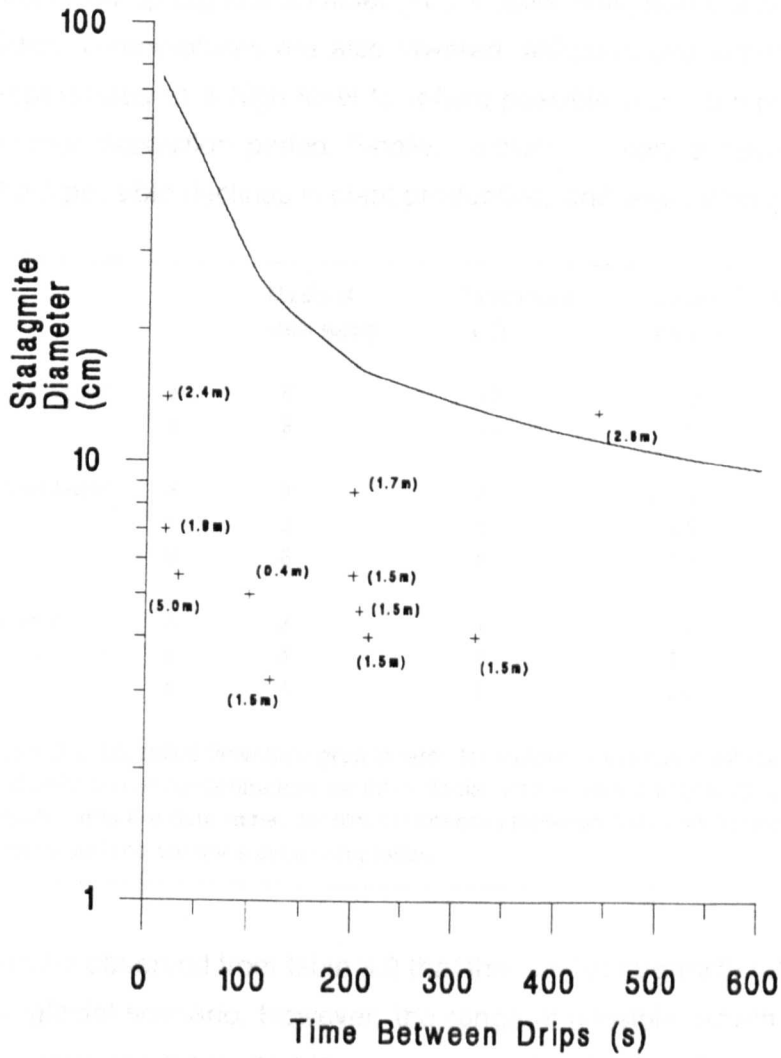

Figure 3.14. Drip rate / stalagmite diameter relationship as proposed by Dreybrodt (1988) (solid line), and as measured in this study in G.B. Cave and Lower Cave (points), with drip fall heights shown in brackets.

modelled for three possible scenarios; inter-glacial, inter-stadial and glacial conditions in the United Kingdom. In the former, water availability is assumed to be for 6 to 9 months of the year, with limited supply only in the summer when evaporation may exceed precipitation. Mean annual temperature is assumed to be 10 °C, the same as that today, and calcium ion concentrations 2.0 mmol l^{-1}, again typical of values measured today. For inter-stadial and glacial conditions, these variables are altered to reflect a deterioration in climate. The length of water availability is decreased to reflect only spring and summer groundwater flow, with the ground assumed frozen in winter. Temperatures are also lowered, although one scenario ("glacial - a") keeps temperatures at a high level to reflect possible warm temperatures during a limited summer deposition period. Finally, calcium ion concentrations are also lowered, to reflect possible declines in plant productivity and vegetation change.

		Months of water supply	Temperature (°C)	Calcium Concentration (mmol l^{-1})	Growth Rate (mm yr^{-1})
"Inter-Glacial"	a	6	10	2.0	0.006 - 0.077
	b	9	10	2.0	0.009 - 0.116
"Inter-Stadial"	a	3	8	1.0	0.001 - 0.008
	b	3	8	2.0	0.002 - 0.032
	c	6	8	2.0	0.005 - 0.063
"Glacial"	a	2	10	2.0	0.002 - 0.025
	b	4	5	1.0	0.001 - 0.014
	c	4	5	2.0	0.002 - 0.030

Table 3.2. Modelled flowstone growth rates for variations in seasonality of water supply, temperature and calcium ion concentrations for inter-glacial, inter-stadial and glacial scenarios. The range of growth rates are determined for film thicknesses between 0.01 and 0.2 mm, the range observed upon flowstone samples depositing today.

It can be observed from table 3.2 that the maximum growth rates are predicted for the inter-glacial scenario. However, the range of possible growth rates under all climatic conditions are large, and is greater than the changes between scenarios, reflecting the importance of the water film thickness term. If film thickness remains constant or exhibits only small variations over time, then the other variables will dominate. Whether this occurs in nature is unknown, but can be tested by analysing flowstone samples which have grown during periods of known Quaternary climate change.

Stalagmite samples may be expected to show similar trends in growth rate under changing climatic conditions, especially if they also exhibit seasonal cessation of water supply, and would respond in a similar fashion to that demonstrated in table 3.2. However, many samples have a continuous water feed, and thus variations in

drip rate become important. Table 3.3 incorporates this variable and shows the sensitivity of stalagmite growth rate to climate change; drip rates are varied in the range 10 to 500 seconds between drips. It can be observed that changes in drip rate have a relatively insignificant effect, and temperature and calcium ion concentration have the greatest influence on growth rate. Again, variations in film thickness would have a significant effect, but if these can be assumed constant for all drip rates, then a precise signal can be obtained. Such a constancy of water film thickness is demonstrated in section 4.3.1.2.

		Time between drips (s)	Temperature (°C)	Calcium Concentration (mmol l^{-1})	Growth Rate (mm yr^{-1})
"Inter-Glacial"	a	10	10	2.0	0.055
	b	100	10	2.0	0.053
"Inter-Stadial"	a	100	8	1.0	0.012
	b	100	8	2.0	0.045
	c	300	8	2.0	0.042
"Glacial"	a	300	10	2.0	0.049
	b	500	5	1.0	0.007
	c	500	5	2.0	0.028

Table 3.3. Modelled growth rates for variations in drip rate, temperature and calcium ion concentrations for stalagmites for inter-glacial, inter-stadial and glacial scenarios. Growth rates are shown for a constant water film thickness of 0.05 mm, a result demonstrated in chapter 4. Water supply is assumed continuous over the course of a year.

In general, significant increases in growth rate of both stalagmites and flowstones may be expected from ameliorations in climate. A more detailed investigation of this record is not possible since precise palaeo-records of drip rate, water flux or calcium concentration are not preserved within speleothems. It has been demonstrated in section 2.2 that calcium concentration cannot be substituted for temperature; and at present, very few speleothem samples have yielded reliable palaeo-temperature signal through $\delta^{18}O$ or D/H records, which would allow the elimination of temperature (for a review see Gascoyne, 1992). In the absence of other records, the palaeoclimate record contained within the growth rate signal cannot be interpreted in terms of absolute changes of temperature, water flux and calcium ion concentrations, since none of the variables are determinable or can be assumed to be constant over time. Furthermore, the possibility of foreign ion effects, turbulent flow conditions and the disagreement between experimental and theoretical growth rate values all suggest that measures of growth rate may not solely reflect changes in climate. A growth rate record from an individual sample growing over one time period cannot therefore be used to infer an unambiguous palaeoclimate signal. Multiple samples

with records preserved over the same time period would allow a more confident interpretation of the growth rate record, if they showed the same relative response to the palaeoclimate signal. Such a record is sought from samples analysed in chapters 4 to 6.

3.4.2 Growth Rate Theory and Growth Hiatuses

Growth rate theory can also provide a better understanding of how changes in palaeoclimate can potentially cause cessation of speleothem growth giving a hiatus, as described in chapter 2.2. From equations (3-3) and (3-6), growth *will* cease when:

a) drip rate or film thickness equals zero. This is likely to occur when annual precipitation is low, and / or evaporation exceeds precipitation.

b) $[Ca] < [Ca_{eq}]$; which occurs when the calcium ion concentration falls below the range 0.56 to 1.00 mmol l^{-1} for mean annual temperatures between 5 and 20 °C and cave pCO_2 levels between $3x10^{-4}$ and $1x10^{-3}$ atm. Calcium ion concentrations may change in response to the many factors discussed in section 2.2.

Growth *may* also cease when:

c) Temperatures are low. Continual temperatures below 0 °C may lead to the ice-locking of water supply and thus cessation of growth. Low temperatures on their own will not necessarily prevent speleothem deposition, since a positive growth rate at this temperature has been proven (Dreybrodt, 1981).

As well as the factors presented above, geological processes may also be important in limiting growth. Sedimentation, either upon the speleothem, or within the fissure feeding the deposit, may terminate growth temporarily or permanently. Flow switching between different routes in the karst aquifer may also cause growth to cease under certain hydrological conditions. Flooding of the cave system would also halt growth, this may occur due to sea-level rise or a rise in groundwater levels.

Growth rate theory demonstrates the potential importance of palaeoclimatic factors in causing growth hiatuses. This will be investigated empirically in chapter 5, where mass spectrometric analyses upon long flowstone sequences will be used to define both variations in growth rate and the timing of growth cessation. The latter will then be compared to the theory presented above.

3.5 Conclusions

Growth rates may provide a relative record of palaeoclimate change. Multiple samples should be obtained for an individual time period in order to confirm this palaeoclimate signal. In theory, increases in growth rate correlate with increasing temperature, water availability and calcium concentrations. Testing growth rate theory in the present day cave environment where these variables are known is undertaken in chapter 4 to provide further confirmation of the validity of the theory. In parallel, studies of Quaternary samples were undertaken using both mass spectrometric uranium series dating (chapter 5) and annual luminescence banding techniques (chapter 6).

CHAPTER FOUR

FIELD MEASUREMENTS OF SPELEOTHEM GROWTH RATE

4.1 Introduction

Sections 3.2, 3.3 and 3.4 described both the kinetic theory of speleothem growth rate, and its potential in providing a palaeoclimate signal. However, as previously stated, the theory has never been tested in the cave environment, due to the difficulties in measuring low rates of growth; the one laboratory experiment on stalagmite growth rate was reported in section 3.3 (Figure 3.2), in order to test the accuracy of the growth rate theory. Further work is necessary on both stalagmites and flowstones in a cave environment, where all the variables affecting growth rate can be determined. Only then can the record of growth rate change derived from mass spectrometric uranium-series (MSU) dating (chapter 5) or annual luminescence banding (chapter 6) be interpreted for the Quaternary.

Two separate groups of experiments were performed. The first experiments were to test assumptions about film thickness variations made in the growth rate model, as noted in section 3.3 and detailed below. The second were to compare growth rates of samples forming today to that predicted theoretically from measurements of the parameters affecting growth rate (calcium concentration, water film thickness, discharge and temperature). This was undertaken for both stalagmites and flowstones.

4.2 Film Thickness Experiments

4.2.1 Methods

The theoretical model of speleothem growth rate makes several assumptions about film thickness variations on both flowstone and stalagmites which need to be tested under either laboratory or field conditions (see section 3.3).

1) That the water film thickness on a stalagmite cap is equal to 0.1 mm, that obtained by Dreybrodt (1980) under laboratory conditions. This can be tested by taking field measurements using a vernier spherometer graduated to a precision of 0.01 mm. The distance to both the water film surface and speleothem surface were

obtained, the difference between them giving the film thickness. At least six measurements of film thickness were obtained per site (e.g. on the cap of a stalagmite).

2) That water film thickness on a stalagmite cap is independent of drip rate. This can be investigated by measuring discharge onto the sample by recording the drip rate of the drip feeding the stalagmite. Water film thickness is also measured, as described above.

3) No studies have been made of film thickness on flowstones, or how it may depend on the nature of the water feeds (single or multiple drip sources), the gradient of the flowstone and total discharge. A laboratory experiment was set up to investigate the interrelationship of these factors upon a perfectly plane surface. Water was dripped onto a a cut section of Carboniferous limestone from one to three burette sources, and the water film thickness measured (in sextuplet) at 5, 10, 15 and 20 cm distances from the drip source(s) using a spherometer. The gradient of the surface was altered between experiments, and discharge was also varied over the range expected for flowstones. The same experiment was also performed in the cave environment, so that a comparison could be made between the plane surface and more typical flowstone surfaces.

4.2.2 Results

4.2.2.1 Field Experiments of Stalagmite Cap Film Thickness.

An estimate of film thickness variability for an individual stalagmite cap was obtained from multiple measurements on 6 samples from Kent's Cavern and Lower Cave. The results from the variability measurements are shown in Table 4.1. The coefficient of variation within individual samples was low, ranging between 2% and 56%. Samples were also used to investigate the film thickness - discharge relationship; no relationship was assumed by Dreybrodt (1980; 1988). The results are shown in figure 4.1; error bars are 1σ errors based on suites of six film thickness measurements made upon each stalagmite cap. The results show that no relationship exists between drip rate and film thickness ($r= 0.299$; $n=6$; insignificant at a 95% level); with the variability of film thickness for each stalagmite greater than any caused by drip rate variations. Hence the assumptions of Dreybrodt (1980; 1988) are correct.

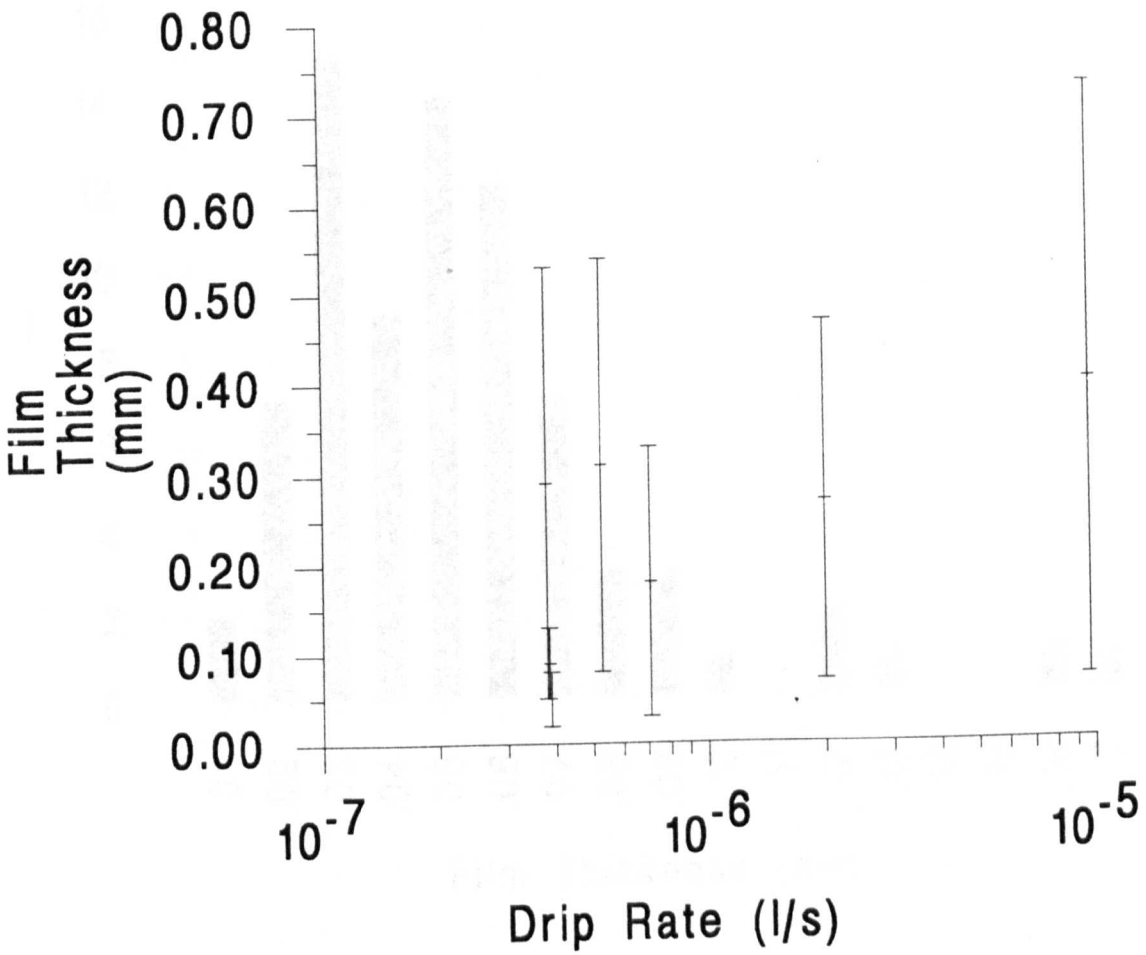

Figure 4.1. Relationship between drip rate and water film thickness on stalagmite caps. Error bars are 1σ.

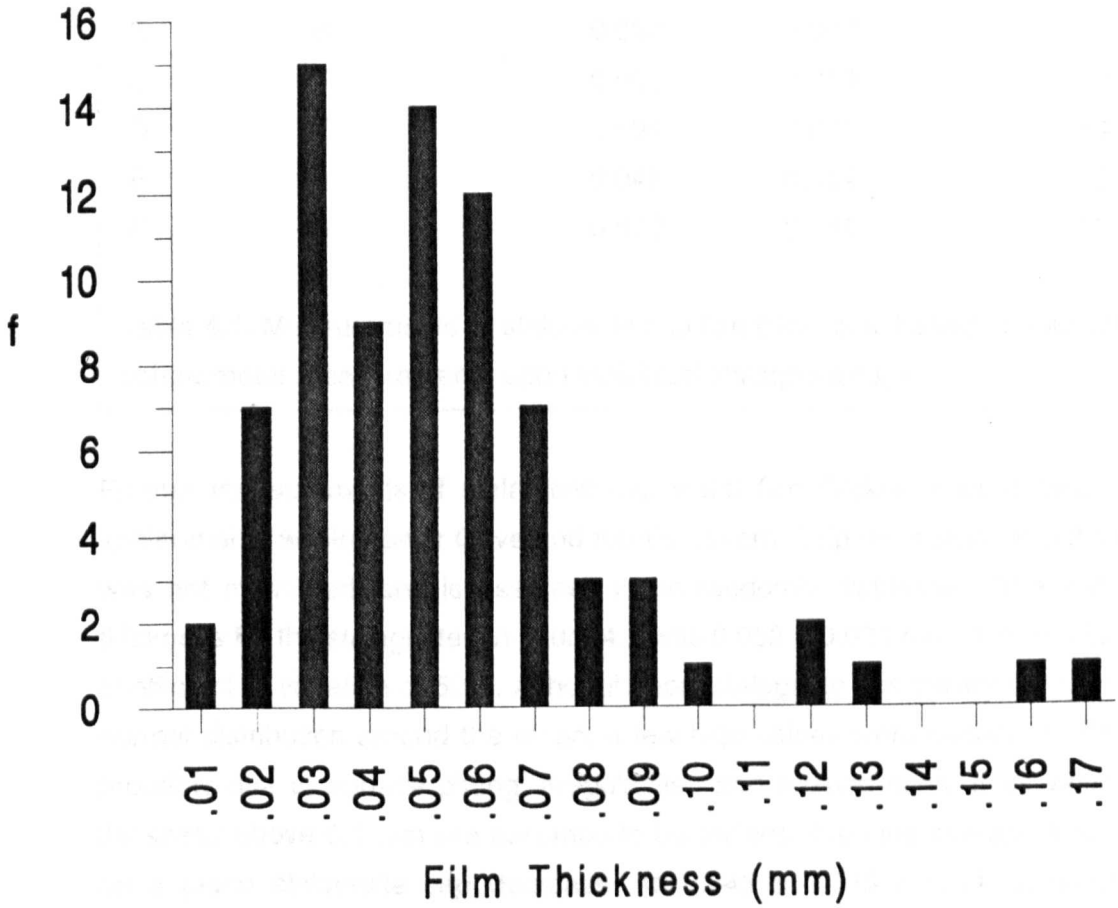

Figure 4.2. Frequency distribution of mean stalagmite cap film thickness measurements.

Sample	*Number of Measurements*	*Mean (mm)*	*1 σ error (mm)*	*Coefficient of Variation (%)*
A	7	0.034	0.016	46
B	6	0.033	0.007	21
C	7	0.064	0.019	29
D	7	0.094	0.051	54
E	6	0.048	0.014	30
F	6	0.078	0.045	56

Table 4.1. Measurements of stalagmite cap film thickness, based on multiple spherometer measurements upon individual stalagmite caps.

Further measurements of stalagmite cap water film thickness were taken from 26 speleothems within Lower Cave and Kent's Cavern. Drip discharge onto the samples was not measured, and is assumed to be randomly distributed. The average film thickness for the stalagmites in figure 4.2 was 0.052 ± 0.031 mm (1 σ; n=78), giving a coefficient of variation of 59%. Although most stalagmite film thicknesses fell within a normal distribution around the mean, a few high values were observed. These were probably due to surface pitting, irregularities and erosion cups. If all values of film thickness above 0.1 mm are assumed to be outliers, then the average film thickness on a plane stalagmite cap decreases to 0.045 ± 0.019 mm (1 σ, n=72) with a coefficient of variation of 43%. Overall levels of film thickness were significantly lower than that recorded by Dreybrodt (1980) in his laboratory experiments.

4.2.2.2 Laboratory Experiments of Flowstone Film Thickness.

The results of the investigation of the variation of film thickness with distance for a constant slope angle are presented in Figure 4.3. They show no significant variation of film thickness with distance (r = 0.03; n = 4; insignificant at a 95% level).

The variation of film thickness with discharge for a differing number of drip sources was investigated in more detail for a slope of constant gradient. The results are shown in figure 4.4. The number of drip sources has no effect on the discharge - film thickness relationship. However, there does appear to be a relationship between the film thickness and drip discharge for all number of drip sources, at a high level of significance:

log (film thickness) = 0.247 + 0.179 x log (drip rate) (4-1)

r = 0.78; n=19; significant at a 95% level.

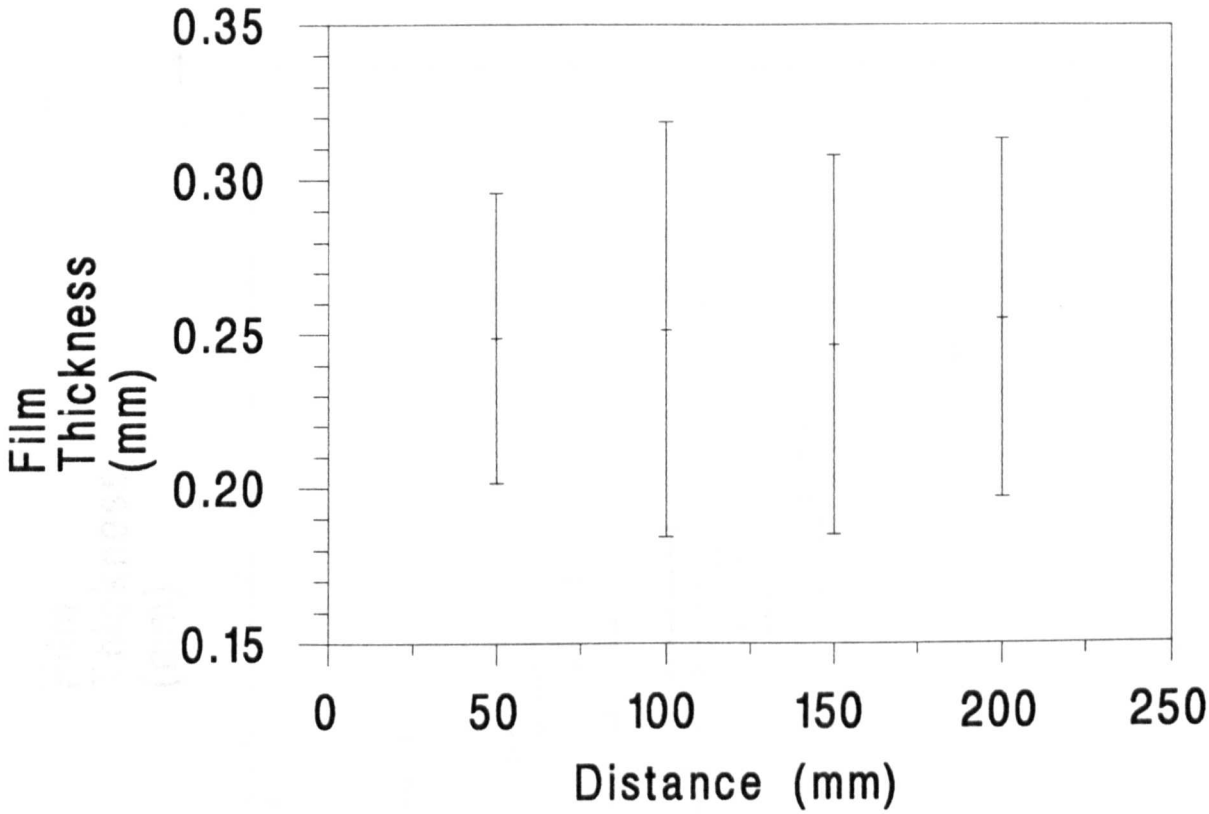

Figure 4.3. Relationship between film thickness and distance from drip source for a plane surface, constant discharge and slope angle. Error bars are 1σ.

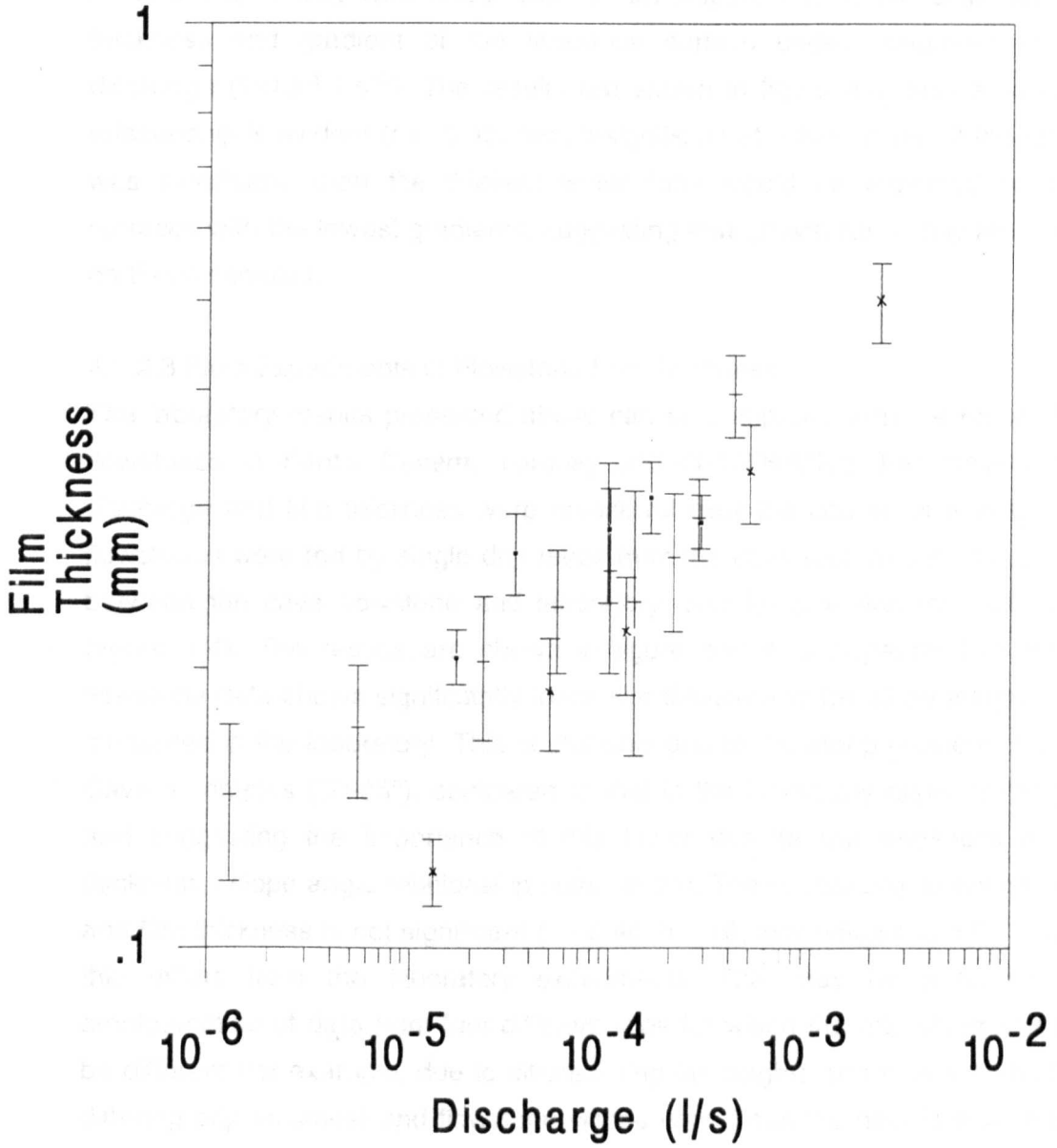

Figure 4.4. Relationship between film thickness and discharge for a plane surface and constant slope angle. Error bars are 1σ. Discharge is from one drip source (bars), two sources (squares) or three sources (crosses).

At no time does the film thickness increase beyond a maximum of 0.45 ± 0.1 mm for a slope angle of 18°.

A third experiment was undertaken to investigate the relationship between film thickness and gradient of the flowstone surface under conditions of constant discharge ($1x10^{-4}$ l s^{-1}). The results are shown in figure 4.5, only a weak inverse relationship is evident (r = -0.45; n=5; insignificant at a 95% level). If the relationship was significant, then the thickest water films would be expected on flowstone surfaces with the lowest gradients, suggesting that growth rates may also be greater on these samples.

4.2.2.3 Field Experiments of Flowstone Film Thickness

The laboratory results presented above can be compared with the results from five flowstones in Kent's Cavern, Torquay (KC-91-1/5/6/8/10). For these sites, both discharge and film thickness were measured over the course of a year. All these flowstones were fed by single drip feeds from the cave roof, and thus a comparison between the cave flowstone and laboratory data for one drip feed can be made (figure 4.4). The results are shown in figure 4.6; it is apparent that the natural flowstone data shows significantly lower film thicknesses for all discharges than that measured in the laboratory. This is probably due to the steep gradient of the Kent's Cavern samples (50-85°), compared to that in the laboratory experiments (10-50°), and suggesting the importance of this factor despite the weakness of the film thickness - slope angle relationship noted above. The relationship between discharge and film thickness is not significant (r = 0.44; n = 16; insignificant at a 95% level) and this differs from the laboratory experiments. This may be a function of the amalgamation of data from four different sites for which the drip characteristics may be different (for example, due to different drip fall heights and thus splash effects, or differing drip volumes) and flowstone slopes vary. Thus the data is broken down for two of the five constituent sites (for which n>4) in figure 4.7. For both these sites, there is no relationship between film thickness and drip rate (r = 0.42, n = 5; and r = 0.81, n = 4; for KC-91-6 and KC-91-10 respectively, both insignificant at a 95% level). This data confirms that a drip rate / film thickness relationship cannot be identified for flowstones in this case. The average film thickness for all Kent's Cavern samples under all discharge conditions was 0.098 ± 0.050 mm (1σ error; n=22), giving an expected 2σ range of values between 0.0 and 0.2 mm. The 1σ errors for all film thicknesses measured in the cave environment were much higher than in the laboratory experiment (a coefficient of variation of ≈50% in the cave against ≈20% in the laboratory); probably an indication of the heterogeneity of the flowstone surface,

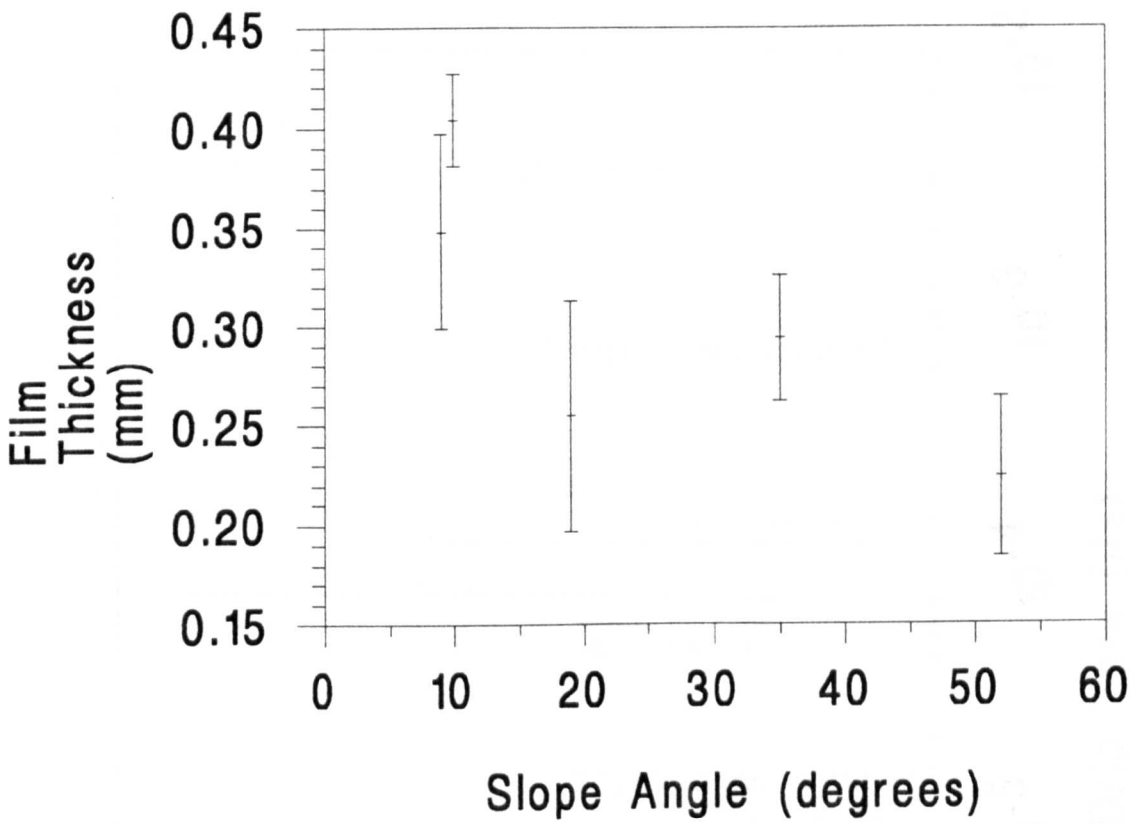

Figure 4.5. Relationship between film thickness and slope angle for a plane surface under constant discharge conditions. Error bars are 1σ.

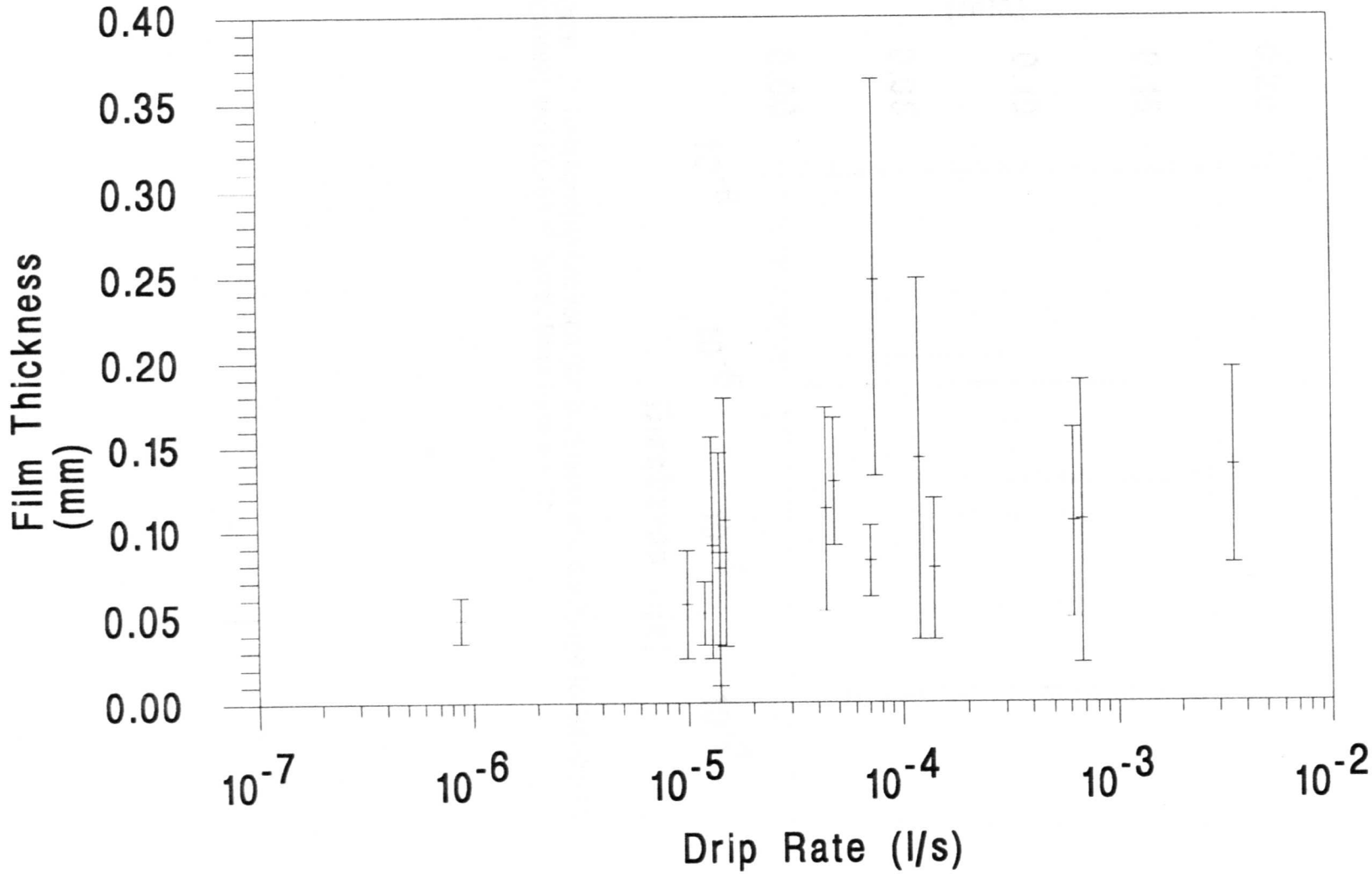

Figure 4.6. Relationship between film thickness and drip rate for Kent's Cavern flowstone sites. Error bars are 1σ.

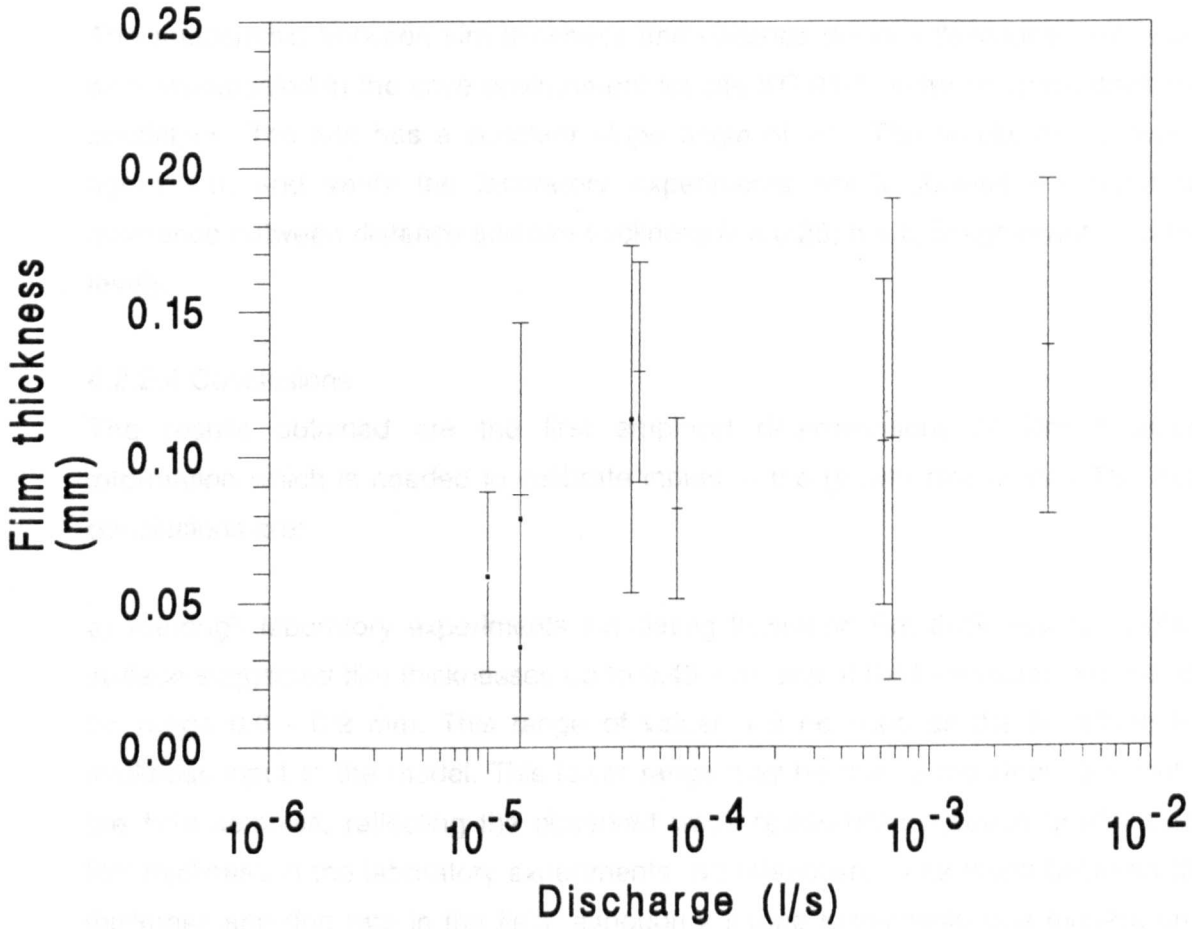

Figure 4.7. Relationship between film thickness and discharge for KC-91-10 (squares) and KC-91-6 (bars). Error bars are 1σ.

which may also be obscuring the expected relationship between drip rate and film thickness.

The relationship between film thickness and distance down a flowstone profile was also investigated in the cave environment for site KC-91-6 under constant discharge conditions. The site has a constant slope angle of 75°. The results are shown in figure 4.8, and verify the laboratory experiments which showed no significant difference between distance and film thickness ($r = 0.25$; $n = 6$; insignificant at a 95% level).

4.2.2.4 Conclusions

The results obtained are the first empirical determinations of film thickness information which is needed to calibrate inputs to the growth rate model. The main conclusions are:

a) Although laboratory experiments simulating flowstone film thickness on a plane surface suggested film thicknesses up to 0.45 mm, actual field measures were in the 2σ range 0.0 - 0.2 mm. This range of values will be used as the flowstone film thickness input to the model. This lower range may be due to the steep gradient of the field samples, reflecting the observed weak relationship between gradient and film thickness in the laboratory experiments. No relationship was found between film thickness and drip rate in the field, although a strong relationship was evident on a plane surface under laboratory conditions. This suggests that other factors, such as flowstone surface heterogeneities, may be obscuring the relationship. Variations in film thickness with distance from the drip source were shown to be insignificant, both in the field and laboratory.

b) The average value of water film thickness on a stalagmite cap was found to be 0.052 ± 0.031 mm (1σ, $n=78$), significantly lower than the figure used by Dreybrodt (1980). This value will subsequently be used in all model predictions. No relationship was found between drip rate and film thickness over the range of drip rates investigated.

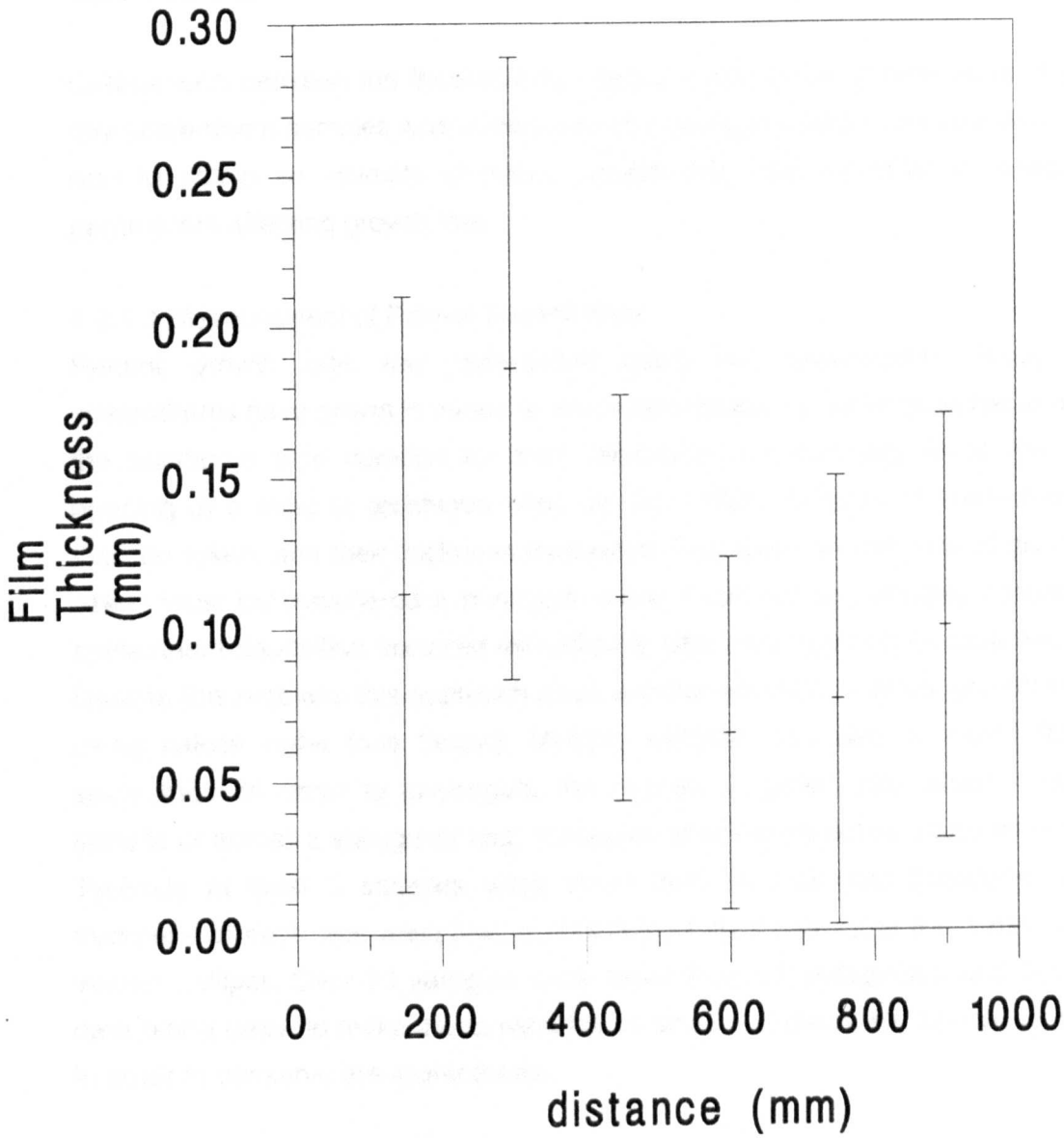

Figure 4.8. Relationship between film thickness and distance for KC-91-6 under constant discharge conditions. Errors are 1σ.

4.3 Testing the Growth Rate Theory

4.3.1 Methods

Comparison between the theoretically predicted and actual growth rates of present day speleothem samples was undertaken by making two sets of measurements. One was to obtain an estimate of recent growth rate, and the other to measure the parameters affecting growth rate.

4.3.1.1 Measurement of Recent Growth Rate.

Recent growth rate was determined using two approaches. Firstly, where speleothems have grown in mines or excavated caves, it may be possible to estimate the maximum time duration for their deposition; for example, since the date of opening of a mine (a technique used by Orr, 1952). Samples of speleothems can then be taken, and their thickness measured. This gives an estimate of growth rate, which must be considered a minimum, since it can not be definitely assumed that speleothem deposition occurred immediately after mine opening or cave excavation. Despite this problem, this approach gives a better estimate of actual growth rate than using calcite slabs (see below). Multiple samples can also be taken from one speleothem in order to investigate the change in growth rate down a flowstone sample or across a stalagmite cap, measures which could not be obtained otherwise. Typically at least 3 samples were taken from an individual flowstone, and the thickness of each was measured a minimum of six times using a 0.1 mm precision vernier calliper. Over 70 samples were taken from 32 stalagmites and flowstones, care being taken to make these samples as small and discretely located as possible in order to conserve the speleothems.

A second approach involved placing thin slabs of calcite onto the surface of the speleothems for a period of 3 to 12 months, and then measuring their mass increase to obtain a growth rate estimate. Samples of approximate dimensions 10.0 x 5.0 x 0.2 mm were cut from a pure marble slab using a precision diamond wire saw, etched using ≈ 4N HCl for 30 s, and subsequently dried at 105 °C for 24 hours, placed to cool in a desiccator, and weighed using a 5 decimal place precision top-pan balance. After being recovered from the field, the slabs were again dried and reweighed. Assuming that growth only occurred on the top surface of the slab, and that the slabs were not significantly thick (with no growth on the sides of the slab), then the increase in mass was converted to a measure of growth rate. From the surface area and change in mass, and exposure time of the slabs, an estimate of weight increase in g

cm^{-2} was obtained, and converted to change in slab thickness (growth rate) using the known density of speleothem calcite (2.75 g cm^{-3}; Hill and Forti, 1986).

Slabs were placed on a variety of speleothems, both those for which an estimate of growth rate was possible from sample thicknesses (to provide a comparison of the precision of the two approaches), and on those for which no other measurements were possible (in order to obtain a growth rate estimate). In order to determine the errors associated with the measurement of such small mass increases, one sample was repeatedly dried, desiccated and reweighed after removal from the cave, to obtain a measure of the accuracy of the weighing and handling procedure. Duplicate slabs were also placed at one site (Lower Cave), in order to obtain an estimate of the variability of growth rate at one site. In previous experiments investigating mass increases of calcite crystals in tufa depositing karst streams, weight increases were shown to vary by a factor of x1.1 - 19 less than that theoretically predicted (Hermann and Lorah, 1988). In a similar experiment, Dreybrodt et al (1992) observed a typical error of ± 20% between duplicate analyses. Such high errors may be due to many factors, and apply to the calcite slab experiments in this study. Berner (1980) demonstrated that seeding was necessary before crystal growth could start from nuclei, and surface roughness variations have also been shown to be important (Compton and Daly, 1986). The latter should not be a factor in this study as all slabs were etched for an equal time period. Physical entrapment of sediments may occur, which could cause a great overestimate of the weight change due to precipitation. Finally, water flow may be diverted around the slabs placed on flowstones, since the minimum slab thickness (0.2 mm) is of the same magnitude as the expected water film thickness (0.0 to 0.2 mm), leading to an underestimate of the growth rate.

Both slab weight increases and sample thickness measurements could be used in combination with estimates of growth rates determined from MSU dating (chapter 5) or from annual luminescence bands (chapter 6). In practice, however, the samples did not contain the luminescence banding signal, and although MSU dating is possible on recent samples (Edwards, 1988; Richards, unpub. data), it was not generally feasible in this study.

4.3.1.2 Measurement of Growth Rate Parameters

As described in section 3.3, three major variables determine growth rates; calcium concentrations, temperature, and water flux (film thickness, water drip rate and seasonality of water flow). All three are measurable in the cave environment, and were determined over the course of an annual field cycle for speleothems whose

growth rate had been determined by the methods outlined above. This cycle took place over the period May 1991 to October 1992, with several interruptions due to injury and MSU dating work in Minneapolis.

Calcium concentrations in the cave waters were measured using standard EDTA titrations. Drip waters were collected in 125 ml glass sample bottles; bottles were filled to the top and stoppered to prevent degassing, and the titrations were performed in the minimum possible time (usually under 24 hours from collection). Samples were collected as close to the water source in the cave as possible (to prevent degassing), taking care not to include particles of bedrock which would contaminate the sample. In many cases, titrations against EDTA were also performed to obtain a total hardness measure, to determine if there was a significant magnesium concentration which may effect growth rates if precipitated. For flowstones, where possible calcium concentrations were also obtained at the base of the deposit to determine the change in calcium saturation over the surface of the speleothem. With stalagmites, water drip rates were frequently so slow as to make the collection of water samples for titration impossible. Occasionally samples were collected from nearby fast dripping sources, although such samples may be expected to poorly estimate actual calcium concentration due to different groundwater residence times.

Film thickness measurements were obtained on speleothems, using the vernier spherometer, at least six measurements of film thickness were obtained per site. Where possible, a measure of discharge onto the sample was also obtained by recording the drip rate of any drip feeding onto the flowstone or stalagmite, to give a record of the seasonal variation of the water flow.

Occasional temperature measurements were made to confirm that drip temperature approximates to the mean annual temperature for the region (9 to 11 °C; Wigley and Brown, 1977). All measurements made in this study varied between 10 and 11 °C. A value of 10 °C is used in all experimental calculations. Cave air pCO_2 was not measured, but assumed to be $3x10^{-4}$ atm. Such an approximation does not have a significant effect on growth rate, as shown in chapter 3.

4.3.2 Flowstone Growth Rate Results

Comparison between theoretical and actual flowstone growth rates was undertaken at several sites, each of which are detailed in this section.

4.3.2.1 Kent's Cavern

An investigation into the growth rate of flowstones within Kent's Cavern was undertaken using 10 flowstones with different hydrological characteristics, the locations of which are shown in figure 4.9. The flowstones were situated below the level of a former stalagmite floor; the part of the cave system dug by Pengelly between 1865 and 1880 during archaeological investigations (Proctor and Smart, 1989). Thus, for this section of the cave, the maximum age of the deposits is known.

The flowstones fall into 3 groups. KC-91-1 (Wolf's Cave), KC-91-6 (High Level Chamber) and KC-91-10 (Charcoal Cave) were observed to have a continuous drip source and remain wet all year around. KC-91-5 (High Level Chamber), KC-91-8 (Wolf's Cave) and KC-91-11 (South Sally Port) were all observed to have water flows for longer than 4 months in a year, mostly during the winter months. KC-91-2 and 3 (North Sally Port) and KC-91-4 (South Sally Port) were observed to be dry in summer, and have a moist water film in winter for less than four months; however, the water source was from seep(s), and no drip sources were evident. For flowstones with a prominent drip source (KC-91-1,5,6,8,10), calcium samples and drip rate and film thickness measurements were collected. Samples were also taken at both the drip source and base of the flowstone where possible. The flowstone thickness was also measured for all 10 flowstones, and the results are shown in table 4.2; calcium concentrations, drip discharges and film thickness measurements are shown in tables 4.3, 4.4 and 4.5.

The measured calcium concentration and film thickness were used as inputs into the growth rate model for the five samples for which both values had been obtained. Values of film thickness of 0.10 ± 0.05 mm (the mean and 1σ error reported in section 4.2.2.3) were used; calcium values used were the mean and 1σ deviation of those obtained over the annual cycle. The partial pressure of carbon dioxide in the cave atmosphere was assumed constant at 3×10^{-4} atm, and the water temperature taken as equal to the mean annual temperature of 10 °C. The calculated growth rate was compared to the (minimum) growth rates determined from sample thicknesses (table 4.6). Except for the top 50 cm of site KC-91-1, which is discussed later, growth rates are lower than that predicted by the theory. However, actual and predicted values all agree within the 2σ errors of the determinations.

If there is an overprediction of growth rate by the theory, it may be explained by either:

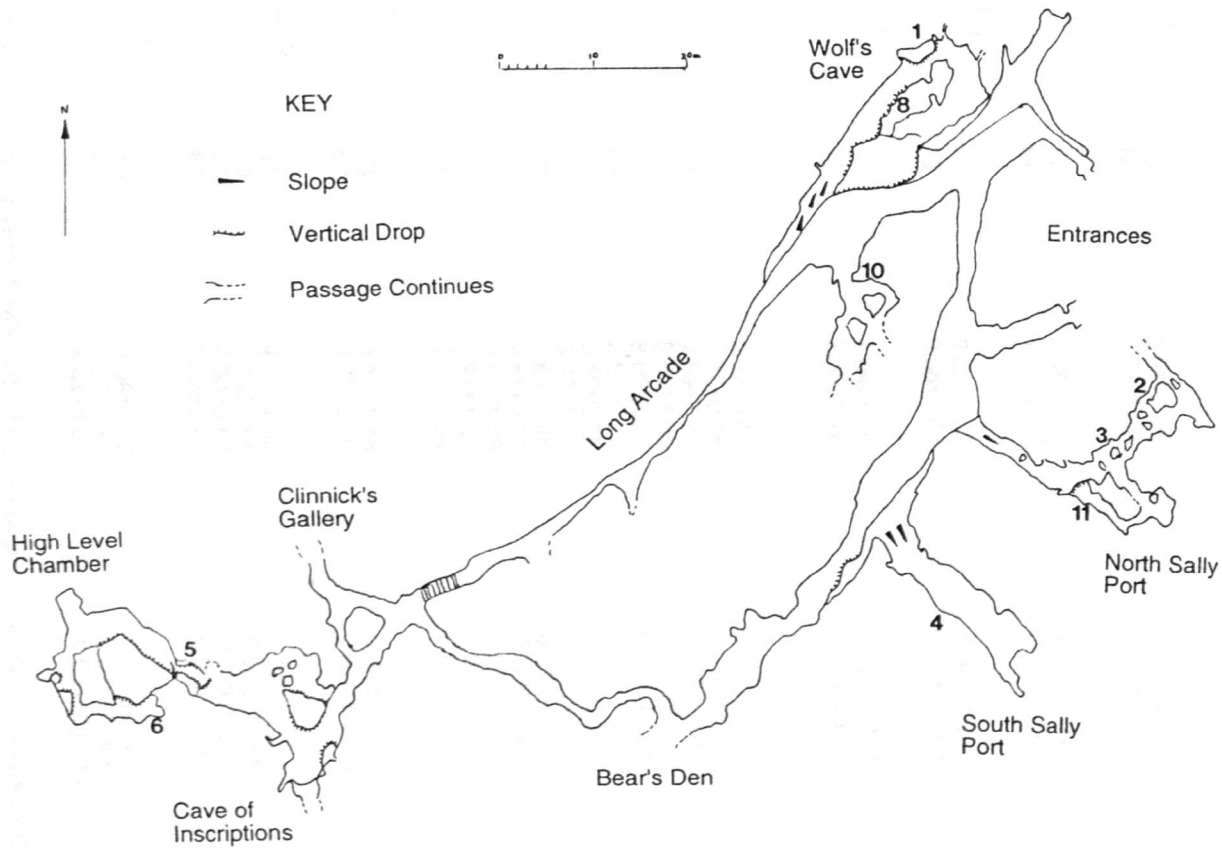

Figure 4.9. Simplified survey of Kent's Cavern (BCRA Grade 5d; modified from Proctor and Smart, 1989), showing positions of flowstone sites (numbered 1-6,8,10,11).

KC-91-1 Angle (deg)	Distance (cm)	Thickness (mm)	Growth Rate (mm yr^{-1})
5	15	30.57±4.75	0.261±0.041
5	30	23.03±6.37	0.217±0.060
5	32	15.88±5.05	0.130±0.041
5	45	23.82±4.36	0.174±0.032
80	75	3.74±1.18	0.033±0.010
70	90	1.98±0.92	0.017±0.008
75	105	1.98±1.00	0.017±0.009
75	120	2.63±0.92	0.023±0.008
80	125	2.12±0.44	0.018±0.004
85	147	1.01±0.60	0.009±0.005
85	150	1.30±0.58	0.011±0.005
KC-91-2			
85	20	2.95±2.00	0.025±0.017
85	42	2.03±1.04	0.018±0.009
KC-91-3			
85	11	1.38±1.16	0.012±0.010
85	84	1.39±0.98	0.012±0.008
KC-91-4			
85	21	0.83±0.62	0.007±0.005
85	53	0.38±0.68	0.003±0.005
KC-91-5			
85	21	1.68±1.36	0.015±0.012
85	42	2.68±1.18	0.023±0.010
KC-91-6			
75	21	3.57±0.56	0.031±0.005
		1.86±0.88	0.016±0.008
75	30	2.69±1.41	0.023±0.012
		3.38±1.49	0.029±0.013
		8.00±3.00	0.069±0.026
75	42	2.86±0.22	0.029±0.022
		0.55±0.32	0.005±0.003
		3.32±2.20	0.029±0.019
75	60	1.84±1.48	0.016±0.012
		2.61±0.76	0.023±0.007
		3.85±1.22	0.033±0.010
75	63	3.97±1.42	0.035±0.014
75	84	1.38±0.34	0.012±0.004
KC-91-8			
85	63	4.12±1.16	0.036±0.010
85	69	5.70±0.66	0.050±0.006
KC-91-10			
50	15	4.36±1.42	0.038±0.012
50	30	5.95±1.84	0.052±0.016
50	45	4.33±0.64	0.038±0.006
50	60	3.25±1.41	0.028±0.012
KC-91-11			
90	10	2.04±0.75	0.018±0.007
45	40	5.25±0.57	0.045±0.005
90	90	5.94±2.40	0.051±0.021

Table 4.2 Kent's Cavern flowstone data. Flowstone angle is measured to the nearest 5°, sampling distance from the drip / seep source to the nearest cm. Uncertainties in flowstone thickness are 1σ derived from multiple measurements made upon each sample. Growth rates are minima, based on sample deposition starting in 1876.

Site	21/6/91	28/6/91	26/7/91	23/8/91	8/11/91	20/12/91	12/2/92	26/3/92	21/5/92	2/7/92	Mean
KC-91-1T	2.07	2.83	3.00	2.80	2.85 (3.18)	2.55	2.29	2.75	-	-	2.64±0.32
B	-	2.13	-	-	-	-	1.80	1.38	-	-	1.77±0.38
KC-91-5	-	Dry	Dry	2.00	1.45	1.23	2.00	Dry	Dry	Dry	1.67±0.39
KC-91-6	0.83	1.23	0.88	1.40	1.73 (2.10)	1.43	1.25	1.70	1.55	1.80	1.38±0.34
KC-91-8T	2.72	Dry	Dry	Dry	2.55 (2.83)	2.33	2.40	2.43	Dry	Dry	2.49±0.15
B	-	Dry	Dry	Dry	2.30 (2.50)	2.22	2.00	-	Dry	Dry	2.17±0.16
KC-91-10	2.70	2.47	2.40	-	2.48 (2.78)	2.27	1.93	2.35	2.35	2.15	2.34±0.22

Table 4.3. Kent's Cavern calcium concentrations of drip sources. Values are in mmol/l. Errors on individual analyses are ±0.05 mmol l^{-1}. Values in brackets are for total hardness. - signifies occasions when drip rates were too low for measurements to be made, dry signifies that no drips were present. Mean and 1σ error are calculated for each site.

Site	*28/6/91*	*8/11/91*	*12/2/92*	*26/3/92*	*21/5/92*	*Mean*
KC-91-1	0.249±0.116	-	0.143±0.106	-	0.052±0.018	0.158±0.125
KC-91-4	-	0.137±0.138	-	0.015±0.089	-	0.117±0.070
KC-91-5	Dry	0.091±0.065	0.048±0.013	0.063±0.027	0.057±0.019	0.069±0.047
KC-91-6	0.106±0.083	0.105±0.056	0.138±0.058	0.082±0.031	0.129±0.038	0.111±0.057
KC-91-8	Dry	0.114±0.056	0.078±0.041	0.106±0.073	0.023±0.025	0.086±0.060
KC-91-10	0.034±0.053	0.113±0.060	-	0.078±0.068	0.057±0.031	0.073±0.061

Table 4.4. Kent's Cavern water film thicknesses. Values are in mm. Errors are one sigma, based on sets of over 6 measurements per site. - signifies that measurements were not determined.

Site	*21/6/91*	*28/6/91*	*23/8/91*	*8/11/91*	*20/12/91*	*12/2/92*	*26/3/92*	*21/5/92*	*2/7/92*	*Mean*
KC-91-1	-	7.5×10^{-5}	2.8×10^{-6}	5.9×10^{-5}	1.1×10^{-4}	1.2×10^{-4}	3.3×10^{-5}	1.2×10^{-5}	2.3×10^{-6}	$5.2\pm4.7\times10^{-5}$
KC-91-5	-	Dry	1.3×10^{-5}	6.3×10^{-7}	5.0×10^{-6}	8.8×10^{-7}	Dry	Dry	Dry	$4.9\pm5.8\times10^{-6}$
KC-91-6	4.4×10^{-4}	6.8×10^{-4}	6.2×10^{-4}	3.1×10^{-4}	5.0×10^{-4}	3.5×10^{-3}	7.1×10^{-5}	4.8×10^{-5}	5.0×10^{-5}	$6.9\pm11.0\times10^{-4}$
KC-91-8	-	Dry	Dry	1.4×10^{-4}	1.6×10^{-4}	1.4×10^{-4}	1.5×10^{-5}	Dry	Dry	$11.0\pm6.7\times10^{-5}$
KC-91-10	1.4×10^{-5}	1.4×10^{-5}	4.4×10^{-5}	3.2×10^{-5}	2.1×10^{-5}	2.4×10^{-5}	1.4×10^{-5}	9.9×10^{-6}	-	$2.2\pm1.2\times10^{-5}$

Table 4.5. Kent's Cavern drip rates. Values are in litres per second. - signifies that drip rates were not determined. Mean and 1σ error for each site is shown.

Site	*Predicted Growth Rate (mm yr^{-1})*	*Actual Growth Rate (mm yr^{-1})*	*Predicted mean - actual mean growth rate (mm yr^{-1})*	*growth rate difference*
KC-91-1	0.15±0.08	0.201±0.049 (top)	-0.050	x0.8
		0.19±0.09 (slope)	+0.131	x7.9
KC-91-5	0.08±0.06	0.018±0.007	+0.062	x4.4
KC-91-6	0.06±0.04	0.024±0.013	+0.036	x2.5
KC-91-8	0.14±0.09	0.039±0.011	+0.101	x3.6
KC-91-10	0.13±0.08	0.041±0.011	+0.089	x3.2
DL-91-1	0.09±0.05	0.019±0.003	+0.071	x4.7
DL-91-2	0.09±0.05	0.018±0.004	+0.072	x5.0
DL-91-3	0.09±0.05	0.019±0.003	+0.071	x4.7
LC-91-1	0.16±0.12	0.009±0.006	+0.151	x11.4

Table 4.6. Comparison of predicted and actual growth rates for all flowstone sites. Predicted mean and 1σ errors are calculated as described in the text. Mean and 1σ errors for the actual growth rate calculated from sample thickness estimates from each of the sites, except LC-91-1, which is calculated from the mean of the slab experiment and ASU results.

1) An error contained within the Plummer et al (1978, 1979) kinetic model upon which the growth rate theory is based (see section 3.3).
2) An error in the formulation in the growth rate model; for example, if a significant rate determining step is not included.
3) Change in the calcium and film thickness values from those measured today over the last 116 years.
4) Sample growth commenced significantly more recently than 116 years ago.
5) Seasonal shut-off of the water flow limits growth rate.
All these explanations are possible; it has already been noted (section 3.3) that the kinetic growth model depends upon the Plummer-Wigley-Parkhurst equations, which are only accurate to within a factor of two. Similarly, the groundwater flow and chemistry at Kent's Cavern may have been altered by the increasing encroachment of domestic housing on the overlying surface (Proctor, pers. comm.). This may be resolved by considering additional evidence from further sites which have not undergone land use change.

Assuming that the field data does provide a reliable record of calcium and film thickness variations, then the relative sensitivity of growth rate to the two variables can be determined. Growth rate and measured calcium levels can be compared from tables 4.2 and 4.3 for the five samples for which calcium concentrations were determined; correlation of the two variables demonstrates that no relationship is apparent ($r = 0.14$; $n = 5$; not significant at a 95% level). The effect of seasonality of discharge on growth rate is investigated in Table 4.7. Having shown that film thickness and discharge levels are not significantly related in the field (section 4.2.2.3), it is assumed that variations in discharge are insignificant compared to seasonality effects. The flowstones are grouped according to continuous flow (group A; KC-91-1/6/10), more than 4 months winter flow (group B; KC-91-5/8/11) and less than 4 months winter flow (group C; KC-91-2/3/4) as noted earlier. The lowest flow samples (group C) have significantly lower minimum growth rates than the highest flow group (A) at a 95% confidence level, and both groups B and A at a lower 90% confidence level. Thus for this site it appears that seasonality of flow may be the most significant factor affecting growth rate. However, sample growth occurred over a time period for which calcium concentration and temperature may have remained constant, and thus sensitivity of growth rate to seasonality of water supply would be more noticeable.

	A	B	C
	Continuous Flow	Discontinuous Flow	Discontinuous Flow
	Discharge >$1x10^{-5}$ l s^{-1}	Discharge >4 months	Discharge <4 months
Number of samples (n)	28	7	6
Growth Rate (mm yr^{-1})	0.049	0.034	0.013
1 σ error	0.065	0.016	0.008
90% C.I. (student's t-test)	0.028-0.070	0.023-0.045	0.006-0.019
95% C.I. (student's t-test)	0.024-0.074	0.020-0.048	0.005-0.021
Significant Difference	Faster than C at 95%	Faster than C at 90%	Slower than B at 90%
			Slower than A at 95%

Table 4.7. Comparison of sample thickness and flow regime. Group C is significantly different from group B at a 90% confidence level; and is different from A at a 95% confidence level.

A sensitivity to seasonally limited discharge may also provide an explanation to the overestimation of growth rate by the theory. For the five samples for which both predicted and actual growth rates could be determined (table 4.6), both KC-91-1 and KC-91-8 had an available water supply for only 4-6 months. If the actual growth rates of these samples (0.018±0.007 and 0.039±0.011 mm yr^{-1}) are multiplied by x2-3, simulating continuous growth, then their growth rates would be 0.036-0.054 and 0.078-0.116 mm yr^{-1} respectively. This would be in closer agreement to that theoretically predicted (0.08 and 0.13 mm yr^{-1} respectively). However, this argument does not explain the overprediction of growth rate for sites KC-91-1, 6 and 10.

Two other important measurements were obtained at Kent's Cavern. Firstly, for two samples (KC-91-5 and 8), calcium determinations were made from both the top and base of the flowstone profile (Table 4.4). All the calcium levels at the base are significantly lower than those at the drip source, but none have reached the equilibrium value expected for 10 °C and $3x10^{-4}$ atm (0.63 mmol l^{-1}), and thus at no time should deposition cease. This result also suggests that maximum growth rates should be lower at the base of the profile, although this is not reflected in the measurements obtained from sample thickness variations (table 4.2). Correlation of the change in calcium down the profile with drip discharge rate should be possible (table 4.8), although from a data set of only 3 points. A slower drip rate does not appear to lead to a greater decrease in calcium concentration down the flowstone. Although this may be expected; a longer residence time upon the flowstone would lead to an increase in degassing and thus greater loss of calcium, this appears to be

obscured here, perhaps due to the ponding of water on the flowstone surface, buffering this effect. This may explain the larger change in calcium concentration observed for KC-91-1 rather than KC-91-8, with the former site having ponding and a shallow gradient.

Site	*Difference in Calcium Ion Concentration (mmol l^{-1})*	*Drip Rate ($l\ s^{-1}$)*
KC-91-1	0.49	$1.2x10^{-4}$
	0.70	$7.5x10^{-5}$
	1.37	$3.3x10^{-5}$
KC-91-8	0.11	$1.6x10^{-4}$
	0.25	$1.4x10^{-4}$
	0.40	$1.4x10^{-4}$

Table 4.8. Comparison between the change in calcium ion concentration between top and base of two flowstone sites, and the drip discharge onto them.

A final important observation is of the extremely high growth rate for the upper part of KC-91-1 which is an order of magnitude higher than that observed on any other flowstone at the site, and agrees with that theoretically predicted. This could be due to turbulent flow occurring (see section 3.3), which would lead to growth rates an order of magnitude higher than under laminar flow conditions. Also, the high growth rates only occur on the flat top of the flowstone, where rimstone pools are present; with lower rates on the steep sloping sides. Thus slope angle may be a more important factor, perhaps causing increased residence times for deposition and high water film thicknesses.

A test for turbulent flow was undertaken on two samples (KC-91-1, KC-91-6) by placing a drop of Rhodamine WT dye onto the flowstone surface and measuring the velocity of the labelled water down the flowstone. Water drip rate and film thickness were also recorded. These variables can then be used to derive the Reynolds Number (R_e), an index of turbulent flow:

$$R_e = \frac{\text{velocity x density x film thickness}}{\text{viscosity}} \qquad (4\text{-}2)$$

Typical flow velocities were in the range 0.01 - 0.2 cm s^{-1} (for drip rates between $4x10^{-5}$ and $8x10^{-4}$ l s^{-1}). Viscosity at 10 °C is 0.01307 $cm^2\ s^{-1}$, density is 1.03 g cm^{-3} and film thickness was that measured on the surface of the sample. For KC-91-1, film thickness on the low gradient on which rimstone pools were visible was 6.4 mm (1σ uncertainty = 3.2 mm; n=14), significantly deeper than that observed on the steeper

sloping face of the sample (0.158 ± 0.125 mm (table 4.4)). Despite this difference, the calculated Reynolds numbers (Table 4.9a) were in the range 0 - 3, and demonstrate no likelihood of turbulent flow occurring.

(a)

Sample	*Drip Rate* ($l\ s^{-1}$)	*Velocity* ($cm\ s^{-1}$)	*Assumed Film Thickness* (cm)	*Reynolds Number*
KC-91-1	1800	.037	.6	1.7
KC-91-1	1800	.054	.6	2.6
KC-91-6	16000	.13	.015	0.2
KC-91-6	2400	.083	.015	0.1

(b)

Sample	*Time* (d)	*Initial Weight* (g)	*Final Weight* (g)	*Growth Rate* ($mm\ yr^{-1}$)
POOL-1	80	.06454	.06561	0.0065±.0048
POOL-2	80	.07646	.08226	0.0263±.0195
FILM-1	80	.07199	.07346	0.0072±.0054
FILM-2	80	.11335	.11493	0.0004±.0003

Table 4.9 Results of the testing of high growth rate conditions. (a) Turbulent flow measurements made upon KC-91-1 and KC-91-6. (b) Growth rates determined from the placing of calcite slabs upon ponded and non-ponded sections of KC-91-1. 2σ errors are assumed to be ±75%, for justification see section 4.3.2.3.

The presence of the rimstone pools may be the factor causing increased growth rate, although it has been demonstrated that this is not via an increase in film thicknesses generating turbulent flow. Other factors could be used to explain the higher growth rate. Under 'typical' growth conditions, growth rate is limited by the thickness of water films; faster growth would be possible in the pools due to the thicker water film. Alternatively, the ponding may permit a continual supply of water supply to be present, giving continuous deposition, whereas lower down the sample the flowstone may become dry under some conditions. This would allow complete degassing to occur, and thus explain the good agreement between predicted and actual growth rates at this location. However, throughout the year of observations, a water film was observed over the whole sample.

To further examine these hypotheses, calcite slabs were placed upon flowstone site KC-91-1. Two slabs were placed within the pools and two others placed upon planar

sections of the sample with 'normal' growth rates. The results from this experiment are shown in Table 4.9b and show that there is no significant difference between growth rates determined from the two sets of slabs, neither of which exhibit an elevated growth rate. Later results (section 4.3.2.4) present additional data on the effects of rimstone pools from Ravens Well.

4.3.2.2 Dolebury Levy

Dolebury Levy is an adit situated in the Lower Limestone Shales of the Carboniferous Limestone Series at Rowberrow, Mendip. The levy is sited within a National Trust nature reserve, land use has been unchanged for several centuries. The adit was excavated by Dr Benjamin Somers in 1830 in search of haematite and ochre (Gough, 1967 (revised edition), pp173-5; 243-5). Sample locations are shown in figure 4.10. At the three sample sites, subsamples for thickness determination were collected, and calcium concentrations, film thicknesses, and drip rates recorded. The results are recorded in table 4.10.

For sample DL-91-1, both drip rate and calcium values were obtainable; for the other samples only drip rates were measurable due to the very low discharge. Film thickness measurements were taken for all samples when wet and measured 0.048 ± 0.040 mm (1σ; n=53). This value was used in the growth rate model. These measurements were frequently prevented by flooding of parts of the adit, limiting access to the flowstones. Thus film thickness measurements were not frequent enough to allow a comparison with different drip rates. Comparison of the model results with minimum growth rates determined from actual sample thicknesses is shown in table 4.6 for DL-91-1. As for Kent's Cavern, the model overpredicts growth rate, although the growth rates do agree within 2σ errors. This may be explained by the flow regime, with the site becoming dry in the summer months (table 4.10), although again the underestimation may be due to the flowstone not forming immediately after the excavation of the mine.

Calcium concentration measurements were not possible for DL-91-2/3; two titrations from fast dripping sources near the samples measured 1.63 and 1.90 mmol l^{-1}, the same concentration as that measured at DL-91-1. All three sites are in the same bedrock, at a similar depth and with identical surface vegetation; therefore no significant difference in calcium concentration would be expected. Flow was continuous throughout the year for both samples, but the drip rate of DL-91-3 was significantly higher than that of DL-91-2 (table 4.10). Comparing the growth rates of the two samples determined from the sample thicknesses, there is no difference

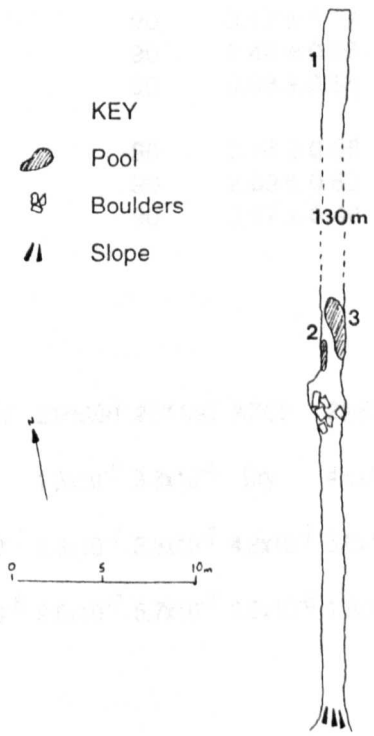

Figure 4.10. Survey of Dolebury Levy (BCRA Grade 1), showing locations of flowstone sites 1-3.

(a)

Site	*Distance (cm)*	*Angle (°)*	*Thickness (mm)*	*Min. growth rate (mm yr^{-1})*
DL-91-1				
	20	90	3.43 ± 0.42	0.021±0.003
	40	90	3.05 ± 0.92	0.019±0.006
	40	90	2.95 ± 0.66	0.018±0.004
	60	90	2.66 ± 0.56	0.016±0.005
DL-91-2				
	30	90	2.26 ± 0.90	0.014±0.006
	60	90	3.17 ± 1.14	0.020±0.007
	90	90	2.46 ± 0.66	0.015±0.004
	110	90	3.38 ± 0.56	0.021±0.003
DL-91-3				
	30	90	3.16 ± 0.86	0.020±0.005
	50	90	2.69 ± 0.88	0.017±0.006
	75	90	3.17 ± 0.40	0.020±0.003

(b) Drip Rate (l s^{-1})

Site	*2/5/91*	*10/9/91*	*21/10/91*	*27/11/91*	*8/7/92*	*28/8/92*	*21/10/92*	*mean*
DL-91-1	2.8×10^{-4}	Dry	1.3×10^{-5}	3.3×10^{-4}	Dry	4.6×10^{-4}	3.3×10^{-5}	$2.7\pm1.9\times10^{-4}$
DL-91-2	-	5.4×10^{-7}	8.3×10^{-7}	3.3×10^{-7}	4.2×10^{-7}	5.0×10^{-7}	5.0×10^{-7}	$5.4\pm1.7\times10^{-7}$
DL-91-3	-	1.7×10^{-6}	9.6×10^{-7}	6.7×10^{-7}	2.5×10^{-6}	1.9×10^{-6}	1.3×10^{-6}	$15.0\pm6.7\times10^{-7}$

(c) Calcium (mmol l^{-1})

Site	*2/5/91*	*10/9/91*	*21/10/91*	*27/11/91*	*8/7/92*	*28/8/92*	*21/10/92*	*mean*
DL-91-1	1.92	Dry	1.75	2.03	Dry	1.85	1.95	1.90±.106

Table 4.10. Results of experiments upon the Dolebury Levy flowstones. (a) Sample details. (b) Drip rates. (c) Calcium ion concentration.

between that of DL-91-2 and DL-91-3; and both are of a similar magnitude to DL-91-1. Growth rates are again less than those predicted by the model (assuming calcium concentrations are the same as those on DL-91-1) (table 4.6). This suggests that drip rates, although significantly different between DL-91-2 and 3, were so low as not to significantly affect film thickness and thus growth rate. This was confirmed by the film thickness measures; DL-91-2 averaged 0.047 ± 0.019 mm (n=14), DL-91-3 averaged 0.038 ± 0.027 mm (n=15), not significantly different at 95% confidence levels, and the same as those for DL-91-1. This corroborates results from Kent's Cavern, where no relationship was found between drip rate and film thickness. Growth rates of DL-91-2 and 3 were similar to those of DL-91-1, despite the latter shutting off during the summer. If seasonality is an important factor affecting growth rate, it might be expected that DL-91-2 and 3 would have higher levels. This was not observed here; however, DL-91-2 and 3 were observed to be partially dry over some or most of their surface areas, even with an active drip source. Thus their extreme low flow, although continuous, would appear to be limiting growth rate, and having a similar influence as seasonal shut-off. If true, this result suggests that evaporation would be occurring over parts of the flowstone for some or all of the year, but how this may effect growth rate is not known.

Calcite slabs were placed at all 3 sites over the period September 1991 to October 1992; data and results are shown in table 4.11. As can be seen, all samples demonstrated a mass increase, which could then be converted into a growth rate. Comparison of growth rates measured using the slab technique and minimum growth rate levels obtained from sample thickness measures show no relationship (tables 4.6 and 4.10), although results are of the correct order of magnitude. This can largely be attributed to the large errors associated with these experiments (see section 4.2.1.1 and following section).

Sample	*Slab* (d)	*Time* (days)	*Initial Weight* (g)	*Final Weight* (g)	*Growth Rate* mm yr^{-1}
DL-91-1	K	406	.06412	.06454	.0125±.0094
DL-91-2	J	406	.06829	.07199	.0178±.0134
DL-91-3	I	406	.07365	.07646	.0023±.0017

Table 4.11. Dolebury Levy calcite slab results. Growth rate is calculated using equations presented in section 4.2.1.1. Errors are assumed to be 75% (2σ), see following section for justification.

The results for Dolebury Levy corroborate those from Kent's Cavern, in that the growth rate theory is again shown to overpredict the actual growth rates. In particular, the undisturbed nature of the site allows us to be very certain that the calcium and film thickness values measured today are representative of values over the last 100 years.

4.3.2.3 Lower Cave

Lower Cave is situated at the base of the Avon Gorge behind the former site of Hotwells Railway Station, now adjacent to the A4 'Portway'. The cave was discovered during the construction of the station site in 1865, when it was stripped of most of its formations. The cave has remained relatively undisturbed since 1922, when the railway was closed and the new Portway built (Mockford and Male, 1974). Although the site was primarily used in this study to investigate stalagmite growth rates, one flowstone, LC-91-1, was also analysed. It's location is shown in figure 4.11.

Drip discharge, calcium concentration and film thickness measurements were made at the site over the period 1991-92. Flowstone thickness was measured by sampling; and a basal section was dated by alpha spectrometric uranium series (ASU) dating. This would provide an estimate of recent growth rate; and also constrain the age of sediments underlying the flowstone, which contained many 'Earliest Holocene' frog remains (Currant, pers. comm.). Two sets of duplicate calcite slabs were placed 2 cm apart on the flowstone, in order to obtain both a growth rate estimate and a measure of variability across the sample.

Drip discharge variation is shown in table 4.12; at no time during the year was flow observed to cease. Film thickness measurements were taken throughout the year, and averaged 0.183 ± 0.130 mm (1 σ; n = 20). This value is significantly higher than that obtained at either Kent's Cavern or Dolebury Levy. This may be due to the lower flowstone surface gradient here (10° - 60°), but more likely due to the soft nature of the calcite from which the flowstone was forming, which caused significant instability whilst making spherometer measurements. Calcium titrations were performed on the drip waters, and calcium concentrations averaged 2.06 ± 0.31 mmol l^{-1} (1σ error; n = 4).

Results from the calcite slab experiments are shown in table 4.12. Slab H was dried, desiccated and reweighed ten times after removal from the site, in order to obtain an estimate of the error in the weighing procedure. The multiple weighings gave a mean mass of 0.130934 ± 0.000169 g (1 σ), which gives an error for the preparation and

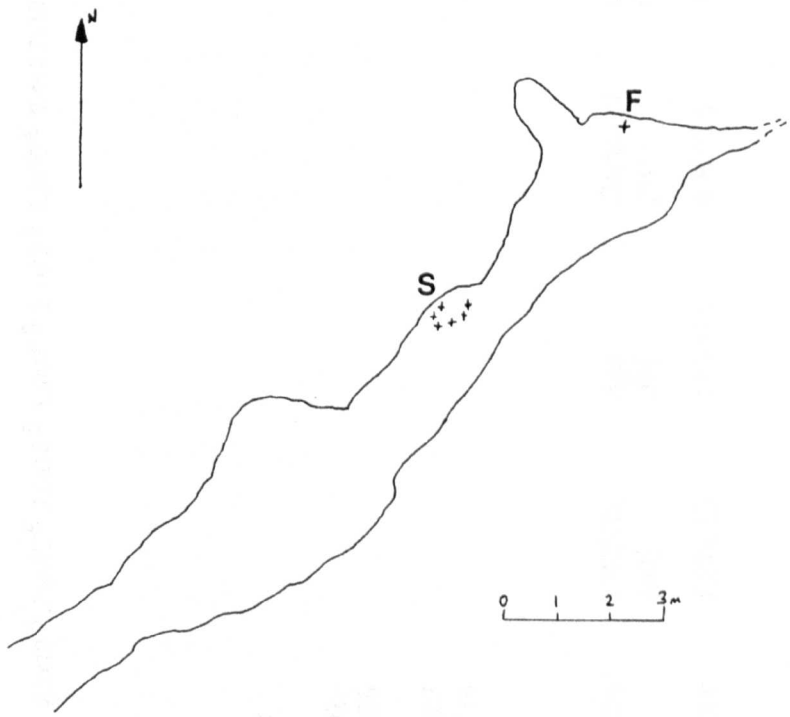

Figure 4.11. Survey of Lower Cave (BCRA Grade 4; Speleological Group, Rodway School, 1973), showing location of flowstone site LC-91-1 (F) and stalagmite sites LC-92-1 to 6 (S).

(a) Drip Rate ($l\ s^{-1}$)

	18/10	*7/11*	*27/11*	*2/1*	*10/1*	*30/1*	*7/2*	*2/3*	*12/7*	*24/7*	*5/8*	*Mean*
LC-91-1	6.0×10^{-6}	3.8×10^{-5}	2.1×10^{-5}	9.4×10^{-6}	1.0×10^{-4}	2.3×10^{-5}	7.9×10^{-6}	2.0×10^{-5}	1.4×10^{-5}	2.1×10^{-5}	6.3×10^{-6}	$2.4\pm2.7\times10^{-5}$

(b) Slab Experiments

Slab	*Time (d)*	*Surface Area (mm^2)*	*Initial Weight (g)*	*Final Weight (g)*	*Growth Rate mm yr^{-1}*
C	98	141.6	.10849	.11174	.031±.023
D	98	140.4	.12385	.12444	.006±.005
G	326	141.6	.11176	.11481	.009±.007
H	326	140.4	.12444	.13091	.019±.014

(c) ASU Result

Sample	*Distance from Surface (mm)*	*$^{234/238}U$ [act]*	*$^{230}Th/^{234}U$ [act]*	*$^{230/232}Th$ [act]*	*Age (ka)*	*Corrected (ka)*	*Growth Rate (mm yr^{-1})*
LC-91-1	58±15	1.47±.11	.105±.008	2.67±.23	11.9±1.6	6.86±2.5	.0085±.0061

Table 4.12. Lower Cave flowstone data. (a) Drip rate data. (b) Calcite slab data. Slabs C and D, and G and H, form duplicate pairs. Growth rate is calculated by the method shown in section 4.3.1.1. (c) Growth rate derived from the alpha spectrometric dating. The corrected age is calculated using the method of chapter 5.

weighing procedure of under 1%. Variation between the duplicates placed on the sample was significantly greater, a 75% 2σ error between duplicates C and D and 40% 2σ error between G and H necessary to explain the differences between the means. This is at the same level as errors reported by Hermann and Lorah (1988) and Dreybrodt et al (1992), and confirms the large errors associated with the slab technique (section 4.3.1.1). A 75% 2σ error is assumed for all growth rates determined from calcite slab experiments preformed at other sites.

Growth rate estimates from the calcite slabs and ASU dating (table 4.12) are compared to theoretically predicted growth rates at 10 °C, cave atmosphere pCO_2 of $3x10^{-4}$ atm, and the measured range of film thickness and calcium concentration. The results are shown in table 4.6. Both the alpha spectrometric and slab measurements appear to underestimate with the theoretical growth rate, it must be noted that the large error terms associated with both the slab experiments (±75%) and the alpha-spectrometric date (due to the thorium contamination) mean that the growth rates may actually be higher or lower than theoretically predicted at 2σ. Results from Lower Cave are not precise enough to further conclusions made in the earlier sections.

4.3.2.4 Other Sites (Stump Cross, Ravens Well)

Many other sites were investigated whilst searching for suitable recent flowstone samples whose age was known and for which calcium concentrations and water discharge could be measured. For several (G.B. Cave, Single Way Mine, Devils Hole), slabs were placed, but were either washed off the sample or precipitated onto the sample over the course of the year, preventing any results from being obtained. In other instances, limited, but useful results were obtained.

Flowstone samples were collected from Raven's Well, a hand dug adit system underneath Temple Meads and Redcliffe, Bristol. The system was originally dug in 1366, and extended in 1651 (Mockford and Male, 1974); a flowstone sample was collected from near the entrance, which is presumed to date from 1366. The flowstone itself was dry, and appeared not to have water flowing over it for a considerable period. Water samples from drip sources were collected from a different (wet) part of the adit (but within the same mudstone bedrock). Calcium concentrations averaged 3.31 ± 0.29 mmol l^{-1} (n=4), magnesium concentrations 3.08 ± 1.25 mmol l^{-1} (n=3). The dryness of the flowstone sample today is presumed to be caused by development of the Temple Meads Station complex over the last 120 years.

Thickness measures were taken on three subsamples of the flowstone. These averaged 14.58 ± 3.47 (n=23), 9.32 ± 3.05 (n=18) and 18.98 ± 1.88 mm (n=10). The first two subsamples were taken from random locations, and are not significantly different. The third was taken from a section which in cross-section appeared to have consisted of a gour pool, and this sample had a significantly higher growth rate. Since all subsamples come from the same sample which grew over the same period of time, this must represent a faster growth rate. Fast flowstone growth was also found where rimstone pools were present on KC-91-1, and these results suggest that care must be taken when interpreting flowstone growth rates when such features are present.

Crude growth rates for the sample can be calculated assuming that growth commenced in 1366 and terminated at ≈ 1900. This gives growth rate estimates of 0.027, 0.017 and 0.036 mm yr^{-1}, which are of the expected order of magnitude.

Another growth rate estimate was obtained from Stump Cross sample SC-90-6M, which had been collected for MSU and ASU analysis (see chapter 5). The uppermost growth layer of this sample was actively growing today, and has an average thickness of 2.28 ± 1.25 mm. This layer would have started to grow around 1880, when local mining activity lowered the groundwater levels and exposed the cave artificially (Dickinson, 1972; see chapter 5 for detailed justification). This gives a growth rate of 0.020 mm yr^{-1}; although no calcium or film thickness measurements were obtained, this result is again of the expected order of magnitude.

4.3.2.5 Conclusions

Flowstone growth rates were measured on fifteen flowstones from five cave and mine systems. Measured growth rates were minima, and ranged between 0.014 and 0.201 mm yr^{-1}. These are in the range predicted by the growth rate model for modern temperature, calcium ion concentration, water film thickness and cave air pCO_2 conditions. For nine samples, these variables could be precisely determined, and thus a direct comparison to the theory made (table 4.6). For eight sites, growth rates were overpredicted by the model by between x2.5 and x11.4, although growth rates agree within 2σ errors. This may be due to the actual growth rates only being minima, the effect of seasonally limited water supply, or an error in the theory or in the Plummer et al (1978, 1979) kinetic model upon which the theory is based. When seasonality of flow was considered for samples, it accounted for the overprediction,

but this factor does not explain all growth rate overprediction, as this also occurred for sites with continuous discharge.

One exceptional result was for site KC-91-1, which has a near level gradient and highly developed rimstone pools, and for which growth rates exceeded those predicted. This was also observed in one other sample with rimstone pools, suggesting that this factor was important in generating elevated growth rates, although the reason for this is unclear.

Comparison of flowstone growth rates and calcium ion concentration and seasonality of discharge was undertaken for the Kent's Cavern sites. No relationship was found between growth rate and calcium ion concentration, perhaps due to changes in this variable with recent land use change. Growth rates were shown to slowest for Kent's Cavern sites with seasonally limited water supplies, demonstrating the importance of this factor, although this result was not observed at Dolebury Levy.

4.3.3 Stalagmite Growth Rate Results

Stalagmite growth rate data was collected from four cave and mine locations. The results are discussed below.

4.3.3.1 Lower Cave

Flowstone within Lower Cave has been described in section 4.2.2.3. In addition, six stalagmite samples were analysed for growth rate variation, shown in figure 4.11.

Drip rates onto LC-92-1/2/3/4/5/6 were measured throughout 1991 - 1992, to obtain a record of relative drip rate variation. This is shown in figure 4.12. Calcium samples were also obtained, although because of the slow drip rates samples were collected over a 24 hour period and thus considerable degassing may have occurred. For all samples, calcium concentrations averaged 2.19 ± 0.16 mmol l^{-1} (1 σ error; n= 12), not significantly different from those obtained from the flowstone LC-91-1. At the end of the year, the samples were removed from the cave, and their thickness measured. One sample, LC-92-1, was growing on the bedrock rather than on sediments, and was not removable for thickness measurement. Another, LC-92-6, was found to have an irregular growth thickness, due to entrained sediments, and has a high uncertainty in the thickness measurements.

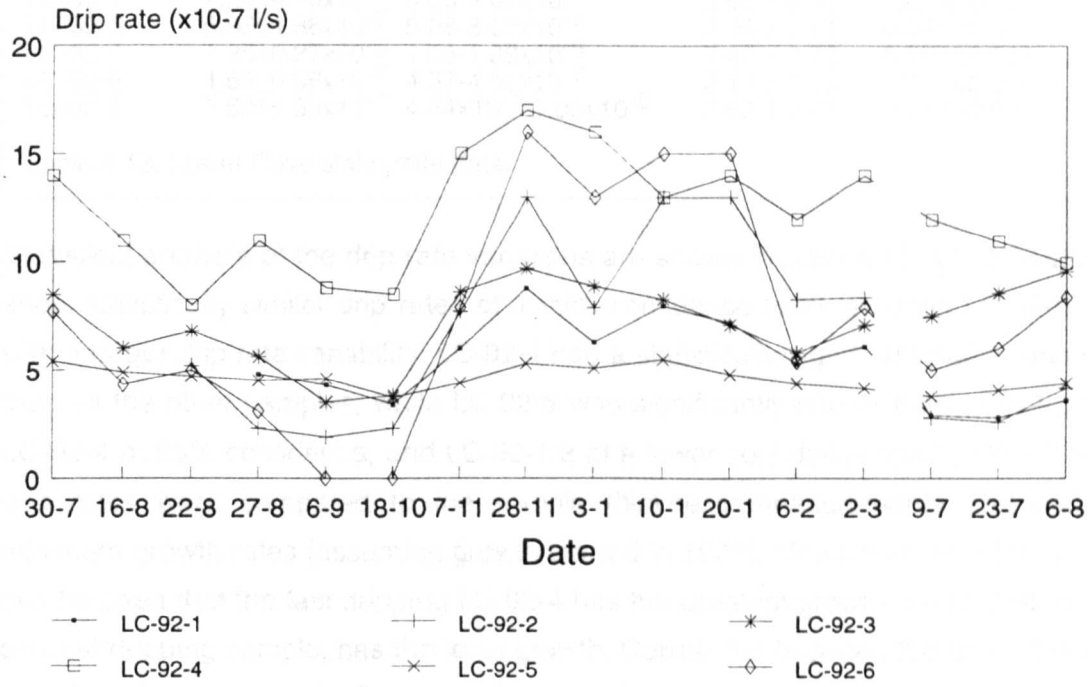

Figure 4.12. Drip discharge data for Lower Cave stalagmites LC-92-1 to 6.

Sample	*Drip Rate* ($l\ s^{-1}$)	*95% C.I.* (*t-score*)	*Sample Thickness* (*mm*)	*Minimum growth rate* ($mm\ yr^{-1}$)
LC-92-1	$5.75\pm1.86\times10^{-7}$	$4.50\text{-}6.99\times10^{-7}$	-	-
LC-92-2	$7.25\pm4.10\times10^{-7}$	$4.65\text{-}9.86\times10^{-7}$	3.06 ± 0.98	0.044±0.014
LC-92-3	$6.95\pm1.86\times10^{-7}$	$5.88\text{-}8.03\times10^{-7}$	3.05 ± 0.81	0.044±0.012
LC-92-4	$1.25\pm0.27\times10^{-6}$	$1.08\text{-}1.39\times10^{-6}$	4.44 ± 0.75	0.063±0.011
LC-92-5	$4.68\pm0.56\times10^{-7}$	$4.37\text{-}4.00\times10^{-7}$	2.14 ± 1.13	0.031±0.016
LC-92-6	$7.50\pm5.33\times10^{-7}$	$4.44\times10^{-7}\text{-}1.06\times10^{-6}$	3.68 ± 1.77	0.052±0.025

Table 4.13. Lower Cave stalagmite data.

Statistical analysis of the drip rate variations are shown in table 4.13. LC-92-1/2/3 all show statistically similar drip rates at a 95% confidence level, as does LC-92-6, but with a larger drip rate variability. LC-92-4 had a statistically significant higher drip rate than all the other samples, while LC-92-5 was significantly slower than LC-92-3 and LC-92-4 at 95% confidence, and LC-92-1/2 at a lower confidence level (90%). These drip rates were compared to the sample thickness measurements and derived minimum growth rates (assuming growth started in 1922), also shown in table 4.13. It can be seen that the fast dripping LC-92-4 has the greatest growth, and LC-92-5, the slowest dripping sample, has the least growth. Correlation between the drip rates and growth rate is shown in figure 4.13; a weak relationship is visible which is not statistically significant ($r = 0.45$; $n = 5$; not significant at a 95% level). Thus under conditions of constant temperature and calcium concentration, a weak control of growth rate by drip discharge has been demonstrated in the cave environment.

Minimum growth rate values obtained from the sample thicknesses can be compared to the modelled growth rate. Calcium concentrations, drip rate and film thickness are all known; temperature is assumed 10 °C, a pCO_2 of 3×10^{-4} atm, and a 90% drop replacement. The results are shown in table 4.14. A better agreement is evident between modelled and actual growth rates than at the previous sites, and gives some support for the accuracy of the growth rate model, despite both the measured growth rates and calcium ion concentrations being minima.

4.3.3.2 Brownes Folly Mine

Brownes Folly Mine (also known as Farleigh Old Mine), Bathford, was opened ≈1860 for the extraction of bathstone from the Jurassic limestone (Price, 1984). It has been disused for many years, and is well decorated with stalagmites. It is sited within a nature reserve, and overlying land use has remained unchanged since the discontinuation of mining.

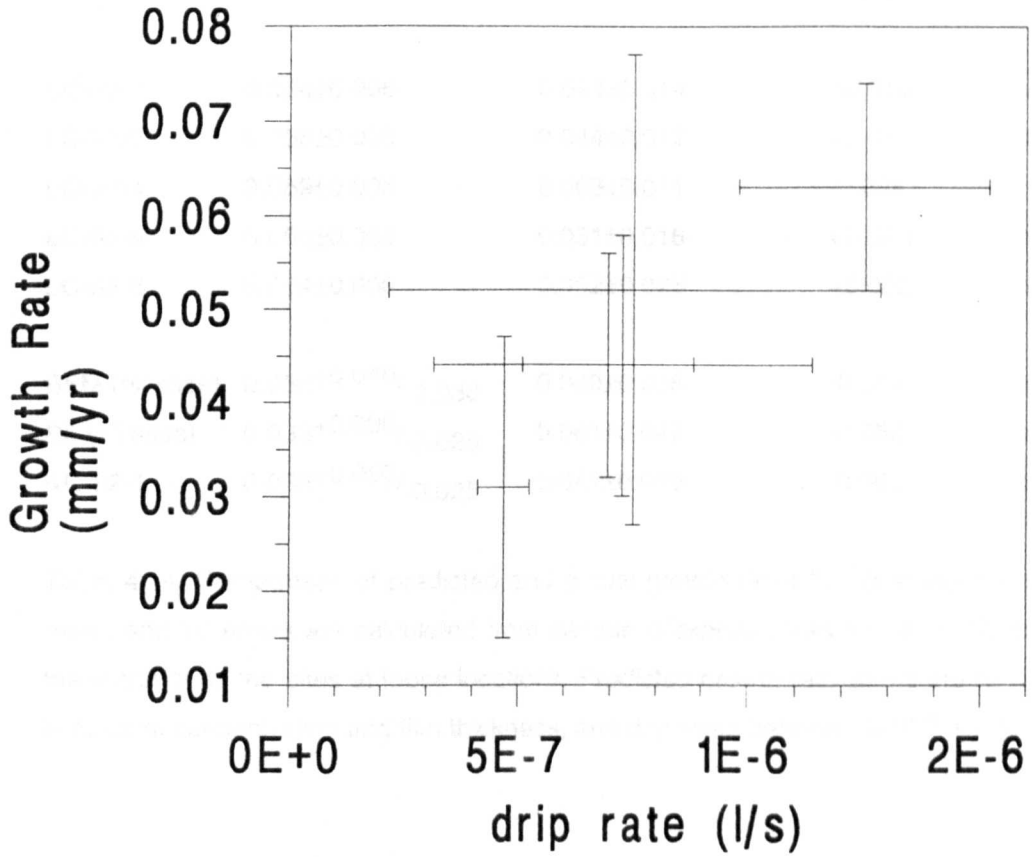

Figure 4.13. Relationship between growth rate and drip rate for Lower Cave stalagmites LC-92-2 to 6. Errors are 1σ, derived from variations in drip rate and stalagmite thickness.

Site	*Predicted Growth Rate (mm yr^{-1})*	*Actual Growth Rate (mm yr^{-1})*	*Predicted - Actual Growth Rate (mm yr^{-1})*	
			mm yr^{-1}	*difference*
LC-92-2	0.054±0.006	0.044±0.014	+0.010	x1.2
LC-92-3	0.056±0.006	0.044±0.012	+0.012	x1.3
LC-92-4	0.059±0.006	0.063±0.011	-0.004	x0.9
LC-92-5	0.054±0.006	0.031±0.016	+0.023	x1.7
LC-92-6	0.054±0.006	0.052±0.025	+0.002	x1.0
BFM (all sites)	$0.066^{+0.040}/_{-0.030}$	0.080±0.058	-0.014	x0.8
SL (all sites)	$0.036^{+0.090}/_{-0.025}$	0.081±0.042	-0.050	x0.4
KC-92-1	$0.036^{+0.090}/_{-0.025}$	0.041±0.010	-0.005	x0.9

Table 4.14. Comparison of predicted and actual growth rates for all stalagmite sites. Actual mean and 1σ errors are calculated from sample thickness measurements; SL and BFM are the mean of all the sites at those locations. Predicted growth rate errors are for 1σ variations in calcium concentration and film thickness, and drip rates between $5x10^{-6}$ and $5x10^{-8}$ l s^{-1}.

Eleven whole stalagmite samples were collected from the Front Passage / St Pauls area of the mine (see Irwin and Knibb, 1977, for survey), and these were sectioned so that their thickness could be determined. Water samples were collected from nearby fast flowing drips; this may lead to significant inaccuracy in the calcium determinations. These had an average calcium concentration of 2.57 ± 0.09 mmol l^{-1} (n=7; 1 sigma errors); molar Mg/Ca ratios were typically 0.04 ± 0.05. Water film thickness on the stalagmite caps was taken to be the average for stalagmite caps; 0.052 ± 0.031 mm (see section 4.2.2.1). The thicknesses of the stalagmites and the derived minimum growth rates are shown in table 4.15.

Sample	*Thickness (mm)*	*Minimum Growth Rate (mm yr^{-1})*
BFM-92-1	2.48 ± 0.47	0.019±0.004
BFM-92-2	4.73 ± 0.36	0.036±0.003
BFM-92-3	3.65 ± 0.62	0.028±0.005
BFM-92-4	5.06 ± 0.58	0.038±0.004
BFM-92-5	3.53 ± 1.03	0.027±0.008
BFM-92-6	10.20 ± 0.64	0.077±0.005
BFM-92-7	24.42 ± 3.75	0.185±0.028
BFM-92-8	12.48 ± 0.99	0.095±0.008
BFM-92-9	22.68 ± 2.58	0.172±0.020
BFM-92-10	11.24 ± 2.05	0.085±0.016
BFM-92-11	15.46 ± 1.49	0.117±0.011

Table 4.15. Brownes Folly Mine stalagmite sample thicknesses.

The growth rates obtained from the mine samples were compared to the theoretical growth rates predicted from the kinetic model. Calcium concentration and film thickness values were those described above; temperature was assumed to be 10 °C and cave pCO_2 $3x10^{-4}$ atmospheres. 90% drip replacement and a continuous drip discharge were assumed, the latter as discharge was observed to be occurring during the summer. The results of the model run over the range of drip rates $5x10^{-8}$ - $5x10^{-6}$ l s^{-1} (1 drip / second to 1 drip / hour; that observed in the field) are shown in figure 4.14. Growth rates are of the correct level, and some are approximately a factor of x2 higher than theoretically expected, independent of the range of possible drip rates, although all are within the 2σ error range of the model predictions. Better agreement between measured and modelled growth rates from the stalagmites compared to the flowstone data presented earlier suggests that continuous discharge may be an important factor, as this is the only significantly different factor between the two sample types. Continuous drip discharge onto the Brownes Folly stalagmites would allow continuous speleothem growth, and thus a higher growth rate. However, this does not explain the much larger range of observed growth rates, and the underprediction for some samples. This may be due to a wide range of calcium

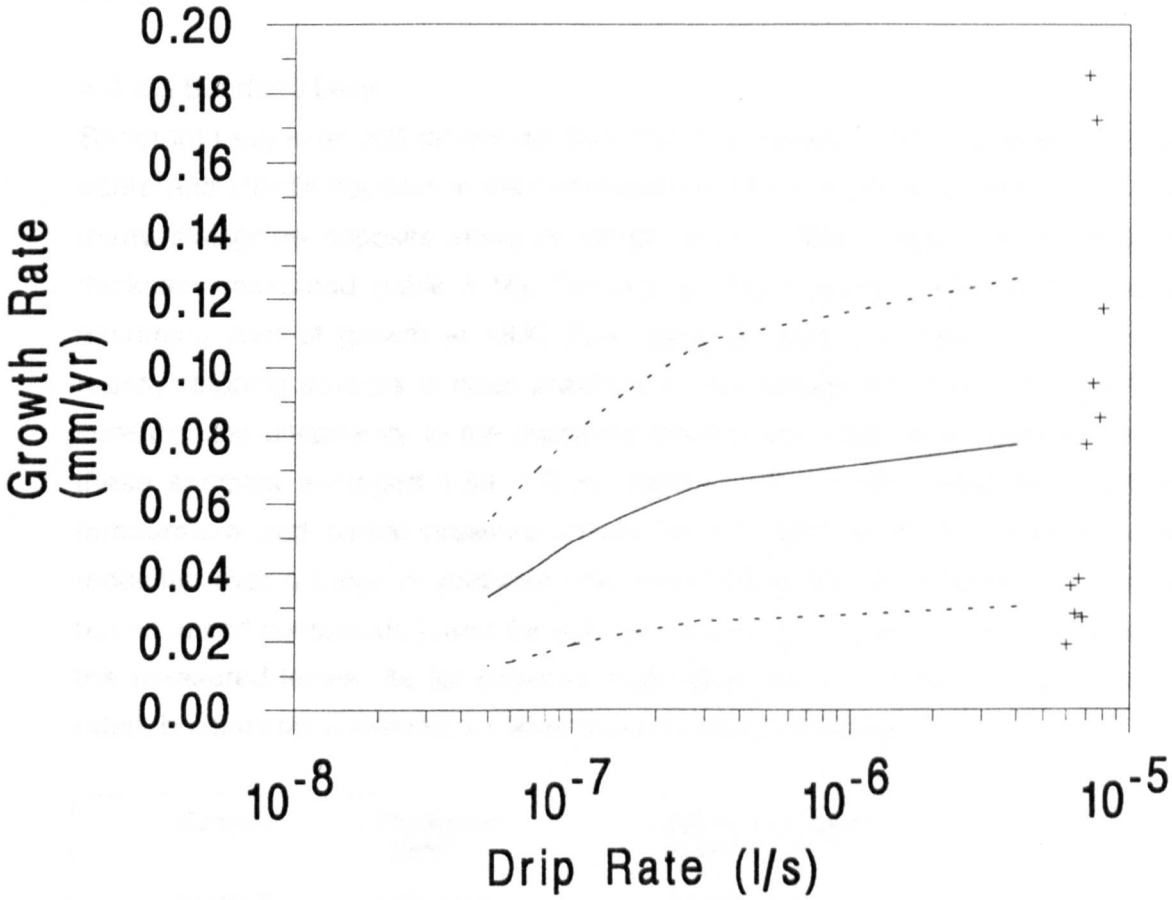

Figure 4.14. Relationship between predicted and actual growth rates for the Brownes Folly Mine stalagmites. Mean predicted growth rate is shown by a solid line, predicted $\pm 1\sigma$ errors (derived from 1σ errors in calcium concentration and film thickness) by dashed lines. Actual growth rates shown by crosses, error bars are omitted for clarity.

variation between drips which was not distinguishable by the measurements taken, or some as yet unknown factor which causes elevated growth rates for stalagmite samples.

4.3.3.3 Sandford Levy

Sandford Levy is an adit driven into Sandford Hill, Mendip, ≈1830, to search for lead, ochre and blende deposits in the Carboniferous limestone (Gough, 1967). It contains many stalagmite deposits along its length, four of which were removed and their thickness measured (table 4.16). Derived minimum growth rates were calculated assuming start of growth at 1830. Drip samples were also taken, but from more rapidly dripping sources in close proximity to the stalagmites. This may again bring considerable uncertainty to the predicted growth rate. Calcium concentrations from these samples averaged 1.59 ± 0.06 mmol l^{-1} (1 σ; n=6). Using film thickness, temperature and partial pressure values as in earlier sections, growth rate was modelled over a range of probable drip rates (actual drip rates were not measured but assumed continuous), and the results are shown in figure 4.15 and compared to the measured levels. As for Brownes Folly Mine, there is a wide range of growth rates, but they fall within the 2 σ error range of those predicted.

Sample	*Thickness (mm)*	*Minimum Growth Rate (mm yr^{-1})*
SL-92-2	4.47 ± 0.25	0.028±0.002
SL-92-3	17.0 ± 0.50	0.105±0.003
SL-92-4	11.2 ± 1.63	0.069±0.010
SL-92-5	19.7 ± 0.41	0.122±0.003

Table 4.16. Sandford Levy stalagmite data

4.3.3.4 Kent's Cavern

One stalagmite sample was taken from the High Level Chamber area of Kent's Cavern (see figure 4.9). All the samples were forming on sediments which had last been disturbed by digging in 1876. The thickness was 4.80 ± 1.15 mm, giving a minimum growth rate of 0.041 mm yr^{-1} . Calcium concentrations were not taken, but are assumed to be the mean of those at flowstones KC-91-5 and 6, which are closest to the site (1.46 ± 0.36 mmol l^{-1}; n=14). The growth rates were then modelled as in previous sections, and compared to the actual thickness measured. The result is shown in figure 4.16, and growth rates agree within the 1σ errors of that predicted by the theory.

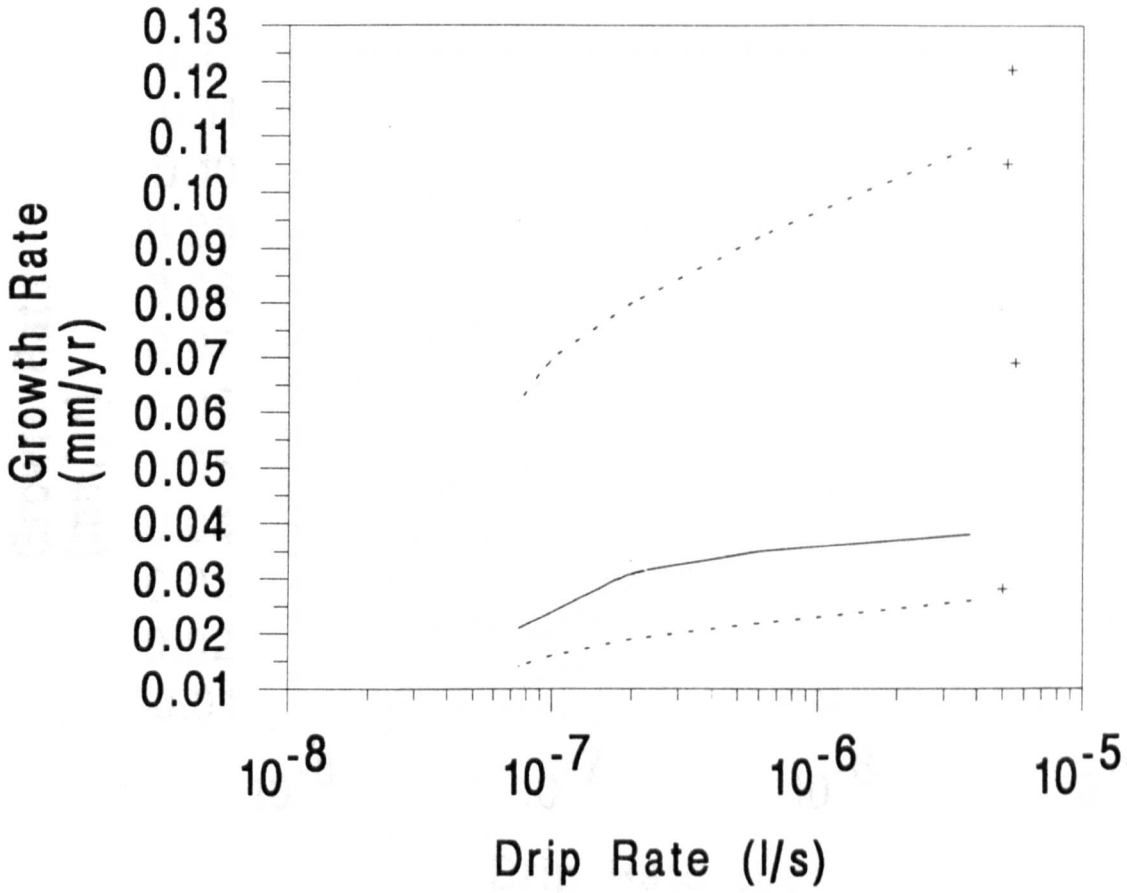

Figure 4.15. Relationship between predicted and actual growth rates for the Sandford Levy stalagmites. Mean predicted growth rate is shown by a solid line, predicted ±1σ errors (derived from 1σ errors in calcium concentration and film thickness) by dashed lines. Actual growth rates shown by crosses, error bars are omitted for clarity.

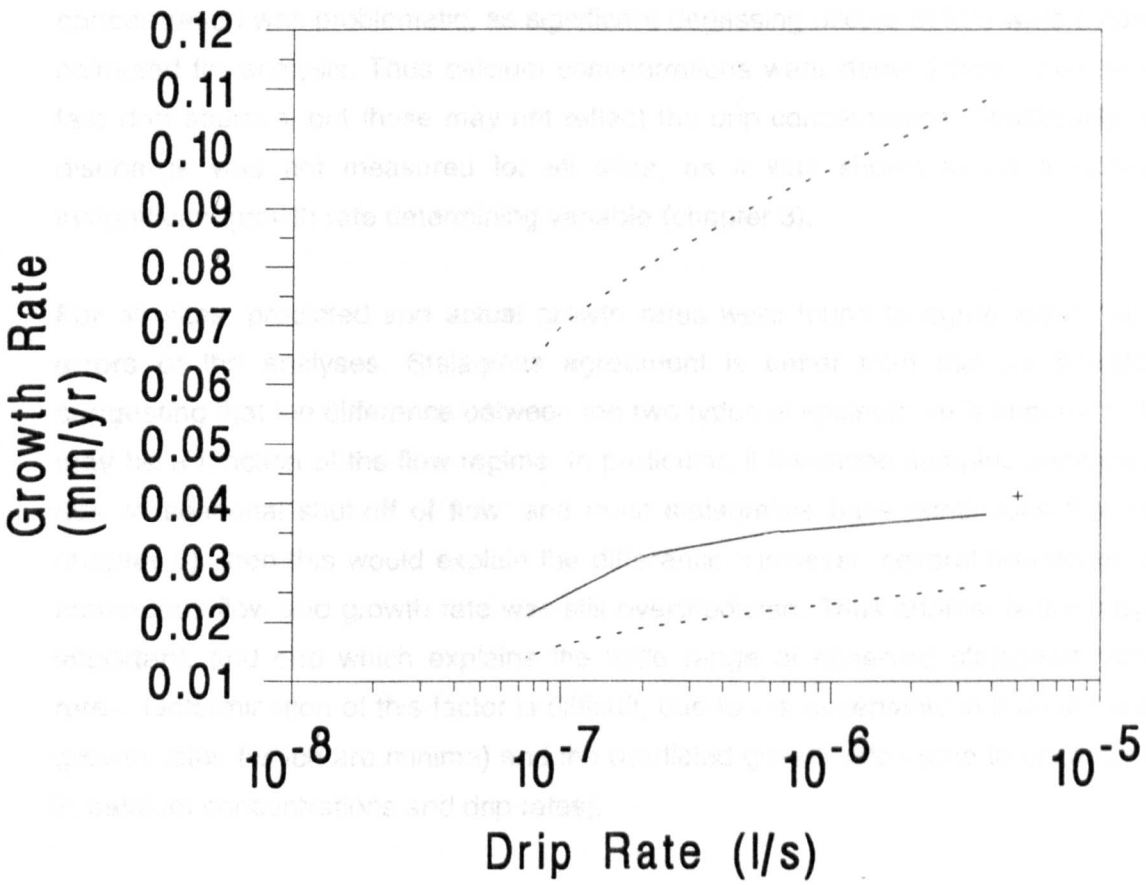

Figure 4.16. Relationship between predicted and actual growth rates for Kent's Cavern stalagmite KC-92-1. Mean predicted growth rate is shown by a solid line, predicted $\pm 1\sigma$ errors (derived from 1σ errors in calcium concentration and film thickness) by dashed lines. Actual growth rates shown by crosses, error bars are omitted for clarity.

4.3.3.5. Conclusions

Stalagmite growth rates were measured in four cave and mine systems, a comparison of results is shown in table 4.13. For all sites, determination of calcium concentration was problematic, as significant degassing occurs before waters can be collected for analysis. Thus calcium concentrations were derived from other nearby fast drip sources, but these may not reflect the drip concentration. Additionally, drip discharge was not measured for all sites, as it was shown to be a relatively insignificant growth rate determining variable (chapter 3).

For all sites, predicted and actual growth rates were found to agree within the 2σ errors of the analyses. Stalagmite agreement is better than that for flowstone, suggesting that the difference between the two types of speleothem is important. This may be a function of the flow regime. In particular, if flowstone samples underpredict due to seasonal shut-off of flow, and most stalagmites have continuous flow (see chapter 3), then this would explain the difference. However, several flowstones had continuous flow and growth rate was still overpredicted. Thus another factor may be important, and one which explains the wide range of observed stalagmite growth rates. Determination of this factor is difficult, due to the uncertainty in both the actual growth rates (which are minima) and the predicted growth rates (due to uncertainties in calcium concentrations and drip rates).

For one location, Lower Cave, stalagmite sites also had drip discharge measured over the course of a year. This variable was found to weakly correlate with growth rate. Thus under conditions of constant temperature and calcium ion concentration, the (relatively weak) relationship between growth rate and drip discharge may be observed.

4.4 Conclusions

The growth rate theory can be tested against the minimum growth rate of recent speleothems, for which all the growth rate determining variables can be measured. Analyses of both flowstones and stalagmites have shown that the modelled growth rates agree at a 2σ level. In general, better agreement occurred for stalagmites, and for one flowstone at Kent's Cavern, where rimstone pools were present. Most flowstones had significantly lower growth rates than predicted, possibly due to limited water supply due to seasonal shutoffs, the fact that growth rates are minima, or errors within the Plummer et al (1978, 1979) kinetic equations upon which the growth rate model is based. Precise conclusions were not possible due to both growth rates

being minima and the large errors associated with both film thickness and calcium concentrations.

More precise results are needed in which actual growth rates are accurately constrained and not minimum estimates. This can be achieved through the use of annual luminescence bands or MSU dating, both of which provide absolute growth rate measurements. The former was sought in this study, but banding was not preserved in any of the samples collected. The latter technique was feasible, but not a practical use of resources at the current time, but may have future research potential.

Important palaeoclimatic conclusions can be made from the work presented in this chapter. Where comparisons between seasonally limited and continuous flows were available, flowstones with continuous flow had statistically significant high growth rates compared to those with summer shut-off. For stalagmites at Lower Cave, drip rate was found to be the most important variable determining growth rate. However, all these results were obtained under conditions of constant calcium concentration and temperature. Thus a result which appears to be suggesting that growth rates can be successfully used as an indicator of palaeodischarge must be treated with extreme caution at this stage; what is now necessary are empirical measurements of growth rates over times of known temperature and / or calcium flux. This is pursued in the following chapters, by MSU dating and luminescence band analysis of samples which have grown over glacial / interglacial cycles.

CHAPTER FIVE

MASS SPECTROMETRIC MEASUREMENT OF THE TIMING AND RATE OF SPELEOTHEM GROWTH

5.1 Introduction

Chapter four demonstrated how theoretical growth rate could be tested against actual rates measured in the cave environment today, and it was concluded both that theoretical and actual growth rates agree within 2σ errors, and that under some conditions a potential palaeoclimate signal may be obtained. This assessment of the theory was made under present day conditions of temperature, groundwater flux and calcium ion concentration. What is now needed is an examination of an ancient growth rate record from the Holocene, during which time the changes in several of the growth rate determining variables are known from other palaeoclimate records. If successful, the record can be applied to speleothems growing earlier in the Quaternary. However, even in the Holocene, calcium concentrations are unknown, and precipitation poorly constrained, and for earlier Quaternary periods many or all of the variables are unknown. Thus in this chapter it is assumed that the growth rate theory does precisely predict growth rates at a 2σ confidence level, and thus growth rates determined by mass spectrometry are used to gain an insight into variations in the magnitude of the growth rate determining variables.

A growth rate record can be determined by obtaining two uranium series dates along the long axis of growth of a speleothem, and then measuring the distance between the two dated sections. This was first undertaken using alpha-spectrometric uranium-series (ASU) analyses. Results for stalagmites are summarised in Ford and Williams (1989, p345), and demonstrate a range of growth rates from 0.002 to 0.36 mm yr^{-1}. These analyses had large associated errors, due to two factors. Firstly, the large sample sizes associated with alpha-spectrometry (25-100 g) cause a large time averaging of growth; for example, a 100 g sample may be 5 cm thick, which for a sample growing at 0.01 mm yr^{-1}, consists of 5000 years of growth. Secondly, the error associated with alpha spectrometric dating is typically 10-20% at 2σ errors, which may be large enough to obscure any variation in growth rate.

Recent developments in mass-spectrometric uranium series (MSU) dating has allowed growth rates to be determined by this method for the first time. The technique was first developed on coral samples which have a high uranium concentration (≈ 1-3

ppm; Edwards, 1988), and more recently has been applied to other deposits, such as vein calcite (Winograd et al, 1992) and speleothem (Li et al, 1989; Dorale et al, 1992; Richards et al, in prep). Richards et al (in prep) demonstrated that over 200,000 ions of $^{234}U^{+}$ and $^{230}Th^{+}$ can be collected on a typical analysis, giving a 2σ error of under 1% from samples of a mass of only 0.5 - 2.5 grams. Such small samples can be cut to a thickness of approximately 1-2 mm using diamond bladed cutting equipment; sample cuts made parallel to the direction of growth significantly decrease the time averaging effect. For instance, a 1 mm thick sample would only span a time range of ± 100 years if the sample grew at 0.01 mm yr^{-1}, which is typically smaller than any error from the counting statistics. Thus MSU dating can be used to obtain high precision growth rates measured over long time periods.

MSU dating can also provide a more precise determination of the timing of growth hiatuses. This has already been applied to speleothems from submerged sea-caves in the Bahamas (Li et al, 1989; Richards et al, in prep). No work has been undertaken on terrestrial samples, which may respond to a palaeoclimatic shut-off as demonstrated in chapter 2. Mass spectrometric dating is thus used here both to precisely constrain periods of speleothem growth and growth cessation, and to determine speleothem growth rates.

Finally, $^{13}C/^{12}C$ ratios obtained in association with the mass spectrometric determinations may provide additional information on both the mechanisms of speleothem growth and growth rate change. Firstly, flowstone deposition may occur at a fast enough rate to cause kinetic fractionation of $^{13}C/^{12}C$ & $^{18}O/^{16}O$ ratios; Gascoyne (1992) observed that 5 out of 11 flowstones analysed from Yorkshire had undergone isotopic fractionation. This prevents a palaeotemperature signal being obtained from the ^{18}O data, but it may be possible to observe a strong correlation between increasing growth rate and increasing fractionation of ^{13}C and ^{18}O. Secondly, as introduced in chapter 2, $^{13}C/^{12}C$ ratios may reflect the type of plant community present on the surface above the speleothem, or distinguish whether the samples formed from a non-biogenic source. This may provide additional information on the growth process occurring, especially important if samples grew during periods of possible glacier cover. Thus carbon and oxygen isotope records are compared, where available, to the records of growth and growth rate change.

5.2 Experimental Method

5.2.1 Mass Spectrometry

The experimental procedure for preparing and analysing samples for mass spectrometric dating has been published elsewhere for both coral samples (Chen et al, 1986, 1992; Edwards et al, 1987; Edwards, 1988) and speleothems (Lundberg, 1990; Richards et al, in prep). The procedure followed here closely follows that of Edwards (1988), and detailed descriptions can be found there. Only an outline of the experimental method is presented, except where procedures or results differed from those cited above.

MSU speleothem analysis was undertaken at the Minnesota Isotope Laboratory, Department of Geology and Geophysics, University of Minnesota, in association with Larry Edwards. Samples were first cut using either a diamond wire saw or a slow speed diamond blade saw. The samples were cut parallel to the axis of growth, typical sample width being 1.5 to 3.0 mm, depending on the friability of the calcite. Sample weights ranged between 0.8 and 2.5 g, depending on the sample age and ^{238}U concentration. Cut samples were cleaned in super-pure water in an ultrasonic water bath; dried; weighed to five significant figures, and then transferred to a clean laboratory for chemical analysis.

The samples were first dissolved in a minimum of superpure* 7N HNO_3. To this solution, a known weight of both uranium and thorium spikes was added. The uranium was a double spike of approximately equal ratios of ^{233}U - ^{236}U, and two dilutions were used. For low uranium concentration samples (under 200 ppb ^{238}U), DIL-3F was used, which had a concentration of 0.132128 picomoles g^{-1} (≈ 28 pg g^{-1}) ^{233}U. Approximately 1-3 g of this spike were added to samples, in order to obtain a ratio of ^{235}U / ^{233}U of ≈ 10 (Edwards, 1988). DIL-2F had a concentration of x8 that of DIL-3F (0.951011 picomoles g^{-1}; ≈ 200 pg g^{-1} ^{233}U), and was used for samples of higher uranium concentration (200 - 3000 ppb). The thorium spike, DIL 2 of concentration 0.23708 picomoles g^{-1} ^{229}Th, was added in a fixed amount of 1.0-1.5 g. This gave approximately 5000 cps ^{229}Th during a typical mass spectrometry run, and an optimum ionisation efficiency for Th analyses (a total load of $<10^{13}$ atoms of thorium).

The sample was dissolved to dryness, redissolved in a minimum of superpure $HClO_4$, and dried down again. The sample was dissolved in approximately 4N HCl, and

* superpure reagents are double-distilled in quartz.

transferred to a centrifuge tube. Two drops of pure $FeCl_3$ were added, and then superpure concentrated NH_4OH was added dropwise until a brown iron precipitate formed. The sample was then centrifuged three times, the supernate being discarded each time, and the precipitate taken up in superpure water.

The sample was then taken up in superpure 7N HNO_3, and uranium and thorium were separated using a standard ion exchange column procedure. Initial columns were of 0.45 ml volume filled with Dowex AG1X8 anion exchange resin. After prewashing with 7N HNO_3, and the addition of the sample, the columns were washed with up to 1.8 ml of 7N HNO_3 to extract the iron, then 1.35 ml of 6N HCl to extract thorium and 1.8 ml of 1N HBr to extract uranium. The uranium and thorium elutes were both dried down, and taken up in 7N HNO_3 prior to the second column stage. These columns were of 0.15 ml volume, and after the addition of the sample, the columns were washed as before but with elutant volumes decreased by one third. The uranium and thorium separates were dried down and finally taken up in 14N HNO_3.

For analysis on the Finnigan MAT-262 the samples were loaded onto filaments. The uranium was loaded onto double Rembar rhenium filaments. The sample was dissolved in one drop of 0.1 N HNO_3, and approximately half of this was loaded onto the filament at a current of 0.8 A. The second half was stored in case of a run failure, or to perform a duplicate analysis. When the sample had dried onto the filament, the current was turned up to 1.3 A for 30 s, and then 1.6 A for 30 s, to remove water, sodium and potassium. The sample was then ready for analysis. Thorium samples were loaded onto a single Rembar rhenium filament which had already been run as a blank to test for high levels of ^{232}Th in the filament. The filament was first loaded with a graphite coating at 1.0 A, and when dry, the sample (dissolved in 0.1 N HNO_3 as for the uranium) was added at the same current. When fully loaded, the current was slowly increased to ≈ 2.0 A, to burn off any water and rare earth metals, and also to fuse the graphite and sample to the filament. The sample was then ready to run.

Samples were run on a Finnigan MAT-262 thermal ionisation mass spectrometer. Uranium analyses were run at typical evaporation currents of 0.6 to 1.1 A and ionisation currents of 3.5 to 4.5 A, an operating temperature of 1750-1850 °C. Ions were measured in the order $^{233\text{-}234\text{-}234\text{-}234\text{-}234\text{-}235\text{-}236}U^+$, background intensities were measured at masses of 233.5, 234.4 and 235.5, to enable any correction to occur for the tail of the large (unmeasured) $^{238}U^+$ beam. Each ion was collected for 4 s, and 11 scans made up one block of data, from which isotope ratios were

calculated. Typical runs lasted for 2 to 16 blocks (between 30 minutes and 3 hours), and between $1x10^4$ and $3x10^6$ ions of $^{234}U^+$ were counted. A typical run is shown in figure 5.1a. Thorium analyses were run at ionisation currents of 4.0 - 5.0 A (1950 - 2100 °C), the sample having previously been left at 1600-1700 °C (≈ 3.5 A) for 1 hour. Thorium ions were collected in the order $^{229\text{-}230\text{-}230\text{-}232}Th$, $^{229}Th^+$ and $^{232}Th^+$ were collected for 4 s on each run, $^{230}Th^+$ for 8 s. A block of data was complete after 8 such scans, and runs typically lasted for 2 to 10 blocks (20 minutes to 1 hour). Run temperatures were often adjusted between blocks, to keep them below the temperature at which the graphite burns off. A typical run is shown in figure 5.1b.

The raw data was converted into isotopic data using a Microsoft Excel spreadsheet and uranium series ages calculated iteratively from the decay equations using TK Solver on an Apple Macintosh microcomputer.

Several aspects of the procedure detailed above differ significantly from that published elsewhere, or additional difficulties were encountered which require further explanation. These points are detailed below.

(a) The first samples passed through the chemical separation procedure had a significant brown colouration when dissolved down for the final time. This was originally thought to be due to incomplete iron extraction. To prevent this, iron chloride addition was cut down to one drop, and the iron elution stage during uranium and thorium separation increased from 1 column volume to 4 column volumes. However, some samples still showed a brown colouration. It is now thought to be due to the presence of organic matter, which was not destroyed by the perchloric acid dry down procedure. It is thought that the presence of organics was responsible for the beam instability that often occurred in uranium runs (figure 5.1c), which often lead to the errors obtained from the run statistics being greater than the counting statistics. The failure of several analyses which had very low uranium concentrations (less than 100 ppb ^{238}U) may also be due to organic matter preventing a stable uranium ion beam from forming (see section 5.4.2.2). Future UV or heat lamp treatment of samples should overcome this problem.

(b) The Rembar single filaments used for the thorium analyses were routinely run as blanks (with only graphite loaded onto them) over the range 1950-2100 °C. The total number of counts per second of $^{230}Th^+$ and $^{232}Th^+$ were recorded at these temperatures, in order to determine the number of these ions which originated from the filament. This was because high thorium abundances were found in some

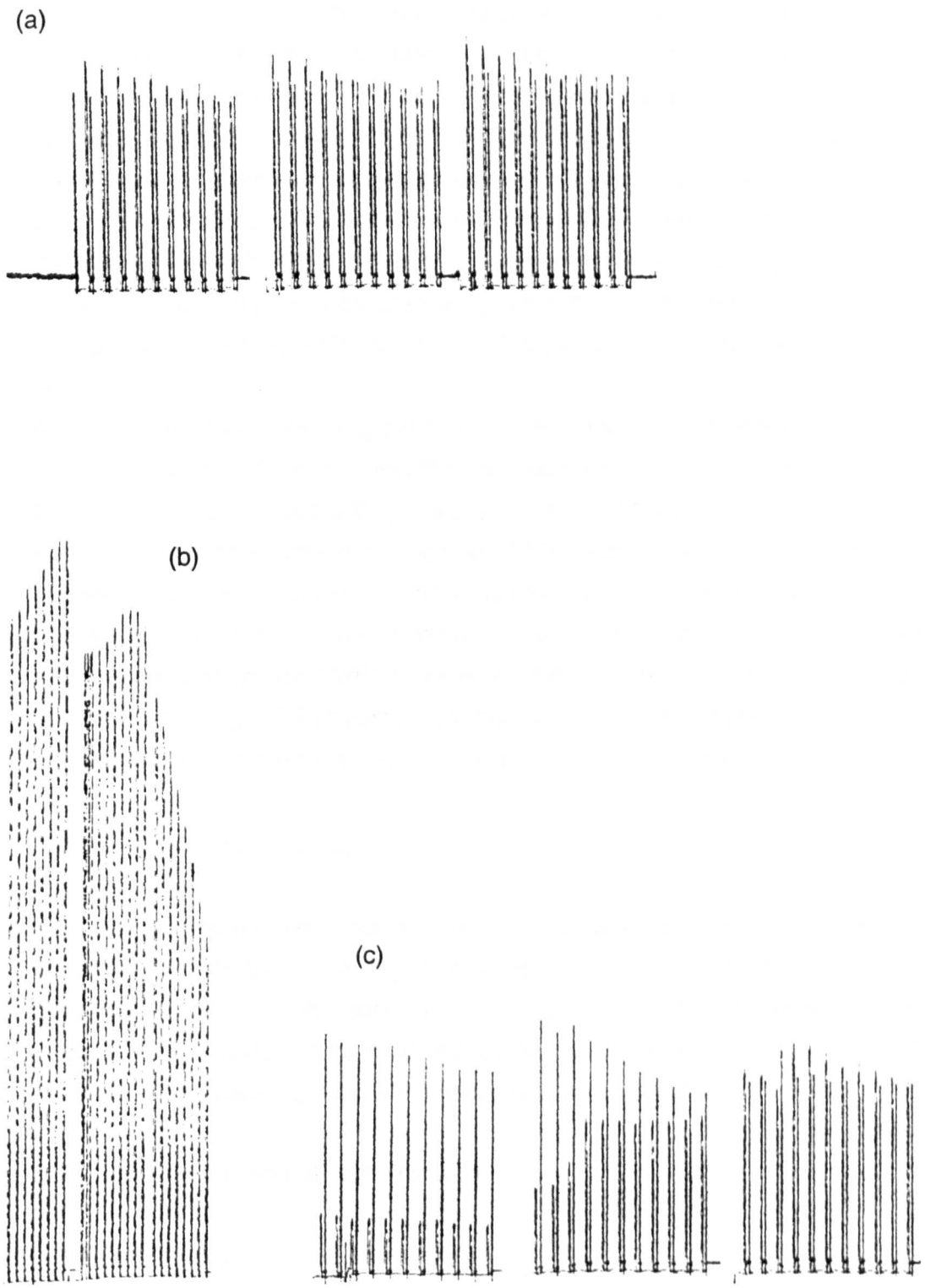

Figure 5.1. (a) Typical uranium analysis. Three blocks of eleven scans of data are shown. (b) Typical thorium analysis. Three blocks of eight scans are shown. (c) Unstable uranium run. Three blocks of data showing beam instability (current and temperature are not changed). In all cases, the vertical height of the bars is proportional to the ion beam size.

filament batches in earlier investigations (60 cps to 40,000 cps of $^{232}Th^{+}$; Edwards, 1988). Edwards (1988) also demonstrated that the concentrations of uranium ions were always insignificant compared to that obtained from the samples (60 - 3000 cps $^{238}U^{+}$). In this work no $^{230}Th^{+}$ was ever measured at running temperatures, whilst typically 100 to 4000 cps of $^{232}Th^{+}$ were recorded. The latter value was often of the same order of magnitude as the number of $^{232}Th^{+}$ cps derived from the speleothem samples themselves. Thus for some samples a large component of the error term in the ratios of $^{230}Th/^{232}Th$ is due to this filament source of ^{232}Th. However, the activity ratios of the samples was always greater than 100, irrespective of the error introduced by filament ^{232}Th, and thus did not affect the age determinations.

(c) One sample was limited by high ^{232}Th abundance in the speleothem. This caused a high count rate of $^{232}Th^{+}$ ions; the maximum count rate on the ion counter of the Finnigan MAT-262 is 600,000 cps. Sample SU-80-11A was run at this maximum level on the $^{232}Th^{+}$ ion beam (of an average of 531,000 cps $^{232}Th^{+}$), thus limiting its run temperature and number of $^{230}Th^{+}$ ions collected. This sample had a $^{230}Th/^{232}Th$ activity ratio of 5.1±0.1, the highest measured on the mass spectrometer, and provides a limit to the "dirtiest" samples measurable using this technique. Such samples with large ^{232}Th beams also required an age correction for the effect of the tail of this beam on the measured ^{230}Th and ^{229}Th isotopic abundance.

5.2.2 Carbon Isotope Analysis

^{13}C determinations were made using a standard oxygen and carbon isotopic extraction line at the University of Minnesota in association with Emi Ito. 15 mg powdered speleothem samples were dissolved in 30 ml of dilute H_3PO_4, and the evolved CO_2 trapped and collected using standard procedures. ^{18}O and ^{13}C isotopes were analysed using a Finnigan mass spectrometer.

5.3 Holocene Speleothem Growth

5.3.1 Introduction

A record of Holocene growth rate change is necessary to test the growth rate theory over a time period for which variations in the growth rate determining variables would have occurred. Over the Holocene, other palaeoclimate records exist which allow temperature and precipitation to be measured with various degrees of accuracy. However calcium ion concentrations are unknown, but if temperature and

precipitation can be determined, relative changes in calcium concentration can be obtained from the measured growth rate.

One such Holocene growth rate record can be calculated from mass spectrometric dates published for a stalagmite from Cold Water Cave, Iowa (Dorale et al, 1992). In this work, the uranium series dates were used to constrain a ^{13}C and ^{18}O isotopic record, but enough detail was given for a growth rate record to be extracted. This data is shown in figure 5.2, and shows a general increase in growth rate over time for the period 8-1 ka, although significant variations in growth rate occur (0.014 to 0.043 mm yr^{-1}). This range of growth rates is of the same order of magnitude to those determined in the cave environment in South West England today (chapter 4).

The actual growth rates can be compared to those predicted theoretically, if the variables determining growth rate are known for Iowa for the period 8-1 ka (table 5.1). An average water film thickness of 0.05 mm upon the stalagmite cap is assumed (see chapter 4), and a mean annual temperature of 10 °C. The latter value is the mean of that determined from oxygen isotope variations along the stalagmite profile, which reached a maximum of ≈ 11 °C for the period 5.9 - 3.6 ka, and averaged ≈ 8 °C for all other times. Calcium ion concentrations in modern day drip waters in the cave have not been determined, nor is it known how they have changed over time. Trainer and Heath (1976) measured spring water calcium concentration in Madison County, Iowa (with a range of 4.14 to 5.24 mmol l^{-1}), and Dupage County, Illinois (with a range of 2.84 to 4.76 mmol l^{-1}). However, this range of calcium concentrations is very high, and there is no reason why calcium values obtained today should have any relationship to those occurring in the past, since the region is currently intensively farmed and has thus undergone a significant vegetation change since the Holocene. Present day drip rates are also unknown, and a drip discharge of $1.5x10^{-5}$ to $1.5x10^{-7}$ l s^{-1} (one drip every 100 to 1000 seconds) is assumed. Table 5.1 demonstrates that if the measured growth rates are used to predict the palaeo-calcium ion concentration, concentrations of under 2.0 mmol l^{-1} are most likely for the period 8-1 ka. Such calcium ion concentrations have been recorded today in North American spring waters (Drake, 1983), and would not be considered unreasonable during the Holocene. No testing of the accuracy of the growth rate theory can be made from this sample, although it does suggest that groundwater calcium concentrations have increased since the introduction of intensive farming methods in the region.

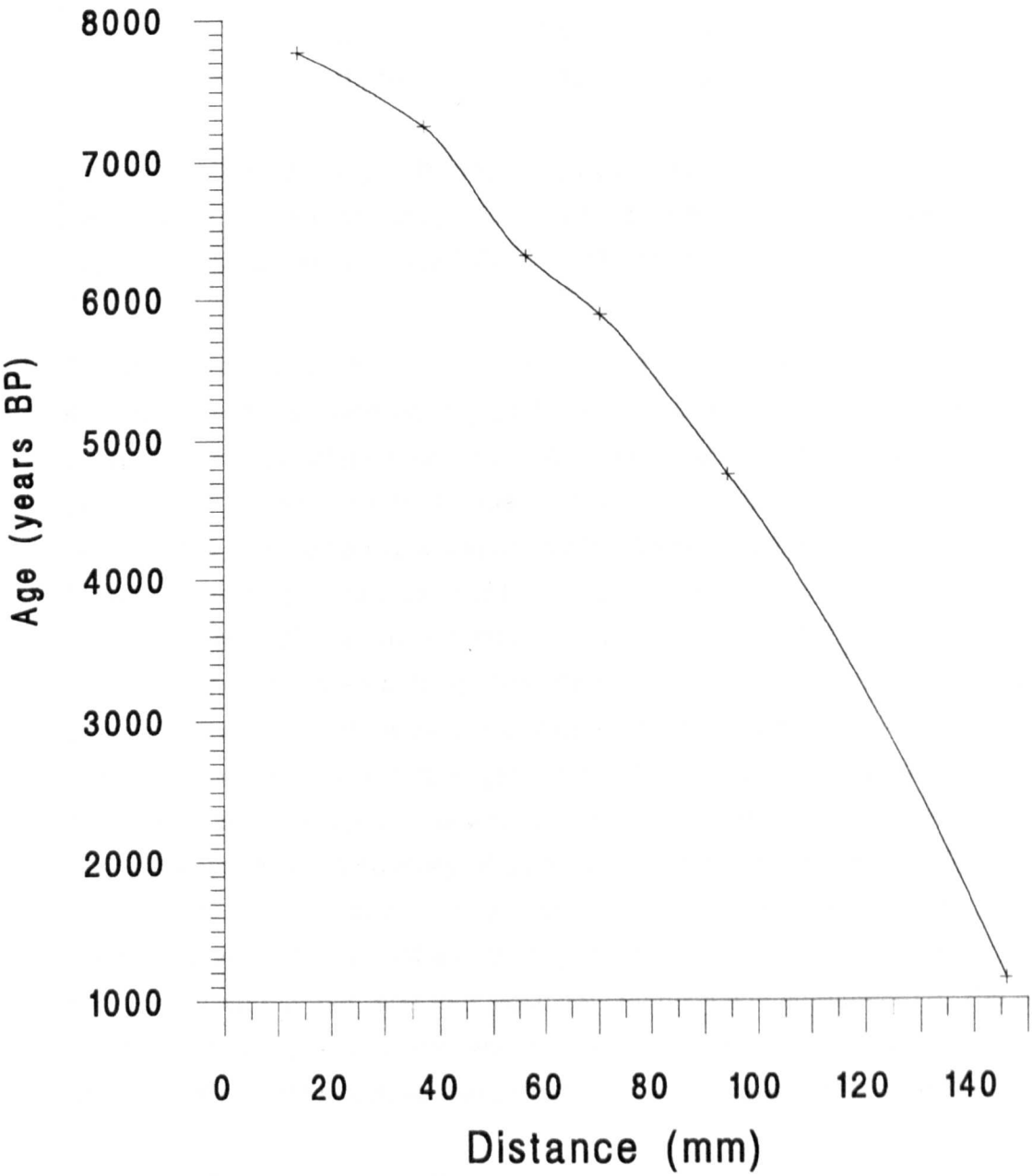

Figure 5.2. Variation in growth rate over the period 8000 to 1000 years b.p. for stalagmite 1s (after Dorale et al, 1992). Error bars are not shown, but are smaller than the symbols used.

	Calcium Ion Concentration (mmol l^{-1})			
Discharge ($l\ s^{-1}$)	1.0	2.0	3.0	4.0
$1.5x10^{-6}$	0.014	0.053	0.091	0.129
$5x10^{-7}$	0.013	0.046	0.084	0.120
$3x10^{-7}$	0.012	0.045	0.078	0.110
$1.5x10^{-7}$	0.010	0.038	0.065	0.093

Table 5.1. Theoretical growth rates for varying calcium ion concentrations and drip discharges for the Iowa stalagmite. Growth rates determined by mass spectrometry are in the range 0.01 to 0.043 mm yr^{-1}.

Growth rate trends over time can also be investigated for the Iowa stalagmite. Figure 5.2 demonstrates an increase in growth rate over time, with the fastest rates between 7.2 and 6.3 ka and after 4.8 ka. This can be compared to changes in temperature and precipitation for the region. Temperature was demonstrated to increase by 3 °C between 5.9 and 3.6 ka (Dorale et al, 1992). This would increase growth rate by 30% (assuming an initial temperature of 8 °C, drip discharge of $1.5x10^{-6}$ l s^{-1} (1 drip every 100 seconds), and calcium concentrations between 1.0 and 2.0 mmol l^{-1}). Such an increase is not observed in the growth rate record of the sample, but may be due to a decrease in drip rate or the seasonal availability of water due to increasing aridity. A transition from forest to prairie vegetation has been observed over the period 8-3 ka, suggesting an increase in aridity (Chumbley et al, 1990). This has been explained due to the increased frequency of summer Pacific air (Baker et al, 1992), and may have countered any increase in growth rate from temperature increases. However, changes in vegetation would also be expected to change the calcium concentrations in an unknown manner, and thus absolute determination is impossible. The general trend of increasing growth rate over time does not reflect the changes in temperature or precipitation, and suggests that calcium concentration is the dominant variable.

A record of growth rate change needs to be obtained from a region where the variables influencing growth rate can be precisely determined. One such record was obtained from Sutherland, from a region where recent dripwater calcium ion concentrations have been determined from previous studies, and temperature changes are well known (the sample also has an annual banding record as presented in chapter 6). This record is presented below.

5.3.2 The Sutherland Record

Sutherland stalagmite SU-80-11, was collected from Uamh an Tartair, part of the Cnoc Nan Uamh System, Traligill, Assynt, by Pete Smart in 1980. The cave is at an altitude of 221 m, and is developed in the dolomites of the Cambro-Ordovician Durness limestone. The bedrock has a high magnesium content, which is reflected in the geochemistry of the groundwaters (Mg/Ca ratio of 1.0; Trudgill et al, 1980), but not in speleothems, as a Mg/Ca ratio of over 2.9 is required for magnesium deposition (Fischbeck and Muller, 1971). The high magnesium concentration in the groundwaters is not enough to affect growth rate, as magnesium has insignificant influence below a concentration of 2.0 mmol l^{-1} (Dreybrodt et al, 1987); present day groundwaters have a magnesium concentration of ≈1.3 mmol l^{-1}.

A survey and detailed cave description is presented in Lawson (1988), and the sampling location of SU-80-11 is shown in Atkinson et al (1986). It is a stalagmite which shows continuous growth with no visible hiatuses, and was actively forming when collected. It had been previously dated by alpha spectrometry, with dates obtained between 9±1 and 5±1 ka (1σ errors; Atkinson et al, 1986). The sample shows luminescence banding (chapter 6, this study), and mass spectrometric dating could therefore be used both to test the annual nature of this banding, and to assess the growth rate model.

Six samples of 2 g or less were cut parallel to the growth banding from a 4 mm thick central section cut down the long axis of growth (SU-80-11A, B, C, D, E, and H; sampling locations shown in figure 5.3). SU-80-11D was subsequently divided into two, to provide duplicate analyses, and this was prepared and run by David Richards, SU-80-11H was dated by Andy Farrant. All other samples were run by the author.

5.3.3 Results

The dating results are shown in table 5.2. The analyses fall in stratigraphic sequence, and differ from each other at a 2σ level. The duplicate analyses of sample D agree within the 2σ error of the ages. Except for SU-80-11A, $^{230}Th/^{232}Th$ activity ratios are above that requiring correction for significant detrital thorium contamination. The former had a $[^{230}Th/^{232}Th]_{act}$ ratio of ≈5, and the mass spectrometer run was at the maximum possible beam intensity on the ion counter (< 600,000 cps $^{232}Th^{+}$). For all analyses, low abundances of ^{230}Th were present (380 to 960 million atoms/g of speleothem), due to the young age of the stalagmite. However, 3000 to 9000 counts

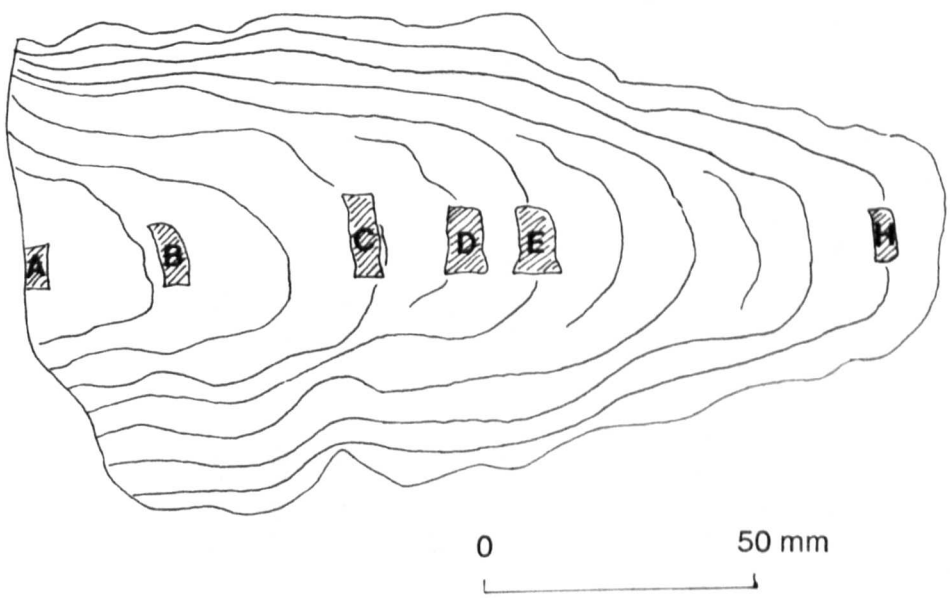

Figure 5.3. Stalagmite sample SU-80-11, showing the locations of the MSU samples.

Sample Name[a]	Distance down axis[a]	^{238}U conc ng g^{-1}	$^{234}U/^{238}U$ x 10^6	$^{230}Th/^{232}Th$ x 10^6	$\delta^{234}U(0)$[b,e] per mil	$\delta 234U(T)$[b,e] per mil	$[^{230}Th/^{238}U]$[c,e] act	Age[d,e] years B.P.	Modified Age[f] years B.P.
SU-80-11A	2mm	247.61±0.75	64.64±0.36	26.3±0.9	181.2±6.6	185.7±6.8	0.0878±.0029	8340±290	6970±750
SU-80-11B	28mm	254.76±0.75	64.38±0.43	110.1±3.0	176.5±7.8	179.0±7.9	0.0506±.0014	4730±130	4540±160
SU-80-11C	64mm	237.11±0.48	66.84±0.27	148.7±4.5	221.4±4.9	223.6±5.0	0.0378±.0011	3370±100	3270±110
SU-80-11D(1)	80mm	329.49±0.30	65.97±0.12	149.9±2.3	205.6±2.1	207.4±2.2	0.0339±.00046	3103±43	3014±62
SU-80-11D(2)		329.56±0.24	65.90±0.11	147.0±6.5	204.4±2.1	206.2±2.1	0.0333±.00141	3051±131	2962±138
SU-80-11E	96mm	302.95±1.11	67.31±0.31	1622±95	230.1±5.6	231.9±5.7	0.03042±.00077	2680±70	2670±70
SU-80-11H	162mm	300.64±0.99	65.57±1.26	186.7±1.26	198.4±23.0	198.8±23.0	0.00904±.00159	823±146	798±150

[a] Sample location and distances shown in Figure 5.3; SU-80-11D(1) and SU-80-11D(2) are replicate analyses of different aliquots of the solution derived from sample SU-80-11D.

[b] $\delta^{234}U = \{[(^{234}U/^{238}U)/(^{234}U/^{238}U)eq]-1\}x10^3$, where $(^{234}U/^{238}U)eq$ is the atomic ratio at secular equilibrium and is equal to $5.472x10^{-5}$. $\delta^{234}U(0)$ is the measured value. $\delta^{234}U(T)$ is the initial value and is equal to $[\delta^{234}U(0)][e(\lambda^{234}T)]$

[c] Calculated from the atomic $^{230}Th/^{238}U$ ratio by multiplying by $\lambda_{230}/\lambda_{238}$.

[d] Ages are calculated using $[^{230}Th^{238}U]act -1 = e^{-\lambda 230T} + (\delta^{234}U(0)/1000)(\lambda_{230}/\lambda_{230}-\lambda_{234})(1-e^{-(\lambda 230-\lambda 234)T})$ where T is the age in years.

[e] Values for decay constants are $\lambda_{238}=1.551x10^{-10}$ yr^{-1} (Jaffey et al, 1971), $\lambda_{234}=2.835x10^{-6}$ yr^{-1} (de Bievre et al, 1971; Lounsbury and Durham, 1971), and $\lambda_{230}=9.195x10^{-6}$ yr^{-1} (Meadows et al, 1980)

[f] Modified ages assume an initial $^{230}Th/^{232}Th$ atomic ratio of $4.4±2.2x10^{-6}$ (method 1, equation 8 from Schwarz (1980)). This is the value for a material at secular equilibrium, with a crustal $^{232}Th/^{238}U$ value of 3.8. The error is arbitarily assumed to be 50%. The error in the modified age for SU-80-11A is large due to detrital contamination and the uncertainty in the initial $^{230}Th/^{232}Th$ ratio used in correcting for this contamination. This initial ratio may be significantly in error. Kaufman (1993) notes a global range of initial $^{230}Th/^{232}Th$ atomic ratios of $3.6x10^{-6}$ to $26.9x10^{-6}$; such a modified ratio would make ages significantly younger than quoted here.

Table 5.2. Uranium / Thorium isotopic data and mass-spectrometric ages for SU-80-11.

of $^{230}Th^{+}$ were counted in each mass spectrometer run (except sample SU-90-11H, with only 130 counts of $^{230}Th^{+}$), giving counting statistics comparable to the run statistics, and overall 2σ errors of 2-5%.

The results are shown graphically in figure 5.4. Growth commenced at 6.97±0.75 ka, and continued to the present day. Growth rates calculated from the age determinations demonstrate a gradual increase in growth rate over the period 7 to 3.5 ka. Initial growth rate is approximately 0.011 mm yr^{-1}. The maximum growth rate of 0.055 mm yr^{-1} occurs between samples C and E. The annual banding record (see chapter 6) shows that growth rate continues at this level for short periods over the 120 - 160 mm section of the sample. Since the sample was still actively growing when collected, growth rate must slow down significantly sometime over the last 1.5 ka. The average growth rate between sample H and the stalagmite cap is 0.010±0.004 mm yr^{-1}.

Finally, the mass spectrometric ages are consistently ≈2 ka younger than those previously obtained by alpha spectrometry. This is discussed in detail in the following section.

5.3.4 Interpretation

5.3.4.1 Testing the Growth Rate Theory.

The growth rate record obtained from the mass spectrometric ages can be compared to that predicted from theory. Growth rate was predicted only for the section between subsample 'H' and the stalagmite cap (0.010±0.004 mm yr^{-1}), as known present day values for the variables affecting growth rate can be employed.

In modelling growth rate, temperature was assumed to be 8 °C (the present mean annual temperature), water film thickness was taken as 0.05 mm (see chapter 4), and calcium ion concentration of the drip waters 1.33±0.24 mmol l^{-1}. The latter was the average of 40 measures of cave and spring seeps in the catchment measured by Pete Smart (unpublished data). It was assumed that this value had not changed significantly since the time of speleothem growth, an assumption considered in greater detail later. Stalagmite growth rate was modelled for drip discharges in the range $1.5x10^{-5}$ to $1.5x10^{-7}$ l s^{-1} (10 - 1000 seconds per drip), a range that was considered suitable for a stalagmite of 8 cm diameter.

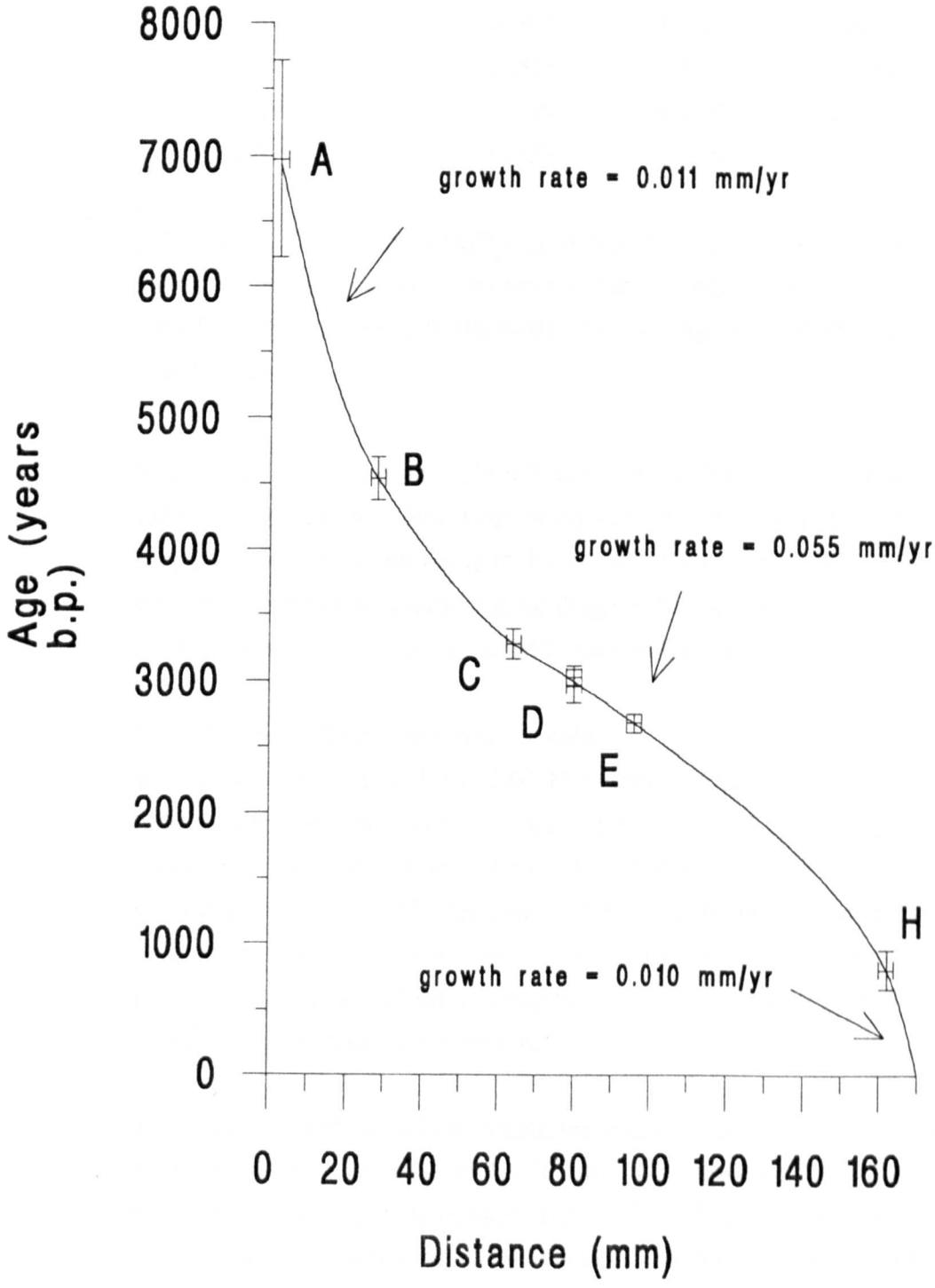

Figure 5.4. Variations in growth rate for sample SU-80-11, constrained by the MSU analyses.

	Calcium Ion Concentration (mmol l^{-1})		
Drip Discharge ($l\ s^{-1}$)	*0.85*	*1.33*	*1.81*
$1.5x10^{-5}$	0.007	0.022	0.039
$1.5x10^{-6}$	0.007	0.021	0.037
$5.0x10^{-7}$	0.007	0.020	0.035
$3.0x10^{-7}$	0.006	0.019	0.033
$1.5x10^{-7}$	0.005	0.016	0.028

Table 5.3. Theoretical growth rate of SU-80-11 calculated for varying drip rates and 2σ range of calcium ion concentrations. Recent measured growth rate was 0.010±0.004 mm yr^{-1}, demonstrating a good agreement between the theoretical and actual rates.

The results are shown in table 5.3, and demonstrate that theoretical growth rates are within the 2σ range of that determined from the MSU analysis. Precise comparison is difficult due to the uncertainty in the actual growth rate (0.010±0.004 mm yr^{-1}) and in the calcium determinations, but do suggest that either an overprediction is occurring by the theory, or that calcium concentrations have increased in recent years.

5.3.4.2 Growth Rate and Palaeoclimate

The growth rate record for SU-80-11 shows a gradual increase over the period 7 to 3.5 ka, with a maximum growth rate in the period 3.5 to 2.5 ka, and then a decrease sometime over the period 1.5 to 0 ka. These changes may be due to a gradual variation in any one of drip rate, calcium concentration or temperature. Possible changes in these variables over the period 7 ka to 0 ka can be determined from other contemporaneous Holocene records from the region, and their significance in controlling growth rate determined.

The most accurate data is available for mean annual temperature, with many records demonstrating an increase of 1-2 °C from that observed today during the period 8 ka to 5 ka, and then a subsequent drop of 1-2 °C until today (Simmons et al, 1981). Thus growth rate would be expected to increase over the period 8-5 ka, instead the stalagmite increases in growth rate over the period 3.5 to 2.5 ka, when temperature is known to have declined. Hence another variable must be more important.

Variations in precipitation are less well known; it has been suggested that precipitation was 10% lower than today during the Boreal (9-7 ka), and 10% higher than present during the Atlantic (7-5 ka) (Simmons et al, 1981), although the error

associated with these values are unknown. Again, such small shifts in precipitation are unlikely to cause a large enough change in drip rate to significantly change growth rates. Table 5.4a shows the effect of changing both temperature and drip rate, assuming an average drip discharge of $8x10^{-7}$ l s^{-1} (one drip every 200 seconds), and that a 10% change in precipitation leads to a 10% change in drip rate. Again drip rate variations do not generate growth rate variations large enough to explain that actually observed. Even if the 10% change in precipitation triggered a 50% change in drip rate, the shift in growth rate would still be too small to explain the observed growth rate variations. Furthermore, the trend of increasing precipitation to a maximum in the Atlantic period would be expected to give the fastest growth rate then, whereas maximum growth rate occurs after this period, between 3.5 ka and 2.5 ka.

One possible explanation may be that the drip feeding the sample was only active all year round during the period of maximum growth rate, and that it shut off during the summer for the other growth periods. This would lead to a significant increase in growth rate, perhaps by 100% if drip water supply increased from 6 to 12 months, or by 300% if availability increased from 3 to 12 months. Such a shut-off was observed for slowly dripping stalagmites which are actively forming today (two out of eleven samples; chapter 4). Additional evidence that this may have occurred comes from the annual growth banding record (chapter 6), since the majority of banding is only present in the section of the sample growing at the fast growth rate (0.055 mm yr^{-1}). Preservation of banding is thought to rely on seasonal differentiation of drip waters, suggesting that at lower growth rates such a differentiation is not possible. This could be explained by the drip source drying up during the summer, perhaps due to decreased precipitation or an evaporation deficit, preventing the transmission of the summer banding signal. However, if a seasonal shut-off of water supply was occurring, it again disagrees with the timing of the changes in precipitation thought to occur over the Holocene.

(a)

Time (ka)	*Growth Rate (mm yr^{-1})*	
	Actual	*Predicted*
7-5	0.011±0.005	0.026
5-3.5	0.028±0.002	0.021
3.5-2.5	0.055±0.002	0.021
2.5-0.8	0.034±0.002	0.021
0.8-0	0.010±0.004	0.021

(b)

Time (ka)	*Predicted Calcium Ion Concentration (mmol l^{-1})*
7-5	0.79-1.08
5-3.5	1.50
3.5-2.5	2.10
2.5-0.8	1.55
0.8-0	0.81-1.03

Table 5.4. (a) Comparison of measured and theoretical growth rates for sample SU-80-11. Drip rates and temperature are varied as detailed in the text; calcium ion concentrations are held constant. (b) Modelled changes in calcium ion concentrations, based on the measured growth rates and the drip rate and temperature changes detailed in the text. The ranges of calcium ion concentrations in some instances are due to the uncertainties in the growth rate measurements.

Calcium ion concentration variations are not known for the last 7 ka, but can be calculated from the measured growth rates and known temperature and precipitation variations. The results are shown in table 5.4b. To explain the change in growth rate from 0.011 to 0.055 mm yr^{-1} in terms of calcium variations requires a change from 0.94 to 2.1 mmol l^{-1}. This requires a significant change in soil pCO_2; a doubling of calcium concentration requires a fivefold increase in soil pCO_2 (assuming open system evolution). This may be caused by vegetation changes or increases in plant productivity. Several pollen and fossil tree stump records are preserved for Assynt for the time sample SU-80-11 grew (Birks, 1975), and give a record of vegetation change. These show an increase in blanket bog formation after 5.5 ka, with an acceleration after 4.5 ka. Additionally, from 4.0 to 3.5 ka, pollen diagrams show a widespread decrease in *Pinus* throughout north west Scotland, from both lowland

and high altitude sites. Previous to this a significant proportion of the arboreal pollen record reflected a *Betula - Corylus* population. The widespread geographical spread of the *Pinus* decline convinced both Pennington et al (1972) and Birks (1975) that the increased wetness in the Atlantic period triggered this change in vegetation, rather than any anthropogenic effect.

Thus during the period of speleothem growth, the overlying plant communities may have undergone very significant shifts, triggered by comparatively small changes in climatic conditions. How this was reflected in the local plant community in the Traligill Basin, and subsequently in the dissolved calcium ion concentrations reaching the sample, is not known. To explain the increased growth rate, the changes in vegetation would have to be such that groundwater calcium concentrations were significantly increased. Present day vegetation in the Traligill Valley is of both *Calluna* with acidic peat soils, and also grassland with sparse *Betula nana* and brown earth soils. A shift to the former may have resulted in a decrease in the soil pCO_2 in recent years. Changes in vegetation in the Holocene away from the *Pinus* vegetation, which is known to have comparatively poorly developed soils, may also have increased the soil pCO_2.

Changes in the calcium ion concentration may also occur due to increases in plant productivity with rising solar insolation (see chapter 2). Over the period of growth of SU-80-11, insolation declines from 508 W m^{-2} to 476 W m^{-2}. If the insolation variations caused a change in plant productivity and thus dissolved calcium ion concentration, then a decrease in growth rate would be expected to occur over the period of growth of SU-80-11. This is not observed, and thus it appears that solar insolation levels do not have a direct influence on the growth rate of this sample.

SU-80-11 shows an increase in growth rate between 3.5 and 2.5 ka, a time for which temperatures and precipitation had started to decline. Of the two, only variations in the seasonal supply of drip water can explain the observed increase in growth rate, but if true probably demonstrates a non-linear relationship between precipitation variations and growth rate change. Calcium ion concentration increases may also have occurred, increasing growth rate in this time of climatic deterioration. Pollen evidence suggests that it is possible that significant calcium ion concentration changes could have occurred over the period in question due to shifts in vegetation type.

5.3.4.3 Timing of Growth

The mass spectrometric dates also provide a precise determination of the commencement of growth of SU-80-11. Atkinson et al (1986) suggest that speleothem growth in the cave was limited by flooding during the last glaciation, with the basal date of 9±1 ka obtained by alpha-spectrometry on this sample marking the earliest time of water recession. Using mass spectrometry, growth commencement was timed at 6.97±0.75 ka (the large error is associated with the uncertainty caused by the high $^{230}Th/^{232}Th$ activity ratio). The timing of growth commencement can be compared to potential factors which cause speleothem growth to occur (section 3.4.2).

(a) Drip rate commencement. The record of precipitation for the period 9 to 0 ka obtained from pollen records suggests that changes in precipitation would only vary by ± 10% of that occurring today, as detailed above. Unless a non-linear relationship between drip rate and precipitation occurred, it is unlikely that low levels of precipitation would be an important factor in limiting the start of growth of SU-80-11.

(b) Severe temperature conditions, such as the freezing of the soil and bedrock, preventing groundwater flow, could cause growth cessation. However, this is again unlikely to be a factor, as temperature records show mean annual temperatures within 2 °C of that of today prior to when growth commenced at 7 ka.

(c) Calcium ion concentrations below that of atmospheric equilibrium concentration would limit growth. The variations in growth rate have already suggested that changes in calcium ion concentration may have occurred during the course of speleothem deposition. The average initial growth rate measured 0.011 ± 0.005 mm yr^{-1}. Assuming temperature of 8 °C, and a drip discharge of $5x10^{-7}$ to $1.5x10^{-6}$ l s^{-1} (200 ± 100 seconds per drip), such a growth rate requires a calcium ion concentration of between 0.79 and 1.08 mmol l^{-1}. This range is not significantly above the calcium ion concentrations necessary for saturation to occur (0.60 to 0.70 mmol l^{-1} at 5-10 °C). Thus concentrations may have initially been below atmospheric equilibrium concentration, and explain why growth first started at 7 ka.

(d) Other factors. Hydrological factors may be important in preventing speleothem growth due to cave flooding, a mechanism previously suggested by Atkinson et al (1986) as being the cause of the initial lack of growth. However, a glacial meltwater origin was proposed for the flooding, and a younger basal date of 6.97±0.75 ka makes this unlikely, as all evidence suggests that the Late Devensian ice sheet

would have left the region by 13 - 12 ka (Sutherland, 1991). However, sediment deposited by this glaciation may have blocked the cave, the timing of growth commencement may represent the clearing of these deposits.

Thus it is difficult to explain the timing of the commencement of growth of SU-80-11 in terms of a palaeotemperature or precipitation signal. The most likely cause of growth commencement is due to the clearance of the sediment blockage of the cave, although it may also be explained by an increase in calcium ion concentrations above the level required for saturation to occur, or a non-linear relationship between drip rate and precipitation. This again suggests that growth periods can not be explained in a simple relationship to climate change, but to a more complex combination of geological, climatic and vegetation changes.

5.3.4.4 Comparison of MSU and ASU Dates

It is important to note the discrepancy between the mass spectrometric dates with the previously published alpha spectrometric ages. The latter were performed at the Scottish Universities Research Reactor Centre, East Kilbride, in the early 1980's, and published in Atkinson et al (1986). 'Top', 'Middle' and 'Bottom' analyses were performed (the cutting diagrams for which are unavailable), and when corrected for the half-life value used for ^{230}Th (see chapter 2), gave ages of 5.6±1.1 ka, 7.9±1.2 ka and 9.1±1.2 ka respectively (1σ errors). When compared to the MSU ages in table 5.2, it is apparent that the analyses do not agree at a 2σ level, even if the dates are left uncorrected for the thorium half-life variations.

The reason for this discrepancy is unclear, but must put into some doubt the accuracy of these early alpha-spectrometric dates. The MSU age analyses would be considered correct, as work by Edwards (1988) has shown precise agreement between MSU dates and ages determined from annual band counting in corals. More recent work from the Minnesota Isotope Laboratory has also yielded recent (<100 year) ages on actively forming samples (Richards, unpublished data; Asmerom, unpublished data). The inaccuracy of the ASU ages can not be due to an incorrect ^{230}Th half-life being used, as even the corrected ages do not agree. Lundberg (1990) demonstrated a consistent 20% overprediction in the age of samples for ASU compared to MSU age determinations at McMaster University. This was ascribed to the early use of standard grade iron chloride which had a considerable ^{230}Th component; MSU analyses using 99% purity iron chloride yielded precise ages. It is not known whether this could provide an explanation here; the iron chloride used in

the Minnesota Isotope Laboratory is derived from meteoritic iron and superpure HCl, and no ^{230}Th has been observed in blank (control) analyses.

5.3.5 Conclusions

The recent growth rate of stalagmite sample SU-80-11 shows a good agreement with that theoretically predicted within the 2σ uncertainties. When compared over the period 7-0 ka, the growth rate record suggests that either changes in the calcium concentrations of the waters may have occurred, or a seasonal drip water shut-off mechanism was acting. The former may be due to a significant change in vegetation type occurring over the period 3.5-2.5 ka. This correlates with the timing of the *Pinus* decline in the region. These vegetation changes occurred despite only relatively small variations in climate over this time; thus stalagmite growth rate may be affected by changes in vegetation cover rather than directly by changes in temperature or precipitation. If calcium ion concentration variations dominate the growth rate signal, then it does generate a more complex palaeoclimate signal than one which can be explained solely in terms of temperature or precipitation alone. This complexity could also increase because both the calcium and drip rate signals could interact. If a shut-off occurred such that drip waters only occurred in winter months, then this would be at the time of year when calcium concentrations are at their lowest, and may be below saturation. This may further decrease growth rate, and provide another non-linear relationship between growth rate and palaeoclimate change. The timing of the onset of speleothem growth is also of interest, as the commencement was not immediately after the end of glaciation, but showed a 5 ka lag. Other factors such as sediment blockage, calcium undersaturation or a non-linear response to precipitation may thus be more important.

Differing growth rate trends between the samples from Sutherland and Iowa over the same time period demonstrate that growth rate responds to the different palaeoclimatic and palaeoenvironmental changes in these regions. What are now needed are multiple records obtained from one region over the same time period, in order to test whether the growth rate and growth records from these samples respond to an overriding palaeoclimate signal.

5.4 Late Quaternary Speleothem Growth

5.4.1 Introduction

Speleothem growth rate variations are now examined over a longer period of time (200 ka) using two coeval samples. Two long flowstone sequences, both of which had previously been dated by alpha-spectrometry, were collected from North West Yorkshire from Stump Cross Caverns (Sutcliffe et al, 1985), and Lancaster Hole (Gascoyne et al, 1983). For both samples, palaeoclimate change over the last 200 ka is poorly understood, with very few records of temperature change, and virtually no information on variations in precipitation and calcium. Thus the growth rates obtained are used to give an insight into the variations of these variables.

5.4.2 The Stump Cross Record

5.4.2.1 Site Description

Stump Cross Caverns are situated on Greenhow Hill, between Wharfedale and Nidderdale, at an altitude of 361 m a.s.l.. They form part of the Stump Cross / Mungo Gill cave system, developed in an outlier of the Upper Carboniferous Great Scar Limestone. The cave was originally discovered by Victorian miners, exploring the many lead and fluorospar rich veins within the Great Scar limestone on Greenhow Hill. The system follows both the strike of the limestone (east-west) and the direction of jointing (north-south), resurging at an altitude of 310 m to the south west at Dry Gill.

Flowstone samples SC-90-5/6 were collected from the top of Bowling Alley passage, one of two main fossil streamways in the high level series of the cave (at a depth of 15 m below the surface), by Angus Tillotson and Pete Smart in 1990 and the author in 1992. A survey is presented in figure 5.5. The Bowling Alley descends on a very gentle gradient to it's termination where a narrow fissure carries water down to the middle levels of the cave; water backs up here in very wet conditions. The flowstone sampling site is stratigraphically consistent with sample sites IIIA/B of Sutcliffe et al (1985), where equivalent flowstone samples were alpha-spectrometrically dated in order to determine the age of a *Gulo gulo* (wolverine) deposit found at several locations within the Bowling Alley (sites IIIA/B/C in Sutcliffe et al, 1985).

Sample SC-90-5/6 consists of a 1m thick flowstone sequence, the base of which sits upon finely laminated sediments containing flowstone fragments. The flowstone

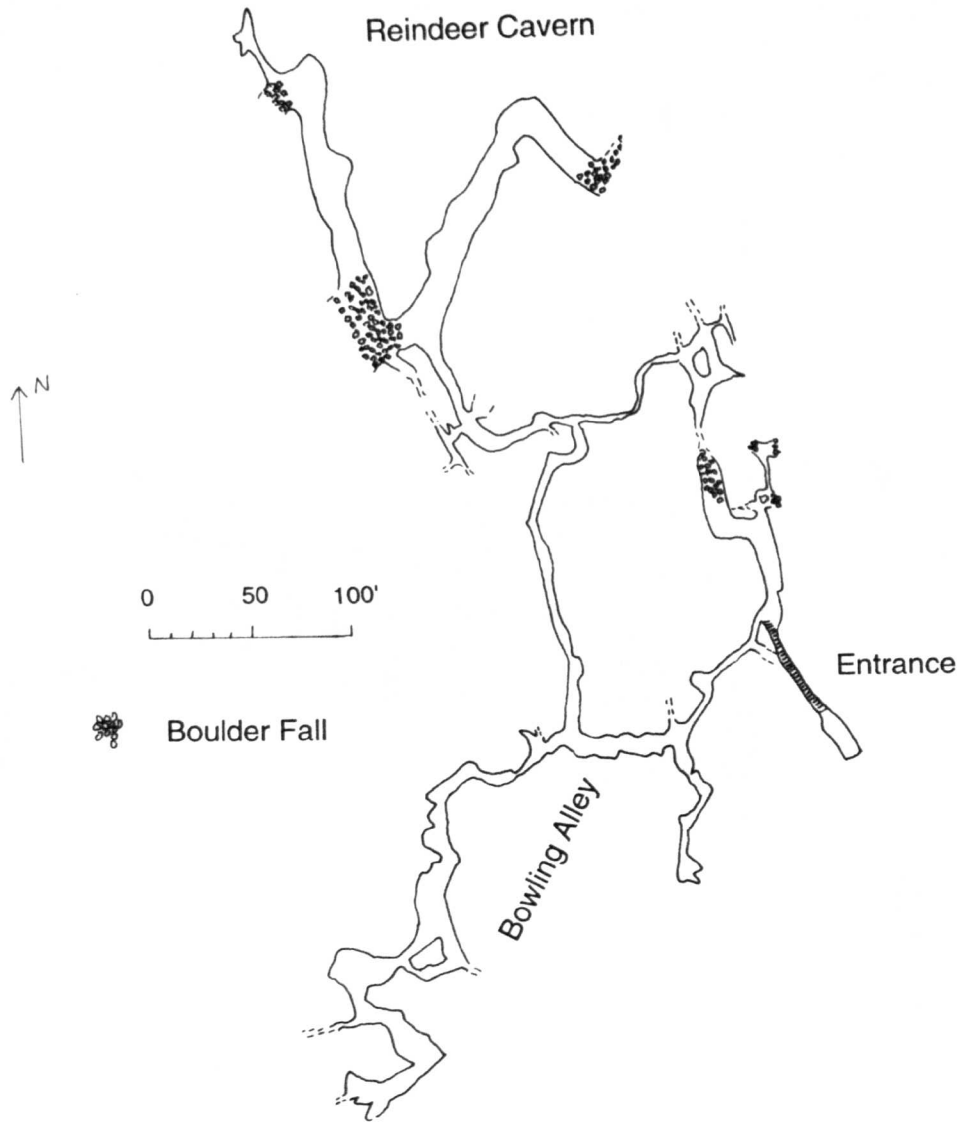

Figure 5.5. Survey of the entrance section of Stump Cross Caverns, showing sampling locations mentioned in the text.

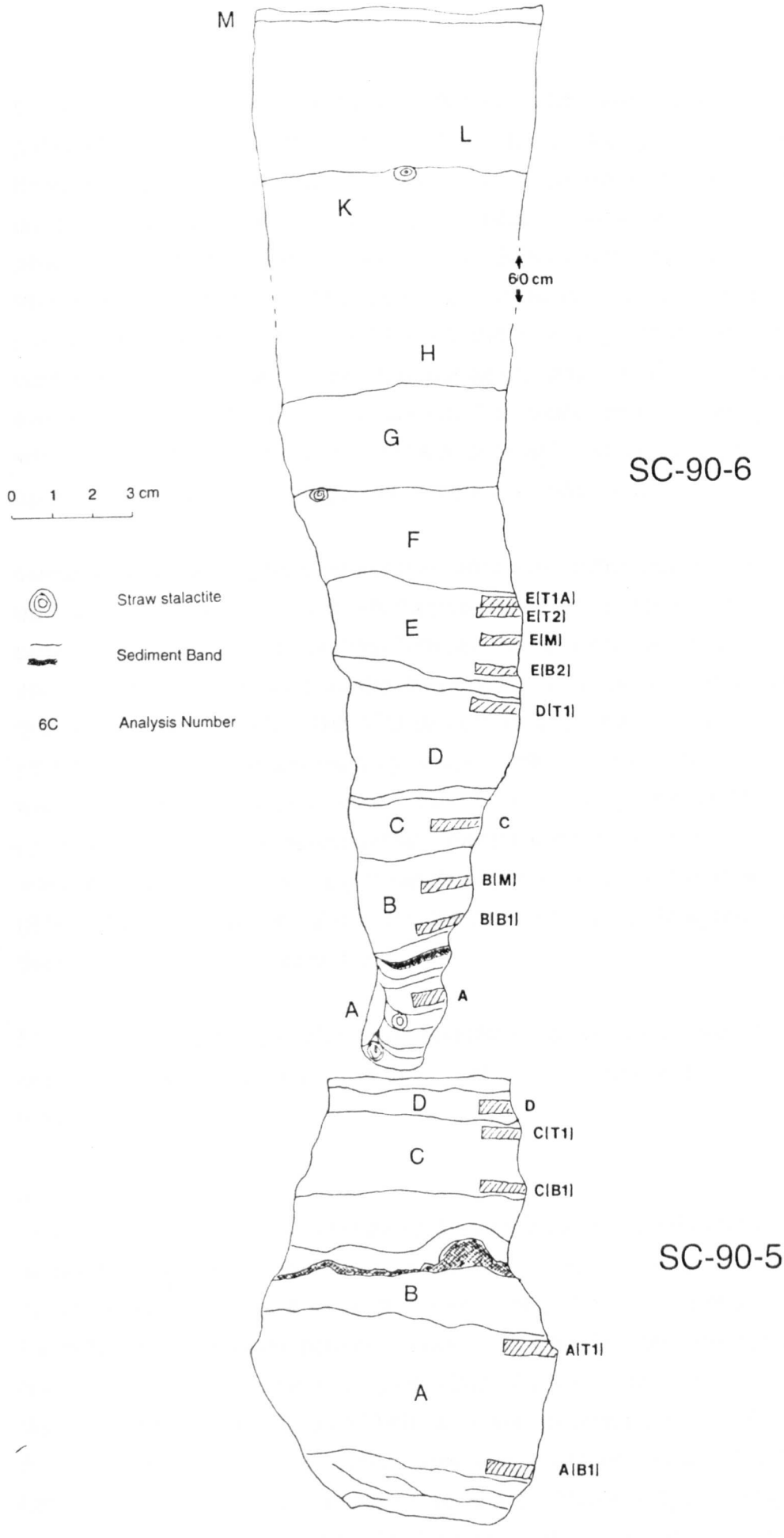

Figure 5.6. Flowstone SC-90-5/6, showing location of MSU samples.

sequence contains many sediment bands (Figure 5.6), which were thought to signify palaeoclimate events. The sediment band below the growth phase SC-90-6A contains much detrital material, stalactites, stalagmite fragments and limestone clasts. Broken straw stalactites are also visible in the sediments between growth phases F and G, and K and L. Samples SC-90-5 (growth sections A to D) and SC-90-6 (sections A to D) comprise pure white, massive, coarsely crystalline columnar calcite. In sections E to L in SC-90-6 there is a gradation to more detritally contaminated, cream or light brown colour calcite; and the crystal structure becomes less massive and appears more porous. The sequence is capped by section M, which is only 3 mm thick, and consists of pure white dense columnar calcite, which appears to be actively forming under present day conditions.

Samples were taken initially for alpha spectrometric dating from growth sections SC-90-5A/6B/6F/6G/6H/6K/6L; typically they consisted of bulk samples of 50-100 g of the purest calcite available, taken from between the sediment bands. The samples were dissolved and analysed using standard alpha spectrometric procedures based on that of Gascoyne (1977a). The ASU dates were obtained either to provide an initial age estimate (samples analysed by Angus Tillotson), or to provide ages for bands with a high detrital content, which would have exceeded the $^{232}Th^{+}$ ion-counting capability on the mass spectrometer. Subsequently, mass spectrometric samples were also cut, comprising 1-2 g of calcite samples were cut to a minimum thickness (2-3 mm) at a distance of 1-2 mm from the sediment bands. Analyses were run using the method described in section 5.2.

Finally, carbon isotopic analysis was undertaken on powders drilled throughout the length of sample SC-90-6 (by Angus Tillotson) to obtain a record of the growth mechanism occurring.

5.4.2.2 Results

The ASU and MSU dates obtained on the sequence are listed in tables 5.5 and 5.6 respectively (all errors are shown as 2σ); and show four major phases of growth. These occur at 168.4±3.4 ka, 79.2±2.4 ka to 52.7±1.4 ka, 35.1±9.9 ka and 9.9±3.2 ka. Where sections of the sequence have been dated by both techniques (SC-90-5A and SC-90-6B), agreement is good within 2σ error. This is in contrast to the disagreement between ASU and MSU analyses observed in section 5.3.4.4. Sample SC-90-6F, above the highest MSU dated sample (SC-90-E(T1A); dated at 53.4±1.8 ka), is from a highly contaminated section ($[^{230}Th/^{232}Th]_{act}$ = 2.8), and has a corrected age which is stratigraphically consistent with the MSU analysis within 2σ

Sample[a]	*Uranium Conc.* (ppm)	$^{230}Th/^{234}U$ [act]	$^{234}U/^{238}U$ [act]	$^{230}Th/^{232}Th$ [act]	*Age* (ka)	*Age (corrected)*[b] (ka)
SC-90-5A	1.030±0.010	0.7921±0.0208	1.5165±0.0053	203±28	148.5±23	-
SC-90-6B	0.070±0.001	0.5707±0.0139	1.311±0.0259	63±8.0	88.0±9.1	-
SC-90-6F	0.166±0.001	0.3812±0.0114	1.1458±0.0135	2.8±0.1	51.5±4.6	35.1±9.9
SC-90-6G	0.140±0.002	0.1060±0.0089	1.2270±0.0177	8.3±1.7	12.1±2.6	8.9±3.5
SC-90-6H	0.085±0.001	0.1199±0.0125	1.1954±0.0197	10.5±4.4	13.8±3.6	11.7±4.7
SC-90-6K	0.0708±0.002	0.0848±0.0032	1.1134±0.0210	4.3±0.2	9.6±0.8	7.8±1.6
SC-90-6L	0.052±0.001	0.1131±0.0040	1.1134±0.0165	6.3±0.5	13.0±1.1	11.3±2.8

[a]. Samples 5A and 6B analysed by Angus Tillotson.

[b]. Corrected ages assume an initial $^{230/232}Th$ atomic ratio of $4.4\pm2.2\times10^{-6}$ (method 1, equation 8 from Schwarcz (1980)). This is the value for a material at secular equilibrium, with a crustal $^{232}Th/^{238}U$ of 3.8. The error is arbitarily assumed to be 50%; errors also include those from counting statistics.

Table 5.5. Alpha Spectrometric Age Determinations for the Stump Cross flowstone.

Sample[a]	Distance[a] (mm)	^{238}U conc ng g^{-1}	$^{234}U/^{238}U$ x10^{6}	$^{230}Th/^{232}Th$ x10^{6}	$\delta^{234}U(0)$[b,e] per mil	$\delta^{234}U(T)$[b,e] per mil	$^{230}Th/^{238}U$[c,e] [act]	$^{230}Th/^{232}Th$ [act]	Age[d,e] ka
SC-90-5A(B1)	3.0	1067±1	83.5±0.1	7826±135	525.4±2.0	848.7±9.8	1.2895±0.0137	1455±25	169.2±3.9
SC-90-5A(T1)	32.0	929±3	82.5±0.2	12575±110	506.9±4.0	817.6±8.5	1.2699±0.0076	2338±21	168.6±2.4
SC-90-5C(B1)	69.0	727±5	82.6±0.8	8135±662	509.5±14.7	813.3±28.5	1.2593±0.0214	1512±123	165.0±7.0
SC-90-5C(T1)	88.0	830±2	80.6±0.2	1932±26	472.5±3.8	764.8±10.7	1.2416±0.0133	359±5	169.9±4.0
SC-90-5D	92.0	1038±3	79.5±0.3	190±2	452.4±5.0	724.9±10.3	1.2102±0.0097	35±0.3	166.3±3.1
SC-90-6A	113.0	161±1	66.6±0.5	373±8	216.4±9.7	270.9±12.2	0.6412±0.0124	69±1.4	79.2±2.4
SC-90-6B(B1)	132.0	69±1	64.6±1.7	291±5	180.6±30.2	225.3±37.8	0.6148±0.0111	54±0.9	78.2±3.7
SC-90-6B(M)	140.0	94±1	63.0±1.1	24954±5106	151.7±20.0	188.6±24.9	0.5905±0.0090	4640±950	76.7±2.6
SC-90-6C	155.0	60±1	62.0±0.5	63±1	133.6±8.6	165.9±10.7	0.5792±0.0072	11.8±0.1	71.6±1.9
SC-90-6D(T1)	183.0	160±2	62.0±1.6	336±7	133.5±29.5	158.1±35.0	0.4836±0.0104	63±1.0	59.7±2.8
SC-90-6E(B2)	195.0	142±2	65.7±1.6	4250±179	200.9±28.9	233.1±33.6	0.4646±0.0085	790±33	52.4±2.1
SC-90-6E(M)	205.0	122±1	65.7±0.5	2688±196	201.3±9.0	233.7±10.5	0.4668±0.0093	500±37	52.7±1.4
SC-90-6E(T2)	208.0	88±1	64.4±1.3	2363±116	176.2±23.1	206.0±27.0	0.4728±0.0105	439±22	55.1±2.2
SC-90-6E(T1A)	210.0	72±1	64.3±0.4	213±6	174.6±6.3	203.1±7.4	0.4605±0.1220	40±1.0	53.4±1.8

[a] Sample location and distance shown in figure 5.6.

[b] $\delta^{234}U = \{[(^{234}U/^{238}U)/(^{234}U/^{238}U)eq]-1\}x10^{3}$, where $(^{234}U/^{238}U)eq$ is the atomic ratio at secular equilibrium and is equal to $5.472x10^{-5}$. $\delta^{234}U(0)$ is the measured value. $\delta^{234}U(T)$ is the initial value and is equal to $[\delta^{234}U(0)][e(^{\lambda 234}T)]$

[c] Calculated from the atomic $^{230}Th/^{238}U$ ratio by multiplying by $\lambda_{230}/\lambda_{238}$.

[d] Ages are calculated using $[^{230}Th^{238}U]act\ -1 = e^{-\lambda 230T} + (\delta^{234}U(0)/1000)(\lambda_{230}/\lambda_{230}-\lambda_{234})(1-e^{-(\lambda 230-\lambda 234)T})$ where T is the age in years. Where there is a high concentration of detrital ^{232}Th, then corrected ages are calculated. These assume an initial $^{230}Th/^{232}Th$ atomic ratio of $4.4\pm2.2x10^{-6}$ (method 1, equation 8 from Scwarcz (1980)). This is the value for a material at secular equilibrium, with a crustal $^{232}Th/^{238}U$ value of 3.8. The error is arbitarily assumed to be 50%. Only SC-90-6C required a detrital age correction.

[e] Values for decay constants are $\lambda_{238}=1.551x10^{-10}\ yr^{-1}$ (Jaffey et al, 1971), $\lambda_{234}=2.835x10^{-6}\ yr^{-1}$ (de Bievre et al, 1971; Lounsbury and Durham, 1971), and $\lambda_{230}=9.195x10^{-6}\ yr^{-1}$ (Meadows et al, 1980)

Table 5.6. Uranium/Thorium isotopic data and mass spectrometric ages for the Stump Cross flowstone.

age errors at 35.1±9.9 ka. Alpha-spectrometric analyses on sections SC-90-6G/H/K/L show that growth occurred at 9.9±3.2 ka; a hiatus between bands K and L marked by fallen stalactite fragments does not appear to mark an event of significant temporal duration.

The MSU dates (Table 5.6) show good stratigraphic consistency, confirming that this terrestrial flowstone is a closed system suitable for uranium series dating. The five dates from sample SC-90-5 are in chronological order at 2σ significance levels (figure 5.7) and show identical uranium isotopic signals. They also demonstrate that the speleothem growth was rapid, and that the events depositing the sediments were of limited temporal duration (less than 10^3 years), since there is no apparent differences between ages obtained either side of the sediment bands. SC-90-6 shows the same internal isotopic and stratigraphic consistency as SC-90-5, and again the sediment depositing events appear to be of a short duration. Of significant importance is the variation in uranium concentration between SC-90-5 and SC-90-6; with a decrease from 800 ppm to 80 ppm of ^{238}U. This demonstrates a significant change in the uranium concentrations in the groundwater feeding the flowstone. The low levels of uranium in SC-90-6 lead to difficulties in analysing many of the samples. In particular, dates on sections B(B2), B(T), D(B1), D(B2) and E(B1) all failed to run on the mass spectrometer, thought to be due to high organic matter concentrations preventing a stable uranium beam from developing for samples with low uranium concentrations.

5.4.2.3 Interpretation

5.4.2.3.1 Timing of Growth. The Stump Cross flowstone sequence does not follow the expected pattern of growth in interglacial and interstadial periods (chapter 2). The growth of SC-90-5/6 occurs within both interglacial, interstadial and glacial oxygen isotope stages; the growth at 168.4±3.4 ka correlates with isotope event 6.42 within stage 6 (Martinson et al; 1987); that between 79.2±2.4 and 52.7±1.4 ka grows throughout stage 4 and the start of stage 3, that at 35.1±9.9 ka within stage 3; and that at 9.9±3.2 ka within stage 1. Interpretation of such a complex growth record in terms of a single simple palaeoclimate control is difficult. In particular, growth during periods of probable climatic deterioration at 166 ka and 79-52 ka was not expected.

Growth theory imposes several useful limits the conditions prevailing during active growth in the inter-stadial and glacial periods. Firstly, calcium ion concentration must be above equilibrium with atmospheric carbon dioxide, which is in the range 0.60 to 0.70 mmol l^{-1} for temperatures in the range 5 - 10 °C. This indicates the presence of a biogenic source of CO_2 at these times (a non-biotic growth mechanism is not

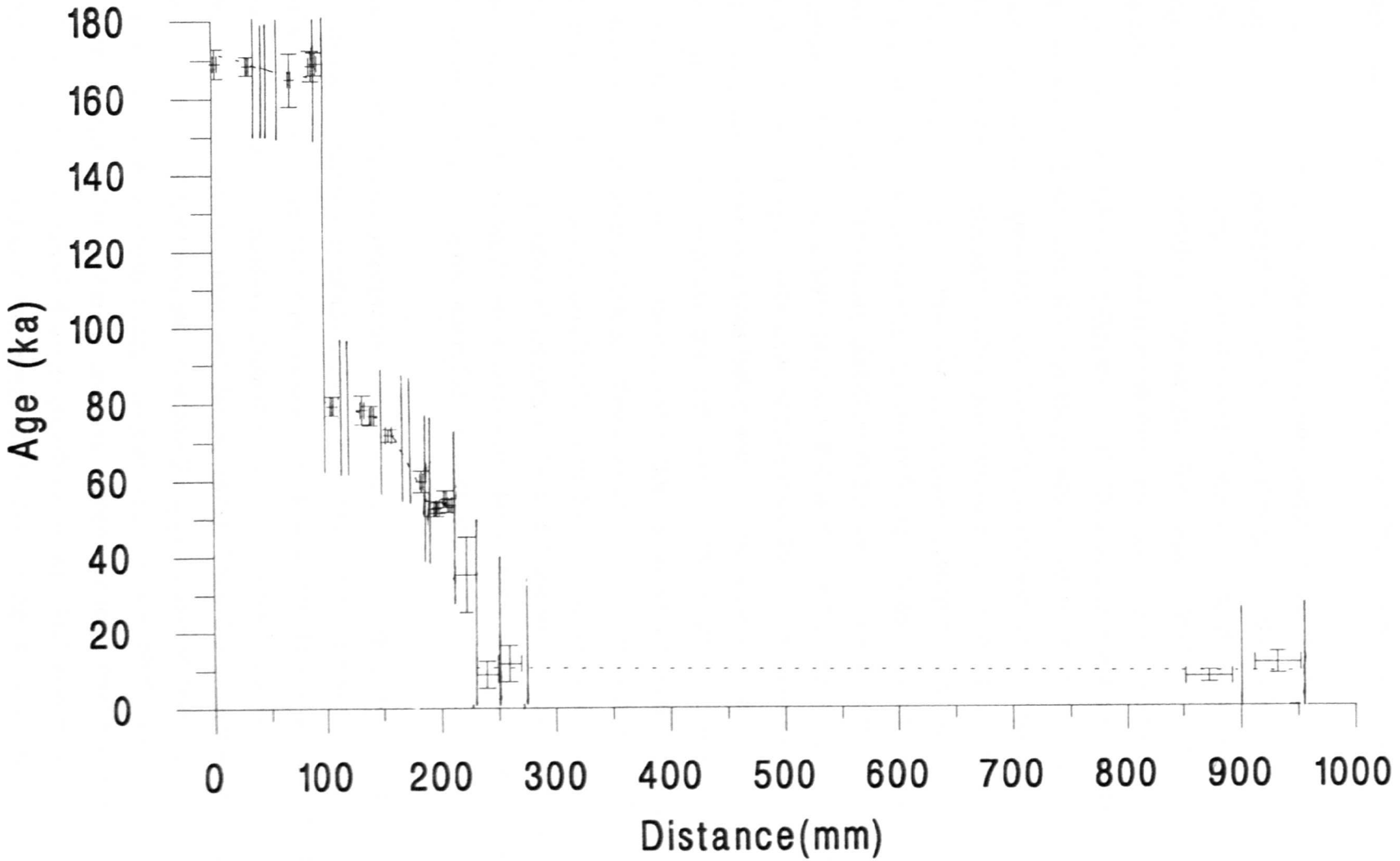

Figure 5.7. Graph showing the relationship between the age of sample SC-90-5/6 and the distance up the sequence. Sediment bands are shown as solid lines, minimum growth rates by dashed lines.

thought likely, since elevated ^{13}C values do not occur, see section 5.4.2.3.3). Secondly, there must be a significant groundwater recharge, conditions being neither too arid, nor sufficiently cold for development of a continuous permafrost zone.

Comparison of these conditions with regional palaeoclimate is difficult, due to both paucity of suitable terrestrial records, and poor dating of those available. A spatially constrained record is that of glacial extent. Three possible glacial events occurred during the time of deposition of the sample. The stage 6 (Wolstonian) glaciation is considered to be the most severe of the three, with deposits as far south as Norfolk and the Isles of Scilly (Rice and Douglas, 1991). This glaciation would be expected to cover the Stump Cross site, although the growth at 168.4±3.4 ka may precede the glacial maximum. A stage 4 (the Irish Midlandian) glaciation has not been recognised in England; although deposits have been assigned to this age in Ireland (Hoare, 1991) and also TL dated to this time in Denmark (Kronberg and Mejdahl, 1990). Glacial cover would not be considered likely at Stump Cross. The extent and timing of the stage 2 (Late Devensian) glaciation in England is well known (Catt, 1991; Sutherland, 1991). Catt (1991) reviewed the evidence for glacier cover in the Yorkshire region during the maximum glacial extent. Ice streams are known to have flowed down Nidderdale and Wharfedale and into the Vale of York, but only for a limited distance down Airedale, the next valley to the south. All these ice flows originated from the uplands to the north-west, but it is not known whether ice covered the interfluves between the valleys. In these areas drift deposits underlie the blanket peat, but could be formed by periglacial processes or a pre-Devensian ice sheet. In contrast significant quantities of Devensian till and moraines can be found in the valley floors. Thus it is not known if ice covered the surface at Stump Cross at this time, though glaciers were present in the main valleys.

Whether such climatic deterioration would affect speleothem growth is unknown. Groundwater recharge may cease if glacier is cold-based, or if continuous permafrost develops; however the former is not considered likely for UK ice sheets with the spatial extent of the glaciers explicable by warm-based glaciers moving on deformable sediments (Boulton and Jones, 1979). Thus the presence of growth within isotope event 6.42 and stages 4 and 3 suggests that continuous permafrost had not developed at these times. However, warm based glaciers may produce significant groundwater recharge, as may discontinuous permafrost, and such conditions may have prevailed when growth occurred. Recharge under a warm-based glacier may be due to flow generated by the melting of ice and snow on the glacier surface by insolation, which is then concentrated by the supra-glacial stream

network and sub-glacial conduit system and may recharge the aquifer with substantial flows (Smart, 1983). It may also occur due to surface meltwater building up at the glacier front and building up a pressure head which draws flow into the aquifer (Ford, 1979). A record of palaeotemperature during the last glacial maxima from coleoptera indicates a mean annual temperature of -8 °C, with a summer mean of 5-10 °C (Atkinson et al, 1987), which may melt glacier ice, snow or discontinuous permafrost and explain the growth in stages 6 and 4 if similar conditions prevailed.

The palaeoclimate records give only limited evidence, but suggest that the Stump Cross flowstone growth record during periods of climatic deterioration may be explicable by warm base glacier cover or discontinuous permafrost. Both of these would provide a groundwater source of potentially saturated calcium for part or all the year. Lack of growth in stage 2 and the latter part of stage 6 may suggest a change in conditions to either the formation of continuous permafrost or the flooding of the caves. However, if conditions were favourable for speleothem growth to occur in the glacial and inter-stadial stages, then it would also be expected that growth would occur in the other more climatically favourable interglacials. Thus an explanation has to be sought for the reason for growth cessation within isotope stage 5 and the limited growth in the Holocene (9.9±3.2 ka).

Changes in precipitation may explain the growth rate record. GCM models have shown that up to 50% increases in precipitation may have occurred from glacial to interglacial periods due to the re-establishment of the jet stream over mid-latitudes (Kutzbach and Wright, 1985). One could speculate that this could lead to changes in flow routing in the aquifer during such periods, away from the source which feeds the sample here. However, active growth was occurring today (layer M), in an inter-glacial period, which suggests that growth would also be possible in previous interglacial periods. Another possible explanation would be that increased precipitation could raise the groundwater level in the limestone aquifer and flood the cave which was previously above the water table. If this mechanism occurred, then the periods of flowstone growth are providing a record of groundwater oscillations and thus periods of increased aridity.

Using a uniformitarianistic argument, it may be possible to determine the validity of this argument by comparison with conditions in the cave today. Being in an inter-glacial period at the current time, one would expect the cave to be flooded today. However, this is not the case, and significant flooding never occurs (Gordon Hanley, pers. comm.). The actual level of the water table today is at least 40 m below the

surface, judged by the depth at which sumping occurs in the cave. However, this low groundwater level is due to recent anthropogenic alterations of water flow within the limestone aquifer, with adits driven through the aquifer at depth to drain mine workings (Dickinson, 1972). It may be possible that without these the cave would be flooded today, and by inference, would also have been so in previous interglacials.

As well as high groundwater levels, 'backing-up' of water flowing down the Bowling Alley could also be an important factor in flooding in the passage, as waters discharging down gradient may do so at too great a rate to pass through the fissure at the end of the passage. It may be possible that increased precipitation or individual large storm events could cause flooding, which took days or months to drain away, independent of the groundwater level. However, major storm events today do not cause any significant backing-up or serious flooding of the passage, although drainage conditions may have changed over time. The presence of large amounts of flood debris within the sample (limestone clasts and stalagmite and straw stalactite fragments in SC-90-6A; between SC-90-6F and G and K and L), suggest that the force of water within the passage was such to dislodge them. Water would have to reach the passage roof to explain the presence of straw stalactites within the flowstone. Thus significant flooding of the passage has occurred, between 168.4±3.4 and 79.2±2.4 ka, 35.1±9.9 ka and 9.9±3.2 ka, and within the period 9.9±3.2 ka.

The short period of growth at 9.9±3.2 ka, which occurs at the Holocene climatic optimum, suggests that a simple flooding hypothesis can not explain why growth ceased during the last interglacial. Furthermore, four ASU dates from the Bowling Alley from Sutcliffe et al (1985) suggested that growth occurred within isotope stage 5. One sample (108±36 ka) was within 2σ error range of the growth phase commencing at 80±2 ka. Another of the analyses (116±18 ka; 2σ errors) came from very near the sequence analysed by MSU in this study, and the discrepancy between the ASU and MSU analyses can not be explained. The other two samples were dated to 110±26 ka and 118±24 ka (both errors 2σ), suggesting that flooding did not occur at this time as they were from a lower elevation to the flowstone sequence SC-90-5/6. The reason why deposition did not occur at this time for SC-90-5/6/ is not known.

Overall, the record of the timing of the growth phases from the Stump Cross sample is complex, and again demonstrates that the timing of growth does not respond to a conventional palaeoclimate signal. Both ice cover and flooding may have limited growth during both inter-glacial and glacial periods. Growth may have occurred during periods of relative aridity, when a fall in the water table allowed the cave to be

exposed. Further evidence supporting this growth record may come from any palaeoclimatic information contained within the growth rate record. This is investigated in the following section.

5.4.2.3.2 The Growth Rate Record. A record of growth rate can be determined for the four phases of growth. However, absolute growth rates were not always determinable from the MSU analyses for two reasons. Firstly, growth rate was often so fast that age determinations overlap at a 2σ level. This allowed only a minimum growth rate to be estimated. Secondly, the presence of the sediment bands complicates growth rate determinations, since each represents a hiatus of an unknown (but short) duration. Several of the bands have been dated to show that they are of short duration, and thus minimum growth rates can be estimated (figure 5.7). Despite these complications, the minimum growth rates obtained for the three phases have distinctly different growth rates.

The first period of growth (168.4±3.4 ka) had a minimum growth rate of 0.008 mm yr^{-1}. The second period of growth between 79.2±2.4 and 52.7±1.4 ka has a highly variable growth rate. At ≈ 78 ka the initial growth rate was at a minimum rate of 0.005 mm yr^{-1}, and the slowest rate at ≈ 70-55 ka was 0.002 mm yr^{-1}. Growth rate increased again at ≈ 54 ka to 0.004 mm yr^{-1}. Growth rates were not determined for the growth phase at ≈ 35 ka as only one analysis was obtained by ASU due to the high detrital thorium content of this layer. During the last period of growth, at 9.9±3.2, only a minimum growth rate was again obtainable due to the lower precision of the ASU analyses, and gave a comparatively fast rate of 0.18 mm yr^{-1}.

Thus growth rates varied by a minimum of x90 over the last 200 ka. The growth rates can be compared with those theoretically expected (chapter 3.2). Firstly, one can determine what conditions would be necessary to give the high growth rate observed in the Holocene of at least 0.18 mm yr^{-1}. Model results are shown in table 5.7a for varying climate conditions. For the Holocene maxima temperature is assumed to be 10 °C, the mean annual temperature predicted by Simmons (1981). Film thickness is modelled for 0.05 to 0.2 mm, the range observed upon flowstones under all conditions today (section 4.3.1). Calcium ion concentrations were allowed to vary between saturation (0.7 mmol l^{-1}) and a maximum of 3.0 mmol l^{-1}, the latter value being 50% greater than the maximum observed in the region today (Pentecost, 1992). It is assumed that groundwater is available for between 6-12 months of the year, with the possibility that the flowstone remained dry in the summer months, as observed in this study (7 out of 13 samples, chapter 4). Table 5.7a shows that a

specific range of conditions are necessary to explain the high growth rate. Firstly, a growth rate of 0.18 mm yr^{-1} can be explained by values of calcium ion concentrations, film thickness, temperature and seasonality of water supply within the expected range. More specifically, such a high growth rate would most likely with film thicknesses within the range 0.1 to 0.2 mm, and with a seasonal water supply available for at least 8 months of the year, suggesting fast and near continuous flows.

(a) Calcium concentration (mmol l^{-1})	Temperature (°C)	Film Thickness (mm)	Water Availability (months)
2.4	10	0.2	8
2.0	10	0.2	12
3.0	10	0.1	12
(b)			
2.2 - 3.3	5-10	0.05	4
1.7 - 2.4	5-10	0.05	6
1.5 - 2.1	5-10	0.1	4
1.2 - 2.6	5-10	0.1	6
1.2 - 1.5	5-10	0.2	4
1.0 - 1.2	5-10	0.2	6

Table 5.7. Conditions necessary for a growth rate of (a) 0.18 mm yr^{-1}, (b) 0.002 mm yr^{-1}

It is also possible to model the observed minimum growth rate of 0.002 mm yr^{-1}. These results are shown in table 5.7b. Again, such a growth rate is predictable by the theory under the expected conditions of temperature, film thickness, calcium ion concentration and seasonality. In this case, temperature is assumed to be 5-10 °C, the range of summer maxima predicted for the last glaciation by Atkinson et al (1987), and the water availability is limited to a maximum of 6 months to reflect discharge only in the summer. Table 5.7b demonstrates that the most probable explanations for the decrease in growth rate would be due to a decrease in the calcium ion concentration as well as the decrease in ground-water availability to under 6 months duration.

Growth rates have been shown to be of the correct order of magnitude to that theoretically predicted. However, the measurements suffer from being minimum estimates, due to insufficient precision available from the MSU analyses, and the presence of the sediment bands which are of an unknown duration. Growth rate is observed to be the fastest within the Holocene, and slower within the glacial and interstadial growth phases within isotope stages 6 and 4. This suggests that both calcium concentration and the length of available water supply decreased in the latter periods. Empirical evidence for these observations is not available. It has already been hypothesized in section 5.3 that a change in vegetation cover may cause a significant change in calcium ion concentrations, with up to a 1.3 mmol l^{-1} change in concentration necessary to explain the record of growth rate change for the Sutherland stalagmite. Recent studies have also shown changes in groundwater calcium concentrations have occurred by up to 0.9 mmol l^{-1} between 1940 and 1983 due to land use change in the Mendip Hills (Richards, 1987). Thus a decrease in concentration between interglacial and interstadial or glacial periods as suggested here would not be unreasonable. Such a decline may be due to either a change in vegetation type, a decrease in the amount of vegetation, or a decrease in plant productivity during a period of insolation minima and low temperatures. A continuous pollen record for the region during the early Devensian would help distinguish which factor was operating.

5.4.2.3.3 The carbon isotope record. The ^{13}C record for the Stump Cross sample may be useful in distinguishing the mechanisms of speleothem growth. This is particularly important for this sample, as growth occurred during periods of possible glacier cover, and so a non-biogenic growth mechanism may be possible. Carbon and oxygen isotope records are shown in figure 5.8. Measurements were also taken on samples of the Great Scar limestone bedrock, and the recently growing band SC-90-6M. These measured 0.0 and -0.5 per mil respectively.

All values of ^{13}C fall in the range -6.5 to +0.5 per mil, which is outside that expected if a non-biogenic source of CO_2 was present. They do fall within the range expected if a C4 photosynthetic pathway plant population was present, which is unexpected as such plants would not be found in this region during glacial time, since they require a minimum temperature of 10 °C (Brook et al, 1990; Ito, Pers. Commun.). Thus some other explanation must be sought for such high ^{13}C values.

One possible explanation would be that the sample was fed by a fast flow water supply, such that a significant proportion of the dissolved CO_2 was still in equilibrium

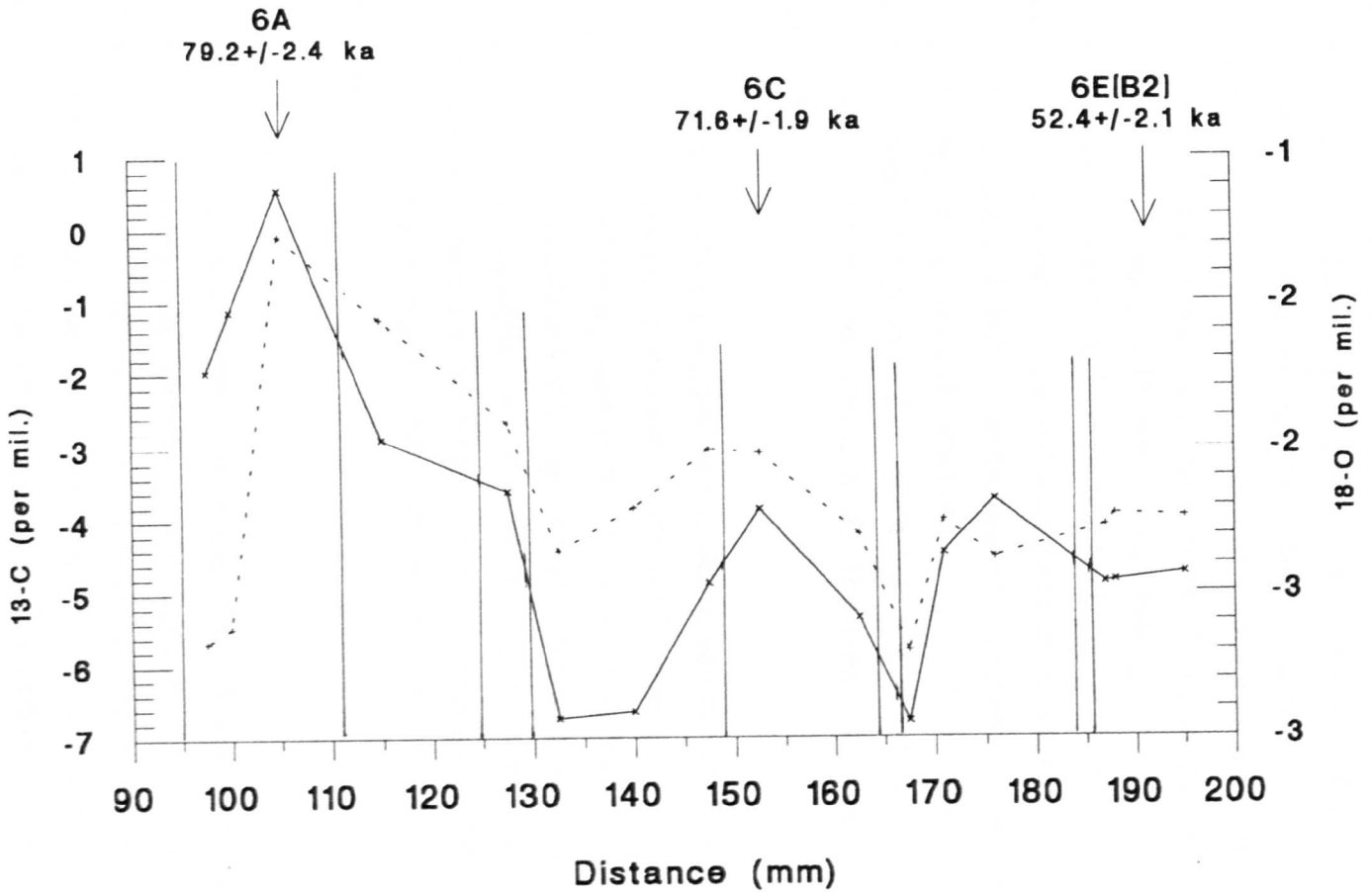

Figure 5.8. Carbon (solid line) and oxygen (dashed line) isotope analyses upon the Stumps Cross flowstone. The section has been dated as shown. Sediment bands are represented by solid lines.

with the atmosphere when it entered the cave system, yet was still saturated with calcium to allow subsequent flowstone deposition. However, even if this occurred, the proportion of carbon dioxide in the atmosphere (0.03%) relative to that in the soil (3%) is so low that it would have relatively little impact on the ^{13}C levels. Even if 50% of the water was still in equilibrium with the atmosphere, this would only contain under 1% of all the carbon in the waters, and hence the elevated ^{13}C values are not explained by this mechanism. Perhaps a more likely explanation is that significant degassing had already occurred within the aquifer, perhaps as the deposition of an earlier flowstone. If the waters remained saturated then they may deposit subsequent flowstones with ^{13}C values reflecting those having undergone significant fractionation. In a semi-dynamic model of carbon fractionation, Dulinski and Rozanski (1990) showed that ^{13}C values of 0 per mil could be reached within 30 minutes of the first degassing, and after only 20% of all the available calcium had been deposited. Such conditions may be applicable for flowstone samples, for which degassing may have occurred earlier in the cave system, since they are often associated with fast flow routes and conduit rather than fissure feeds. This area is a focus for continuing research (chapter 7).

It was also hoped to be able to compare the ^{13}C record with the record of growth rate change, to determine whether an increase in growth rate, due to increased water flux over the sample, caused an increase in the fractionation of the carbon isotopes. However, due to the inadequacies in the growth rate record as detailed previously, such a relationship is not investigatable. However, if there is a significant growth rate decline, then the lack of change in the fractionation record may suggest that a decline in calcium ion concentration may be more important than any decline in water flux over the sample.

5.4.2.4 Conclusions

The record of growth and growth rate of the Stump Cross flowstone is complex and does not provide a simple palaeoclimate record. Explanation of the record of the timing of growth is possible, although somewhat speculative in nature. The growth rate record suffered from the fast growth rate and frequent sediment banding which allowed only minimum growth rates to be calculated. Comparisons of this record with a duplicate speleothem growing over the same time period is now necessary, especially to investigate if growth rate variations occur between interglacial and glacial periods, and to try to obtain another record of potential growth rate slowing within isotope stage 4. This is sought below.

5.4.3 The Lancaster Hole Record

5.4.3.1 Site Description

A flowstone sequence was collected from Lancaster Hole, Yorkshire, part of the 50 km long Ease Gill Caverns system on Casterton Fell, west Yorkshire Dales, by Angus Tillotson and Pete Smart in 1990. The cave is situated at an altitude of 294 m a.s.l. and has formed within the White Scar limestone sequence. The flowstone was collected from Collonade Chamber in the upper levels of the system (figure 5.9). The samples were collected from a location for which a stratigraphically equivalent flowstone had previously been dated by alpha-spectrometry, and known to have grown from ≈ 140 to ≈ 40 ka (Samples 77120A and 77120B in Gascoyne et al, 1983).

Overlying the bedrock was 10 cm of coarse, poorly sorted muddy gravels containing rounded to sub-angular sandstone clasts and large amounts of angular limestone. The flowstone sequence overlaid these sediments. Seven growth phases were present within the flowstone, separated by sediment layers of less than 1 mm thickness. The flowstone was not actively forming when collected. Subsequent to flowstone deposition fine grain sediments had been deposited, the basal material consisted of finely bedded sands, which was overlain by horizontally bedded mud. The passage had been hydrologically active since flowstone and sediment deposition, removing the sediments from the centre of the passage. This had exposed the flowstone sequence and gave rise to some disruption of the flowstone.

The 330 mm long growth sequence is shown in figure 5.10. Twenty ≈ 1 g sub-samples were cut parallel to growth layers with a diamond bladed slow-speed saw. Samples were cut both adjacent to the growth hiatuses (to determine the precise timing of growth termination), and within growth phases (to obtain a measure of growth rate variations). Three sample pairs (5C(T1) and 5C(T2); 6A(T) and 6A(T)dup; 6A(B) and 6A(B)dup) provided sample duplicates from the same growth layer; another sample (5B(M)) was analysed as a machine duplicate to determine machine stability. The results are shown in Table 5.8 and Figure 5.11.

5.4.3.2 Results

Sample LH grew in seven short growth phases; 128.8±2.7 ka; 103.1±1.8 ka; 84.7±1.2 ka; 57.9±1.1 ka; 50.6±1.1 ka; 47.6±1.0 ka and 36.9±0.8 ka. All analyses give ages in correct stratigraphic order, and all duplicates show agreement at 2σ levels. Multiple age determinations from within each growth phase showed continuous, rapid growth. No significant changes in growth rate are visible within each growth phase.

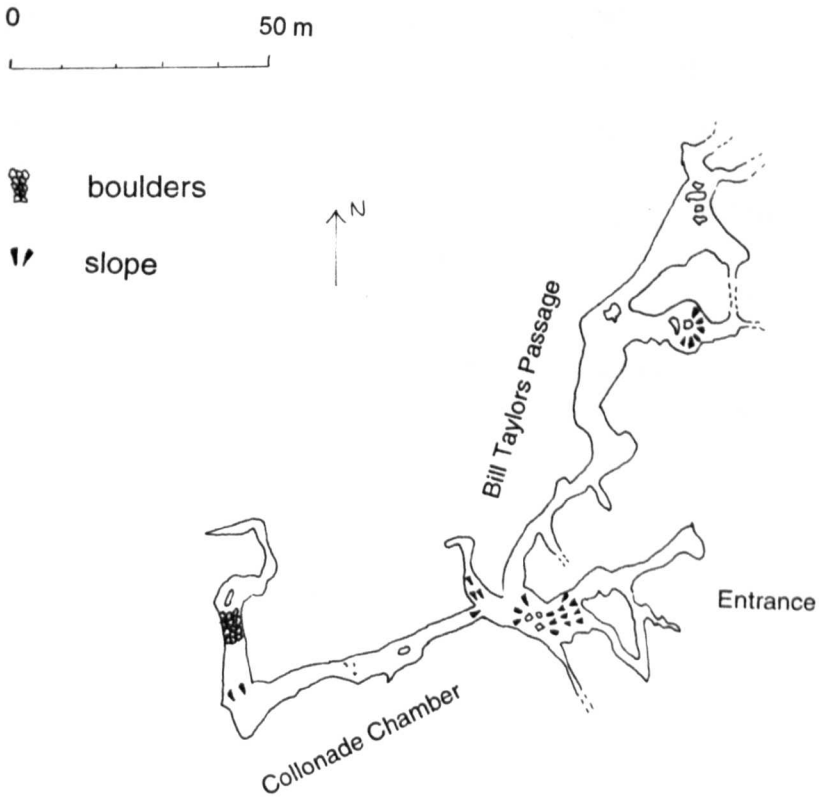

Figure 5.9. Survey of the entrance series of Lancaster Hole, showing sampling location and names of passages mentioned in the text.

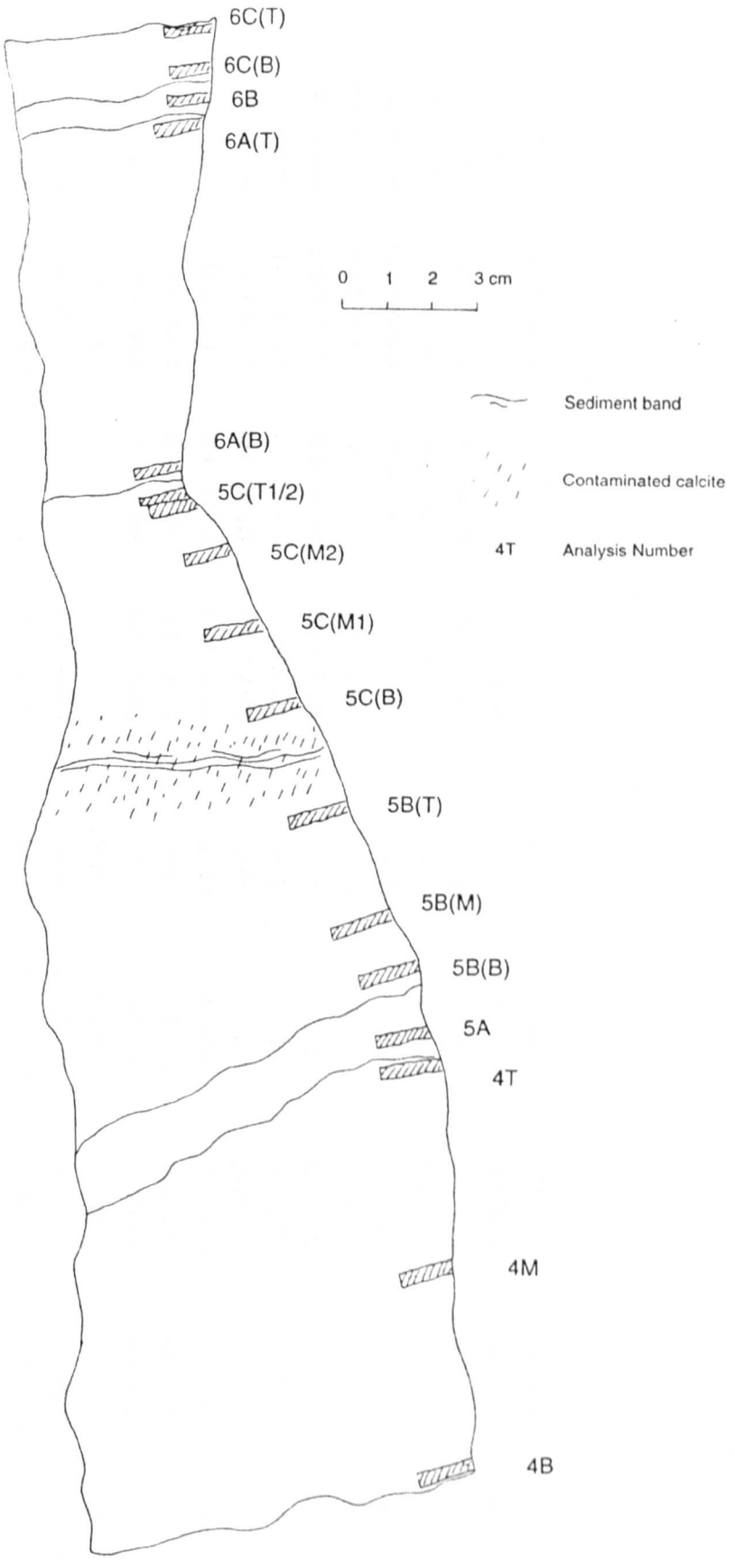

Figure 5.10. Flowstone LH-90-4/5/6, showing MSU sampling locations and the position of sediment bands.

Name[a]	Distance[a]	^{238}U conc.	$^{234}U/^{238}U$	$^{230}Th/^{232}Th$	$^{230}Th/^{232}Th$	$\delta^{234}U_{(0)}$[b,e]	$\delta^{234}U_{(T)}$[b,e]	$^{230}Th/^{238}U$[c,e]	Age[d,e]
	(mm)	*(nm g^{-1})*	*($x10^6$)*	*($x10^6$)*	*(act)*	*(per mil)*	*(per mil)*	*(act)*	*(years)*
LH-90-4B	1.5	16.22±0.11	67.18±0.30	39000±1400	7300±300	227.65±5.55	331.74±8.40	0.8929±0.0074	132820±2400
LH-90-4M	45	5.49±0.011	70.04±0.28	62050±14090	>10000	280.00±5.28	399.85±8.19	0.9079±0.0132	125680±3390
LH-90-4T	90.5	7.27±0.039	66.23±0.35	293800±27500	>10000	210.47±6.45	302.26±9.45	0.8604±0.0062	127780±2180
LH-90-5A	97	5.28±0.021	79.83±0.38	594400±385900	>10000	458.88±6.95	614.67±9.81	0.9316±0.0089	103110±1760
LH-90-5B(B)	110	7.12±0.030	86.02±0.38	174800±34600	>10000	571.95±6.95	727.60±9.25	0.8869±0.0085	84900±1310
LH-90-5B(M)	122	4.82±0.011	86.53±0.26	232590±20120	>10000	581.36±4.75	738.71±6.20	0.8896±0.0040	84490±670
LH-90-5B(M)mdup	122	4.84±0.021	85.95±1.05	4015300±4969700	>10000	570.68±19.11	727.76±24.69	0.8924±0.0072	85760±1890
LH-90-5B(T)	148	2.07±0.006	86.66±0.38	15920±340	3000±60	583.72±6.94	740.02±9.01	0.8851±0.0054	83690±910
LH-90-5C(B)	172	1.55±0.005	84.61±0.75	1137±19	211±3	546.30±13.78	645.34±16.41	0.6638±0.0073	58770±1090
LH-90-5C(M1)	192	1.53±0.004	83.03±0.61	1610±23	300±4	517.42±11.16	608.41±13.22	0.6366±0.0063	57143±920
LH-90-5C(M2)	210	1.70±0.013	80.86±1.58	2552±130	475±25	477.71±28.78	562.73±34.01	0.6245±0.0061	57780±1680
LH-90-5C(T2)	221	1.53±0.007	81.22±0.57	1837±38	340±10	484.27±10.48	568.94±12.46	0.6194±0.0090	56830±1180
LH-90-5C(T1)	224	1.47±0.029	80.87±2.07	5556±7	103±1	477.97±37.85	564.59±44.91	0.6328±0.0138	58750±2620
LH-90-6A(B)	230	1.76±0.037	77.59±3.70	2126±150	395±30	417.97±67.53	489.37±79.28	0.5805±0.0202	55630±4330
LH-90-6A(B)dup	230	1.75±0.003	80.89±0.30	2674±191	497±36	478.34±5.42	554.26±6.58	0.5744±0.0109	51960±1250
LH-90-6A(T)	304	0.67±0.001	75.31±0.29	259±23	48±4	376.22±5.37	428.93±8.38	0.4850±0.0403	46250±4700
LH-90-6A(T)dup	304	0.75±0.001	75.65±0.29	211±4	39±1	382.48±5.33	439.82±6.25	0.5131±0.0081	49270±990
LH-90-6B	310	0.93±0.001	76.45±0.39	1094±31	203±6	397.04±7.13	454.40±8.26	0.5044±0.0081	47600±990
LH-90-6C(B)	316	1.91±0.004	77.02±0.44	2958±352	550±65	407.53±8.13	453.32±9.14	0.4172±0.0093	37560±1020
LH-90-6C(T)	327	1.56±0.003	76.12±0.37	2275±132	423±25	391.03±6.72	433.13±7.49	0.3982±0.0060	36080±670

[a] Sample location and distances shown in Figure 5.10; LH5(B) and LH5(B)mdup are replicate analyses of different aliquots of the solution derived from sample LH5(B), LH5A(T) / LH5A(T)dup and LH5A(B) / LH5A(B)dup are duplicate analyses of different samples from the same growth layer.

[b] $\delta^{234}U = [[(^{234}U/^{238}U)/(^{234}U/^{238}U)eq]-1)x10^3$, where $(^{234}U/^{238}U)eq$ is the atomic ratio at secular equilibrium and is equal to $5.472x10^{-5}$. $\delta^{234}U(0)$ is the measured value. $\delta^{234}U(T)$ is the initial value and is equal to $[\delta^{234}U(0)][e(^{\lambda 234}T)]$

[c] Calculated from the atomic $^{230}Th/^{238}U$ ratio by multiplying by $\lambda_{230}/\lambda_{238}$.

[d] Ages are calculated using $[^{230}Th/^{238}U]act -1 = e^{-\lambda 230T} + (\delta^{234}U(0)/1000)(\lambda_{230}/\lambda_{230}-\lambda_{234})(1-e^{-(\lambda 230-\lambda 234)T})$ where T is the age in years.

[e] Values for decay constants are $\lambda_{238}=1.551x10^{-10}\ yr^{-1}$ (Jaffey et al, 1971), $\lambda_{234}=2.835x10^{-6}\ yr^{-1}$ (de Bievre et al, 1971; Lounsbury and Durham, 1971), and $\lambda_{230}=9.195x10^{-6}\ yr^{-1}$ (Meadows et al, 1980)

Table 5.8. Uranium / Thorium isotopic data and mass-spectrometric ages for the Lancaster Hole flowstone.

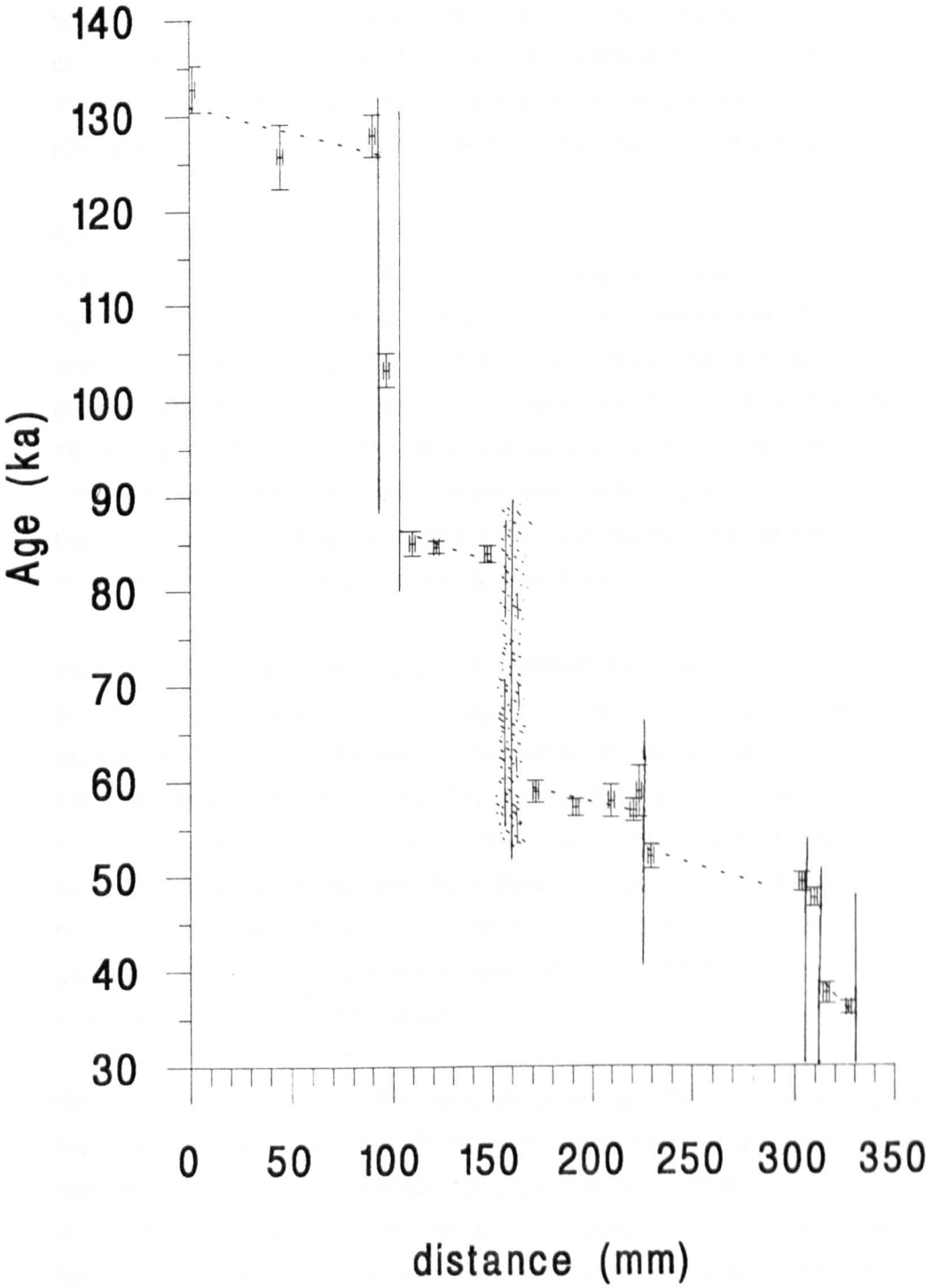

Figure 5.11. Graph showing the relationship between the MSU age analyses and distance down the flowstone profile. Sediment bands are marked by solid lines, minimum growth rates by dashed lines.

Correlations between the timing of these growth phases and other palaeoclimate records are shown in figure 5.12. A strong relationship is visible between the speleothem growth phases and periods of climatic improvements from both the ice core and marine oxygen isotope records (Martinson et al, 1987; Dansgaard et al, 1993), but the most remarkable is that with the predicted solar insolation levels (Berger and Loutre, 1991), calculated from the theory of Milankovitch (1941).

5.4.3.3 Interpretation

5.4.3.3.1 Timing of Growth Phases. The growth phases of the Lancaster Hole flowstone occur only during interglacial and interstadial periods; substages 5e, 5c and 5a, and four interstadials within stage 3. However, the duration of the growth phases are much shorter than the accepted length of isotope substages 5e/c/a (~ 10-20 ka; Martinson et al, 1987; Dansgaard et al, 1993). The close correlation between the flowstone growth phases and the timing of insolation maxima suggests the dominance of this factor upon the timing of growth, through its influence on one or more of the variables affecting speleothem growth.

No growth was observed at the last insolation maxima (9 ka), nor was the sequence actively forming today. This is thought to be due to changes in the hydrology of the aquifer during the last glaciation. None of six massive fossil flowstone sequences in the Collonades Chamber / Bill Taylors Passage of the cave was observed to be actively depositing, and none of their water feeds are active. Where water is discharging into the passages, the waters are aggressive and are eroding both fossil speleothems and bedrock. The presence of glacial till deposited in the Devensian glaciation is proposed to have blocked the former flow routes and decreased the calcium concentration of the water.

Several of the factors which have been shown to affect speleothem growth could be the limiting factor in the interglacial and interstadial growth periods under consideration here. In particular, for growth to occur, both calcium ion concentration has to be above atmospheric equilibrium concentration, and a groundwater supply has to be available. Temperature is also a factor, but would not be expected to be limiting during these periods in the British Isles, as many records demonstrate that temperatures would be expected to be above freezing for most or all of the year. Guiot et al (1989) predict mean annual temperatures of 8-10 °C for Grande Pile in stage 5, and 3-8 °C in stage 3; slightly cooler conditions would be expected in Yorkshire. The beetle record for the Upton Warren predicts summer temperatures of

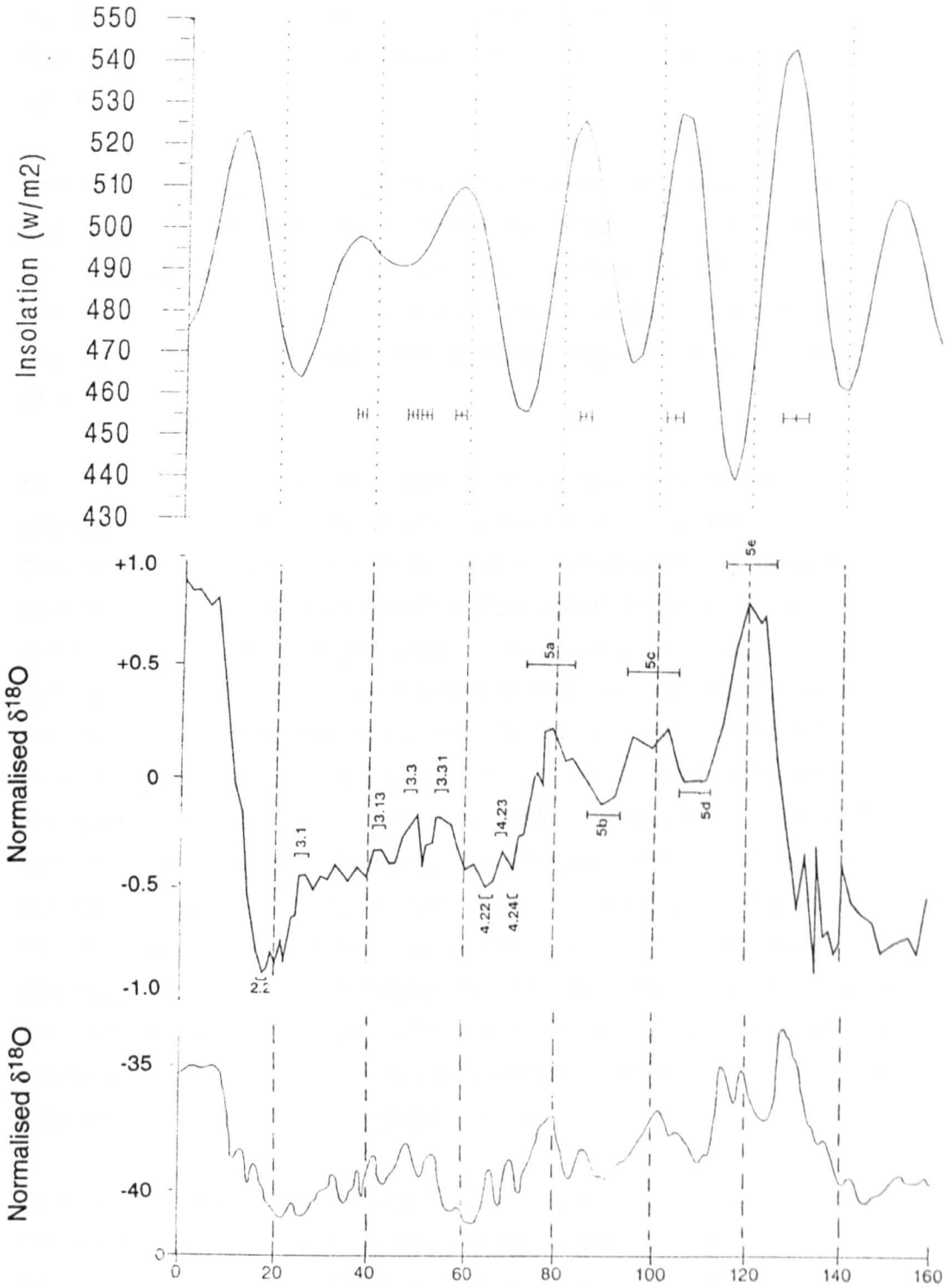

Figure 5.12. Comparison of the growth record of the Lancaster Hole flowstone (horzontal error bars) and three palaeoclimate indicators for the period 0 to 160 ka. From top to bottom, solar insolation for July, 60 °N (Berger and Loutre, 1991), the normalised marine oxygen isotope record (Martinson et al, 1987) and the Summit ice core oxygen isotope record (Dansgaard et al, 1993).

18 °C within stage 3 (Coope, 1977); and that from Chelford (correlated to stage 5c; Ehlers et al, 1991) suggests maximum summer temperatures of 15 °C (Coope, 1959).

Calcium concentrations rising above atmospheric equilibrium concentrations may also explain growth at the insolation maxima. However, this is not thought probable, as it implies that at other times the waters would be aggressive, and dissolve the flowstone. No dissolution surfaces are observed in this sequence, and thus it must seem probable that the cessation of water supply feeding the sample may limit growth.

For changes in groundwater supply to cause growth commencement, then some change must occur during the insolation maxima which causes flow on the flowstone. This may occur due to a significant increase in precipitation at these times, perhaps such that overcame a previous soil moisture deficit. However, no records exist which show such an increased precipitation only during the insolation maxima of the substages, though this may be due to a lack of good precipitation records and their poor temporal constraint at these times. As noted in section 5.4.2.3.1, GCM models for mid-latitudes have predicted up to 50% increases in precipitation from glacial to interglacial periods. Furthermore, the pollen record from Grande Pile shows increased precipitation in interstadial and interglacial periods (Guiot et al, 1989), but not for such a short duration, and without a strong correlation to the insolation maxima. Another explanation may be due to a switch in groundwater flow paths, diverting flow onto the flowstone. Causes of such a switch have to remain speculative, but may be due to changes in the groundwater level, altering the flow routes within the aquifer, or due to increased levels of precipitation quantity or intensity, diverting water into high flow routes.

Several factors may be significant in causing flow cessation upon the flowstone. What is necessary is some threshold to be overcome, which in turn has to respond rapidly to changes in insolation. Further evidence may come from the growth rate record, which may give a record of changes in water flux between growth phases. This record is examined below.

5.4.3.3.2 The Growth rate record. Growth rates were determined for five of the seven growth phases. Two growth periods (in substage 5c and at 48 ka within stage 3) were too short for multiple analyses and thus a growth rate record was not determinable. For the growth phase at 51 ka, only top and bottom dates were

obtained, and thus no information on potential variations in growth rate within the growth phase is available. For several of the growth phases, only minimum growth rates were obtainable from the MSU analyses due to the fast rate of growth. Growth rate data are tabulated in table 5.9.

Time of Growth (ka)	*Growth Rate*
129	0.033 - 0.12
103	-
85	> 0.011
58	> 0.012
51	0.015 - 0.15
48	-
37	> 0.003

Table 5.9. Growth rate data for the Lancaster Hole flowstone derived from MSU analyses.

The growth rates are of the order of magnitude expected, and fall within the range of those observed today and also those of the Stump Cross and Sutherland samples. The absolute growth rates can be explained by the climatic conditions occurring at the times of growth. It can be assumed that film thickness is in the range 0.05 to 0.2 mm, the range observed upon flowstones today. Mean annual temperature is assumed to be 10-12 °C, within the range predicted for the stage 5 interglacial and interstadial periods by other palaeoclimate records (Coope, 1959, 1977; Guiot et al, 1989). Seasonal availability of water is assumed to occur from 6 months (with a soil moisture deficit in summer) to 12 months (with no limitations on water availability). For a minimum growth rate of 0.01 mm yr^{-1} to occur, then calcium ion concentrations would fall in the range 1.4 to 3.2 mmol l^{-1} (Table 5.10a). This is in agreement with that observed in the region today (Pentecost, 1992).

The lack of variation in growth rate within each growth phase can provide insight into the mechanisms limiting growth. If calcium concentrations were thought to limit growth rate, then a decrease in growth rate would be expected as the growth hiatuses were approached due to a decline in calcium concentrations. Similarly, if both temperature and precipitation decreased as the glacial stages were approached, a growth rate decrease would also be expected. However, none of these trends are observed. Table 5.10b shows that the decreases in growth rate that would be expected if these changes occurred would be of the order of magnitude x2-12.

(a)

Calcium Conc. (mmol l^{-1})	Temperature (° C)	Film Thickness (mm)	Months of available water supply
3.2	10	0.05	12
2.7	12	0.05	12
1.5	10	0.20	12
1.4	12	0.20	12
2.3	10	0.20	6
2.1	12	0.20	6

(b)

Conditions	*Growth Rate (mm/yr)*	*Change in growth rate.*
(a) Temperature = 10 °C, film thickness = 0.01 mm, continual water supply, calcium concentration = 2.0 mmol l^{-1}	0.0100	N/A
(b) As (a), but only 4 months available water	0.0033	x 0.33
(c) As (a), calcium concentration = 1.35 mmol l^{-1}	0.0048	x 0.5
(d) As (a), calcium concentration = 0.83 mmol l^{-1}	0.0010	x 0.1
(e) As (a), temperature = 8 °C, film thickness = 0.05 mm	0.0047	x 0.5
(f) temperature = 8 °C, film thickness = 0.05 mm, 4 months water supply, calcium concentration = 1.35 mmol l^{-1}	0.0008	x 0.08

Table 5.10. (a) Conditions necessary for a growth rate of 0.01 mm yr^{-1}. (b) Effect of changing climate on growth rate.

However, the MSU analyses may not be precise enough to constrain such variations for such short duration growth periods of rapid growth rate observed here.

5.4.3.4 Conclusions

The seven periods of growth correlate with the insolation maxima within the period 140-30 ka, and correlate with the three substages of isotope stage 5, plus four interstadial events from stage 3. A good agreement is observed between the dates presented here and those performed on an identical flowstone sequence by Gascoyne et al (1983). The strong correlation of the growth of this flowstone with solar insolation maxima shows the significance of the latter on terrestrial systems. Although responding to the 'classic' palaeoclimate signal of growth in times of climatic improvement, no other samples have been observed to grow for such short a duration. This may be due to the improved precision of MSU dating, further samples may be observed to grow in such a manner in future studies. Within isotope stage 3, the growth record showed subtle differences to the insolation maxima, demonstrating how terrestrial palaeoclimate records may differ from that expected. In particular, the growth phases at 51 and 48 ka fall within a insolation plateau region, suggesting that some other factor is causing palaeoclimatic improvement. Growth rates were shown to be similar to those observed today, and showed no significant variations over time, although the latter may just be due to the difficulty in resolving growth rate change using MSU dating.

The timing of the growth phases strongly correlate with the periods of significant north west European speleothem growth frequency presented in chapter 2, and confirms the accuracy of the latter technique for large data sets. In particular, the growth phases at 58 and 51 ka demonstrate that the double peak in the growth frequency record at this time is probably a true feature. The growth phases at 48 and 37 ka are not observed in the growth frequency record, but may be subsumed in the peaks at 56-49 ka and 42-35 ka. Of particular interest is the growth phase at 85 ka, correlating with sub-stage 5a, which is poorly recorded in the growth frequency record. The reason for this discrepancy is unknown.

This sequence provides for the first time a terrestrial record from the British Isles of consecutive interstadial / interglacial periods, and furthermore, a precise timing of each, although the precise palaeoclimate conditions at these times are not known. The flowstone growth phases may provide a framework into which type-sites such as the Chelford sands formation (Worsley, 1992), Brimpton (Bryant et al, 1983) and the Upton Warren interstadial complex (Coope, 1975; 1977), which are at present

undatable, may be correlated. A tentative correlation by Ehlers et al (1991), placed the Chelford in isotope stage 5c, Brimpton in 5a, and Upton Warren in stage 3. It would also suggest that the idea of a stage 3 inter-stadial complex occurred, with several periods of climatic improvement, rather than just one or two events. The Oerel and Glinde interstadials of Behre (1989) may correlate with the growth phases at 58 and 51 ka, as they have been shown to stratigraphically overly Odderade (sub-stage 5a) deposits. The poorly dated Denekamp, Hengelo and Moershoofd interstadials may correlate with some or all of the peaks at 48 and 37 ka, radiocarbon analyses has placed them between 32 ka and the age limit of the technique.

5.4.4 Comparison of Yorkshire Records

Comparison of the two growth rate records from Stump Cross and Lancaster Hole was not possible due to the lack of correlation in the timing of the growth of each sample. Two periods of overlap occurred, one at ≈ 58 ka, which was of too short a duration for any trends in growth rate to be made, and the other at ≈35±10 ka, for which the age error was too large to constrain any correlations. Growth was so fast during the former time period that only minimum growth rates were obtainable, and thus a comparison between absolute growth rates was not possible either. The suggestion from the Stump Cross sequence that growth rates were lower in interstadial and glacial periods requires further testing; growth rates from Lancaster Hole were generally faster, but again most growth rates were minima. Analysis of further samples from this region would be informative in providing further records of growth and growth rate.

The lack of agreement in the timing of growth of the two samples puts into doubt the conventional interpretations that sediment bands indicate palaeoclimatic hiatuses, and that growth only occurs in periods of climatic improvement. The Stump Cross sample demonstrates that climatic conditions in Yorkshire over the last 200 ka appear to be favourable enough to support active speleothem deposition for most of the time. This has implications for the mechanisms of growth of the Lancaster Hole sequence; if temperature and precipitation are known not to be limiting during the interstadial periods, it suggests that either calcium ion concentrations or some non-linear response (such as flow switching) may be the limiting factors. Caution must now be taken in the interpretation of a growth signal from just one speleothem sample, duplicate samples growing over the same time period are necessary to precisely constrain any palaeoclimate signal.

The growth and growth rate signals also have important implications for other speleothem studies. In particular, combining both the growth of the Stump Cross and Lancaster Hole samples provides a record of growth for a large part of the last 170 ka. This provides an excellent framework for other investigations (trace element, isotopic and palaeomagnetic work). Furthermore, the high growth rate provides a high resolution record; if sampling is possible at a 1 mm frequency, then with a growth rate of 0.1 mm yr^{-1} a record of 10 year variations is possible. However, long records of such high growth rates may be hard to obtain as observed in the Lancaster Hole record, as it is rare to see flowstone sequences thicker than 3-4 m in caves today, which may only reflect a maximum of 30-40 ka of growth.

5.5. Uranium Isotopic Signals

The MSU analyses also provide precise information on the uranium isotopic signatures of the samples. Both the initial $\delta^{234}U$ and ^{238}U concentrations can be precisely measured over long time periods, and these reflect the uranium signature of the groundwaters feeding the speleothem. It has been suggested that the trends in the isotopic signature may vary due to different oxidising conditions, alpha-recoil effects and weathering (Osmond and Ivanovitch, 1992). The oxidation state of the soil and groundwaters above the cave limits the uranium mobility in the groundwaters. Uranium is more mobile in oxidising conditions, and will be leached. Under reducing conditions, uranium ion concentrations should build up. Alpha-recoil effects affect the $\delta^{234}U(0)$ concentrations of the soil and groundwater (where $\delta^{234}U$ is proportional to $^{234}U/^{238}U$; see table 5.3). If there is a long residence time of uranium, then recoil can cause fractionation of ^{234}U, which is mobilised into the groundwater system. Hence $\delta^{234}U(0)$ increases in the groundwaters, and decrease in the soil. However, as residence times decrease and leaching of uranium increases, then $\delta^{234}U(0)$ values approach equilibrium. Finally, weathering has an important effect on the uranium isotopic signature, by either mobilising more uranium through in-situ erosion, or adding or removing it from the system due to erosive movements.

The uranium isotope signature is shown for the Lancaster Hole (figure 5-13), Stump Cross (figure 5-14) and Sutherland (figure 5-15) samples. For clarity, uranium concentrations are plotted against distance down the profile. Different signatures are visible for each of the samples over time.

The Stump Cross flowstone shows the simplest isotopic signal. The two phases of growth dated by the MSU analyses have distinctly different isotopic signatures, with

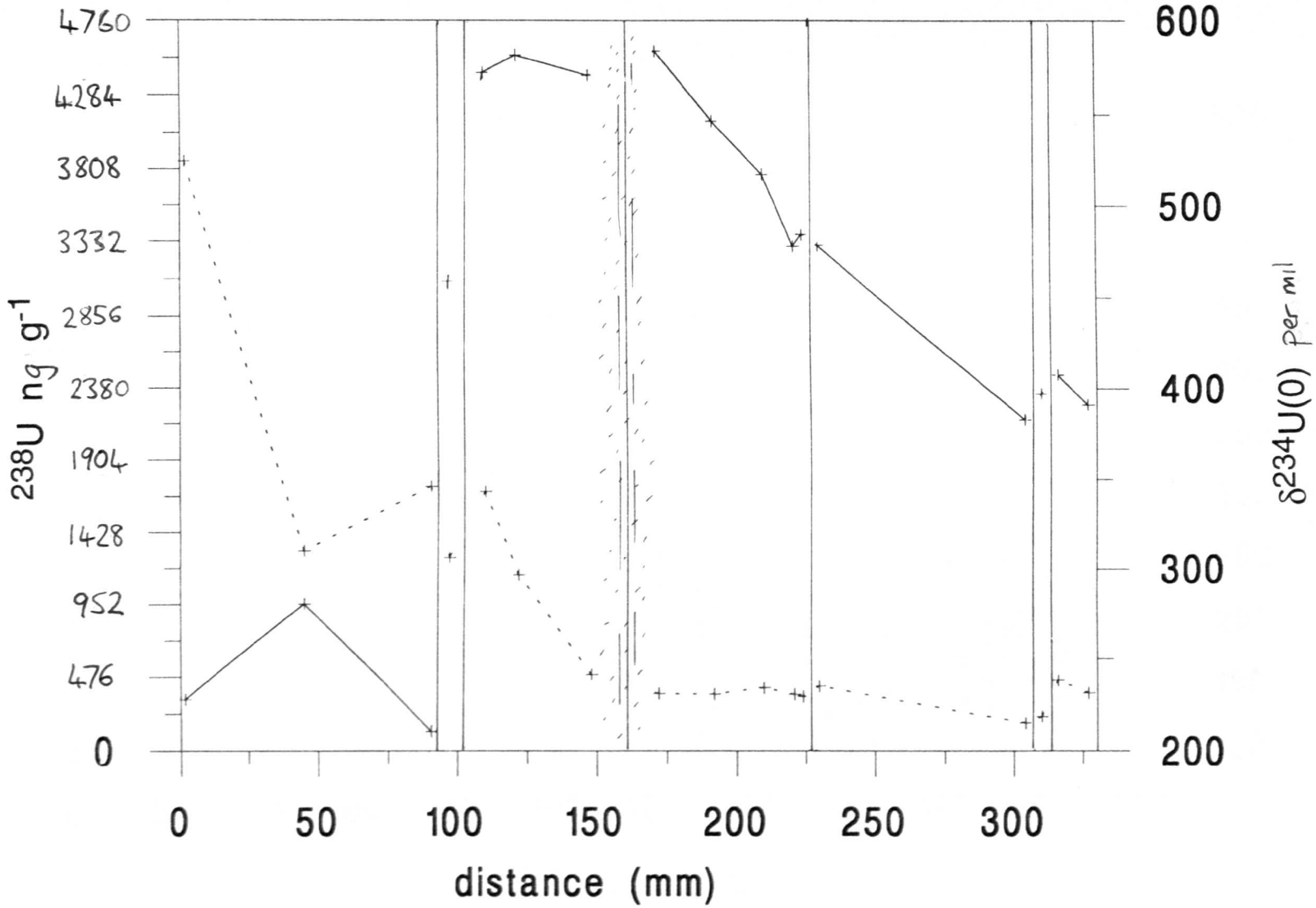

Figure 5.13. Uranium isotopic information from the Lancaster Hole flowstone. Sediment bands are marked by vertical lines, ^{238}U by the dashed line and $^{234}U(0)$ by the solid line. Error bars are removed for clarity but are smaller than the symbols used.

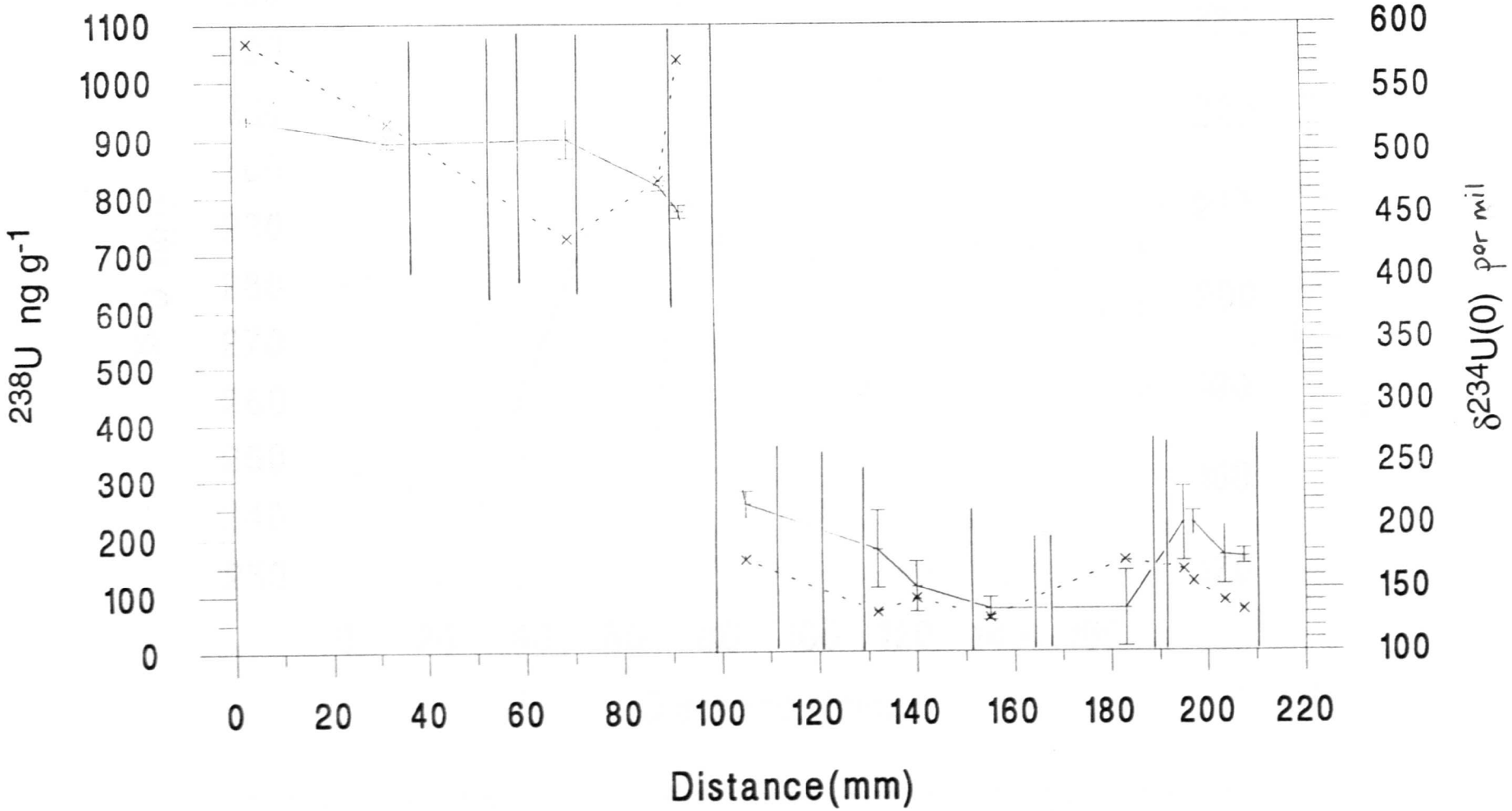

Figure 5.14. Uranium isotopic composition of the Stump Cross flowstone. Sediment bands are marked by vertical lines, ^{238}U by dashed lines and $^{234}U(0)$ by solid lines. Errors in the ^{238}U determinations are smaller than the symbols used.

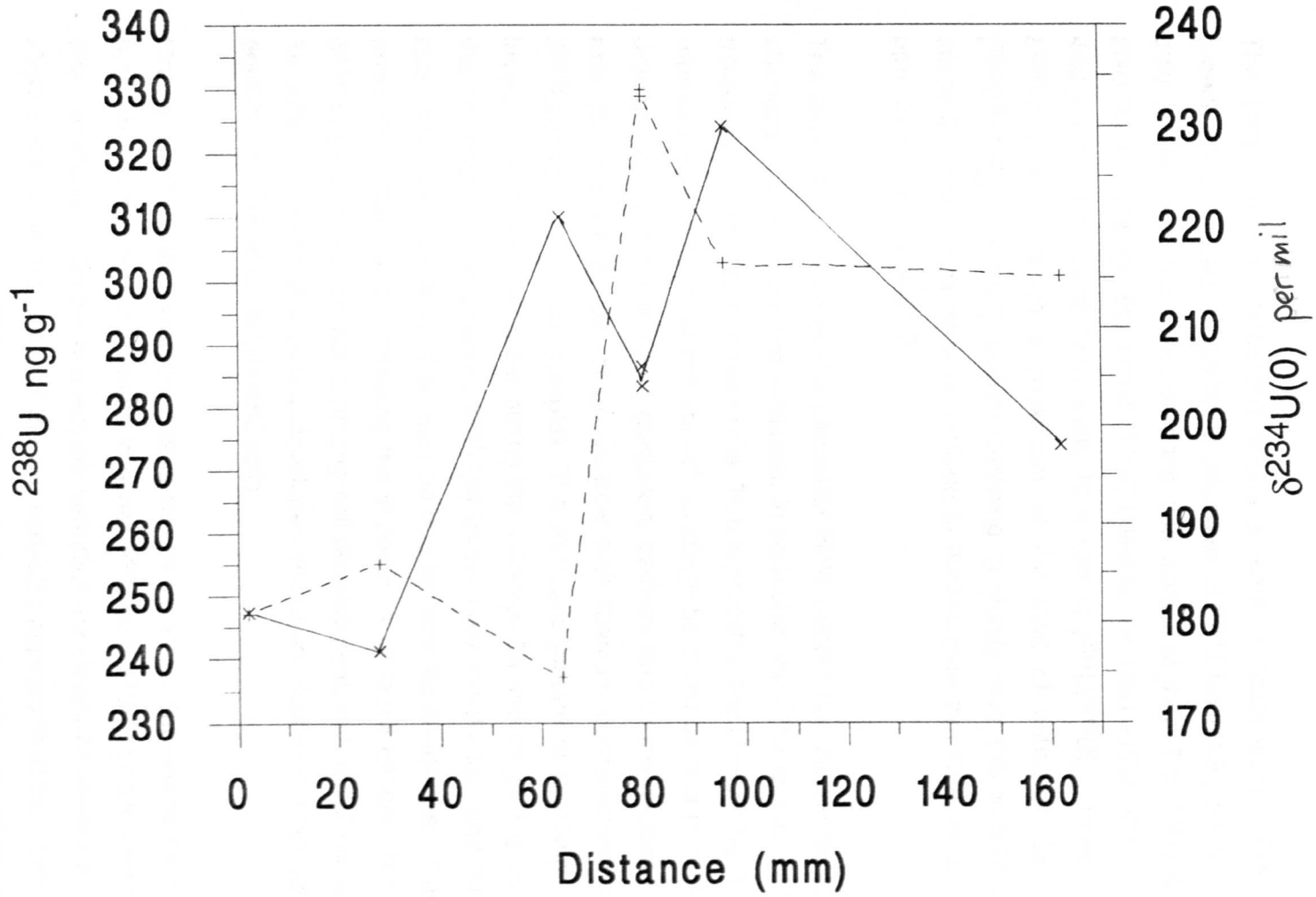

Figure 5.15. Uranium isotopic composition of the Sutherland stalagmite. ^{238}U variations are shown by dashed lines and $^{234}U(0)$ by solid lines. Errors in the ^{238}U and $^{234}U(0)$ determinations are smaller than the symbols used.

elevated ^{238}U and $\delta^{234}U(0)$ within the 169-166 ka growth phase. Subsequent decreases in ^{238}U and $\delta^{234}U(0)$ may be due to glacial scouring, removing a high uranium concentration source. Both growth phases also demonstrate a more gradual decrease in $\delta^{234}U(0)$. This may be due to the increased effects of leaching of the uranium over time, with no replenishment occurring from weathering and erosion.

The Lancaster Hole flowstone shows a more complex signal. The substage 5e growth phase shows a significant decrease in ^{238}U from 3.8 ppm to 1.8 ppm over only 2-5 ka. $\delta^{234}U(0)$ concentrations also decline slightly. The ^{238}U concentrations also fall in substage 5c, whilst $\delta^{234}U(0)$ levels rise from 210 per mil in substage 5e to 460 per mil in this stage (equivalent to a rise in $[^{234}U/^{238}U]_{act}$ from 1.21 to 1.46). $\delta^{234}U(0)$ levels reach a maximum at the start of substage 5a (a maximum $[^{234}U/^{238}U]_{act}$ of 1.57), before declining gradually over this substage and within stage 3. ^{238}U concentrations continue to decline over this time, reaching only 0.35 ppm by the end of stage 3.

The isotopic signature of the Lancaster Hole sample can be explained in terms of changes in weathering and oxidation. In particular, the ^{238}U record shows a gradual decrease in concentration over time. This is probably due to leaching. The initial high uranium concentration at the start of substage 5e could be due to replenishment of uranium during the preceding glaciation, perhaps due to the deposition of uranium rich till, or the exposure of an upslope high uranium concentration bedrock. The $\delta^{234}U(0)$ record is more complex. The expected pattern of leaching and declining levels of $\delta^{234}U(0)$ only occur during the substage 5a and stage 3 growth phases. In the previous growth periods, $\delta^{234}U(0)$ levels were initially low and then showed a rapid increase over time. This may be due to reducing conditions occurring, limiting uranium mobility and increasing the importance of recoil effects. Alternatively, the $\delta^{234}U(0)$ levels may reflect changing soil development, with initial levels in substage 5e reflecting those of a poorly developed soil upon glacial till, later values those in equilibrium with better developed soils.

Only a short duration isotopic record can be obtained Sutherland stalagmite. Figure 5.15 shows that no major shifts in either ^{238}U or $\delta^{234}U(0)$ occur over the growth of this sample, and that the two isotopic variables are closely correlated to each other. A slight increase in the levels of the two variables appears to occur towards the end of the samples growth. This may be related to increased weathering in the Atlantic period, providing new uranium sources, although a trend of decreasing uranium concentration over time would be more expected.

Further information can be obtained from the uranium isotopic data which forms part of the MSU analyses. Sometimes this can provide information on weathering and oxidation conditions, which may provide additional palaeoclimatic information. The Lancaster Hole sample demonstrates highly variable levels of ^{238}U and $\delta^{234}U(0)$ over very short (1-5 ka) time periods, which has not been observed before. Further MSU analyses of additional flowstone and stalagmite sequences may demonstrate this to be a common occurrence. However, in this instance it does prove that the sample is a perfectly closed system suitable for uranium-series dating.

5.6. Conclusions

Variations in growth rate have been determined by MSU techniques for several samples over the last 200 ka. For samples growing over the Holocene, the precision of the technique allowed precise determinations to be made. For older samples, however, the technique could only constrain minimum growth rates. This is due to growth rates being in the range 0.001 to 0.2 mm yr^{-1}. Thus 10 cm of speleothem growth at 100 ka growing at 0.2 mm yr^{-1} would consist of 500 years of growth, whereas the precision on an analysis of that age is around 1%, or ±1000 years. Mass spectrometry would be more suitable for samples with much slower growth rates than measured here. Table 5.11 shows the possible age ranges for which growth rates can be determined for samples of all ages by MSU dating. Samples from the Bahamas have growth rates x100 lower than those measured in this study (Li et al, 1989; Richards, unpublished data), and would be more suitable for MSU dating.

	Growth Rate (mm yr^{-1})				
	0.1	*0.05*	*0.01*	*0.005*	*0.001*
Age Range (ka)	0-5	0-25	0-50	0-250	0-500

Table 5.11. Growth Rates determinable using MSU dating techniques. Dating is from 1 mm subsamples at 10 mm distance apart. A precision of 1% is assumed for the MSU analyses.

Where both minimum and absolute growth rates were obtained, they were found to be of the expected order of magnitude. For SU-80-11, the variables determining growth rate could also be measured, and a good agreement was observed between the theory and actual values. For the older samples, direct comparison with the theory was not possible, but relative changes in the variables could be determined. In

general, the palaeoclimate information which could be obtained from the growth rate record was limited.

The MSU ages determined for the periods of growth commencement and cessation provided some surprising results. Samples were shown to grow in both glacial and interglacial periods. Sediment bands within the samples were also shown to be of either hiatuses of long duration (10^{3-4} years) or temporary short term events (10^{1-2} years). Furthermore, although all the hiatuses were linked to palaeoenvironmental change, this was due to both flooding of the cave system as well as deteriorations in climate. It is argued that caution should be exercised when interpreting sediment bands within a speleothem both in terms of whether it signifies a growth hiatus and in the palaeoclimatic information it may provide.

Of the variables that determine speleothem growth and growth rate, changes in calcium ion concentration and water flux were often important. In particular, the growth record of SU-80-11 was best explained by either a change in calcium ion concentration or a complex response to precipitation change. This makes any palaeoclimate signal contained in the sample more difficult to interpret, as calcium ion concentration changes are driven by vegetation change. The latter may lag behind climate change, cause increases in calcium ion concentrations in a time of climatic deterioration, and is in itself influenced by temperature, precipitation, soil moisture deficit and vegetation dynamics. Growth trends in the Yorkshire samples were better explained by changes in water flow, possible by changes in groundwater flows within the aquifer or through flooding of the caves. This again gives a complex palaeoclimate signal, with potential mechanisms for growth cessation in both glacial and interglacial periods.

Although mass spectrometry provided precise determinations of the timing of growth phases, a more precise measure of growth rate change is needed. Further growth rate information can be obtained on an annual basis by the analysis of annual luminescent bands. This technique is applied in the next chapter, and allows both an annual record of growth rate to be obtained and also a record of inter-annual changes in growth. The latter variability can then be used to gain further information on the growth rate determining variables.

CHAPTER SIX

LUMINESCENCE BANDING, GROWTH RATES AND PALAEOCLIMATE

6.1 Theory of Luminescence Banding

The observation that cave speleothems are luminescent was first made by cavers experimenting with underground flash-photography, who noticed an 'after-glow' effect (O'Brien, 1956). This was not theoretically explained until the experimental work of White and Brennan (1989). They examined speleothems under 365 and 253.7 nm ultra-violet light, and observed that all emitted a blue-green fluorescence (figure 6.1). The source of this luminescence could be either organic or inorganic in nature; however the knowledge that humic and fulvic acids are present within speleothems (Lauritzen et al, 1986) and are luminescent in the blue spectral region, suggested the dominance of an organic source. Recent work by Pedone et al (1990) has compared organic and manganese induced luminescence, and demonstrated that only organically activated luminescence is characterised by significant shifts in wavelength and increasing luminescence intensity with shorter wavelength excitation. Manganese activated luminescence showed no wavelength shift and greatest intensity under visible (green) excitation. Further work in this area is necessary to investigate other possible inorganic luminescence activators. If an organic source does dominate, then such organics could be introduced from the overlying soil and vegetation by the percolation waters feeding the speleothems.

Simultaneous work by Shopov et al (1989, 1990, 1991) has also suggested an organic luminescence source. Using a UV laser, a flowstone sample was observed to have regular peaks and troughs in luminescence intensity up the growth axis, giving a banding effect. This banding was not present throughout the sample; however, assuming a constant growth rate, spectral analysis was applied to the banding intensity signal, to determine its periodicity (figure 6.2). As seen in the figure, a weak 11 *f* periodicity is present, which could be expected to be related to the 11 year sun-spot cycle. Changes in solar intensity over this period may affect plant productivity, humic and fulvic acid concentrations in the soil and groundwater, and thus the intensity of luminescence preserved in the speleothems. Consequently, the 1 *f* luminescence peaks would be expected to be annual, with luminescence peaks occurring in the summer, when maximum biomass is present.

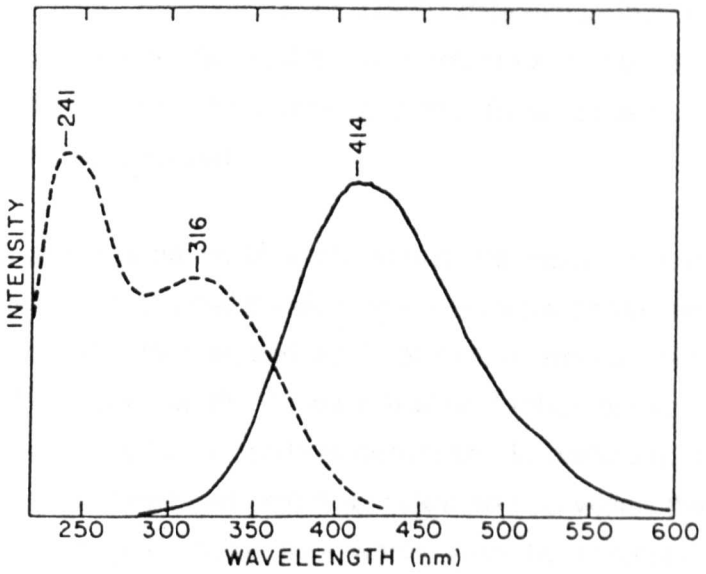

Figure 6.1. Excitation spectrum (dashed line) and emission spectrum (solid line) for a light brown coloured stalagmite (from White and Brennan, 1989)

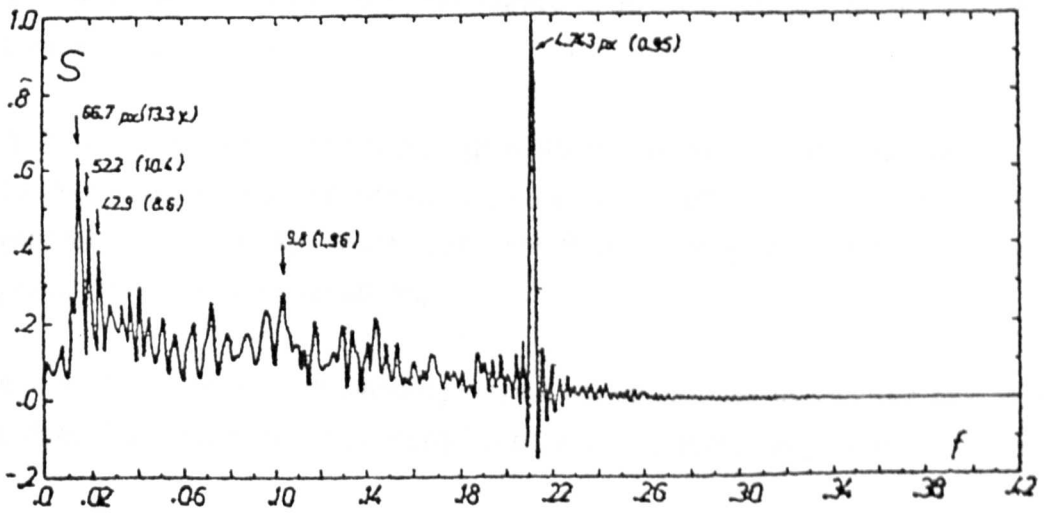

Figure 6.2. Time-series spectra of the luminescence intensity of a flowstone. Frequency of banding is labelled both in terms of digitised pixel width and in years (in brackets), assuming that the intensity peak every 4.743 pixel widths is the annual signal (after Shopov et al, 1989)

Annual luminescence bands have also been observed in corals. Isdale (1984) made the first observation of the phenomenon in an Australian Barrier Reef sample; an annual nature of the banding was demonstrated by comparison with annual growth bands in the coral. Boto and Isdale (1985) determined that the luminescence came from terrestrial fulvic acids, input to the nearshore zone by rivers. More recently, Klein et al (1990) have used luminescent banding in fossil corals to investigate precipitation changes in the Sinai Desert.

If the luminescence bands in speleothems are indeed annual in nature, then the distance between individual bands forms a perfectly preserved signal of growth rate variations from year to year, and would provide a very high resolution record of such variations. However, for this to be possible, further development of the work by Shopov et al (1989, 1990, 1991) is necessary. In particular, they only reported the signal in one cave flowstone, and it is not known how widely the luminescence bands are preserved in speleothems as a whole. Also, by assuming constant growth rate over the whole of the sample, in order to interpolate between the different regions of signal preservation, there is a possibility of introducing harmonics into the power spectrum which are a function of the number of such regions. This could then generate the 11 *f* signal, suggesting the 1 *f* signal may not be annual. Thus several investigations are needed to:

1. Determine the frequency of signal preservation, to discover the practicality of its use in measuring growth rate.

2. Verify the annual nature of the signal, using MSU dating over a period for which banding is preserved.

3. Assess the consistency of the signal along individual growth bands within samples, to determine whether variations in yearly band width are due to internal variations (ripples, angle of deposition, turbulent flow) or external variations (temperature, precipitation, calcium variations).

4. Finally, if the growth banding shows variations due to external influences, the palaeoclimatic signal can be investigated with respect to the growth rate model.

6.2 Experimental Method

In this study over 40 samples were screened to determine the presence or absence of growth banding (Table 6.1). The method employed long wavelength UV excitation (320-420 nm), the same source as used by Isdale (1984), Boto and Isdale (1985) and Klein et al (1990). Samples were cut into 2 mm thick sections parallel to the axis of growth, and observed under a standard Weiss microscope fitted with an IV FI epi-Fluorescence condenser containing a 50 W super-pressure mercury lamp. A 418 nm barrier filter, 320-500 nm exciter filter and a microscope magnification of x64-100 was used. Significant banding was only observed in three samples (two flowstones and one stalagmite), while three other samples had very poorly defined or sparse growth banding.

Where banding was observed, the signal was recorded and analysed. In all cases this involved long exposure photography using Kodalith Ortho 6556 (Type 3) film. Exposure times varied with the intensity of luminescence, sample colour and section thickness, typical exposures were between 10 and 30 s. Standard development techniques were used, and the resulting negative was then analysed in one of three ways:

1. The negative was digitised using a digital scanner, and displayed using UNIRAS graphics on a Sun Workstation. The digital image could be manipulated using smoothing filters, typically a 5 pixel (125 μm) filter was used, in order to measure peak band width. This technique offered the potential for high precision measurement of band width. Disadvantages include the high memory cost (a 5 x 40 mm digitised section of a negative fills a 5.25" disk), logistical problems in transferring data between computer systems, the time taken in scanning, data transfer and computer processing, and difficulties in quantifying any errors which may be incorporated in the scanning process.

2. The negatives could be projected onto a plane surface and then banding measured using a ruler. Typically, distance between bands would average 20-40 mm on the projected surface, measurable to 1 mm accuracy giving an error on measurement of 2-5%. However, in most cases it was found that projection lead to a loss of visual discrimination between bands, and that precise measurement was impaired.

Name	*Location*	*Type*	*Colour*	*Depth*
Banding Present				
HQ-91-1	Holcombe Quarry, Mendip Hills	S	brown	10-15 m
CC-1B	Corbridge Cavern, Devon	F	red/brown	<20 m
SU-80-11	Assynt, Sutherland	S	yellow	<20 m
CC-51B	Corbridge Cavern, Devon	F	red/brown	<20 m
CC-50		F	red/brown	<20 m
GWYR-92-1	Bacon Hole, Gower	S	brown	<10 m
Banding Absent				
GB-89-25-5B	Grand Bahama, Bahamas	F	pure	≈ 20 m
DL-91-1	Dolebury Levy, Mendip Hills	F	pure	≈ 50 m
KC-91-1	Kent's Cavern, Devon	F	red/brown	<20 m
KC-91-5		F	red/brown	<20 m
KC-91-6		F	red/brown	<20 m
KC-91-8		F	red/brown	<20 m
KC-91-11		S	red/brown	<20 m
KC-92-1		F	red/brown	<20 m
SU-80-13	Assynt, Sutherland	S	yellow	<20 m
RW-91-1	Raven's Well, Bristol	F	grey/brown	<10 m
SL-92-2	Sandford Levy, Mendip Hills	S	pure	20-50 m
SL-92-3		S	pure	20-50 m
SL-92-5		S	pure	20-50 m
GWYR-92-2	Bacon Hole, Gower	S	brown	<10 m
GWYR-92-3		S	brown	<10 m
GWYR-92-4	Minchin Hole, Gower	S	brown	<30 m
GWYR-92-5		S	brown	<30 m
BFM-92-6	Brownes Folly Mine, Bath	S	pure	<10m
BFM-92-8		S	pure	<10 m
BFM-92-9		S	pure	<10 m
BFM-92-10		S	pure	<10 m
BFM-92-11		S	pure	<10 m
SC-90-5	Stumps Cross, Yorkshire	F	pure	≈12 m
SC-90-6		F	pure	≈12 m
LC-92-2	Lower Cave, Bristol	S	pure	≈40 m
LC-92-3		S	pure	≈40 m
LC-92-4		S	pure	≈40 m
LC-92-5		S	pure	≈40 m
LH-90-4	Lancaster Hole, Yorkshire	F	pure	<30 m
LH-90-5		F	pure	<30 m
LH-90-8		S	pure	<30 m
LH-90-12		S	pure	<30 m
MQ-91-1	Minera Quarry, N. Wales	S	yellow/brown	unknown
CC-28	Corbridge Cavern, Devon.	F	red/brown	<20 m
GB-91-1	G.B. Cave, Mendip Hills	S	pure	>80 m
GB-91-2		S	pure	>80 m
GB-91-7		S	pure	>80 m

Table 6.1. Speleothem samples analysed for luminescence banding, including sampling location, type (stalagmite or flowstone), colour and depth.

3. The negatives were analysed using a light table, a x2 negative magnifier where necessary, and a 0.02 mm graduated vernier. Band width on the negatives typically measured 0.6-2.0 mm; assuming measurement to the nearest 0.02 mm, errors would amount to 1-3%. This was the technique generally used, and a more realistic fixed measurement error of ±0.1 mm was assumed (5-12%; equivalent to ±0.005 mm yr^{-1} for the magnification used).

6.3 Frequency of Preservation of Growth Banding

Shopov et al (1989) list the conditions they considered necessary for growth banding to be preserved in a sample. In particular, they suggest a sample must be from a shallow depth "so to be more likely to be affected by climatic variations on the surface"; not consist of "single crystal, macro-crystal, lake or aragonitic speleothems"; or "be affected by other inorganic luminescent minerals such as Mn^{2+}, Sn^{2+} or U^{4+}, which may obscure the signal".

Each of these points can be considered in turn with respect to the samples analysed in this study. With respect to sample depth, of the six speleothems containing banding, all came from within 30 m of the surface, yet many non-banded samples also came from similar locations. Contrary to the views of Shopov et al (1989), there appears to be no reason why near surface samples should be effected by climate change. Instead, increased preservation of banding may be due to changes in the characteristics of the aquifer in the upper ≈30 m. Greater fracturing and the increased likelihood of low storage would lead to shorter groundwater residence times (Smart and Friedrich, 1987). This would enable the differentiation of winter (low luminescence) and summer (high luminescence) waters, generating banding within the samples.

Shopov et al (1989) also suggested that crystal structure was important for the preservation of banding, although their reasoning is not clear. In this study crystal structure was typically length-fast, columnar calcite (Kendall and Broughton, 1978), with horizontal layering consisting of fluid inclusions or particulates, often to the extent that syntaxial crystal growth was disrupted. Instead of crystal structure, sample colour appears to be a more important factor. Table 6.1 shows that luminescence banding is more likely in impure (coloured) samples; none of the banded samples were pure, while 23 of the 37 non-banded samples were. This corroborates results by Gascoyne (1977b), who found no correlation between trace elements and colouration in speleothems, and suggested that colouration had an organic source.

The third factor proposed by Shopov et al (1989) was that inorganic luminescence sources should be absent, as they would obscure the banding signal. All the samples analysed in this study demonstrated high levels of luminescence, irrespective of banding, which would be due to either inorganic or organic sources. Recent work has suggested that inorganic interference of the banding signal may be less important, as some inorganic minerals luminesce at longer wavelengths than organic sources (Pedone et al, 1990; see section 6.1). In addition, humic and fulvic acids are known to complex positively valent ions, including luminescent minerals such as Mn^{2+}, Sn^{2+} and U^{4+} (Aiken, 1985). Thus they will be present in the same locations as the organic luminescence sources, and may potentially enhance the banding signal.

Samples analysed in this study suggest that both colour (indicating the presence of organic material) and shallow sample depth (leading to a greater probability of seasonal differentiation of groundwater feeding the sample) are important factors for banding preservation. As well as these, climatic conditions would also be expected to be a factor, as significant precipitation is necessary in both summer and winter in order that waters of both high and low fulvic and humic acid concentration are transported onto the speleothems. Thus samples from seasonally arid locations may not be expected to preserve banding, as may samples from the U.K. if climate changed such that groundwater recharge occurred only during one season.

Although low signal preservation hampers use of luminescence banding in palaeoclimatic studies, if luminescence banding provides a detailed palaeoclimate signal not obtainable elsewhere, or which can be used in association with other high resolution signals (^{13}C, ^{18}O, trace elements) then the additional screening necessary to find suitable samples may be worthwhile. Conservation interests also have to be considered, only 10% of all samples analysed in this study preserved banding, which may result in an unacceptably large number of samples being removed from the cave environment.

6.4 Evidence of Annual Nature of Banding

The demonstration by Shopov et al (1989) of luminescence peaks at 11 *f* and 1 *f* intervals (section 6.1) suggested that banding occurred on an annual basis. However, a more rigourous proof is necessary if band width is to be used to determine annual growth rates. This has been undertaken by MSU dating of a section of a speleothem

sample over which the age could also be determined by band counting (on the assumption that they are annual in nature).

The most suitable sample was SU-80-11 from Sutherland, Scotland, a 170 mm long stalagmite which contained a total of 308 luminescence bands. These were not however continuous, and attention was focussed on a 32 mm section of the sample in which a dense luminescence banding record was present (figure 6.3). Assuming annual growth, the 242 luminescence bands gave an average growth rate of 0.0549 ± 0.0026 mm yr^{-1} (2 standard errors of the mean). For the section between MSU dates SU-90-11C and E, this gives an age difference of 586 ± 28 years, compared with the age difference from the MSU ages of 600 ± 130 years (Table 5.1). Thus there is very good agreement at 2σ levels between the two techniques, and it can be concluded with certainty that the banding is indeed annual in nature, as suggested by Shopov et al (1989; 1990), and can be used for growth rate analysis.

6.5 Internal Consistency of Growth Banding

Before the distance between annual growth bands can be used in growth rate determination, the consistency of the signal has to be proven within individual growth bands. This consistency is investigated for both stalagmites and flowstones.

For stalagmites, it has been suggested from theory that growth rates should be dependent only on external factors such as water film thickness, temperature, calcium concentration and drip rate once an equilibrium deposition state has been reached (Dreybrodt, 1988; see chapter 3). It has also been shown by Dreybrodt and Lamprecht (1981) that stalagmites will reach equilibrium deposition state irrespective of initial growth surface (surface irregularities or an angled slope) once stalagmite height has reached approximately twice its diameter. Thus for such a stalagmite, the width of each growth band should be constant wherever measured along the band, and variations between bands only depend on external factors.

In the case of flowstones, individual growth bands may not show consistency along their length. Most flowstone surfaces show irregularities, such as ripples and gour pools, dependent on sample gradient and water flux. Such structures may affect growth band widths; if internal consistency within a growth band can not be proven, their use as an indicator of external (palaeoclimatic) change can not be justified at an annual level.

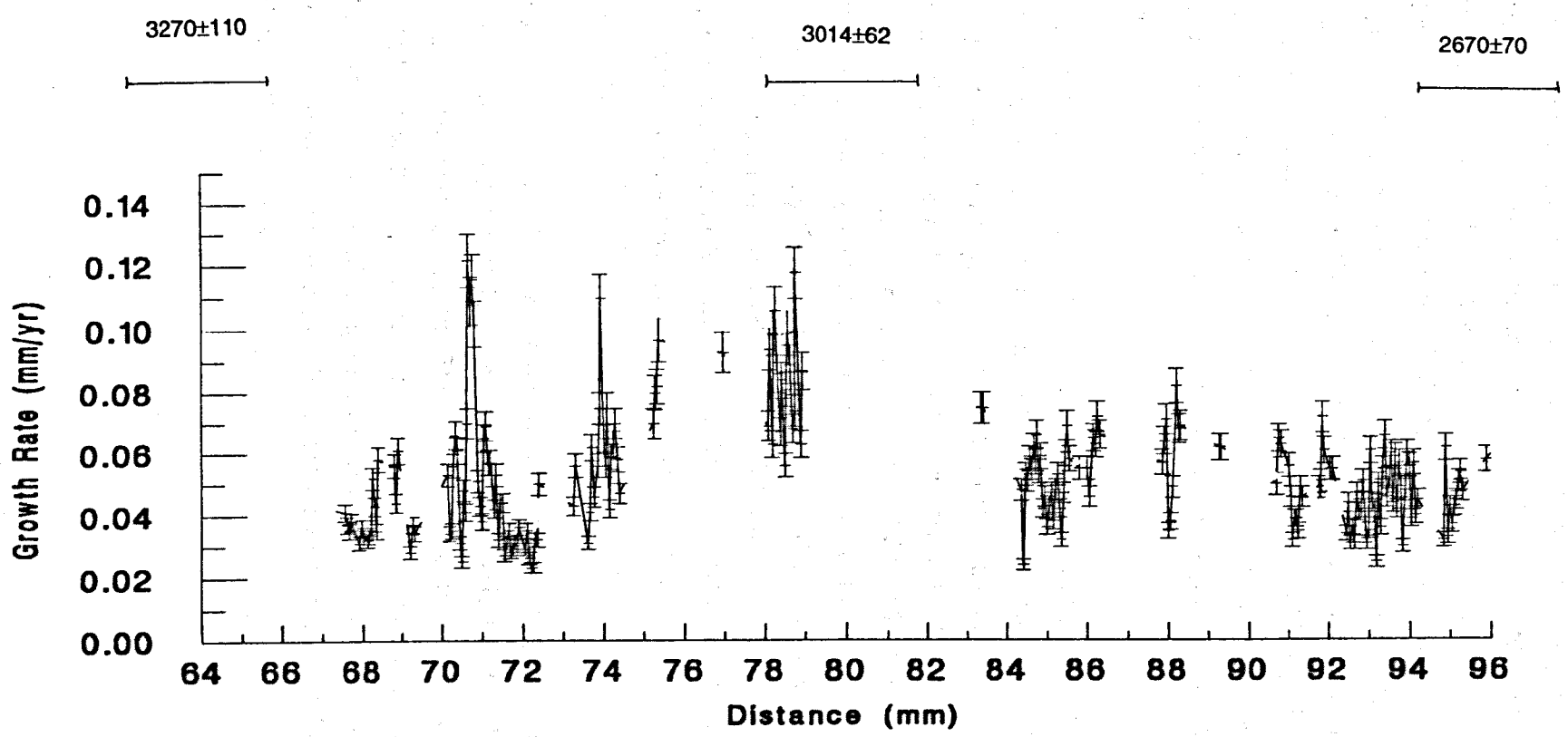

Figure 6.3. Growth rate record of SU-80-11 between 64 and 96 mm, also showing the MSU analyses on this section (in years b.p.). Error bars represent the measurement error.

The internal consistency of the signal within a stalagmite was tested using sample HQ-91-1, a wide stalagmite boss with a flat cap of age 277 ($^{+46}/_{-32}$) ka from Holcombe Quarry, Mendip Hills. Duplicate growth banding records were determined at the one location along the sample where records overlapped (figure 6.4). Correlation between the two was made using prominent marker bands (those either particularly luminescent or wide). Correlations are shown in figure 6.5. There was no statistical difference between the mean growth rates (0.026 ± 0.006 mm yr^{-1} and 0.025 ± 0.008 mm yr^{-1}) at a 99% level (students t-test). The cross-correlation coefficient between the two profiles was 0.663 (n=15; significant at a 99% level), demonstrating that the same temporal trends were being exhibited in both records. Both measures demonstrate the consistency of growth rate variations across the sample.

Testing for consistency within a flowstone was possible using sample CC-1B, from Corbridge Caverns, Berry Head, a sample previously analysed by Proctor and Smart (1991) (figure 6.6). At two points along the profile the luminescence banding could be correlated (figure 6.7a,b). As can be seen, band widths vary significantly between sections. The growth rate records in sections 'a' and 'b' were significantly different at 99% confidence (student's t-test; average growth rates of 0.079 ± 0.031 mm yr^{-1} and 0.036 ± 0.009 mm yr^{-1}) and in sections 'c' and 'd' at 98% confidence (average growth rates of 0.043 ± 0.019 mm yr^{-1} and 0.028 ± 0.009 mm yr^{-1}). Cross-correlations were low, sections 'a' and 'b' having a negative correlation coefficient of -0.574 (n=9; significant at a 90% level), sections 'c' and 'd' a correlation coefficient of 0.284 (n=22; insignificant at all levels).

Consistency in both the magnitude and temporal trends in luminescence band width are demonstrated for stalagmite sample HQ-91-1, but not for flowstone CC-1B, results which were expected. Thus there is no reason why variations in annual growth band width in flat-capped stalagmite samples do not reflect annual variations in the external factors affecting growth rate. In flowstones, a more accurate measure of growth rate variation would be a time average over a longer period of time, perhaps 50-500 years.

Figure 6.4. Stalagmite sample HQ-91-1, showing the location of banded sections.

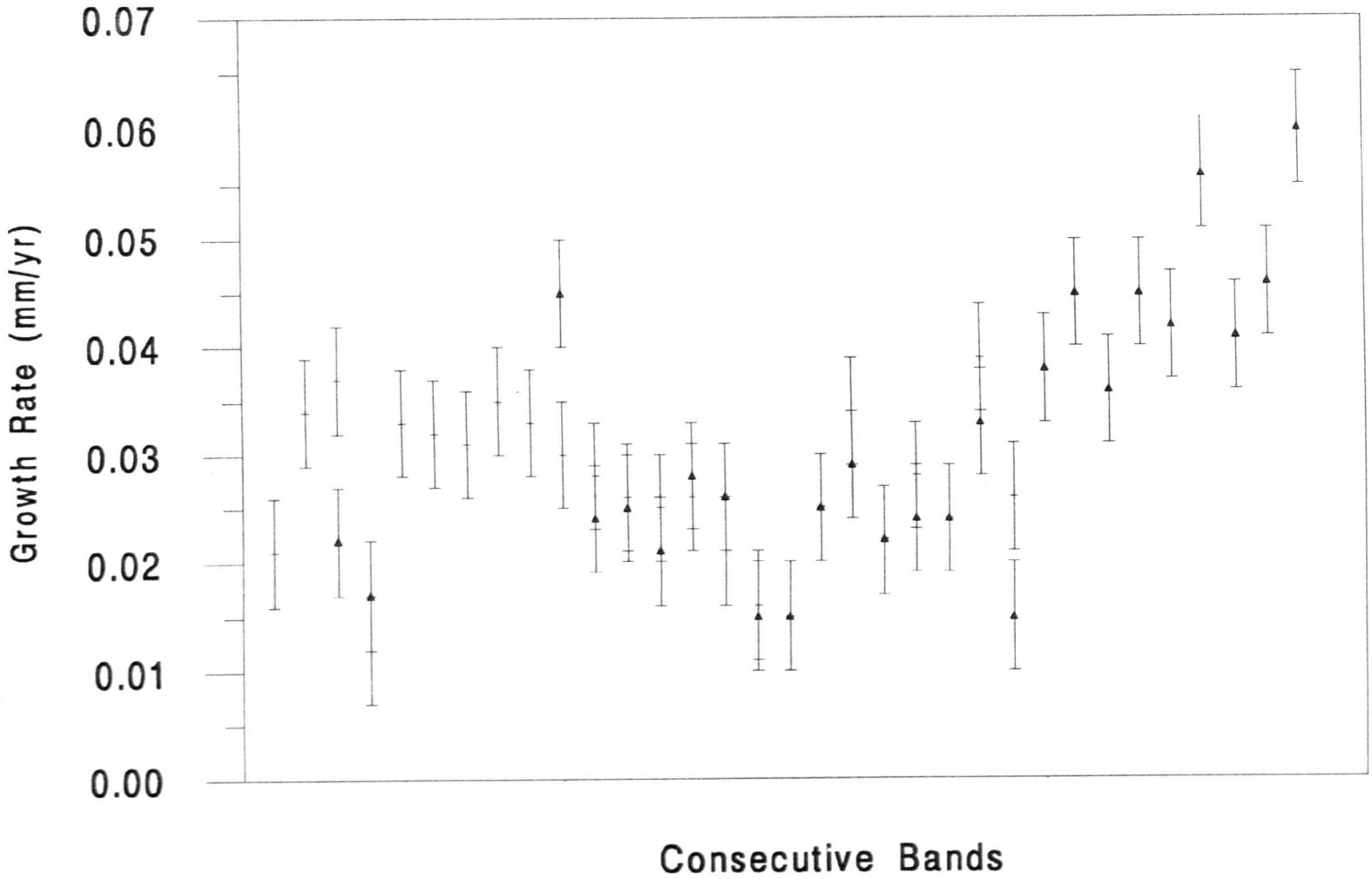

Figure 6.5. Comparison of parallel growth rate records from stalagmite HQ-91-1, marked by bars and triangles. The records overlap for 15 consecutive years, error bars represent measurement errors.

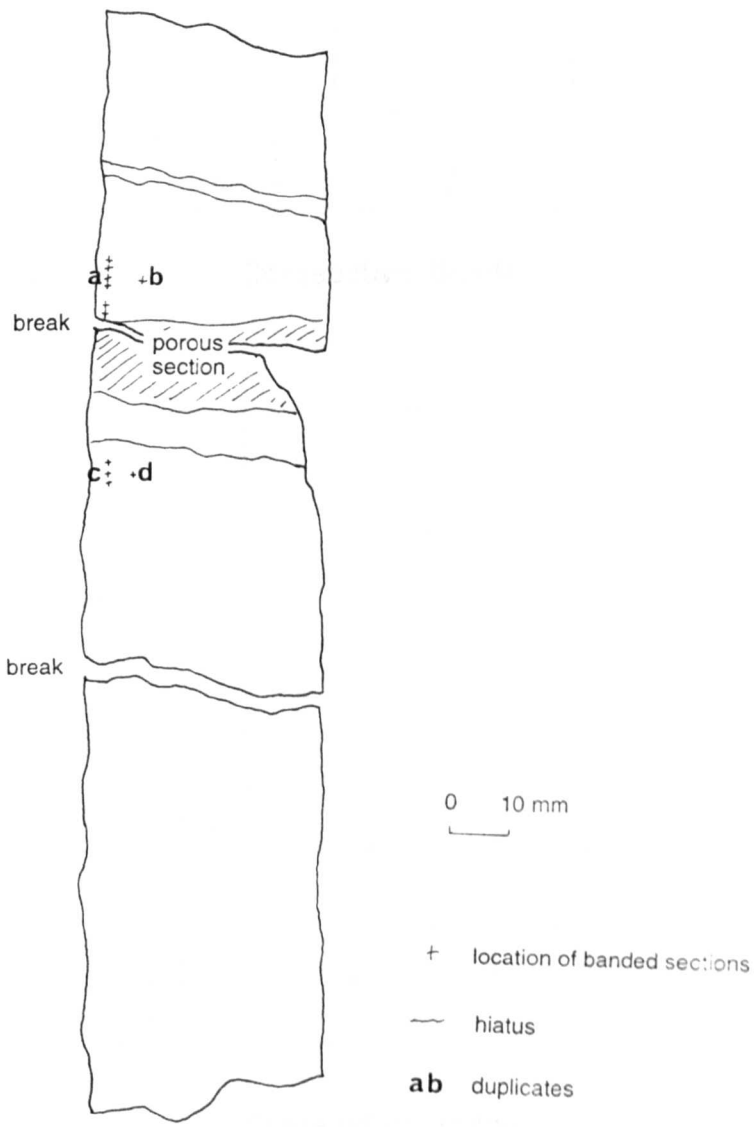

Figure 6.6. Flowstone sample CC-1B, showing the location of banded sections.

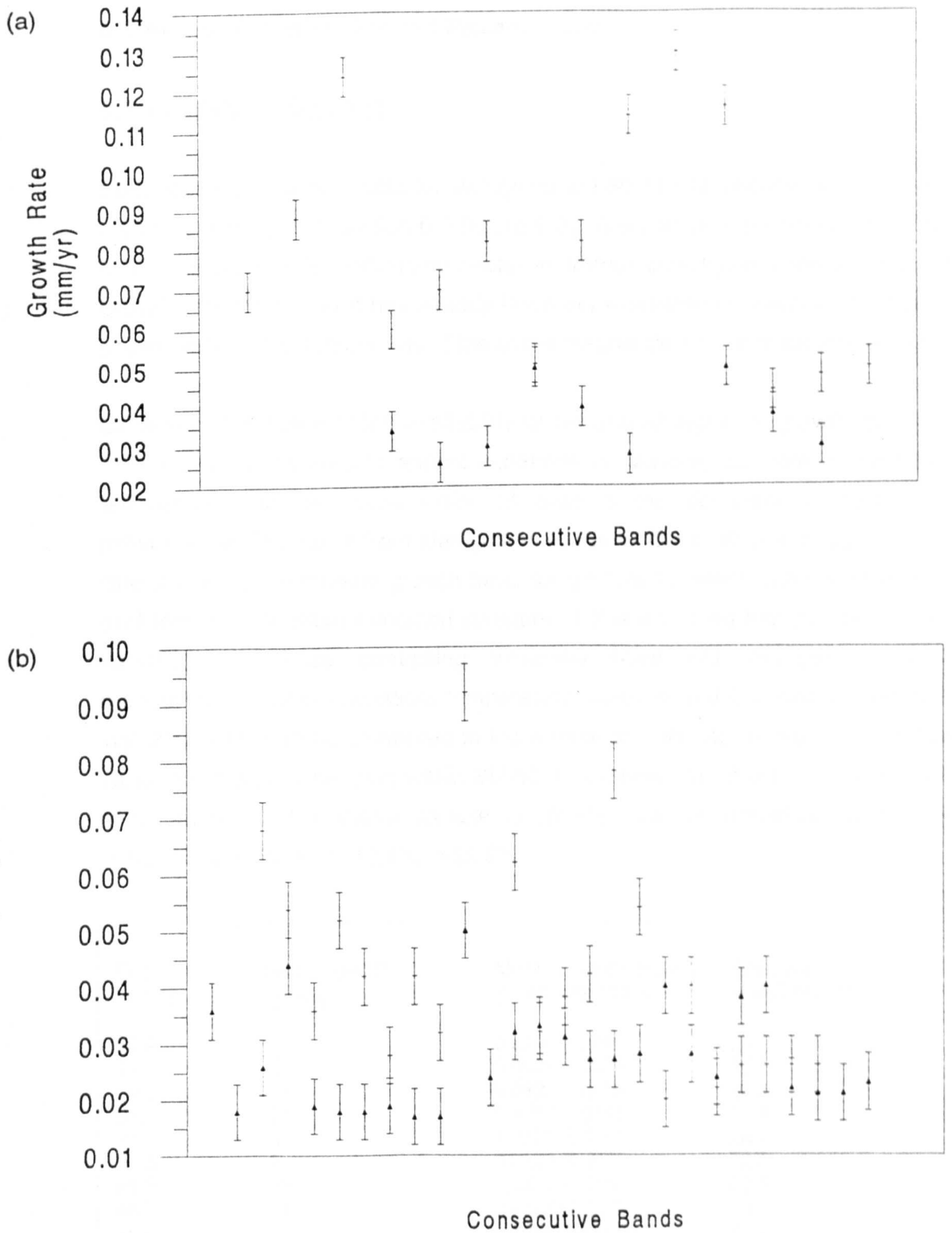

Figure 6.7. Comparison of duplicate growth rate records for flowstone CC-1B. Error bars represent measurement errors. (a) Comparison of duplicate sections 'a' (triangles) and 'b' (bars). (b) Comparison of duplicate sections 'c' (triangles) and 'd' (bars).

6.6 Annual Growth Rates and Palaeoclimate

6.6.1 Stalagmite SU-80-11

Luminescence banding data for stalagmite SU-80-11 has already been presented for part of the sample in section 6.3 (figure 6.3). The complete record is shown in figure 6.8. This sample is particularly useful in further investigating the accuracy of the growth rate theory, as it has already been demonstrated in chapter 5 that the recent growth rate of the sample was of the same magnitude as that theoretically expected.

Of more importance is the availability of an annual signal of growth rate variation. This can be compared to annual variations in calcium, drip rate, precipitation and temperature, to determine which (if any) is the dominant variable. Evidence presented in Chapter 4 from stalagmites in Lower Cave, Bristol, suggested that drip rate levels can determine growth rates for periods for which calcium concentrations and temperature have remained constant. If it is assumed that the factors affecting variations in these controlling variables have not changed since today, measurements of precipitation, temperature, calcium and drip rate variability for the last 200 years can be compared to the annual growth rate record. The coefficient of variation of growth banding within SU-80-11 is shown in table 6.2; overall coefficient of variation for the whole sample is 37.7%, but for individual growth banding sequences varies from 13.4% to 26.8%.

Position (mm)	Record Length (years)	Mean & Standard Dev. growth rate (mm yr^{-1})	Coefficient of variation (%)
68.4	10	0.0389, 0.0092	23.7
74.4	9	0.0647, 0.0174	26.7
78.9	18	0.0831, 0.0168	20.3
84.5	25	0.0499, 0.0106	21.4
88.3	9	0.0593, 0.0159	26.8
91.3	8	0.0428, 0.0079	18.5
94.2	36	0.0452, 0.0103	22.7
98.3	11	0.0723, 0.0097	13.4
159.7	9	0.0582, 0.0123	21.2
163.4	12	0.0599, 0.0157	26.3

Mean of all coefficients of variation = 22.1 ± 4.2 %

Table 6.2. Inter-annual variability measurements of growth rate of SU-80-11.

Records of inter-annual variation of calcium hardness in low discharge conditions such as stalagmite drips are sparse, as most records are obtained during 1 year

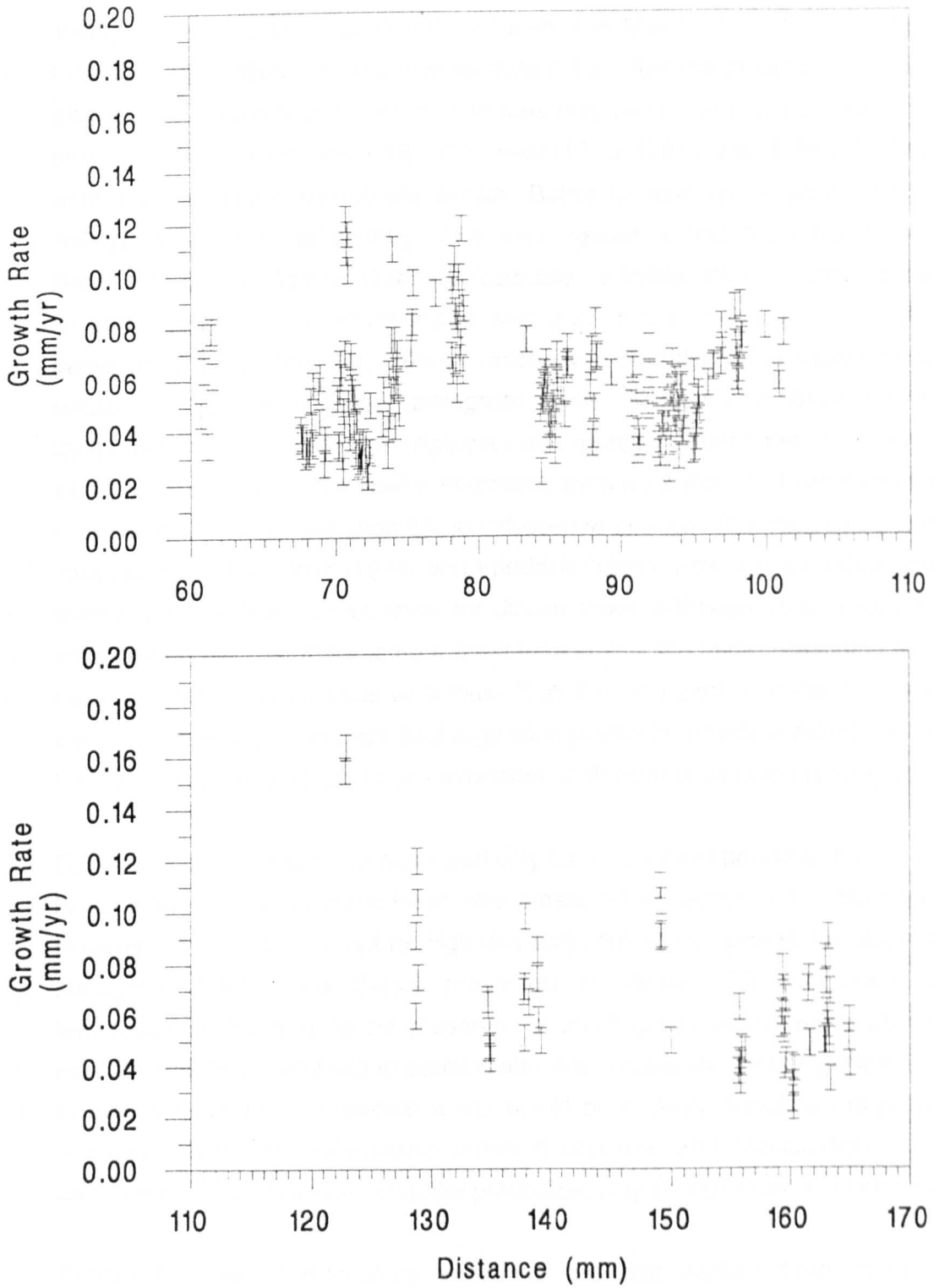

Figure 6.8. The complete growth rate record from sample SU-80-11. Error bars represent measurement errors.

research studies (for example Stenner, 1973; Pitty, 1974; Friedrich, 1981). A very limited record is available from one flowstone feed in G.B. Cave ('GOTO' in Friedrich, 1981), which has been analysed by Smith and Mead, 1962; Stenner, 1973; and Friedrich, 1981. However, the Stenner data is for a five month period only, due to the effects of the 1968 Mendip storm, and thus only two records are available. In 1962, calcium concentration was 1.19 ± 0.11 mmol l^{-1}; in 1981 it was 1.25 ± 0.14 mmol l^{-1}, both concentrations statistically similar. Better records are available from spring risings throughout the country. One such record is that from Coldbath Spring, Broadfield Down, Barrow Guerney (courtesy of Bristol Water Works; table 6.3a). Mean annual calcium concentration was 3.27 ± 0.11 mmol l^{-1}; a coefficient of variation of 3.3%. However, calcium variability in high discharge situations does not reflect that in low discharge stalagmite feeds. Shuster and White (1971), from measures of hardness from Appalachian springs, determined that *intra*-annual variation of calcium concentration decreased from a coefficient of variation of 10-24% in conduit springs to less than 5% in diffuse-flow springs. This result was verified by Jacobson and Langmuir (1974) and Friedrich (1981), although the latter noted less than a 9% coefficient of variation for diffuse flows. Although these records are for intra-annual records, there is no *a priori* reason why the same reasoning should not be applicable to *inter*-annual variations. Thus it is accepted here that the variation of calcium concentration in high-discharge springs should provide a maximum expected for stalagmite samples, and a 3% maximum coefficient of variation is adopted.

Drip rate variation has been measured only for a maximum period of 1 year, and then in very few studies. A compilation was presented in section 3.3.3. No inter-annual records are available except for high discharge limestone springs, not appropriate to stalagmite feeds. The theory presented in section 6.3 suggested that for luminescence banding to be preserved a short groundwater residence time and significant summer and winter precipitation was necessary. Thus significant variation in drip rate would be expected which would be strongly correlated to precipitation variability. Since the relationship between drip rate and precipitation can not be determined, and depends on aquifer properties, only precipitation is considered here.

Precipitation and temperature variations are documented from meteorological observations. Precipitation values were compiled for Sutherland for the last 20 years from Scottish Meteorological Office Data, and are shown in table 6.3a; data from two sites show coefficients of variation of 16.5% and 12.7% respectively. In comparison, mean annual temperature variations show a lower coefficient of variation (table 6.3a).

(a)

Calcium

Coldbath Springs, Bristol

1969-1977	mean = 3.25 mmol l^{-1}; σ = 0.10 mmol l^{-1}	coefficient of variation = 3.2%
1980-1991	mean = 3.24 mmol l^{-1}; σ = 0.09 mmol l^{-1}	coefficient of variation = 2.9%

Precipitation

Cassley, Sutherland	18 year record	Mean = 2012 mm; σ = 332 mm coefficient of variation = 16.5%
Knockan, Sutherland	22 year record	Mean = 2075 mm; σ = 263 mm coefficient of variation = 12.7%

Temperature

Central England

1720-1760	mean = 9.28 °C; σ = 0.67 °C	C.V. = 7.2%
1760-1800	mean = 9.06 °C; σ = 0.59 °C	C.V. = 6.5%
1800-1840	mean = 9.12 °C; σ = 0.68 °C	C.V. = 7.5%
1880-1920	mean = 9.13 °C; σ = 0.52 °C	C.V. = 5.7%

Mean coefficient of variation = 6.7 ± 0.8 %

(b)

Variable	*2σ Inter-annual variability (%)*	*Change in growth rate (mm yr^{-1})*[a]
Calcium	6	± 0.005
Drip Rate	30[b]	± 0.005
Temperature	10	± 0.003

[a] Assuming initial values of calcium concentration of 1.5 mmol l^{-1}, 200 s between drips and a temperature of 10 °C.
[b] Assuming that drip rate variability is equal to precipitation variability.

Cumulative 2σ variability = ± 0.013 mm yr^{-1}
Measured 2σ variability in sample = ± 0.011 mm yr^{-1}

Table 6.3. (a) Inter-annual variations of growth rate determining variables calcium concentration, precipitation and temperature. (b) Comparison of inter-annual variability of growth rate determining variables and inter-annual growth rate variations.

Data compiled from Manley (1974) for four 40 year periods of temperature data for England show a mean inter-annual coefficient of variation of 6.7 ± 0.8%.

Comparison between the variability of growth rate and that of calcium concentrations, precipitation and temperature are shown in table 6.3b. The effects of 2σ variations in each of the variables are shown, assuming mean values of calcium concentration of 1.5 mmol l^{-1}, temperature of 10 °C and a drip discharge of 1 drip per 200 s, and that variations in precipitation equivalently effect drip rate. The results show that the cumulative effects of inter-annual variability in calcium, temperature and precipitation would explain the variability in growth rate, although a simple cumulative effect is unlikely as all the variables are inter-dependent.

This result further corroborates the growth rate theory, which predicts that all three variables should determine growth rate. Better results could be obtained if multiple growth rate records were available for the same time period; this would allow investigation of the relationship between drip rate and precipitation. Different samples from the same location growing at the same time would be expected to have differing growth rates due to variations in water flow path. Furthermore, the growth rates of different samples growing at the same time at different sites would be effected by variations in aquifer characteristics and overlying vegetation. Duplicate samples were sought in the course of this thesis, but were hampered by the low preservation levels of the luminescence signal. This would be expected to be a continuing problem in all further research. Thus neither the relationship between variations in drip rate and precipitation, nor a precise palaeoclimate signal, has been determined at this time.

Of particular interest is the 'spike' in growth rate visible at about 70 mm down the profile (figure 6.9). This shows a C.V. over a 11 year period of 45%, and a tripling of growth rate over three years, far in excess of that explicable by temperature, calcium or precipitation variations under normal conditions. One possible explanation may be the influence of other factors on growth rate. In particular, ash deposits from the Hekla 3 volcanic eruption in Iceland have been observed in Northern Scotland (Dugmore, 1989). The effect of the eruption is also seen in tree ring data from Ireland (Baillie and Munro, 1988); 90% of all trees analysed showed a significant tree-ring narrowing starting at 1159 B.C., with recovery complete by 1140 B.C.. The event has also been dated to ≈ 1150 B.C. from the Greenland ice core record (Hammer et al, 1980). This record suggested that $60x10^6$ tons of acid (H_2SO_4 + HX) were deposited globally by the event. Extrapolating from the date on SU-80-11C by assuming an average growth rate of 0.055 mm yr^{-1}, the growth rate peak occurred at 1155 ± 110

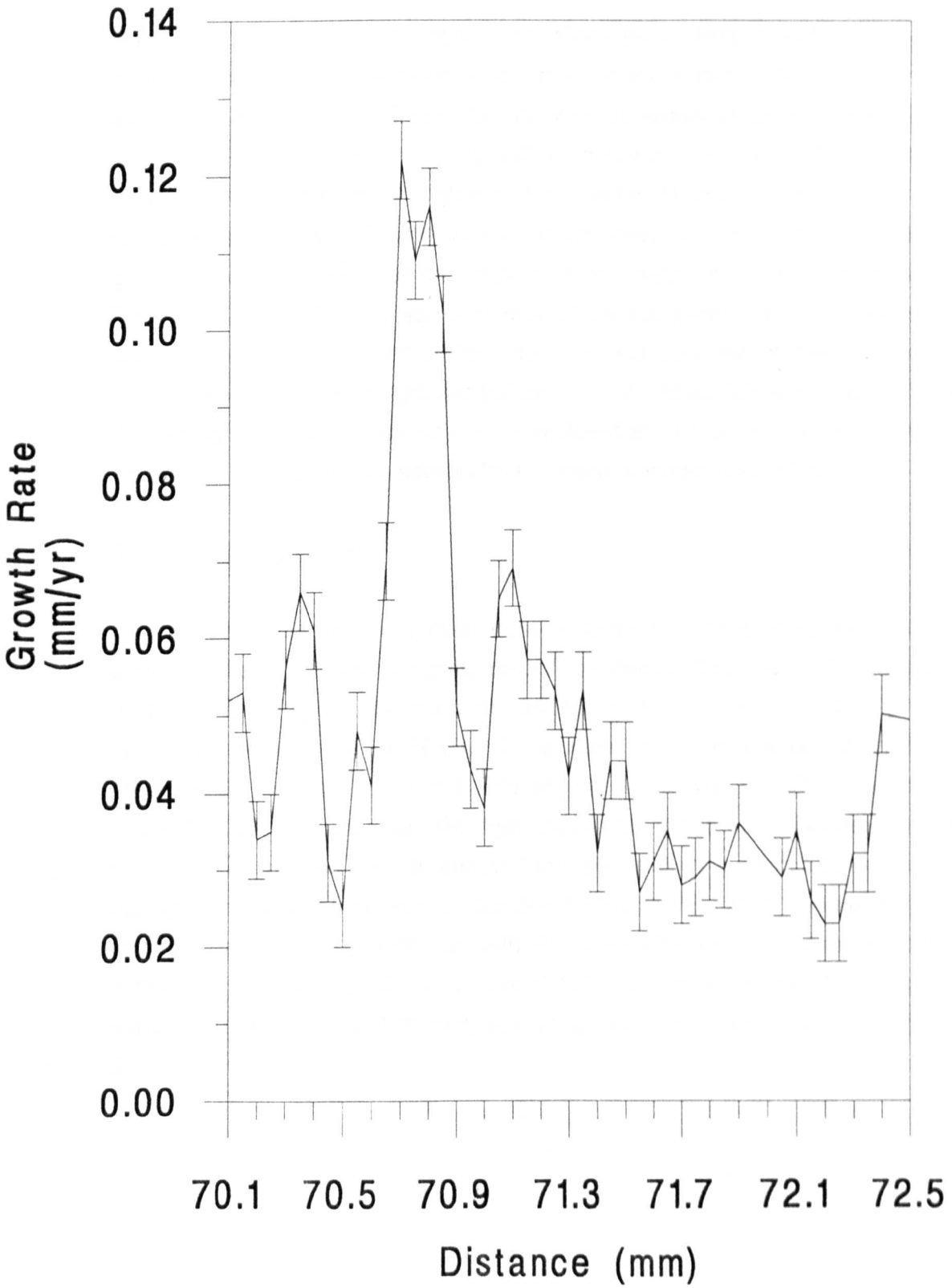

Figure 6.9. A growth rate spike in sample SU-80-11. The section of the sample at 70.5 mm has an age of 1155±110 B.C. by interpolation from the MSU analyses, and correlates with the Hekla 3 volcanic eruption. Error bars represent measurement errors.

B.C., in agreement with the timing of the Hekla event. How a volcanic eruption would affect speleothem growth rates is not clear, as the acidity of the ash may cause an increased dissolution of limestone, as well as significantly increase precipitation. Temperature may also be expected to decrease; however the Pinatubo 1992 eruption caused a decline in global temperatures of less than 1 °C (Pearce, 1983), which would not significantly effect growth rates. Other factors may also cause growth rate spikes, such as the effect of mans alteration of the overlying vegetation. Further analysis of other samples may show the presence of growth rate spikes elsewhere. Meanwhile, ion-probe trace element analysis in this segment of the sample would provide insight into the cause of the spike (for example, a silicon peak if volcanic ash was the cause). If no explanation of the peak is possible, then the spike may show a definite palaeoclimatic signal not observed elsewhere.

6.6.2 Stalagmite HQ-91-1

Correlations between the growth band records for one part of this sample were shown in figure 6.5; the complete record is shown in figure 6.10. Mean growth rate from the banding is calculated as 0.0263 ± 0.0104 mm yr^{-1}, giving an overall coefficient of variation of 39.6%. Comparison between this growth rate and that theoretically predicted is difficult. The sample was dated by ASU to have grown at 277 ($^{+46}_{-32}$) ka (Table 6.4a); the high uncertainty of the analysis does not constrain its growth to any one climatic period. Thus the calcium concentration or temperature during sample formation cannot be determined for HQ-91-1. Figure 6.11 shows a comparison of actual growth rate with that theoretically predicted for a mean annual temperature of 10 °C, calcium values of 1.0, 2.0 and 3.0 mmol l^{-1}, and an average water film thickness of 0.05 mm, assuming accurate prediction by the growth rate theory.

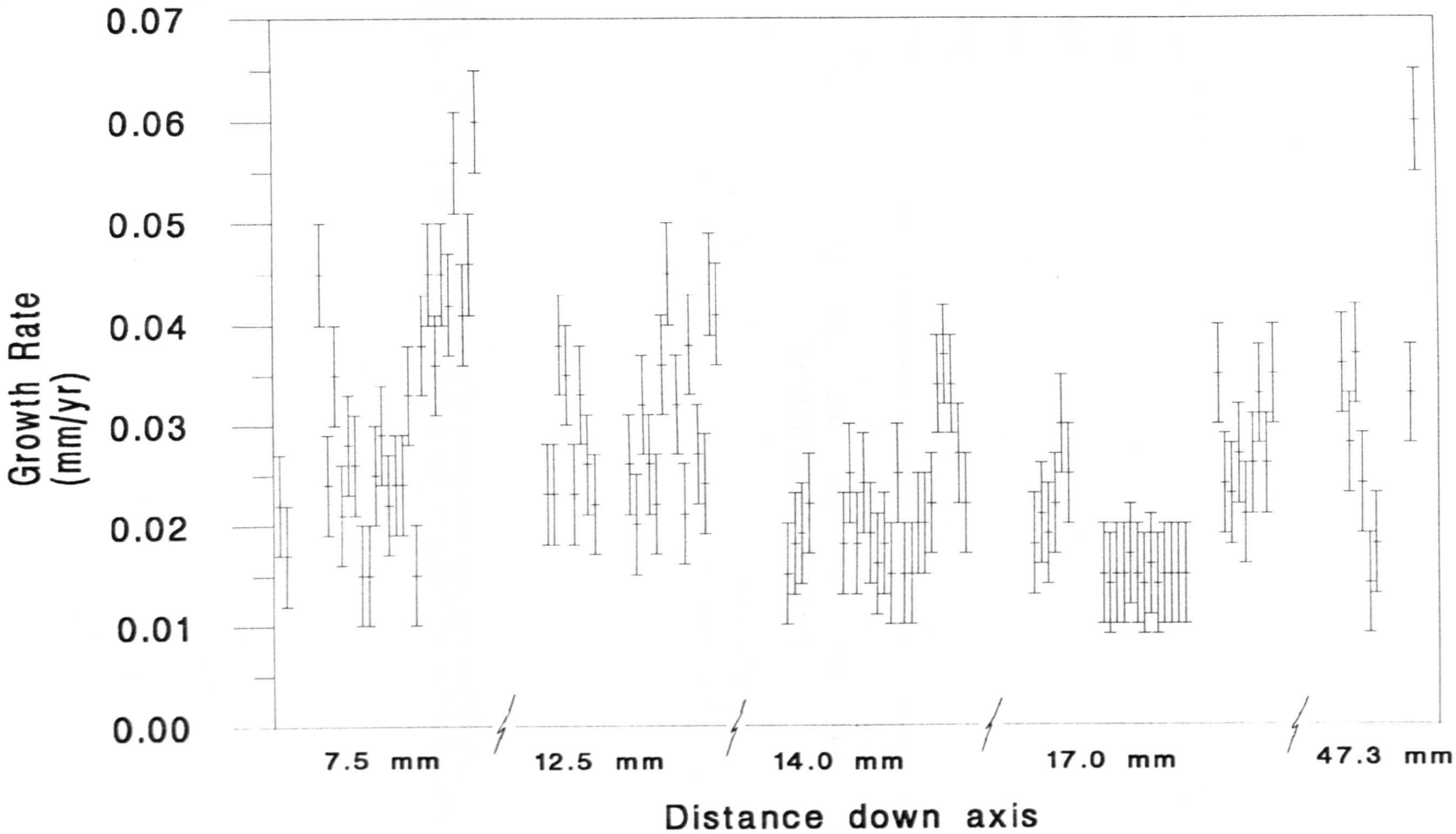

Figure 6.10. The growth rate record for stalagmite HQ-91-1, for the five locations where banding was preserved. Error bars represent measurement errors.

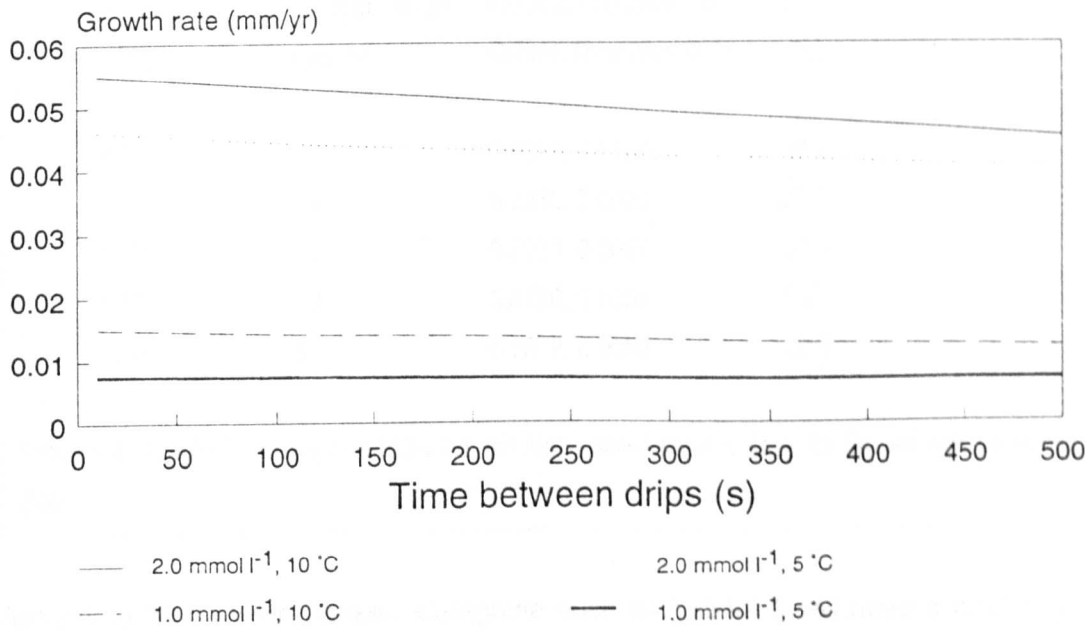

Figure 6.11. Theoretical growth rates for various calcium concentrations, temperatures and drip rates. Actual growth rate of HQ-91-1 was 0.026±0.010 mm yr^{-1}.

(a)

U conc. (ppm)	$^{234}U/^{238}U$ [act]	$^{230}Th/^{234}U$ [act]	$^{230}Th/^{232}Th$ [act]	Age (ka)
.33±.01	1.180±.013	0.9655±.0285	34.9±1.1	276.9^{+46}_{-32}

(b)

Position (mm)	Record Length (years)	Mean & Standard Dev. Growth Rate (mm yr^{-1})	C.V. (%)
7.5	24	0.0325, 0.0127	39.2
12.5	14	0.0310, 0.0086	27.7
14.0	19	0.0223, 0.0067	30.0
17.0	13	0.0150, 0.0008	5.2
17.3	9	0.0278, 0.0053	18.9

Table 6.4. Results for stalagmite HQ-91-1. (a) Alpha-spectrometric data. (b) Growth rate variability data.

Assuming that a wide bossed stalagmite such as HQ-91-1 will have a relatively fast drip rate (faster than 1 drip every 500 s), then initial calcium concentrations of under 1.0 mmol l^{-1} and / or temperatures under 10 °C appear to provide the best explanation of low growth rate. However, because both the temperature and calcium ion concentration during sample formation are unknown, the model can not be constrained further. Looking at the variability of growth rate (Table 6.4b); the C.V. for individual growth sequences is higher and more variable than that for SU-80-11, ranging from 5.2% to 39.2%. Since HQ-91-1 is a larger stalagmite than SU-80-11, with a wider boss and non 'minimum-diameter' form, it would be expected to have higher drip rates and a higher variability of flow. This may explain the observed increase in growth rate variability.

Little useful palaeoclimatic information can be obtained from HQ-91-1; too many variables are unknown, and the preserved luminescence record is too incomplete. A longer, more temporally consistent record is necessary from duplicate samples in order to obtain a satisfactory record.

6.6.3 Flowstone CC-1B

Growth rate information for part of this sample has previously been presented in section 6.5. The complete growth rate record for CC-1B is presented in figure 6.12, and yields a mean growth rate of 0.022 ± 0.009 mm yr^{-1}. This is lower than for the stalagmite samples, and inter-annual variability is higher (with a coefficient of variation of 41.4%).

Limited information is available on the period of growth of the sample. Dates reported by Proctor and Smart (1991) show a complete stratigraphic inversion, but do overlap at 2σ errors. This is shown in figure 6.13, and gives a minimum growth rate of 0.021 mm yr^{-1}, which is in agreement with the luminescence banding record. If a growth rate of 0.02 ± 0.01 mm yr^{-1} is assumed over the whole of the sample (170 mm), this gives an overall growth period of 8500 ± 4000 years at about 170 ka. This shows remarkable agreement with the growth of SC-90-5 during this time period (section 5.4.2), correlating with oxygen isotope stage 6.2 (Martinson et al, 1987), and verifying that conditions were suitable for speleothem growth at this time. Absolute growth rates are also similar, those in SC-90-5 being constrained to a minima of 0.011 mm yr^{-1} by MSU dates (section 5.2).

Limited information is obtainable from the absolute growth rate. Comparisons with modelled flowstone growth rates (table 3.2), suggests that a growth rate of 0.022 ± 0.009 mm yr^{-1} would be explicable by a combination of low calcium concentrations (less than 2.0 mmol l^{-1}), lower mean annual temperatures than today and seasonally limited water availability (assuming that the theory accurately predicts growth rate). Precise determination of the value of any one of these variables is impossible for the time sample CC-1B grew. However, it does give a limited insight into the palaeoclimatic conditions at the time.

Variability of the growth rate record within the sample is the highest of the three samples studied (table 6.5). Increasing coefficient of variability is observed from constant diameter stalagmite SU-90-11 (22%) to stalagmite boss HQ-91-1 (24%) to flowstone CC-1B (35%). This suggests the presence of a palaeoprecipitation signal. For flowstone samples, this may be due to the introduction of seasonality and film thickness variables, both of which have a more significant effect on growth rate than drip rate (chapter 3). However, it may also be a function of the increasing importance of measurement error as growth rate decreases, or be explained by variability caused by variations in flowstone structure, such as the ripple and pool effect of micro-gours.

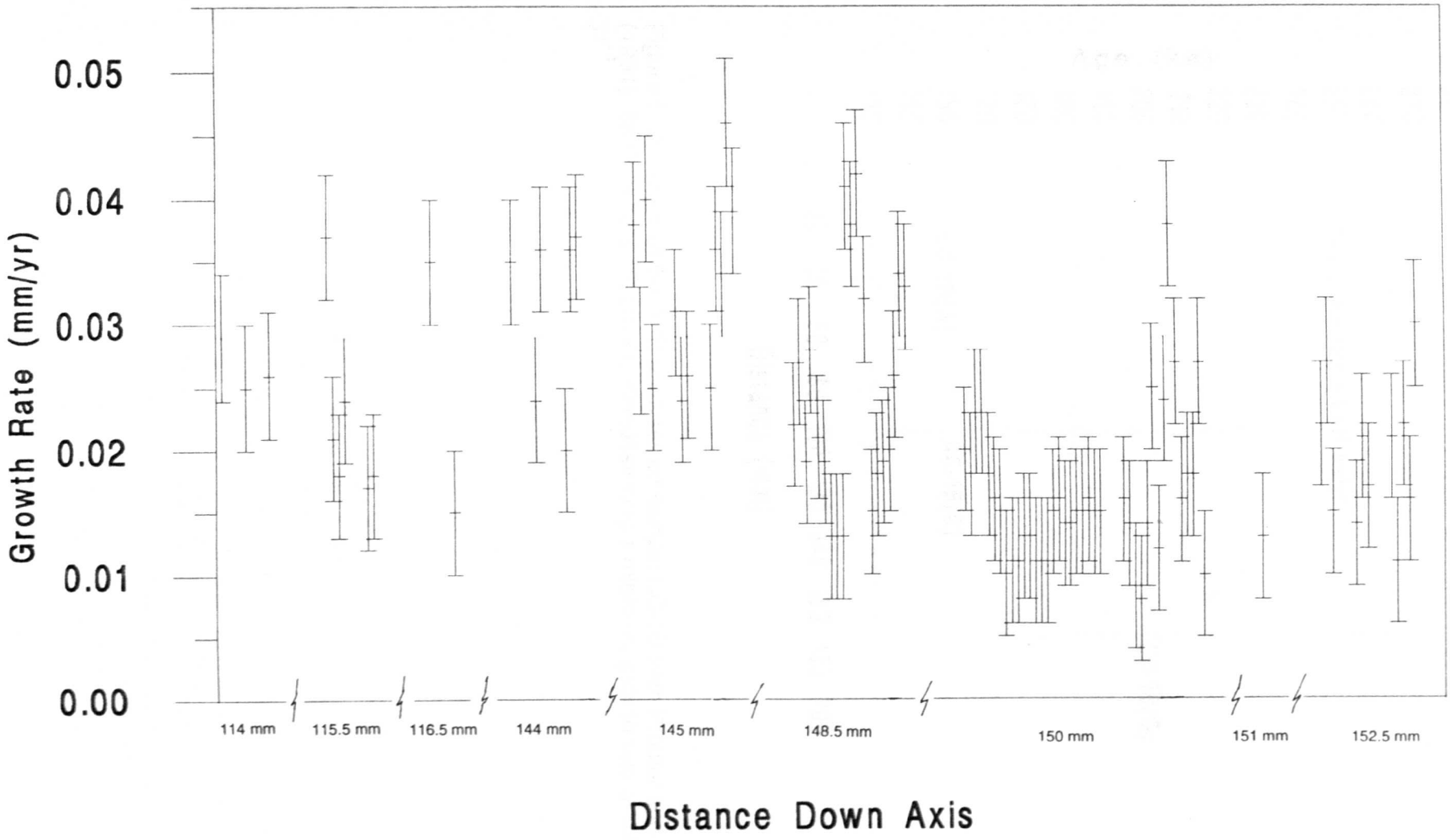

Figure 6.12. Growth rate record for flowstone CC-1B for the nine locations where banding was preserved. Error bars represent measurement errors.

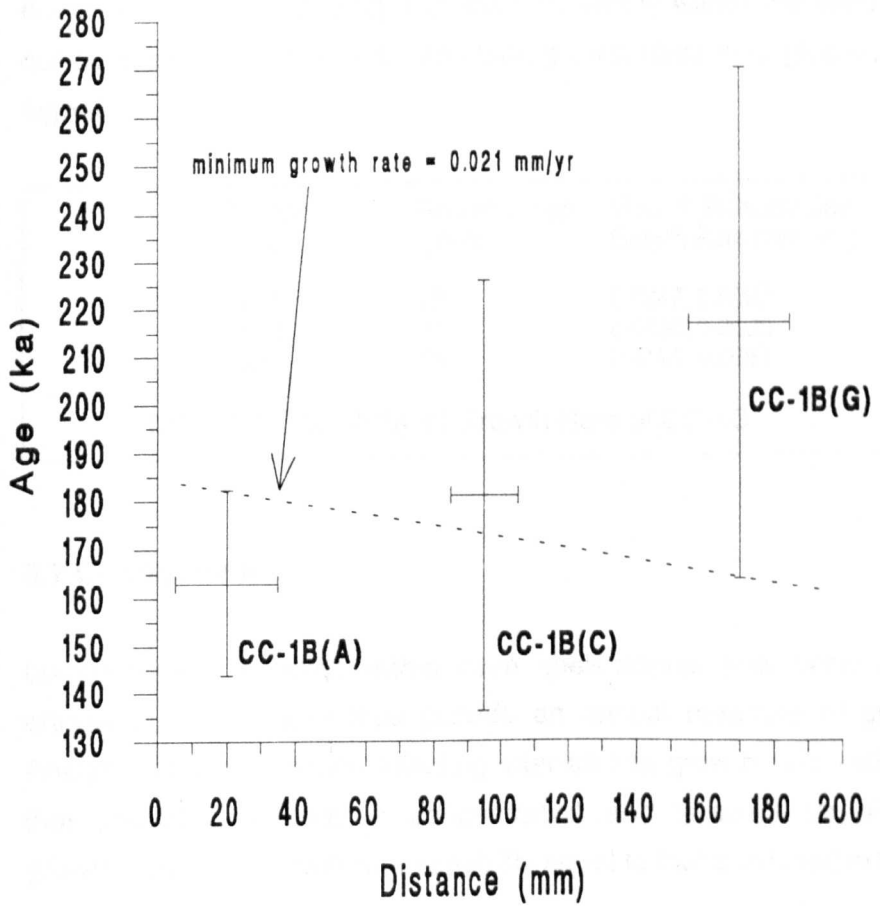

Figure 6.13. Graph of the ASU analyses on sample CC-1B from Proctor and Smart (1991). 2σ error bars are shown, demonstrating a minimum growth rate of 0.021 mm yr^{-1}.

Thus at an annual level, little useful palaeoclimatic information can be obtained from flowstones growth banding. However, variability within the sample can be averaged out over longer time periods, and then growth rates may give a useful palaeoclimatic signal.

Position (mm)	Record Length (years)	Mean & Standard Dev. Growth Rate (mm yr^{-1})	C.V. (%)
148.5	20	0.0247, 0.0093	37.9
150.3	24	0.0150, 0.0035	23.5
150.8	15	0.0191, 0.0081	42.2

Table 6.5. Variability of Growth Rate of CC-1B

6.7 Conclusions

Luminescence banding within cave speleothems has been demonstrated to be annual in nature, and thus provide an annual measure of growth rate variation. Analysis of the variables affecting inter-annual growth rate variability demonstrated that precipitation, calcium concentration and temperature all significantly effect growth rate, with growth rate variability equal to that predicted in theory (table 6.3b).

The high variability of growth rate, together with the discontinuous preservation of luminescent banding, puts the spectral analytical work of Shopov et al (1989) into some doubt, because they assumed a constant growth rate for their flowstone sample for the regions for which banding was not preserved. This is unlikely to be true, and thus the temporal basis of their record must be put into some doubt. A sample with a continuous banding record would prove whether an 11 year luminescent intensity peak is present.

Absolute growth rates from an individual sample can not be directly related to a palaeoclimate signal, since they are a function of flow routing and aquifer characteristics rather than palaeoprecipitation. Comparison between samples which have undergone the same changes in temperature and calcium concentration over the same time is necessary to give a record of relative palaeoprecipitation levels, but due to the low levels of banding preservation, multiple samples are hard to obtain. Annual growth banding in flowstones is suggested to be influenced by the morphology of the sample, and average band width over a large number of years would provide a more accurate measure of growth rate. Thus for flowstones, little

further information is available from luminescent banding than that provided by MSU analyses.

Further research could potentially provide additional palaeoclimatic information from luminescence bands. In particular, the individual widths of the 'summer' and 'winter' bands would give an indication of the relative duration and amount of precipitation within the growing and non-growing seasons. Plate 6.1 shows an image from SU-80-11 and one from CC-1B. Comparison of band widths shows that for SU-80-11 the ratio of 'summer' to 'winter' band width is 1:4, whilst for CC-1B the ratio is more variable and typically from 1:1 to 1:3. This suggests that variations between samples are large, and are related to variations in flow pathways. However, if such variations occur within a sample, a seasonal precipitation signal may be extracted, especially important from samples growing over a glacial - interglacial transition period.

Additionally, the variation of trace elements within the sample can now be analysed on a seasonal basis, with developments in ion-probe techniques giving the necessary resolution. For example, summer maxima of nitrogen and sulphur may be expected (from the humic and fulvic acids); additionally summer maxima of trace elements (Zn, Al, U) which would have entered the sample bonded to the humic substances. This would allow added insight into the mechanisms of speleothems precipitation and geochemistry. Finally, where both a relative precipitation signal and ^{18}O / ^{13}C record are obtainable, the former can potentially be used as an indicator of variations in kinetic fractionation during calcite deposition. It may then be possible to smooth the isotopic signal obtained, and provide improved palaeoclimatic information.

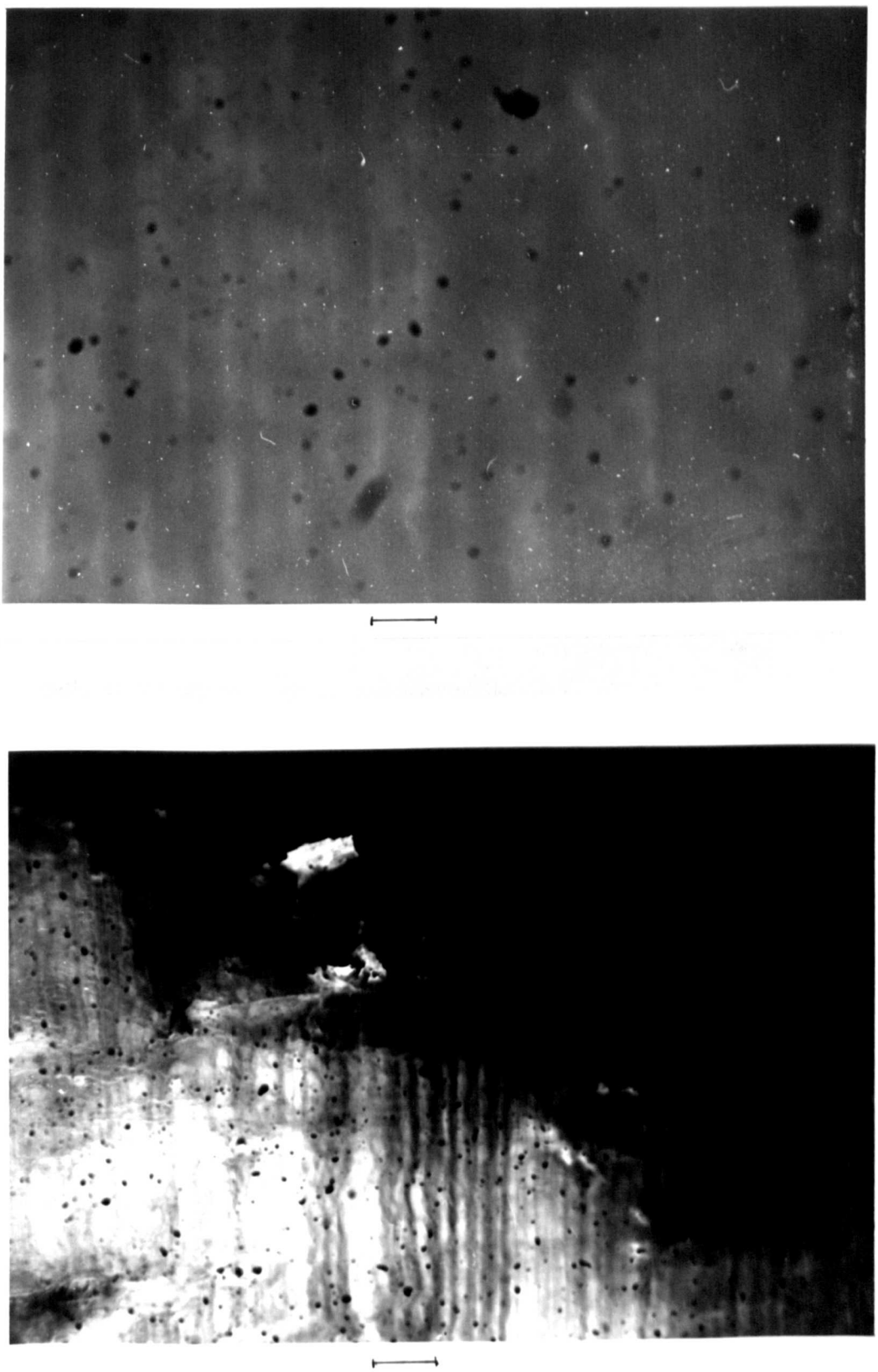

Plate 6.1. Photographs of luminescent banding in stalagmite SU-80-11 (top) and flowstone CC-1B (bottom). Scale bars represents 0.1 mm.

CHAPTER SEVEN

CONCLUSIONS AND FUTURE RESEARCH

7.1 Conclusions

A number of conclusions can be drawn from the work undertaken in this study.

1. Cumulative speleothem growth frequency studies have been demonstrated to provide a useful palaeoclimate record for one region, that of north west Europe. However, it is necessary to have about 500 ASU analyses in such a regional compilation to generate a statistically significant curve which does not suffer from sample bias, and few other climatically homogeneous regions of the world are likely to have such a large data set. Thus few future applications are envisioned, although the technique could be applied to different deposits and dating techniques (such as thermoluminescent dating of loess).

2. Speleothem growth rate was demonstrated to give a potential palaeoclimate signal, through the dependence on water film thickness, drip rate, calcium ion concentration, temperature, and seasonal shut-off of water supply. However, this signal is complex, as the same climate change would cause different growth rates depending on the groundwater flow path feeding individual samples and differences in the overlying vegetation community, causing varying calcium concentrations. Furthermore, although most of the growth rate determining variables increased as climate improved, calcium ion concentration in Quaternary speleothems is not measurable, has a wide range of possible concentrations, can not be substituted for by temperature, and may actually decrease in times of climatic improvement. Calcium concentrations measured in this study were in the range 1.58 to 3.31 mmol l^{-1}, greater than that predicted for 10 °C by Drake (1980, 1983). Thus multiple samples are required to obtain any relative palaeoclimate signal from speleothem growth rate.

3. The growth rate theory was tested for both stalagmites and flowstones for samples which have deposited over the last 200 years, a time for which both temperature and precipitation have remained constant, as has calcium ion concentrations in regions of no land-use change. Both stalagmites and flowstone growth rates agreed with those predicted by the theory within the 2σ error range of the measurements. Flowstone samples had growth rates which were overpredicted by the theory, possibly indicating the importance of seasonally-limited water supplies limiting growth rate. Samples

from Kent's Cavern with continuous water supply had a statistically significant faster growth rate than those with a discontinuous supply, irrespective of the calcium ion concentration of the water. For stalagmites at Lower Cave, samples with the fastest drip rate were observed to have the fastest growth rate, as predicted by theory.

4. MSU analyses were used to obtain a Quaternary record of growth rate change. Recent growth of a sample from Sutherland again showed good agreement between predicted and actual growth rate. Holocene growth, over a period for which temperatures are known to have been near constant, demonstrated a 50% variation in growth rate. Growth rate theory predicted that this could only be due to changes in calcium ion concentration or a seasonal shut-off of the drip feeding the sample, the latter demonstrating a non-linear change with precipitation. MSU analyses on older samples did not give a satisfactory record, as the analytical errors associated with the ages were to large to be able to determine the rate of growth. However, the MSU ages did provide an insight into the timing of growth cessation. Duplicate samples growing over the same time period and in the same region grew at different time periods, one grew only at the insolation maxima, the other both in glacial and inter-glacial periods. The latter proved that growth is climatically possible for most of the last 200 ka, the former suggested in some instances, solar insolation critically limits growth through its effect on temperature, soil pCO_2 and precipitation variations.

5. Luminescent banding was demonstrated to give an annual record of growth rate change, although it is rarely preserved and discontinuous in nature. Banding in flowstones was demonstrated to be a function of flowstone structure, such as rippling, and an average of 50-500 years of bands would give a precise growth rate record. Stalagmites did contain an annual growth rate record, and inter-annual growth rate variations were demonstrated to be equal to those predicted in theory. A growth rate spike was also observed in one instance, growth rate variability was greater than that theoretically possible, and suggested another factor was effecting growth rate. This was proposed to be the influence of the Hekla 3 volcanic eruption, possibly increasing the acidity of the groundwater, the importance of foreign-ion effects on dissolution through the increased sulphur concentration in the atmosphere, through increased precipitation.

7.2 Future Research

Several areas of future research potential have been highlighted by this study. These are considered below:

1. The cumulative growth frequency record from north west Europe showed a significant decrease in speleothem growth in substage 5a. The cause of this decline in growth is unknown, but suggested to be due to a decline in precipitation. Additional records from other deposits at this time would determine whether such a change occurred, such as pollen records with an arid plant community precisely dated to this substage, or the presence of loess at this time.

2. Further testing of the precision of the growth rate theory is also required. The use of recently growing samples from mines and excavated caves only provided a minimum growth rate estimate. An absolute growth rate would provide a more precise record. This could be obtained either by MSU dating of the base of any recently growing samples, or by using luminescence bands. The former was not practical in this study, the latter was not preserved in any of the samples collected. An annual record of growth rate variation from luminescent banding over the last 100 years, a period for which both temperature and precipitation records exist, would provide a most precise test of the palaeoclimate signal contained within the samples.

3. Further records of Quaternary growth rate changes are also required. These would need to come from duplicate samples which are growing at a slower growth rate than analysed in this study. Of particular use could be records from the same time period from both a minimum diameter stalagmite and multiple flowstone samples. If the stalagmites are deposited under isotopic equilibrium conditions, then a record of palaeotemperature may be obtainable from oxygen isotopes and fluid inclusions. Thus growth rate variations would only depend on drip rate and calcium concentration. The former variable has been demonstrated to have a comparatively small effect on growth rate compared to changes in calcium concentration, and thus a record of palaeocalcium concentrations may be obtained. If it can be demonstrated that either the calcium concentration of feeds supplying the stalagmite would be the same as that feeding flowstones in the same cave (through comparison of modern day calcium concentrations), or that relative changes in calcium concentration over time for both stalagmites and flowstones are the same, then both calcium concentration and temperature are known for the flowstone samples. Thus growth rates determined from multiple samples may give a relative palaeoprecipitation signal. However, the whole approach is costly in terms of sample collection and mass-spectrometer time, and may not yield successful results. More realistic future applications of growth rate variations would be when MSU analyses have been obtained to constrain other records such as trace-element and isotopic data. In this

case, changes in growth rate may provide additional limited palaeoclimate information at no extra cost in terms of time or sample destruction.

4. This study has provided new evidence on the timing of terrestrial speleothem growth. In particular, it may be determined that many samples may grow only at insolation maxima, revealing a previously undetermined sensitivity to this factor. It has also been shown that it may be possible for samples to grow during glacial stages. Additional dating of further samples may prove further insight into the causes of the timing of speleothem growth, and the relationship between changes in solar insolation variations, and variations in temperature, precipitation, and plant productivity. Changes in uranium isotopic composition ($^{234}U/^{238}U$; ^{238}U concentration) can also be precisely determined by MSU analyses, further investigations may provide evidence on both groundwater oxidation conditions and landscape evolution.

5. ^{13}C analysis of the Stump Cross flowstone suggested that ^{13}C values in flowstones may record the amount of degassing prior to flowstone deposition, and not changes in vegetation community or the presence of a non-biogenic CO_2 source. Further investigations are needed to test the validity of this argument. ^{13}C analysis of water samples from water feeding both stalagmites and flowstones with the same overlying vegetation cover would test whether elevated ^{13}C values are found today. Such work is currently in progress.

6. Some of the best applications derive from luminescence studies of speleothems. These can be obtained both from variations in band width (growth rate) and band intensity. These provide several records:

a) The simplest application is as a chronostratigraphic marker, which would allow the determination of the age of sections of sample distant from MSU analyses. This may have particular application in constraining the timing of oscillations in both the trace element or isotopic records.

b) Further research is necessary to determine if there is a palaeoclimate signal in the variation of the widths of luminescence bands. This would represent both changes in the duration of these periods, and the timing of groundwater flow during these times. This may give additional palaeoclimate information, for example, a decrease in the width of the "winter" luminescence minima may represent a decrease in groundwater flow at this time, perhaps due to winter freezing.

c) It has been demonstrated that a limited palaeoclimate signal may be obtained from the growth rate record, as detailed earlier. Further applications can be made,

including the comparison of very recent growth rate variation to climate records, as detailed above. Over slightly longer timescales, it may be possible to determine the timing of deforestation by changes in growth rate.

d) Further samples could be analysed to determine the presence of further growth rate spikes. This should be undertaken for the Holocene, for which a good record of volcanic activity exists, to observe whether all spikes correlate with volcanic events. If true, the record can then be extended back into the Quaternary, a time for which volcanic activity is less well recorded.

e) Addition work is necessary on the reasons for banding discontinuity. It has been proposed that it may be due to seasonal shut-off of water supply preventing either periods of luminescent maxima or minima. This can be tested in samples which have formed over the last 100 years, and comparisons made to the precipitation record for this time. If growth banding preservation ceases at a certain precipitation threshold, then flow rerouting could be occurring, explaining the lack of banding. Additionally, samples could be collected from regions of the world where the seasonality of the climate should prevent banding from being preserved, and a statistical study made. However, this would be expensive in terms of conservation , with perhaps 50-100 samples from each region required to give a statistically significant data set.

f) Trace-element studies would provide insights into the transport of trace-elements onto speleothems and the nature of the banding. High resolution studies could determine whether luminescent inorganic minerals are present in the banding maxima, if multiple measurements could be made over an individual band. For a band of 0.1 mm width, a minimum resolution of 0.01 mm is required; recent developments in ion probe techniques will make such a study possible.

g) Additional records may be obtained from variations in banding intensity. The presence of the 11 year solar insolation cycle needs to be verified from multiple samples which contain a continuous banding record. Such preservation may not occur, and thus make verification impossible. Long term variations in intensity may correlate with variations in plant productivity, and may correlate with other palaeoclimate records. Banding does not need to be preserved for such a study, but changes in luminescence intensity for multiple samples deposited over the same time may give a record which correlates with other measures of palaeoclimate change.

h) The importance of organic matter in determining luminescence intensity also needs further investigation and does not require banding to be present. The relationship between luminescence intensity and colour can be studied, to determine whether the colouration (and thus organic matter concentration) of speleothems is related to luminescence. The source of this luminescence may also be investigated using trace element studies. Long term (100-10000 year) variations in trace element

concentrations, determined using standard electron probes or ICPMS techniques, may be correlated to luminescence intensity variations, to determine whether there is an organic or inorganic luminescence source.

BIBLIOGRAPHY

Aiken, G.R., 1985. *Humic Substances in soil, sediment and water: geochemistry, isolation and characterisation.* Wiley, New York. 694pp.

Alley, R.B., Meese, D.A., Shuman, C.A., Gow, A.J., Taylor, K.C., Grootes, P.M., White, J.W.C., Ram, M., Waddington, E.D., Mayewski, P.A., and Zielinski, G.A., 1993. Abrupt increase in Greenland snow accumulation at the end of the Younger Dryas event. *Nature*, 362:527-529.

Amthor, J.S., 1989. *Respiration and Crop productivity.* Springer-verlag, 215pp.

Atkinson, T.C., 1983. Growth mechanisms of speleothems in Castleguard Cave, Colombia Icefield, Alberta, Canada. *Arctic and Alpine Research*, 15:523-536.

Atkinson, T.C., Harmon, R.S., Smart, P.L., and Waltham, A.C., 1978. Palaeoclimate and geomorphic implications of ^{230}Th / ^{234}U dates on speleothems from Britain. *Nature*, 272:24-28.

Atkinson, T.C., Smart, P.L., and Andrews, J.N., 1984. Uranium series dates of speleothems from the Mendip Hills. I Rhino Rift, Charterhouse-on-Mendip. *Proceedings of the University of Bristol Speleological Society*, 17:55-69.

Atkinson, T.C., Lawson, T.J., Smart, P.L., Harmon, R.S., and Hess, J.W., 1986. New data on speleothem deposition and palaeoclimate in Britain over the last 40000 years. *Journal of Quaternary Science*, 1:67-72.

Atkinson, T.C., Briffa, K.R., and Coope, R., 1987. Seasonal palaeotemperatures in Britain during the last 22000 years, reconstructed using beetle remains. *Nature*, 325:587-592.

Baillie, M.G.L. and Munro, M.A.R., 1988. Irish tree-rings, Santorini and volcanic dust veils. *Nature*, 332:344-346.

Baker, A., Smart, P.L. and Ford, D.C., 1993a. Northwest European palaeoclimate as indicated by growth frequency variations of secondary calcite deposits. *Palaeogeography, palaeoclimatology, palaeoecology*, 100:291-301.

Baker, A., Smart, P.L., Edwards, R.L. and Richards, D.A., 1993b. Annual banding in a cave stalagmite. *Nature*, 364:518-520.

Baker, R.G., Mahler, L.J., Chumbley, C.A. and Van Zant, K.A., 1992. *Quaternary Research*, 37:379-389.

Bard, E., Hamelin, B., Fairbanks, R.G. and Zindler, A., 1990. Calibration of the ^{14}C timescale over the past 30,000 years using mass-spectrometric U-Th ages from Barbados corals. *Nature*, 345:405-410.

Barnola, J.M., Raynaud, D., Korotkevich, Y.S., and Lorius, C., 1987. Vostok ice core provides 160000-year record of atmospheric CO_2. *Nature*, 329:408-414.

Bastin, B., 1979. L'Annalyse pollinique des stalagmites. *Annales de la Sociétié Géologique Belgique*, 101:13-19.

Bastin, B. and Gewelt, M., 1986. Analyses pollinique et datation ^{14}C de concrétions stalagmitiques Holocènes: apports complémentaires des deux méthods. *Géographie Physique et Quaternaire*, 40:185-196.

Bastin, B., Quinif, Y., Dupuis, C. and Gascoyne, M., 1988. La sequence sedimentaire de la Grotte de Buhon (Belgique). *Annales de la Sociétié Géologique Belgique*, 111:51-60.

Behre, K.-E., 1989. Biostratigraphy of the last glacial period in Europe. *Quaternary Science Reviews*, 8:25-44.

Berger, A. and Loutre, M.F., 1991. Insolation values for the last 10 million years. *Quaternary Science Reviews*, 10:297-317.

Berner, R.A., 1980. *Early diagenesis: A theoretical approach*. Princetown university Press, Princetown. 250pp.

Birks, H.H., 1975. Studies in the vegetational history of Scotland, IV: Pine stumps in Scottish blanket peats. *Philosophical Transactions of the Royal Society, London, B*, 270:181-226.

Blackwell, B. and Schwarcz, H.P., 1986. U-series analyses of the lower travertine at Ehringsdorf, D.D.R.. *Quaternary Research*, 25:215-222.

Boto, K. and Isdale, P., 1985. Fluorescent bands in massive corals result from terrestrial fulvic acid inputs to nearshore zone. *Nature*, 315:396-397.

Boulton, G.S. and Jones, A.S., 1979. Stability of temperate ice caps and ice sheets resting on beds of deformable sediments. *Journal of Glaciology*, 24:29-43.

Bowen, D.Q., 1990. The last interglacial - glacial cycle in the British Isles. *Quaternary International*, 3/4:41-47.

Brandt, C.J., 1990. Simulation of the size distribution and erosivity of raindrops and throughfall drops. *Earth Surface Processes and Landforms*, 15:687-698.

Broecker, W.S., 1990. Salinity history of the northern Atlantic during the last deglaciation. *Palaeoceanography*, 5:459-467.

Broecker, W.S., Andree, J., Wolfi, W., Oeschger, H., Bonani, G., Peteet, D. and Kennett, J.P., 1988. The chronology of the last deglaciation: implications to the cause of the Younger Dryas event. *Paleoceanography*, 3:1-29.

Brook, G.A., Burney, D.A., and Cowart, J.B., 1990. Desert palaeoenvironmental data from cave speleothems with examples from the Chihuahuan, Somali, Chalbi and Kalahari deserts. *Palaeogeography, Palaeoclimatology, Palaeoecology*, 76:311-329.

Brunnacker, K., Jäger, K.-D., Hennig, G.J., Preuss, J., and Grün, R., 1983. Radiometrische untersuchungen zur datierung mitteleuropaischer travertinvarkommen. *Ethnographisch - Archäologische Zeitschrift*, 24:217-266.

Bryant, I.D., Holyoak, D.T. and Moseley, K.A., 1983. Late Pleistocene deposits at Brimpton, Berkshire, England. *Proceedings of the Geologists Association*, 94:321-343.

Buhmann, D. and Dreybrodt, W., 1985a. The kinetics of calcite dissolution and precipitaion in geologically relevant situations of karst areas: I Open System. *Chemical Geology*, 48:189-211.

Buhmann, D. and Dreybrodt, W., 1985b. The kinetics of calcite dissolution and precipitaion in geologically relevant situations of karst areas: II Closed System. *Chemical Geology*, 53:109-124.

Buhmann, D. and Dreybrodt. W., 1987. Calcite dissolution kinetics in the system H_2O-CO_2-$CaCO_3$ with the participation of foreign ions. *Chemical Geology*, 64:89-102.

Buyanovsky, G.A. and Wagner, G.H., 1983. Annual cycles of CO_2 level in soil air. *Soil Science Scociety of America Journal*, 47:1139-1145.

Catt, J.A., 1991. The Quaternary history and and glacial deposits of East Yorkshire. In: Ehlers, J., Gibbard, P.L. and Rose, J. (Editors), *Glacial Deposits in Great Britain and Ireland*. A.A. Balkema, Rotterdam. pp185-192.

Cerling, T.E., 1984. The stable isotopic composition of modern soil carbonate and its relationship to climate. *Earth and Planetary Science Letters*, 71:229-240.

Chen, J.H., Edwards, R.L. and Wasserburg, G.J., 1986. ^{238}U, ^{234}U and ^{232}Th in sea water. *Earth and Planetary Science Letters*, 80:241-251.

Chen, J.H., Edwards, R.L. and Wasserburg, G.J., 1992. Mass spectrometry and applications to uranium-series disequilibrium. In: Ivanovich, M. and Harmon, R.S. (Editors) *Uranium-series Disequilibrium*, Oxford Science Publications, pp174-206.

Cheng, L., 1977. Dynamic spreading of drops impacting on a solid surface. *Industrial Engineering and Chemical Process Design and Development*, 16:192-197.

Cherdyntsev, V.V., 1971. *Uranium 234*. Jerusalem: Israel Programme for Scientific Translations. pp234.

Chumbley, C.A., Baker, R.G. and Bellus III, E.A., 1990. *Science*, 249:272-274.

CLIMAP Project members, 1976. The surface of the ice-age earth. *Science*, 191:1131-1137.

CLIMAP Project members, 1981. Seasonal reconstruction of the earth's surface at the last glacial maximum. *Geological Society of Amrica Map Chart Serial.* MC-36.

CLIMAP Project members, 1984. The last interglacial ocean. *Quaternary Research*, 21:123-224.

COHMAP Members, 1988. Climate changes of the last 18,000 years: observations and model simulations. *Science*, 241:1043-1052.

Compton, R.G. and Daly, P.J., 1984. The dissolution kinetics of iceland spar single crystals. *Journal of Colloid and Interface Science*, 101:159-166.

Compton, R.G., Daly, P.J. and House, W.A., 1986. The dissolution of Iceland Spar crystals - the effect of surface morphology. *Journal of Colloid and Interface Science*, 113:12-20.

Coope, G.R., 1959. A Late Pleistocene insect fauna from Celford, Cheshire. *Proceedings of the Royal Society, London*, B, 151:70-86.

Coope, G.R., 1975. Climatic fluctuations in north-west Europe since the last Interglacial, indicated by fossil assemblages of Coleoptera. In: A.E. Wright and F. Moseley (Editors), *Ice Ages: Ancient and Modern.* Seel House Press, Liverpool, pp.153-168.

Coope, G.R. 1977. Fossil coleopteran assemblages as sensitive indicators of climatic changes during the last (Devensian) cold stage. *Philosophical Transactions of the Royal Society, London, B*, 280:313-340.

Crowley, T.J., 1989. Palaeoclimate perspectives on a greenhouse warming. In: Berger, A. et al (Editors), *Climate and Geosciences.* Kluwer, Netherlands, pp179-207.

Crowley, T.J. amd North, G.R., 1991. *Palaeoclimatology.* Oxford University Press, 339 pp.

Crowther, J., 1984. Soil CO_2 and weathering potentials in tropical karst terrain, penninsula Malaysia: A preliminary model. *Earth Surface Process and Landforms*, 9:397-407.

Curl, R.L., 1973. Minimum Diameter Stalagmites. *Bulletin of the National Speleological Society*, 35:1-9.

Dansgaard, W., Clausen, H.B., Gundestrup, N., Hammer, C.U., Johnsen, S.F., Kristinsdottir, P.M. and Reeh, N., 1982. A new Greenland deep ice core. *Science*, 218:1273-1277.

Dansgaard, W., Johnsen, S.J., Claussen, H.B., Dohl-Jensen, D., Gundestrup, N.S., Hammer, C.U., Hvidbeg, C.J., Steffensen, J.P., Sveinbjorndottir, A.E., Jouzel, J. and Bond, G., 1993. Evidence of general instability of past climate from a 250 kyr ice-core record. *Nature*, 364:218-220.

de Bievre, P., Lauer, K.J., Le Duigon, Y., Moret, H., Muschenborn, G., Spaepen, J., Spernol, A., Vaninbroukx, R. and Verdingh, V., 1971. The half-life of ^{234}U. In: Hurrell, M.L. (Editor), *Proceedings of the International Conference on Chemical Nuclear Data, Measurement and Applications*. Institute of Civil Engineers, London, pp221-225.

Denton, G.H. and Hughes, T.J., 1981. *The last great ice sheets*. Wiley, New York. pp484.

Derbyshire, E., 1987. A history of glacial stratigraphy in China. *Quaternary Science Reviews*, 6:310-314.

Dickinson, J.M., 1972. *Mines and t'Miners: A history of lead mining in Airedale, Wharfedale and Nidderdale*. 81pp.

Dorale, J.A., Gonzalez, L.A., Regan, M.K., Pickett, D.A., Murrell, M.T. and Baker, R.G., 1992. A high resolution record of Holocene climate change in speleothem calcite from Coldwater Cave, north-east Iowa. *Science*, 258:1626-1630.

Dorr, H. and Munnich, K.O., 1986. Annual variations of the ^{14}C content of soil CO_2. *Radiocarbon*, 28:338-345.

Dorr, H. and Munnich, K.O., 1989. Downward movement of soil organic matter and its influence on trace-element transport (^{210}Pb, ^{137}Cs). *Radiocarbon*, 31:655-663.

Drake, J.J., 1980. The effect of soil activity on the chemistry of carbonate groundwater. *Water Resources Research*, 16:381-386.

Drake, J.J., 1983. The effects of geomorphology and seasonality on the chemistry of carbonate groundwaters. *Journal of Hydrology*, 61:223-226.

Drake, J.J. and Wigley, T.M.L., 1975. The effect of climate on the chemistry of carbonate groundwater. *Water Resources Research*, 11:958-962.

Drever, J.I., 1982. *The geochemistry of Natural Waters*. New Jersey: Prentice-Hall. 388pp.

Dreybrodt, W., 1980. Deposition of calcite from thin films of calcareous solutions and the growth of speleothems. *Chemical Geology*, 29:89-105.

Dreybrodt, W., 1981. The kinetics of calcite precipitation from thin films of calcareous solutions and the growth of speleothems: revisited. *Chemical Geology*, 32:237-245.

Dreybrodt, W., 1982. A possible mechanism for growth of calcite speleothems without participation of biogenic CO_2. *Earth and Planetary Science Letters*, 58:293-299.

Dreybrodt, W., 1988. *Processes in Karst Systems: Physics, Chemistry and Geology.* Springer-Velag, Berlin, 288pp.

Dreybrodt, W. and Lamprecht, G., 1981. Computer-simulation des wachstums von stalagmiten. *Die Hohle,* 31:11-21.

Dreybrodt, W. and Franke, H.W., 1987. Wachstumsgeschwindigkeiten und durchmesser von kerzenstalagmiten. *Die Hohle*, 38:1-6.

Dreybrodt, W., Buhmann, D., Michaelis, J. and Usdowski, E., 1992. Geochemically controlled calcite precipitation by CO_2 outgassing: Field measurements of precipitation rates in comparison to theoretical predictions. *Chemical Geology*, 97:285-294.

Dromgoole, E.L. and Walter,L.M., 1990. Iron and manganese incorporation into calcite: effects of growth kinetics, temperature and solution chemistry. *Chemical Geology,* 81:311-336.

Dugmore, A.J., 1989. Icelandic volcanic ash in Scotland. *Scottish Geographical Magazine*, 105:168-172.

Dulinski, M. and Rozanski, K., 1990. Formation of C-13 C-12 isotope ratios in speleothems - a semidynamic model. *Radiocarbon*, 32:7-16.

Edwards, R.L., 1988. High precision thorium-230 ages of corals and the timing of sea level fluctuations in the late Quaternary. *Unpublished PhD thesis, California Institute of Technology.*

Edwards, R.L. and Gallup, C.D., 1993. Dating the Devils Hole calcite vein. *Science*, 259:1626.

Edwards, R.L., Chen, J.H. and Wasserburg, G.J. 1987. ^{238}U-^{234}U-^{232}Th-^{230}Th systematics and the precise measurement of time over the last 500000 years. *Earth and Planetary Science Letters*, 81:175-192.

Edwards, R.L., Beck, J.W., Burr, G.S., Donahue, D.J., Chappell, J.M.A., Bloom, A.L., Druffel, E.R.M. and Taylor, F.W., 1993. A large drop in atmospheric $^{14}C/^{12}C$ and reduced melting in the Younger Dryas, documented with ^{230}Th ages of corals. *Science*, 260:962-968.

Ehlers, J., Gibbard, P. and Rose, J., 1991. Glacial deposits of Britain and Europe: general overview. In: Ehlers, J., Gibbard, P. and Rose, J. (Editors), *Glacial Deposits of Great Britain and Ireland.* A.A. Balkema, Rotterdam, pp493-502.

Ek, C. and Gewelt, M., 1984. Carbon dioxide in cave atmospheres. New results in Belgium and comparison with some other countries. *Earth Surface Processes and Landforms,* 10:173-187.

Fairbanks, R., 1989. A 17,000 year glacio-eustatic sea level record: Influence of glacial melting rates on the Younger Dryas event and deep-ocean circulation. *Nature,* 342:637-642.

Fish, J.E., 1978. Karst hydrology and geomorphology of the Sierra de El Abra and the Valles-San Luis Potosi Region, Mexico. *Unpublished PhD thesis, McMaster University.*

Fishbeck, R. and Muller, G., 1971. Monohydrocalcite, hydromagnesite, nesqueharite, dolomite, aragonite and calcite in speleothems of the Frankische Scheiz, West Germany. *Contributions to Mineralogy and Petrology,* 33:87-92.

Ford, D.C., (1979). A reveiw of alpine karst in the southern Rocky Mountains of Canada. *Bulletin of the National Speleological Society,* 41:53-65.

Ford, D.C. and Williams, P., 1989. *Karst Geomorphology and Hydrology.* Unwin-Hyman, London. 601pp.

Ford, T.D., Gascoyne, M., and Beck, J.S., 1983. Speleothem dates and Pleistocene chronology in the Peak District of Derbyshire. *Transactions of the British Cave Research Association,* 10:103-113.

Friedrich, H., 1981. The hydrochemistry of recharge in the unsaturated zone with special reference to the carboniferous limestone of the Mendip Hills. *Unpublished PhD thesis, University of Bristol.*

Gams, I., 1981. Contribution to morphometrics of stalagmite. *Proceedings of the 8th International Congress of Speleology,* pp276-278.

Gascoyne, M. 1977a. Uranium series dating of speleothems: an investigation of technique, data processing and precision. *Department of Geology, McMaster University, Technical Memo 77-4.*

Gascoyne, M., 1977b. Trace element geochemistry of speleothems. *Proceedings of the 7th International Congress of Speleology,* pp205-207.

Gascoyne, M., 1979. Pleistocene climates determined from stable isotope and geochronologic studies of speleothem. *Unpublished PhD Thesis, McMaster University.*

Gascoyne, M. 1983. Trace element partition coefficients in the calcite-water system and their palaeoclimate significance in cave studies. *Journal of Hydrology*, 61:215-222.

Gascoyne, M. 1992. Palaeoclimate determination from cave calcite deposits. *Quaternary Science Reviews*, 11:609-632.

Gascoyne, M., Schwarcz, H.P. and Ford, D.C., 1978. Uranium series dating and stable isotope studies of speleothems: Part One. Theory and technique. *British Cave Research Group Transactions*, 5:91-111.

Gascoyne, M., Benjamin, G.J., Ford, D.C. and Schwarcz, H.P., 1979. Sea-level lowering during the Illinoain glaciation: Evidence from a Bahama 'blue hole'. *Science*, 205:806-808.

Gascoyne, M., Currant, A., and Lord, T.C., 1981. Ipswichian fauna of Victoria Cave and the marine palaeoclimatic record. *Nature*, 294:652-654.

Gascoyne, M., Schwarcz, H.P., and Ford, D.C., 1983. Uranium series ages of speleothems from North West England: correlation with Quaternary climate. *Philosophical Transactions of the Royal Society Series B*, 301:143-164.

Gerbaud, A., Andre, M., and Richaud, C., 1977. Gas exchange and nutrition patterns during the life cycle of an artificial wheat crop. *Physiologia Plantarum*, 7:471-478.

Gewelt, M., 1985. Cinétique du concrétionnement dans quelques grottes Belges: apport des datations ^{14}C et ^{230}Th / ^{234}U. *Annales de la Sociétié Géologique Belgique*, 108:267-73.

Gewelt, M. and Juvigne, E., 1986. Les téphra de Remouchamps, un nouveau marqueur stratigraphique dans le Pléistocène supérieur daté par ^{230}Th / ^{234}U dans des concrétions stalagmitiques. *Annales de la Sociétié Géologique Belgique*, 109:489-497.

Gewelt, M., Scharcz, H.P., and Szabo, B.J., in prep. ^{230}Th / ^{234}U and ^{14}C dating of speleothems from Scladina Cave.

Geyh, M.A., 1971. Zeitliche abrenzung von klimaanderungen mit 14C-daten von kalksinter und organischen substanzen. *Beih. geol. Jahr.*, 98:15-22.

Geyh, M.A., 1980. Holocene sea-level history: case study of statistical evaluation of ^{14}C dates. *Radiocarbon*, 22:695-704.

Godwin, H., 1975. *The History of the British Flora*. Cambridge University Press, Cambridge, 541pp.

Gordon, D. 1987. The Pleistocene of the Mendip region: aspects of the absolute dated, faunal and sediment records. *Unpublished PhD thesis, University of Bristol.*

Gordon, D. and Smart, P.L., 1984. Comments on 'Speleothem, travertines and palaeoclimate' by Hennig, G.J., Grün, R. and Brunnaker, K.. *Quaternary Reasearch*, 22:144-147.

Gordon, D., Smart, P.L., Ford, D.C., Andrews, J.N., Atkinson, T.C., Rowe, P.J. and Christopher, N.J., 1989. Dating of Late Pleistocene interglacial and interstadial periods in the United Kingdom from speleothem growth frequency. *Quaternary Research*, 31:14-26.

Gough, J.W., 1967. *The Mines of Mendip*. David and Charles, Newton Abbot, 269pp.

Green, H.S., 1984. *Pontnewyyd Cave*. National Museum of Wales, Cardiff, 227pp.

Grüger, E., 1990. Palynostratigraphy of the last interglacial / glacial cycle in Germany. *Quaternary International*, 3/4:69-79.

Grün, R., Brunnacker, K., and Hennig, G.J., 1982. 230Th / 234U - daten mittel- und jungpleistozäner travertine im raum Stuttgart. *Jahresberichte und Mitteilungen Oberrhanischen Geologischen Vereins, N.F.*, 64:201-211.

Guiot, J., Pons, A., Beaulieu, J.-L., and Reille, M., 1989. A 140000 year continental climate reconstruction from two European pollen records. *Nature*, 338:309-313.

Hammer, C.U., Clausen, H.B. and Dansgaard, W., 1980. Greenland ice sheet evidence of postglacial volcanism and its climatic impact. *Nature*, 288:230-233.

Hansen, G.K. and Jensen, C.R., 1977. Growth and maintainance respiration in whole plants, tops and roots of *Lolium multiflorum*. *Physiologia Plantarum*, 39:155-164.

Harlow, F.H. and Shannan, J.P., 1967. The splash of a liquid drop. *Journal of Applied Physics*, 38:3855-3866.

Harmon, R.S., 1975. Late Pleistocene palaeoclimates in North America as inferred from isotopic variations in speleothems. *Unpublished PhD thesis, McMaster University*.

Harmon, R.S., White, W.B., Drake, J.J. and Hess, J.W., 1975. Regional hydrochemistry of north American carbonate terrains. *Water Resources Research*, 11:963-967.

Harmon, R.S., Thompson, P., Schwarcz, H.P. and Ford, D.C., 1978. Late Pleistocene palaeoclimates of North America as inferred from stable isotope studies of speleothems. *Quaternary Research*, 9:54-70.

Harmon, R.S., Glazek, J., and Novak, K., 1980. ^{230}Th / ^{234}U dating of travertine from the Bilzingsleben archaeological site. *Nature*, 284:132-135.

Harmon R.S., Atkinson, T.C., and Atkinson, J.L., 1983. The mineralogy of Castleguard Cave, Columbia Icefields, Alberta, Canada. *Arctic and Alpine Research*, 15:503-516.

Hedges, R.E.M., 1981. Radiocarbon dating with an accelerator: review and preview. *Archaeometry*, 23:3-18.

Heijnis, H. and van der Plicht, J., 1992. Uranium / thorium dating of Late Pleistocene peat deposits in NW Europe, uranium / thorium systematics and open-system behaviour of peat layers. *Chemical Geology (Isotope Geoscience)*, 94:161-171.

Hendy, C., 1971. The isotopic geochemistry of speleothems I. The calculation of the effects of different modes of formation on the isotope composition of speleothems and their applicability as palaeoclimate indicators. *Geochimica Cosmochimica Acta*, 35:801-824.

Hendy, C. and Wilson, A.T., 1968. Palaeoclimatic data from speleothem. *Nature*, 216:48-51.

Hennig, G.J., 1979. Beiträge zur Th-230 / U-234 altersbestimmung von höhlensintern sowie ein vergleich der erzielten ergebnisse mit denen anderer absolutdatierungsmethoden. *Unpublished PhD Thesis, University of Cologne.*

Hennig, G.J., Herr, W., Weber, E. and Xirotiris, N.I., 1982. Petralona Cave dating controversy. *Nature*, 299:281-282.

Hennig, G.J., Grun, R. and Brunnacker, K., 1983. Speleothems, travertines and palaeoclimate. *Quaternary Research*, 29:1-29.

Hermann, J.S. and Lorah, M.M., 1988. Calcite precipitation rates in the field: measurement and prediction for a travertine depositing stream. *Geochimica Cosmochimica Acta*, 52:2347-2355.

Hill, C.A. and Forti, P. 1986. *Cave Minerals of the World.* Huntsville, USA: National Speleological Society. 238pp.

Hoare, P.G., 1991. Late Midlandian glacial deposits and glaciations in Ireland and the adjacent offshore regions. In: Ehlers, J., Gibbard, P.L. and Rose, J. (Editors), *Glacial Deposits in Great Britain and Ireland*. A.A. Balkema, Rotterdam. pp69-78.

Holland, H.D., Kirsipu, T.W., Huebner, J.S. and Oxburgh, U.M., 1964. On some aspects of the chemical evolution of cave waters. *Journal of Geology*, 72:36-67.

Irwin, D.J. and Knibb, A.J., 1977. *Mendip Underground.* Mendip Publishers, Somerset. 212pp.

Isdale, P., 1984. Fluorescent bands in massive corals record centuries of coastal rainfall. *Nature*, 310:578-579.

Jacobson, R.L. and Langmuir, D., 1974. Dissociation constant of calcite and $CaHCO_3^+$ from 0° to 50 °C. *Geochimica Cosmochimica Acta*, 38:301-318.

Jaffey, A.H., Flynn, K.F., Glendenin, L.W., Bentley, W.C., and Essling, A.M., 1971. Precision measurements of half-lives and specific activities of ^{235}U and ^{238}U. *Physics Review C*, 4:1889-1906.

Jouzel, J., Lorius, C., Petit, J.R., Genthon, C., Barkov, N.I., Kotlyakov, V.M. and Petrov, V.M., 1987. Vostok ice core: A continuous isotope temperature record over the last climatic cycle (160,000 years). *Nature*, 329:403-408.

Kane, D.L. and Stein, J., 1984. Field evidence of groundwater recharge in interior Alaska. In: *Proceedings of the 4th International Conference on Permafrost.* National Academy of Sciences, Washington, pp 572-577.

Kashiwaya, K., Atkinson, T.C. and Smart, P.L., 1991. Periodic variations in Late Pleistocene speleothem abundance in Britain. *Quaternary Research*, 35:190-196.

Kaufman, A., 1993. An evaluation of several methods of determining $^{230}Th/U$ ages in impure carbonates. Geochimica et Cosmochimica Acta, 57, 2303-2317

Kendall, A.C. and Broughton, P.L., 1978. Origin of fabrics in speleothems of columnar calcite crystals. *Journal of Sedimentary Petrology*, 48:519-538.

King, J.W., 1973. Solar radiation changes and the weather. *Nature*, 245:443-446.

Klein, R., Loya, Y., Gvirtzman, G., Isdale, P.J., and Susic, M., 1990. Seasonal rainfall in the Sinai Desert during the late Quaternary inferred from fluorescent bands in fossil corals. *Nature*, 345:145-147.

Köppen, W. and Geiger, R., 1954. *Klima der Erde.* Justus Perthus, Darnstadt.

Kronberg, C. and Mejdahl, V., 1990. Thermoluminescence dating of Eemian and Early Weichselian deposits in Denmark. *Quaternary International*, 3/4:93-99.

Kukla, G., 1987. Loess stratigraphy in central China. *Quaternary Science Reviews*, 6:191-219.

Kukla, G, Heller, F., Ming, L.-X., Chun, X.-T., Sheng, L.-T. and Sheng, A.-Z., 1988. Pleistocene climates in China dated by magnetic susceptibility. *Geology*, 16:811-814.

Kutzbach, J.E. and Wright, H.E., 1985. Simulation of the climate of 18,000 year BP: Results from the North American / North Atlantic / European sector and comparison with the geologic record. *Quaternary Science Reviews*, 4:147-187.

Kyle, H.L., Ardanuy, P.E. and Hurley, E.J., 1985. The status of Nimbus-7 earth-radiation-budget data set. *Bulletin of the American Meteorological Society*, 66:1378-1388.

Latham, A.G. and Schwarcz, H.P., 1992. The Petralona hominid site: uranium-series re-analysis of 'layer-10' calcite and associated palaeomagnetic analysis. *Archaeometry*, 34:135-140.

Latham, A.G., Schwarcz, H.P., Ford, D.C., and Pearce, G.W., 1979. Palaeomagnetism of stalagmite deposits. *Nature*, 280:383-385.

Lauritzen, S.-E., Ford, D.C. and Schwarcz, H.P., 1986. Humic substances in a speleothem matrix. *Proceedings of the 9th International congress of Speleology*, pp77-79.

Lawson, T.J., 1988. *Caves of Assynt.* Grampian Speleological Society Occasional Publication Number 6, 90pp.

Lehman, S.J. and Keigwin, L.D., 1992. Sudden changes in North Atlantic circulation during the last deglaciation. *Nature*, 356:757-762.

Li, W.-X., Lundberg, J., Dickin, A.P., Ford, D.C., Schwarcz, H.P., McNutt, R., and Williams, D., 1989. High precision mass-spectrometric uranium-series dating of cave deposits and implication for palaeocliamte studies. *Nature*, 339:334-336.

Liu, T.S., An, Z., Yuan, B., and Han, J., 1985. The loess-palaeosol sequence in China and climatic history. *Episodes*, 8:21-41.

Lorius, L., Jouzel, J., Ritz, C., Merlivat, L., Batkov, N.I., Korotkevich, Y.S. and Kotlyakov, V.M., 1985. A 150,000 year climatic record from Antarctic ice. *Nature*, 316:591-596.

Lounsbury, M. and Durham, R.W., 1971. The alpha half-life of 234-U. In: Hurrell, M.L. (Editor), *Proceedings of the International Conference on Chemical Nuclear Data, Measurement and Applications, Canterbury.* Institute of Civil Engineers, London, pp215-219.

Lu, Y.C., Prescott, J.R., Robertson, G.B. and Hutton, J.T., 1987. Thermoluminescence dating of the Malan loess at Zhaitang, China. *Geology*, 15:603-605.

Ludwig, K.R., Simmons, K.R., Szabo, B.J., Winograd, I.J., Landwehr, J.M., Riggs, A.C. and Hoffman, R.J., 1992. Mass spectrometric Th-230-U-234-U-238 dating of the Devils Hole calcite vein. *Science*, 258:284-287.

Lundberg, J., 1990. U-series dating of carbonates by mass spectrometry with examples of speleothem, coral and shell. *Unpublished PhD Thesis, McMaster University.*

Mahon, J.D., 1977. Respiration and the energy requirement for nitrogen fixation in nodulated pea roots. *Plant physiology*, 60:817-821.

Manley, G., 1974. Central England temperatures: monthly means 1659-1973. *Quaterly Journal of the Royal Meteorological Society*, 100:389-405.

Martinson, D.G., Pisias, N.G., Hays, J.D., Imbrie, J., Morre, T.C., and Shackleton, J., 1987. Age dating and the orbital theory of the ice ages: development of a high-resolution 0 to 300000 year chronostratigraphy. *Quaternary Research*, 27:1-29.

Massimino, D., Andre, M., Richaud, C., Daguenet, A., Massimino, J., and Vivoli, J., 1981. The effect of a day at low irradience of a maize crop: I Root respiration and uptake of N, P and K. *Physiologia Plantarum*, 51:150-155.

Meadows, J.W., Armani, R.J., Callis, E.L., and Essling, A.M., 1980. Half-life of ^{230}Th. *Physics Review C*, 22:750-754.

Meyer, H.J., 1984. The influence of impurities on the growth rate of calcite. *Journal of Crystal Growth*, 66:639-646.

Milankovitch, M., 1941. Canon of insolation and the ice age problem (in Yugoslavian). *K. Serb. Acad. Beorg.* Special Publication 132. Israel program for scientific translation, Jerusalem.

Miller, T.E., 1982. Hydrochemistry, hydrology and morphology of the Caves Branch karst, Belize. *Unpublished PhD thesis, McMaster University.*

Miotke, F.-D. 1974. Carbon dioxide and the soil atmosphere. *Abh. Karst-u. Hohlenkunde, A9.* Munich, 52pp.

Mockford, D.P. and Male, A.J., 1974. *Caves of the Bristol Region.* 20pp.

Mutchler, C.K. and Larson, C.L., 1971. Splash amounts from waterdrop impact on a smooth surface. *Water Resources Research*, 7:195-200.

Nishimura, S., Miao, J. and Sasajima, S., 1984. Thermoluminescent dating of the Luochuan loess sequence. In: Sasojima, S. and Wang, Y.Y. (Editors), *Recent Research on Loess in China.* Kyoto University, Japan, pp69-78.

O'Brien, B.J., 1956. "After-glow" of cave calcite. *Bulletin of the National Speleological Society*, 18:50-51.

Olsen, L., 1990. Weichselian till stratigraphy and glacial history of Finnmarksvidda, North Norway. *Quaternary International*, 3/4:101-108.

Orr, P.C., 1952. *Excavations in Moaning Cave.* Santa Barbara Museum of Natural History Bulletin No. 1. 19pp.

Osmond, J.K. and Ivanovitch, M., 1992. Uranium-series mobilization and surface hydrology. In: Ivanovitch, M. and Harmon, R.S. (Editors), *Uranium-Series Disequilibrium*. Oxford Science Publishers, pp259-290.

Pearce, F., 1993. Pinatubo points to vulnerable climate. *New Scientist*, 1878:7.

Pedone, V.A., Cercone, K.R. and Burruss, R.C., 1990. Activators of photoluminescence in calite: evidence from high-resolution, laser-excited luminescence spectroscopy. *Chemical Geology*, 88:183-190.

Pennington, W., Haworth, E.Y., Bonny, A.P. and Lishman, J.P., 1972. Lake sediments in Northern Scotland. *Philosophical Transactions of the Royal Society, London*, B, 264:191-294.

Pentecost, A., 1992. Carbonate chemistry of surface waters in a temperate karst region: the southern Yorkshire Dales, U.K. *Journal of Hydrology*, 139:211-232.

Pisias, N.G., Martinson, D.G., Moore, T.C., Jr., Shackleton, N.J.,Prell, W. Hays,J. and Boden, G., 1984. High resolution stratigraphic correlation of benthic oxygen isotopic records spanning the last 300 000 years. *Marine Geology*, 56:119-136.

Pitty, A.F., 1966. An approach to the study of karst water. *University of Hull, Occasional Papers in Geograpy, 5.*

Pitty, A.F., 1974. Karst water studies in and around Ingleborough Cavern. In: Waltham, A.C. (Editor), *Limestone and caves of North West England.* David and Charles, Newton Abbott. pp127-139.

Plummer, L.N., Wigley, T.M.L., and Parkhurst, D.L., 1978. The kinetics of calcite dissolution in the CO_2-water systems at 5 to 60°C and 0.0 to 1.0 atm CO_2. *American Journal of Science*, 278:179-216.

Plummer, L.N., Parkhurst, D.L. and Wigley, T.M.L., 1979. Criticla review of the kinetics of calcite dissolutionand precipitation. In: Jenne, E.A. (Editor), *Chemical modelling in aqueous systems.* American Chemical Society, Washington.

Pons, A., Campy, M. and Guiot, J., 1989. The last climatic cycle in France: the diversity of records. *Quaternary International*, 3/4:49-55.

Poole, D.K. and Miller, P.L., 1982. CO_2 flux from 3 arctic tundra types in north-central Alaska. *Arctic and Alpine Research*, 14:27-32.

Prell, W.L. and Kutzbach, J.E., 1987. Monsoon variability over the past 150,000 years. *Journal of Geophysical Research*, 92:8411-8425.

Price, E., 1984. *The Bath Freestone Workings.* The Resurgence Press, Bath. 74pp.

Proctor, C.J. and Smart, P.L., 1989. A new survey of Kent's Cavern, Devon. *Proceedings of the University of Bristol Speleological Society, 19:422-429.*

Proctor, C.J. and Smart, P.L., 1991. A dated cave sediment record of Pleistocene transgressions on Berry Head, South West England. *Journal of Quaternary Science*, 6:233-244.

Pujol,C. and Turon, J.L., 1986. Comparison des cycles climatiques en domaine marin et continental entre 130000 et 28000 ans b.p. dans l'hémisphère Nord. *Bulletin de l'Association Français pour l'Etude du Quaternaire*, 1-2:17-25.

Quinif, Y., 1986. Datations U-Th dans la grotte de Ramioul. *Bulletin des Chercheurs de Wallonie*, 27:109-120.

Quinif, Y., 1989. Datation d'un interstade au sein de la dernière glaciation. *Speleochronos*, 1:23-28.

Ran, E.T.H., Bohncke, S.J.P., van Huissteden, K.J. and Vandenberghe, J., 1990. Evidence of episodic permafrost conditions during the Weichselian Middle Pleniglacial in the Hengelo Basin (The Netherlands). *Geologie en Mijnbouw*, 69:207-218.

Reddy, M.M. and Nancollas, G.H., 1970. The crystallisation of calcium carbonate I. *Journal of Colloid and Interface Science*, 36:166-171.

Reddy, M.M. and Nancollas, G.H., 1971. The crystalisation of calcium carbonate II. *Journal of Colloid and Interface Science*, 37:824-829.

Reddy, M.M., Plummer, L.N., and Busenberg, E., 1981. Crystal growth of calcite from bicarbonate solutions at constant pH and 25°C: a test of the calcite dissolution model. *Geochimica Cosmochimica Acta*, 45:1281-1289.

Rice, R.J. and Douglas, T., 1991. Wolstonian glacial deposits and glaciation in Britain. In: Ehlers, J., Gibbard, P.L. and Rose, J. (Editors), *Glacial Deposits in Great Britain and Ireland*. A.A. Balkema, Rotterdam. pp25-36.

Richards, D.A., 1987. The influence of post-war land-use change on the total hardness of the waters of the Cheddar Falls, Somerset. *Unpublished Undergraduate Dissertation, University of Bristol.*

Richards, D.A., Smart, P.L. and Edwards, R.L., in prep. Sea levels for the last glacial period constrained using ^{230}Th ages of submerged speleothems. *Submitted to Nature.*

Rind, D. and Peeteet, D., 1985. Terrestrial conditions at the last glacial maximum and CLIMAP sea-surface temperature estimates: Are they consistent? *Quaternary Research*, 24:1-22.

Rosholt, J.N. and Antal, P.S., 1962. Evaluation of the Pa^{231}/U-Th^{230}/U method for dating Pleistocene carbonate rocks. *USGS Professional Paper*, 450-E:108-111.

Rousseau, D-D. and Puisségur, J-J., 1990. A 350000 year climatic record from the loess sequence of Achenheim, Alsace, France. *Boreas*, 19:203-216.

Rowe, P., Atkinson, T.C., and Jenkinson, R.D.S., 1989. Uranium series dating of cave deposits at Creswell Crags Gorge, England. *Cave Science*, 16:3-17.

Sarnthein., M. and Tiedeman, R., 1990. Younger Dryas style cooling events at glacial terminations I-VI at ODP site 658: associated benthic $\delta^{13}C$ anomalies constrain meltwater types. *Paleoceanography*, 5:1041-1055.

Schwarcz, H.P., 1980. Absolute age determination of archaeological sites by uranium series dating of travertines. *Archaeometry*, 22:3-24.

Schwarcz, H.P. and Younge, C., 1983. Isotopic composition of a palaeowater as inferred from speleothem and its fluid inclusion. In: *Palaeoclimates and palaeowaters: a collection of environmental isotope studies*, IAEA, Vienna. pp115-133.

Schwarcz, H.P., Harmon, R.S., Thompson, P., and Ford, D.C., 1976. Stable isotope studies of fluid inclusions in speleothems and their palaeoclimatic significance. *Geochimica Cosmochimica Acta*, 40:657-665.

Schwarcz, H.P., Grun, R., Latham, A.G., Mania, D. and Brunnacker, K., 1988. The Bilzingsleben archaeological site; new dating evidence. *Archaeometry*, 30:5-17.

Shackleton, N.J. 1969. The last interglacial in the marine and terrestrial records. *Proceedings of the Royal Society, London, B*, 174:135-154.

Shackleton, N.J. 1977. The oxygen isotope stratigraphic record of the Late Pleistocene. *Philosophical Transactions of the Royal Society, London*, B, 280:169-179.

Shackleton, N.J., 1993. Last interglacial in Devils Hole. *Nature*, 362:596.

Shackleton, N.J. and Opdyke, N.D., 1973. Oxygen isotope and palaeomagnetic stratigraphy of equatorial pacific core V28-238: Oxygen isotope temperatures and ice volume on a 100,000 and 1,000,000 year scale. *Quaternary Research*, 3:39-55.

Sharp, M., Tison, J-L. and Fierens, G., 1990. Geochemistry of subglacial calcites: implications for the hydrology of the basal water film. *Arctic and Alpine Research*, 22:141-152.

Shennan, I., 1979. Statistical evaluation of sea-level data. In, Tooley, M. (Editor), *I.G.C.P. Project 61, Sea Level Changes Bulletin*. Durham, pp6-11.

Shopov, Y.Y., Dermendjiev, V. and Buykliev, G., 1989. Investigation on the variations of the climate and solar activity by a new method - Ilmza of cave flowstone from Bulgaria. *Proceedings of the 10th International Congress of Speleology*, 95-97.

Shopov, Y.Y., Dermendjiev, V. and Buykliev, G., 1990. Microzonality of luminescence of cave flowstoones as a new direct index of solar activity. *Comptes Rendus de l'Academie Bulgare des Sciences*, 43:9-12.

Shopov, Y.Y., Dermendjiev, V. and Buykliev, G., 1991. A new method for dating of natural materials with periodical macrostructures by autocalibration and first application for study of the solar activity in the past. *Porceedings of the International Conference on Environmental Changes in Karst Areas, Pavoda, Italy.* pp17-22.

Shusen, Z., Minglin, L. and Quangsheng, Q., 1988. The U-series ages of speleothem in karst caves in Eastern China. In: *IAH 21st Congress: Karst hydrogeology and karst environmental protection.* pp241-247.

Shuster, E.T. and White, W.B., 1971. Seasonal fluctuations in the chemistry of limestone springs: a possible means of characterising carbonate aquifers. *Journal of Hydrology*, 14:93-128.

Simmons, I.G., Dimbleby, G.W., and Grigson, C., 1981. The Mesolithic. In: Simmons, I.G. and Tooley, M.J. (Editors) *The environment in British Prehistory.* Duckworth, London. pp82-124.

Simsnek, J. and Suarez, D.L., 1993. *Modelling of* CO_2 transport and production in soil, 1. Model development. *Water Resources Research*, 29:487-498.

Smart, C.C., 1983. The hydrology of the Castleguard karst, Columbia Icefield, Alberta, Canada. *Arctic Alpine Research*, 15:471-486.

Smart, P.L. and Friedrich, H., 1987. Water movement and storage in the unsaturated zone of a maturely karstified aquifer, Mendip Hills, England. *Proceedings of the Conference on Environmental Problems in Karst Terrains and their Solution*, Bowling Green, Kentucky, pp57-87.

Smart, P.L. and Richards, D., 1992. Age estimates for the late Quaternary sea-stands. *Quaternary Science Reviews*, 11:687-696.

Smith, D.I. and Mead, D.G., 1962. The solution of limestone. *Proceedings of the University of Bristol Speleological Society*, 9:188-211.

Smith, D.I. and Atkinson, T.C., 1976. The erosion of limestone. In: Ford, T.D. and Cullingford, C.H.D. (Editors), *The Science of Speleology*, Academic Press, London, pp151-177.

Solomon, D.K. and Cerling, T.E., 1987. The annual CO_2 cycle in a montane soil: observations, modelling and implications for weathering. *Water Resources Research*, 23:2257-2265.

Spaulding, W.G., 1991 Pluvial climatic episodes in North America and North Africa: types and correlation with global climate. *Palaeogeography, Palaeoecology, Palaeoclimatology*, 84:217-227.

Speleological Group, Rodway School, Bristol, 1973. *Caves of the Avon Gorge Part Two.* 76pp.

Stenner, R.D., 1973. A study of the hydrology of GB Cave, Charterhouse-on-Mendip. *Proceedings of the University of Bristol Speleological Society*, 13:171-226.

Stringer, C.B., Current, A.P., Schwarcz, H.P. and Collcutt, S.N., 1986. Age of Pleistocene faunas from Bacon Hole, Wales. *Nature*, 320:59-62.

Stumm, W. and Morgan, J.J., 1981. *Aquatic chemistry.* Wiley, New York. pp780.

Stuttard, M.J., 1990. Formation and control of single water drops for laboratory experiments. *British Geomorphological Research Group Technical Monograph.*

Suarez, D.L. and Simsnek, J., 1993. Modelling of CO_2 transport in soil, 2. Parameter selection, sensitivity analysis and coamparison of model predictions to field data. *Water Resources Research*, 29:499-514.

Sutcliffe, A.J. and Currant, A.P., 1984. Minchin Hole Cave. In: Bowen, D.Q. and Henry, A. (Editors), *Field Guide to Wales: Gower, Preseli, Fforest Fawr.* Quaternary Research Association, Cambridge, pp 33-37.

Sutcliffe, A.J., Lord, T.C., Harmon, R.S., Ivanovich, M., Rae, A. and Hess, J.W., 1985. Wolverine in Northern England at about 83000 years b.p.: faunal evidence for climatic change during isotope stage 5. *Quaternary Research*, 24:73-86.

Sutherland, D.G., 1991. Late Devensian glacial deposits and glaciations in Scotland and the adjacent offshore region. In: Ehlers, J., Gibbard, P.L. and Rose, J. (Editors), *Glacial Deposits in Great Britain and Ireland*. A.A. Balkema, Rotterdam. pp53-60.

Taylor, K.C., Lamorey, G.W., Doyle, G.A., Alley, R.B., Grootes, P.M., Mayewski, P.A., White, J.W.C. and Barlow, L.K., 1993. The 'flickering switch' of late Pleistocene climate change. *Nature*, 361:432-436.

Thompson, P., 1973. Speleochronology and Late Pleistocene climates. *Unpublished PhD Thesis, McMaster University.*

Thompson, P., Schwarcz, H.P., and Ford, D.C., 1976. Stable isotope geochronology, geothermometry and geochronology of speleothems from West Virginia. *Geological Society of America Bulletin*, 87:1730-1738.

Tooley, M.J., 1982. Sea level changes in northern Europe. *Proceedings of the Geologists' Association*, 93:43-51.

Trainer, F.W. and Heath, R.C., 1976. Bicarbonate content of groundwater rock in eastern North America. *Journal of Hydrology*, 31:37-55.

Trudgill, S.T., Laidlaw, I.M.S. and Smart, P.L., 1980. Soil water residence times and solute uptake on a dolomite bedrock - preliminary results. *Earth Surface Processes*, 5:91-100.

Van Vliet-Lanoe, B., 1990. Dynamics and extent of the Weichselian permafrost in western Europe (substage 5e to stage 1). *Quaternary International*, 3/4:109-113

Veum, T., Jansen, E., Arnold, M., Bayer, I. and Duplessy, J-C., 1992. Water mass exchange between the north Atlantic and the Norwegian Sea during the past 28,000 years. *Nature*, 356:783-785.

Villar, E., Bonet, A., Diaz-Caneja, B., Fernandez, P.L., Gutierrez, I., Quindos, L.S., Solana, J.R. and Soto, J., 1985. Natural evolution of percolation water in Altamira Cave. *Cave Science*, 12:21-24.

Wels, G.L., 1983. Late glacial circulation over central North America revealed by aeolian features. In: Street-Perrott, A., Beran, M. and Ratcliffe, R., (Editors), *Variations in the Global Water Budget.* D. Reidel, Netherlands, pp317-330.

White, W.B., 1976. Cave minerals and speleothems. In: Ford, T.D. and Cullingford, C.H.D. (Editors) *The Science of Speleology*, Academic Press, London, pp267-327.

White, W.B. and Brennan, E.S., 1989. Luminescence of speleothems due to fulvic acid and other activators. *Proceedings of the 10th International Conference of Speleology*, pp212-214.

Wigley, T.M.L. amd Brown, M.C., 1977. The physics of caves. In: Ford, T.D. and Cullingford, C.H.D., (Editors), *The Science of Speleology.* Academic Press, London, pp329-358.

Winograd, I.J., Coplen, T.B., Landwehr, J.M., Riggs, A.C., Ludwig, K.R., Szabo, B.J., Kolesar, P.T. and Revesz, K.M., 1992. A continuous 500,000 year climate record from vein calcite in Devils Hole, Nevada. *Science*, 258:255-260.

Woo, M.-K, and Marsh, P., 1977. Effects of vegetation on limestone solution in a small Arctic basin. *Canadian Journal of Earth Science*, 14:571-581.

Worsley, P., 1991. Possible early Devensian glaciation in the British Isles. In: Ehlers, J., Gibbard, P.L. and Rose, J. (Editors), *Glacial deposits in Great Britain and Ireland.* A.A.Balkema, Rotterdam, pp47-52.

Zagwijn, W.H., 1983 Applications of radiocarbon dating in geology. *PACT*, 8:71-80.

Zagwijn, W.H., 1990. Vegetation and climate during warmer intervals in the late Pleistocene of Western and Central Europe. *Quaternary International*, 3/4:57-67.

Zöller, L and Wagner, G.A., 1989.Thermoluminescence dating applied to palaeosols. *Quaternary International*, 1:61-64.

Zöller,L., Stremme, H. and Wagner, G.A., 1988. Thermolumineszenz-datierung an loss-palaoboden-sequenzen von Nieder-, Mittel- und Oberrhein / Bundesrepublik Deutschland. *Chemical Geology (Isotope Geoscience Section)*, 73:39-62.